Biomass Derived Binder

Development of the scientific basis for methodologies that enable the production of renewable sustainable cement based on ashes derived from the conversion of biomass residues as determined by qualitative mineralogical analysis

Carr, Natalie

DOI
10.4233/uuid:12821467-3df9-40ab-a297-159497650b8c

Publication date
2019

Document Version
Final published version

Citation (APA)
Carr, N. (2019). *Biomass Derived Binder: Development of the scientific basis for methodologies that enable the production of renewable sustainable cement based on ashes derived from the conversion of biomass residues as determined by qualitative mineralogical analysis*. [Dissertation (TU Delft), Delft University of Technology]. https://doi.org/10.4233/uuid:12821467-3df9-40ab-a297-159497650b8c

Biomass Derived Binder

Development of the scientific basis for methodologies that enable the production of renewable sustainable cement based on ashes derived from the conversion of biomass residues as determined by qualitative mineralogical analysis.

Dissertation

for the purpose of obtaining the degree of doctor
at Delft University of Technology
by the authority of the Rector Magnificus, prof. dr. ir. T.H.J.J. van der Hagen
chair of the Board for Doctorates
to be defended publicly on Friday 18, January 2019 at 10:00 o'clock

by

Natalie Nicole CARR

Master of Science in Building Materials, Construction Chemicals and Repair,
Technische Universität München, Germany
born in Salt Lake City, USA.

This dissertation has been approved by the promotors

Composition of the doctoral committee:

Rector Magnificus	Technische Universiteit Delft, chairman
Prof. dr. ir. K. van Breugel	Technische Universiteit Delft, promotor
Dr. H.M. Jonkers	Technische Universiteit Delft, promotor

Independent members:

Prof. dr. R.N.J. Comans	Wageningen University & Research
Prof. Dr.-Ing. D. Heinz	Technische Universität München
Prof. dr. S.J. Picken	Technische Universiteit Delft
Dr. Ing. A.J. Saraber	Vliegasunie
Dr. ir. G. van der Wegen	SGS Intron
Prof. dr. ir. H.E.J.G. Schlangen	Technische Universiteit Delft

This dissertation is dedicated to all the emotional support animals of the world.

The pie charts are dedicated to Hannes

because he loves pie and charts,

just not together.

ACKNOWLEDGEMENTS

As is the case with any large endeavor, there are many people who helped me along the way and without whom I would have not made it to this fancy new title. This is my attempt at listing those individuals and explaining the reasons for my gratitude.

Noreen, you sparked an interest in sustainability before I even knew what the word was. You had a monumental role in setting me on this path and demonstrating what strength and determination look like.

Lauren and Brian, thanks for all the love and support. I would not be here without both of you.

Philipp, you supported me and my continued education for many years in many ways. One day you will be fully paid back, with interest.

Prof. Heinz, you introduced me to the wonderful world of concrete when you accepted me into the masters program all those years ago. Thank you for coming back to challenge me at the next stage.

Henk, this all started with your idea and I am grateful for that. You saw the potential in me to take on that challenge and have supported and supervised me along the way. Thank you.

My doctoral committee, thank you all for taking the time to evaluate me and my work. Thank you Prof. van Breugel for the constructive criticism and your eagle eye for editing.

Mladena and Claudia, you are standing by me during my defense as paranymphs but also during the whole process as colleagues, as friends, as irreplaceable supports. There have been a lot of shared tears on our journeys but even more laughs, let's keep in going. We are two thirds of the way to a hattrick.

Daša, I am so glad that I met you. My gratitude for your friendship goes far beyond the support you gave during the PhD process.

Jaap Mulkus, you see everything so clearly and have been instrumental in helping me to see things that way too. Thank you for all the confidence you helped me find in myself.

All my former colleagues at the Microlab, thanks for all the good times and hard work.

All my new colleagues at SGS Intron, thanks for all the good times to come and the hard work to come. Thank you, Ron and Gert for taking a chance on me and having confidence that my PhD would be completed.

Joanna, your diligent and dedicating editing skills have made this dissertation possible. Thank you for all of the hard work and for showing me just how often I use the word "however."

Lisa, thank you for a beautiful cover.

Hannes, you may have only caught the end of this wild ride but you certainly held on tight. Thanks for all of the support, patience, love, encouragement and care giving (for me and Molly). But more importantly thanks for always making me laugh. You are my favorite weirdo and my best friend.

Also, I would like to thank anyone and everyone who is reading this. If your eyes make it here it shows that you care, so thank you!

TABLE OF CONTENTS

LIST OF ABBREVIATIONS

adSTT	Autogenously doped & secondary thermally treated
APC	Air pollution control residue
BA	Bottom ash
BBF	Bubbling fluidized bed
BioSCM	Biomass derived secondary cementitious materials
BioSCMp	Processed biomass derived secondary cementitious materials
C_2S	Dicalcium silicate, belite
C_3A	Tricalcium aluminate
C_3S	Tricalcium silicate, alite
C_4AF	Tetracalcium aluminoferrite
CFB	Circulating fluidized bed
CY	Crop yield
DSC	Differential scanning calorimetry
dSTT	Doped secondary thermally treated
DTA	Differential thermal analysis
ESP	Electrostatic precipitator (ESP)
FA	Fly ash
FB	Fluidized bed
GS	Grate stoker combustion
HAB	Herbaceous and agricultural biomass
HI	Harvest index
LOI	Loss on ignition
OPC	Ordinary portland cement
OR_CB	Organic residues and contaminated biomass
PF	Pulverized fuel combustion

PSFA	Paper sludge fly ash
SCM	Secondary cementitious material
SEEA	System of environmental-economic accounting
SNCR	Selective non-catalytic reduction
STT	Secondary thermally treated
TGA	Thermogravimetry
UAA	Utilized agricultural area
WBFA	Woody biomass fly ash
WWB	Wood and woody biomass
XRD	X-Ray diffraction
XRF	X-Ray fluorescence

List of Figures

List of Tables

CHAPTER 1

INTRODUCTION

ABSTRACT

This chapter contains a detailed explanation of the research project, towards the development of a CO_2 neutral cement. The background and research significance identify the motivation from both an environmental and a political standpoint. The research scope states exactly what is to be achieved within this work. A summary of the project as a whole will be given with the individual objectives broken down. Finally, the content of the individual chapters in this thesis is stated.

1 Background and Research Significance

Lowering greenhouse gas emissions is a task facing all communities. The EU, in particular, has taken steps to fight climate change and reinforce energy security with a series of targets to be met by 2020. The Climate Change and Energy Sustainability target of the Europe 2020 program aims to reduce greenhouse gas emissions to 20% lower than the levels in 1990, obtain 20% of energy from renewable resources, and increase energy efficiency by 20% [1]. With these policies, the EU attempts to transform itself into a highly energy-efficient and low carbon economy [2]. However, in order to achieve these sustainability goals, there must be an investment in, and commitment to, green technologies.

Lowering greenhouse gas emissions is a task facing all industries; the cement industry is no exception. The building materials sector is the third largest CO_2 emitting industrial sector in the world and it is dominated by CO_2 stemming from cement production [3]. For this reason, the cement industry is often flagged as a sector where a positive impact can be made through change [4] [5]. When discussing the overall CO_2 production associated with cement, there are two factors to consider: the high quantity demand and the high energy demand.

Concrete is the most extensively used construction material and its consumption continues to grow, especially in developing and newly industrialized countries. China serves as a good example of growing cement demand. Global cement production grew from 594 Mt in 1970 to 2770 Mt in 2007 and as of 2005 China was responsible for 47% [6, 7].

While the EU and other countries are pushing to place more importance on sustainability and the environment, we still live in a society where monetary constraints determine and direct industrial practices and decisions. However, the cost of energy dominates the production cost of cement accounting for up to 40% [2], thereby making it an attractive area of improvement for industry and policy makers alike. From a large perspective, cement production accounts for about 2% of the global primary energy consumption, or up to 5% of the total global industrial energy consumption [4]. The majority of the energy is invested in fuel to reach the sintering temperatures and electricity for grinding the raw materials and clinker [6].

The combination of large production quantities and massive energy consumption results in significant amounts of CO_2 being released into the atmosphere. As of 2004, Gartner calculated that the world cement production was enough to produce roughly 6 km^3 of concrete a year. Since one cubic meter of concrete represents an average CO_2 emission of 0.2 tons this equates to 1.2 billion tons of CO_2 per year [8]. There are two discrete sources of CO_2 stemming from the cement industry, one being "energy-use" CO_2 and the other "process" CO_2 [9]. While the combustion of fossil fuels necessary to reach the sintering temperatures is mostly responsible for the energy-use CO_2, mining, grinding and homogenizing the raw materials and grinding and homogenizing the clinker still comprise a portion of these emissions [2]. Process CO_2 denotes the chemically produced CO_2 from the decomposition of limestone. The CO_2 emissions resulting from the conversion of limestone into calcium oxide are relatively constant and equate to approximately 540 kg CO_2 per ton of clinker produced. However, since multiple factors are involved, such as the thermal efficiency of the kilns, the CO_2 emissions resulting from the combustion of fossil fuels, per ton of cement produced, fluctuate. In 2006, the global average gross CO_2 emissions per ton of clinker was 866 kg [10]. This value accounts for 5-8% of total anthropogenic atmospheric CO_2 emissions [11]. Net CO_2 emissions from cement production can be drastically reduced or potentially even avoided if the raw material, specifically limestone, required for cement production does not result in net emission of CO_2 in the cement production process [12]

2 RESEARCH SCOPE

This work explores the use of biomass derived ash to replace cement, as well as the raw materials currently used in cement and concrete production to potentially lower CO_2 emissions. If biomass derived ash were to replace cement up to a theoretical replacement of 100%, the use of traditional cement (OPC) could be eliminated and the energy required for its production could therefore be drastically diminished. These two factors have, in turn, the advantage of decreasing the CO_2 emissions associated with cement production.

The combustion of biomass for the purpose of energy production is currently happening all over the world and at varying scales, in line with and as stipulated by the EU's goal to obtain 20% of their energy needs from renewable sources by 2020 [13]. Coupling low operational costs with a continuously renewable fuel, biomass fueled power plants have proven themselves to be a promising renewable energy alternative [14]. These two advantages (low costs and renewability) suggest that biomass combustion will take on a more promising role in energy production.

The conversion of biomass into energy also results in the production of ash. Currently there are few available applications for biomass derived ashes; however, the use of coal-based fly ash has been a valued additive to concrete production for decades. When used to partially replace cement, fly ash has the advantage of conserving energy, resources, and cost while improving durability through the formation of a denser matrix of the resulting concrete [15]. While the substitution of coal with biomass in energy production has substantially lower associated net CO_2 emissions, there are a few challenges that must be addressed e.g. the disposal or re-use of the biomass derived ashes and the impact of the reduction in availability of coal based fly ashes on the cement and concrete industry. Therefore, it is crucial to explore the potential of biomass derived ashes as supplementary cementing materials.

Examination of the chemical and mineralogical composition of biomass-derived ash shows that it also has potential to replace clay and limestone, i.e. the raw materials required for the production of cement. A biomass ash with sufficient quantities and ratio of CaO and SiO_2 can either be found or multiple ashes can be blended together to obtain the desired chemical composition of the raw material required for clinker production. This would yield typical clinker minerals after further heat treatment. Replacement of limestone as raw material feed by biomass derived CaO for the production of clinker would reduce CO_2 emissions drastically due to elimination of the limestone calcination process. The burning of biomass and the resulting CO_2 emission does not contribute net CO_2 into the atmosphere as long as combusted biomass is regrown. By replanting harvested biomass, the emitted CO_2 will be fixed during the process of photosynthesis in the new growth cycle. This cyclical process ensures that no "new" or net CO_2 will be released into the atmosphere [16]. Replacing the traditional raw materials used in the production of Portland cement, limestone and clay, with biomass and agricultural waste products, a bio-based cement will be created that does not further deplete limited resources. Since biomass is a renewable source of raw materials and energy, there is, in principle, no concern over depleting limited supplies. Landscape mutilation resulting from the mining of limestone will also be avoided.

Since firing of the biomass will be done in conjunction with energy production, the ashes, or BioCement (i.e. biomass derived ashes capable of replacing cement), can be viewed as a by-product. In this regard, all of the energy invested in harvesting, processing, and preparing the biomass will be associated with energy production and not BioCement production. The utilization of the ashes also provides a solution to the disposal of the waste which would otherwise contribute to landfilling since this is the most economical solution [17]. The utilization of biomass, particularly those stemming from landscaping and agricultural residues, provides a solution for their disposal as well. However, care must be taken to ensure that nutrient cycles and soil productivity are maintained. To balance the removal of nutrients either the lost nutrients need to be returned (recycling) or new nutrients additions (inputs) are needed [18, 19]. In the case of woody biomass the removal of an entire tree can

remove as much as three times the nutrients as compared to a conventional bole-only harvest since the majority of the above ground nutrients are contained in the branches and foliage [20] [21]. However, the majority of the nutrient capital in a forest ecosystem is located below ground, so utilization of the entire tree will result in only a small percentage of nutrient loss from the forest ecosystem [22].

The objective of this investigation is to evaluate the possibilities to apply biomass derived ash as a partial or even full replacement of cement in the production of cement-based materials. Biomass derived ashes will be studied and their ability to replace cement as a secondary cementitious material (SCM) and also as a suitable replacement of raw materials (limestone and clay) in the current cement production process will be evaluated.

3 Summary and Outline of Thesis

The aim of this project is the development of the scientific basis for methodologies that enable the production of renewable sustainable cement (i.e. BioCement) based on ashes derived from the conversion of biomass residues from agricultural or industrial origin. The development and testing of products derived from biomass ash will also be explored. Within this project, biomass ash and derived products will be developed at the laboratory scale, their mineralogical composition will be determined and used to evaluate their potential performance compared to a SCM, traditional (OPC) cement and clinker raw meal. Additionally, the functionality in terms of strength development of biomass derived ashes will be tested when used to partially replace OPC. The ultimate goal is to prove the possibility of replacing virtually all of traditional Portland cement with a renewable BioCement in typical cement-based products such as concrete. BioCement will be environmentally superior to traditional Portland cement with respect to negligible CO_2 emissions during its production. Through Life Cycle Analyses on the developed biomass ashes (and preferably fully functional BioCement), the environmental impact and the potential to replace Portland cement with BioCement based on material stream volumes will be quantified.

A breakdown of the nomenclature applied to the different products contained within this work can be seen in Figure 1. It is important to note the distinction between current traditionally biomass derived ash and those that have been treated in some manner. For this work, all products will be derived from currently available raw ash; the processes subsequently involved will determine the name of the products. Different standards describe different criterion which must be satisfied for the material to be classified as cement. The European Standard EN 197-1 (called CEM) states that the binder must be comprised of more than 50 M.-% of reactive calcium oxide and reactive silicon dioxides [23, 24]. ASTM C 150 dictates that dicalcium silicate (C_2S or belite) must be in excess of 40% [23]. For this work, in order to be classified as a BioCement, the described binder must be comprised of at least 50 M.-% reactive dicalcium silicate (C_2S) and tricalcium silicate (C_3S or alite) and originate from recent biomass.

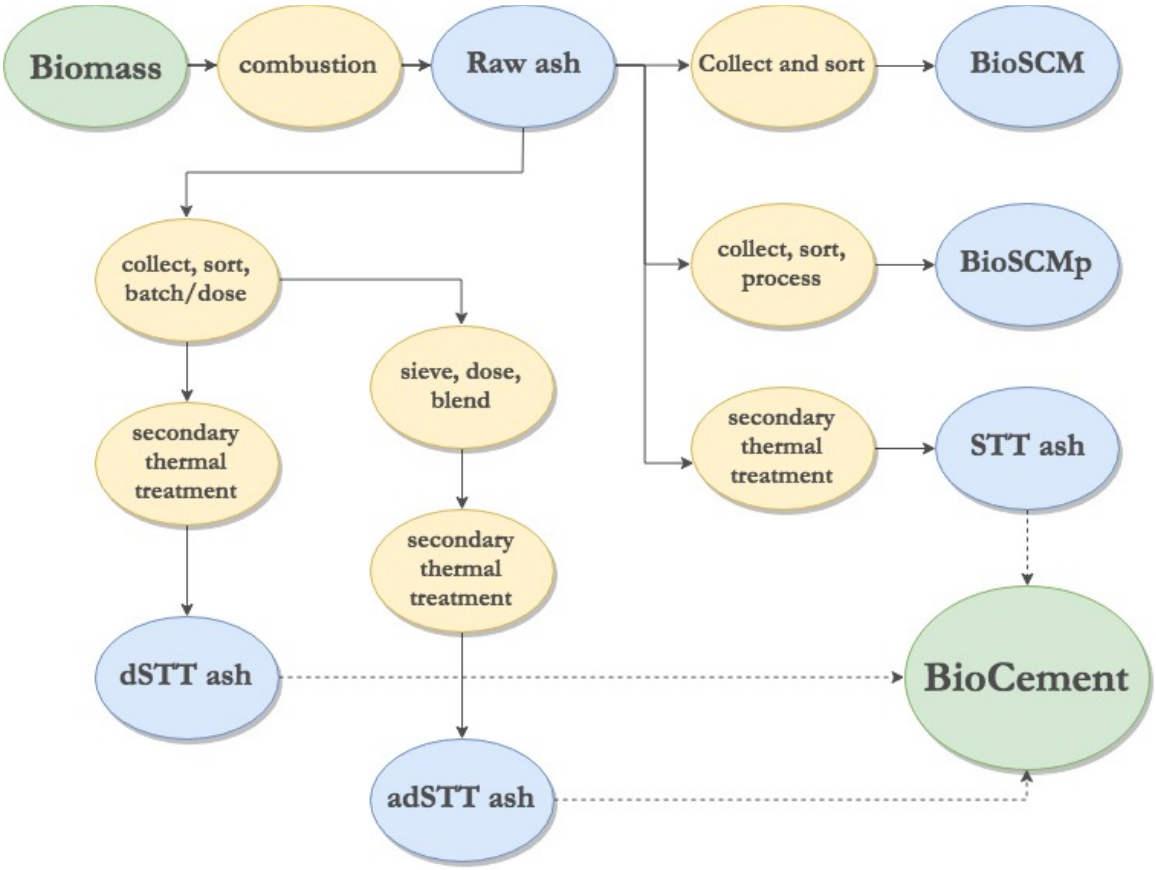

Figure 1: Flow diagram and terminology of the raw materials, conversions, and products discussed in this work; Biomass and Raw ash in chapters 3, BioSCM in chapter 4, BioSCMp in chapter 5, SST ash (secondary thermally treated ash) in chapter 6, and dSTT ash (doped secondary thermally treated ash) and adSTT in chapter 7 (autogenously doped secondary thermally treated ash).

The entire project is divided into eight work packages (a break down can be seen in Figure 2) and the tasks were jointly worked on by three PhD candidates from different disciplines. Work package 1 focuses on the characterization of currently available biomass-derived ashes from different agricultural sources in terms of their chemical composition. This allowed for the establishment of their potential to act as input raw material for the production of BioCement. Work package number 2 concerns the optimization of currently available biomass-derived ashes. Biomass sources were selected for desirable silicon and calcium contents. The relationship between the biomass feedstock and ash properties was established. Furthermore, the silicate and calcium oxide contents in the ash were experimentally optimized and the feasibility of removing undesirable constituents (e.g. salts and trace elements) was theoretically determined. Work package 3 involves the optimization of biomass conversion technology to achieve most desirable ash properties for eventual BioCement production. Work package 4 aims to investigate and optimize the application potential of produced biomass ashes for various concrete- and cement-based construction applications. Work package 5 involves the selection of potential feasible routes for bio-based cement production: from more traditional bio-energy feedstocks to agricultural waste streams. Work package 6 concerns the quantification of the carbon footprint of the produced biomass ashes and eventual BioCement. Comparisons are made

between traditionally produced cement and the novel biomass derived cementitious ashes. Work package 7 goes beyond the carbon footprint to quantify other environmental properties, i.e. investigation into the leaching properties of traditional cement- and Biomass ash -based products at various stages in service life. Work package 8 theoretically explores the potential to scale the process up. The current and future possibilities to replace traditional cement with BioCement will be quantified here.

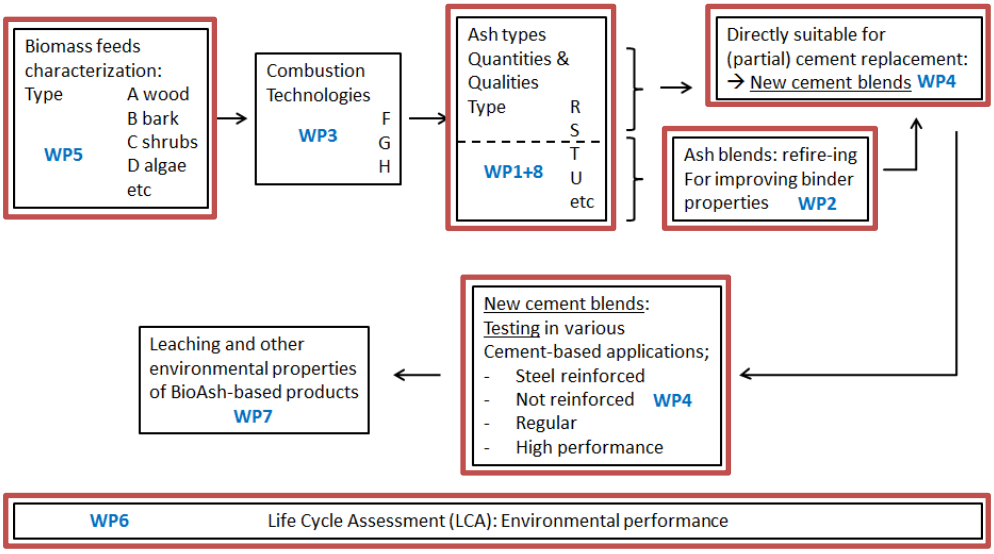

Figure 2: Schematic drawing of entire project objectives. Work packages outlined in red are addressed in this dissertation.

This particular thesis will address the above-mentioned topics in the following chapters:

- Chapter 2: Literature survey.
- Chapter 3: Characterization of currently available biomass derived ashes; WP5, WP1 and WP8.
- Chapter 4: Use of currently available biomass derived ash for cement application as secondary cementing materials (BioSCM); WP4.
- Chapter 5: Modifying currently available biomass derived ash for cement application as secondary cementing materials (BioSCMp); WP2 and WP4.
- Chapter 6: Developing methods of thermal processing to obtain hydraulic minerals from biomass derived ashes (STT); WP2.
- Chapter 7: Modifying biomass derived ash's chemical composition before thermal processing to increase the hydraulic mineral content (dSTT & adSTT); WP2.
- Chapter 8: Quantifying CO_2 emissions associated with the production of BioCement & BioSCM as compared to traditional OPC; WP6.
- Chapter 9: Summary and conclusion.

4 REFERENCES

1. Commission, E., *Energy 2020-A strategy for competitive, sustainable and secure energy.* COM (2010), 2010. **639**.
2. Pardo, N., J.A. Moya, and A. Mercier, *Prospective on the energy efficiency and CO 2 emissions in the EU cement industry.* Energy, 2011. **36**(5): p. 3244-3254.
3. Szabó, L., et al., *CO 2 emission trading within the European Union and Annex B countries: the cement industry case.* Energy Policy, 2006. **34**(1): p. 72-87.
4. Worrell, E., et al., *Carbon dioxide emissions from the global cement industry.* Annual Review of Energy and the Environment, 2001. **26**: p. 303-329.
5. Hendriks, C.A., et al. *Emission reduction of greenhouse gases from the cement industry.* in *Proceedings of the Fourth International Conference on Greenhouse Gas Control Technologies*. 1998.
6. Taylor, M., C. Tam, and D. Gielen, *Energy efficiency and CO2 emissions from the global cement industry.* Korea, 2006. **50**(2.2): p. 61.7.
7. Oss, H.G.v., *US Geological Survey (USGS) Cement - 2007*. 2009.
8. Gartner, E., *Industrially interesting approaches to "low-CO2" cements.* Cement and Concrete Research, 2004. **34**(9): p. 1489-1498.
9. Barcelo, L., et al., *Cement and carbon emissions.* Materials and structures, 2014. **47**(6): p. 1055-1065.
10. Initiative, C.S., *Cement industry energy and CO2 performance: getting the numbers right*. 2009, Geneva: World Business Council for Sustainable Development.
11. Scrivener, K.L. and R.J. Kirkpatrick, *Innovation in use and research on cementitious material.* Cement and Concrete Research, 2008. **38**(2): p. 128-136.
12. Guerrero, A., et al., *Belite cement clinker from coal fly ash of high Ca content. Optimization of synthesis parameters.* Environmental science & technology, 2004. **38**(11): p. 3209-3213.
13. Girón, R.P., et al., *Properties of fly ash from forest biomass combustion.* Fuel, 2013. **114**(0): p. 71-77.
14. Cheah, C.B. and M. Ramli, *The implementation of wood waste ash as a partial cement replacement material in the production of structural grade concrete and mortar: An overview.* Resources, Conservation and Recycling, 2011. **55**(7): p. 669-685.
15. Mehta, P.K. and P.J.M. Monteiro, *Concrete: microstructure, properties and materials*. 2006: McGraw-Hill.
16. McKendry, P., *Energy production from biomass (part 1): overview of biomass.* Bioresource Technology, 2002. **83**(1): p. 37-46.
17. Pels, J.R., D.S. de Nie, and J.H. Kiel. *Utilization of ashes from biomass combustion and gasification*. in *14th European Biomass Conference & Exhibition*. 2005.
18. Gliessman, S.R., *Agroecology: researching the ecological basis for sustainable agriculture*, in *Agroecology*. 1990, Springer. p. 3-10.
19. Anex, R.P., et al., *Potential for enhanced nutrient cycling through coupling of agricultural and bioenergy systems.* Crop Science, 2007. **47**(4): p. 1327-1335.
20. Alban, D.H., D.A. Perala, and B.E. Schlaegel, *Biomass and nutrient distribution in aspen, pine, and spruce stands on the same soil type in Minnesota.* Canadian Journal of Forest Research, 1978. **8**(3): p. 290-299.
21. Phillips, D.R. and D.H. Van Lear, *Biomass removal and nutrient drain as affected by total-tree harvest in southern pine and hardwood stands.* Journal of Forestry, 1984. **82**(9): p. 547-550.
22. Farve, R. and C. Napper, *Biomass fuels & whole tree harvesting impacts on soil productivity—Review of literature.* US For. Serv., San Dimas Technol. Dev. Ctr., San Dimas, CA, 2009.

23. Hewlett, P.C., *Lea's chemistry of cement and concrete*. 2004: A Butterworth-Heinemann Title.

24. EN-197-1, *Cement - Part 1: Composition, specifications and conformity criteria for common cements.* 2011: p. 1-39.

CHAPTER 2

LITERATURE SURVEY

ABSTRACT

This chapter describes the current state of the global cement production process and its contribution to CO_2 emissions. It elaborates on the composition of Portland cement: what is necessary for its functionality and how it is typically manufactured. Furthermore, the conversion of biomass into energy will be expounded. Finally, potential biomass waste streams in The Netherlands, and their suitability as a BioCement precursor based on material streams will be explored. The chapter concludes with the union of these three distinct topics as part of a biobased future. Utilizing the information gained will allow for the production of BioCement, as it will be explored in the subsequent chapters.

1 THE CEMENT INDUSTRY AND CO_2

Concrete is currently the most extensively used construction material and the global consumption of concrete increases every year. As an essential component in concrete, cement consumption also increases annually. Global cement production grew from 594 Mt in 1970 to 2770 Mt in 2007 [1] [2]. Cement production is extremely energy-intensive and accounts for about 2% of the global primary energy consumption, or up to 5% of the total global industrial energy consumption [3, 4]. The theoretical heat requirement for clinker production is calculated to be 1.75 ± 0.1 MJ per kg [5]. In reality, the heat requirement is higher and depends on the specific process applied.

Between the large quantities produced and the huge energy consumption, cement is responsible for significant amounts of CO_2 being released into the atmosphere. The production of cement contributes to CO_2 emissions through two sources: the decomposition of limestone and the combustion of fossil fuel. The CO_2 emissions resulting from conversion of limestone into calcium oxide are fairly constant and equate to approximately 540 kg CO_2 per ton of clinker produced. Since multiple factors are involved, such as the thermal efficiency of the kilns, the CO_2 emissions resulting from the combustion of fossil fuels required for the production of a ton cement fluctuate. In 2006, the global average gross CO_2 emissions per ton of clinker was 866 kg [6]. This value accounts for 5-8% of total human atmospheric CO_2 emissions [7]. Numerous ways to reduce the emission of carbon dioxide in the production of cement have been suggested; improvement in energy efficiency during the production process, replacing high carbon fuels with low carbon fuels to reduce CO_2 emissions, and adopting lower clinker-to-cement ratios in the use of blended cements [8].

The largest proportion of energy consumed in cement manufacturing comes from the fuel that is used to heat the kiln to allow for the chemical reactions necessary to form the clinker minerals. Thus, large gains in energy reduction can come from improved efficiency. The OPEC oil embargo of the mid-1970s lead to the first push for the cement industry to reduce oil dependency and improve energy efficiency. The ensuing research and development sought to refine manufacturing technologies and, as a result, the cement industry adopted new technologies like multistage preheater kilns combined with vertical raw mills (allowing the recovery of waste heat), more efficient closed circuit finish mills and improved clinker coolers [9]. The embargo also ignited interest in alternative fuels, such as coals, cokes, and even waste fuels. These changes lead to roughly a 40% reduction in the fuel energy requirement for clinker manufacturing in North America in the following two decades [6]. Further improvements may still be achieved by applying more energy efficient processing equipment or replacing older installations, however most plants in developed countries have already achieved maximum efficiency. Alternatively, the industry can shift towards new cement production processes or alternative low-energy binders that have yet to be developed [8].

Aside from increasing the energy efficiency of the production process, reducing the carbon content of the fuel can help to lower the overall carbon dioxide emissions. In cement production, more than 90% of the energy used is from the fuels used to heat the kilns (the remaining portion of primary energy is attributed to electricity used in grinding and processing) [8]. The application of waste-derived alternative fuels would help to reduce the net long-term carbon emission though the replacement of primary fossil fuels and help in diminishing the amount of waste material that needs to be disposed. Potential alternative fuels can be categorized as gaseous, liquid or solid. Gaseous alternative fuels include coke oven gases, refinery gases, pyrolysis gas and landfill gas. Liquid alternative industrial by-product derived fuels include halogen-free spent solvents, mineral oils, distillation residues, hydraulic oils and insulating oils. Solid alternative fuels include waste wood, dried sewage sludge, plastic, agricultural residues, tires, petroleum coke, and tar. Alternative fuels could present other problems such as their lack of energy efficiency, low quantity and quality, adverse emissions to the atmosphere other than CO_2, and emission of harmful compounds to terrestrial and aquatic environments, such as deposition of trace elements and heavy metals. Consequently,

individual alternative fuels need to be fully evaluated for their environmental footprint before their application.

Additional measures have been taken to cut CO_2 emissions through the reduction of clinker content using blended cements [8]. In blended cement, a portion of the clinker is replaced with industrial by-products such as coal fly ash, blast furnace slag, silica fume or other pozzolanic materials. The potential for blended cements depends on the availability of the materials as well as the local standards and legislative requirements which may cap the allowable replacement rates. Potential emission reductions in terms of potentially worldwide available volumes of suitable industrial by-products which can be applied for blended cements are estimated to be around 22% [10].

Recently many steps have been taken to combat CO_2 emissions in the cement industry including improving energy efficiency of the kilns, replacing fossil fuel with renewable energy sources, and substituting part of Portland cement with other cementitious materials [6]. While these actions have contributed to making progress in reducing CO_2 emissions, they still do not provide a truly sustainable solution and alternative options must be investigated in order to achieve this objective.

2 Ordinary Portland Cement

Ordinary Portland Cement (OPC) is a polyphase inorganic binder with a complex mineralogical composition resulting from a multi-factor and multi-stage production. Production involves limestone and clay of variable composition and results in a material of variable composition. The four major mineral phases in OPC are alite, belite, calcium aluminate and calcium alumino ferrite. Alite and belite are not stoichiometricly pure compounds, but rather solid solutions which in addition to CaO and SiO_2, incorporate minor amounts of additional oxides. Calcium aluminate and calcium alumino ferrite are compounds based off of alite and belite. In fact, the two calcium aluminate compounds are interstitial phases between the larger crystals of the silicates [11]. The exact individual phase compositions of these four main minerals are dependent on the production process and the chemical makeup of the raw feed. In addition, minor phases, such as periclase, calcium oxide and alkali sulfates can also be found in commercial OPCs. Alite and belite are the most important phases since they contribute the most to the sought after hydraulic properties and subsequent strength. Therefore, the formation and reactivity of these two main phases will be examined in more detail.

2.1 Alite

Alite is the term used for impure forms of tricalcium silicate which can incorporate small amounts of Mg^{2+}, Al^{3+} and Fe^{3+} ions. In cement chemist notation, tricalcium silicate is referred to as C_3S. For simplicity's sake, in this work alite and C_3S will refer to the impure forms of tricalcium silicate. The term tricalcium silicate will refer to only the pure form. C_3S accounts for 50 to 70 wt.-% of clinker and is the most important constituent of OPC due to its high reactivity and contribution to early strength development. Immediately upon mixing with water, 2-10% of the C_3S begins to hydrate before entering a dormant period. After a few hours, the reaction rate begins to increase until around 28 days when a significant fraction of the C_3S has been consumed (i.e. the majority of what will ultimately be consumed). For this reason, C_3S is the most important component for strength development particularly in the first 28 days [5, 12].

2.1.1 Alite Polymorphs and Formation

Alite exhibits seven different polymorphs, depending on impurities and production methods. Of the seven different modifications, there are three crystal systems; three are triclinic (T_1, T_2 and T_3), three are monoclinic (M_1, M_2 and M_3) and one is rhombohedral (R). In clinker, the most commonly occurring modifications are M_1 and M_3 (see Figure 1) [13]. The polymorphs emerge in a successive reversible phase transition when heated, as can be seen in Figure 3 [5].

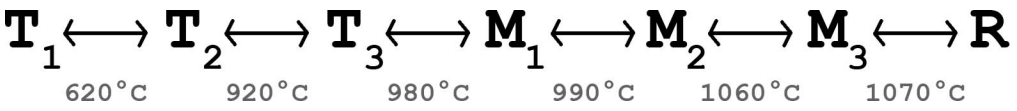

Figure 3: Seven different alite polymorphs and the temperatures of transformation [5, 14].

The polymorphism of tricalcium silicate is quite complex and not as well understood as the other clinker minerals [11]. Structural differences are attributed to shifts in the atomic positions, most notably the oxygen position in the SiO_4 tetrahedra. At room temperature, only the triclinic modification (T_1) of pure C_3S exists. The other six modifications (including the most common M_1 and M_3) are stable at higher temperatures or as solid solutions that have been stabilized with foreign ions [11].

Table 1: Modification of C_3S based on foreign ion concentration [15].

Modification	Fe_2O_3 [M.-%]	Al_2O_3[M.-%]	MgO [M.-%]
T_1	0-0.9	0-0.45	0-0.55
T_2	0.9-1.1	0.45-1.0	0.55-1.45
M_1			1.45-2.0
M_2			>1.2

The impurities, or stabilizing ions, generally found in alite are MgO, Al_2O_3 and Fe_2O_3 and their content can vary greatly from one clinker to another. The atomic radii and the preferred coordination determine the type of substitution. Mg^{2+} is known to substitute directly for Ca^{2+} in the C_3S lattice due to the similarity in their ionic radii [16]. More MgO can be incorporated into C_3S than Al_2O_3 or Fe_2O_3 because the atomic radii of Al^{3+} and Fe^{3+} are less similar to Ca^{2+}. In addition to the size of the ion, synthesis temperature also impacts the solubility limit of foreign ions. Between 1420 and 1550°C the amount of MgO able to be incorporated into C_3S increases from 1.5 wt.-% to 2.5 wt.-% [15]. However, generally more than one type of foreign ion is present in the raw feed and the individual concentrations thereof impact incorporation and polymorph formation. For example the amount of MgO necessary to stabilize a monoclinic C_3S is lower when small amounts of Fe_2O_3 are also present [17]. The complex interactions when multiple ions are in play have been simplified in a table compiled by Stephan et al. [15] based on previous research on the modifications of C_3S with dependence upon the respective concentrations of Fe_2O_3, Al_2O_3 and MgO (Table 1).

Foreign ions are not the only decisive parameter in the polymorphic transformation of C_3S. The temperature and duration of calcination, the evaporation of volatile compounds, the burning grade and intensity as well as the rate and conditions under which the clinker is cooled all impact C_3S modification [18]. The initial properties of the raw meal also influence polymorph formation before conversions even begin. For example, the chemical composition, grain size distribution, mineral composition, contents of minor oxides as well as the macro- and micro-homogeneity of the feed all influence the end mineralogy. Similar to the impact of impurities, small differences in minor oxides and their concentrations could result in large differences in performance amongst cements despite similar amounts of alite in the clinker. Even when the concentrations are low, small deviations in the amount of SO_3, alkali oxides and MgO can significantly influence polymorphism and thus affect strength properties of the resulting hydration products [18].

2.1.2 Alite Identification

Identification and quantification of the individual polymorphs of tricalcium silicate have their advantages despite all alite polymorphs showing a higher rate of hydration than belite. Among the seven polymorphs, there are still differences in the rate of hydration; this is reflected in the resulting strength [18, 19]. Differences were even identified in M_1 and M_3, the two most common C_3S polymorphs in clinker. Stanek and Sulovsky found that the transformation of M_3 to M_1 resulted in a 10% increase in compressive strength of derived specimens [18]. Further connections have been made between the type of stabilizing ion and the resulting compressive strength of the various polymorph derived specimens [20]

Due to very similar X-ray diffraction patterns, tricalcium silicate polymorphs are difficult to distinguish. 'Fingerprint' regions are typically used for the identification of the tricalcium silicate polymorphs, namely peaks in the ranges of 31-33° and 51-52° 2θ [5, 11, 21-23]. However, in clinker, the 31-33° range is less useful for identifying potentially present polymorphs due the presence of other phases, which also form peaks in this range. Since most of the pronounced diffraction peaks in the 31-33° range overlap, the much smaller peaks in the 51-52° range are typically used for identification [23]. The number of peaks located in the 31-33 range can help to identify some polymorphs [24]. However, even with fingerprint regions, identification can still be difficult. In the case of the T_1-T_3 transition one reflection gradually blends into the next, making clear distinctions between polymorphs ambiguous [21].

As a result of the difficulties in characterization using XRD, other methods are often used in conjuncture, such as differential thermal analysis (DTA) and optical microscopy. According to Dunstetter, the M_3 polymorph can only be observed with a high temperature light microscope [11]. Microscopic and diffraction methods are best for the identification of the T_1-T_2 transition, whereas the T_2-T_3 can only be identified with DTA [13, 14, 21]. Identification of the T_3 form is difficult since its structure is not fully understood.

2.2 Belite

The impure dicalcium silicate, C_2S in cement chemist notation, known as belite, is another important constituent of OPC, accounting for anywhere between 15 and 30 wt.% of clinker. In contrast to alite, belite reacts much slower when mixed with water. After an induction period lasting up to two or three days, a noticeable reaction begins. Since the fraction of C_2S hydrated within 28 days is distinctly lower than that of C_3S, it contributes little to the early strength development. After one year, comparable strengths are reached by pure alite and pure belite [5]. In this work, as stipulated for C_3S, C_2S and belite will denote the impure forms, whereas dicalcium silicate will designate the pure form.

Just like tricalcium silicate, dicalcium silicate exists in several different modifications as first observed by Bredig [12, 25]. The different polymorphs of C_2S show markedly different hydration characteristics, significantly more so than those observed for tricalcium silicate. Thus, it is imperative to distinctly identify all five of the C_2S polymorphs. Fortunately all of the research conducted on belite over the past few decades has resulted in the five different polymorphs being well understood regarding formation, structure and reactivity [11, 26-29]. Of the five structural modifications of belite, four are stable in specific temperature ranges and one is metastable [29].

2.2.1 Belite Polymorph Formation

During the production of cement, the raw feed is exposed to increasing temperatures. Eventually when sintering is reached, the CaO and SiO_2 from the raw feed begin to bond and form the high temperature C_2S modifications. At 850°C α'_L-C_2S begins to slowly develop. Further heating above

1177°C transforms the mineral to α'_H-C_2S and then above 1425°C there is a rapid inversion to the α phase (Figure 4).

Upon cooling, it is possible for C_2S to transform into the γ- or β-polymorph. Transformation from the α-C_2S to β-C_2S happens around 675°C; however under 500°C, β-C_2S is metastable [30]. When the temperature drops to the range 400-500°C, β-C_2S transforms reconstructively to γ-C_2S [31]. Due to the reversible polymorphic transformation of β-C_2S to γ-C_2S both phases can coexist in clinker [32]. In fact, the transition from the higher temperature polymorphs is usually incomplete and results in mixtures of the β and γ modifications [33].

The transformation from the β-C_2S to γ-C_2S involves a specific volume increase since the densities of β-C_2S and γ-C_2S are 3.28 g/cm^3 and 2.97 g/cm^3 respectively. This can result in a volume expansion of about 12% and is coupled with a 4.6° angular unit cell change [34]. The stress associated with this expansion is enough to fracture the material and even pulverize the clinker nodules. This well-known phenomenon is referred to as dusting [12]. It has been suggested that dusting could be used to create autogenously pulverizing cement to reduce grinding energy. However, γ-C_2S has an extremely low reactivity, so its content must be limited. A balance would need to be found between energy saving and hydraulic activity [32].

While γ-C_2S is not completely hydraulically inactive, it has a significantly lower reactivity than the other polymorphs, making its presence detrimental to long term strength development [35]. Its reactivity is so low that it is often considered non-hydraulic. Its lack of hydraulic activity has been attributed to its high degree of crystallinity. The regular coordination of the calcium ions with respect to oxygen in the crystal lattice of γ-C_2S, is not as predominant in the other polymorphs [5].

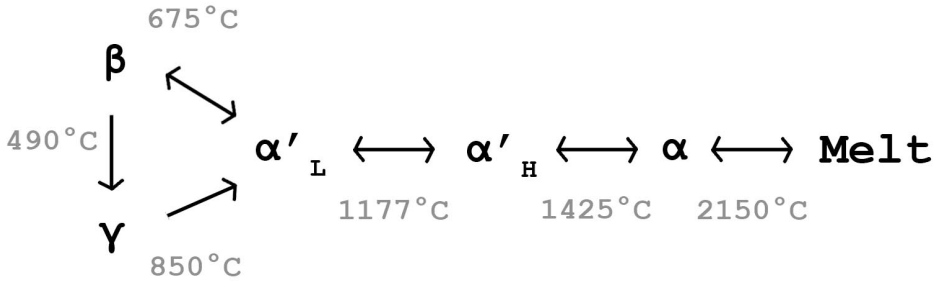

Figure 4: Five different belite polymorphs and the temperatures of transformation [5, 34].

Since the γ-polymorph is the only C_2S modification that exhibits low hydraulic activity, it is generally avoided in industrial clinkers [23]. Extensive research has been done on the preservation of the α- and β-polymorphs upon cooling of clinker and many solutions are possible [12]. Quenching is commonly employed to preserve β-C_2S in clinker. Cooling the nodules as fast as possible limits the time in which they exist in the temperature range where β-C_2S can convert to γ-C_2S. By cooling at a rate exceeding 500 °C/min in the 1300–700 °C range, stabilization of the active forms of dicalcium silicate can be achieved [36].

Furthermore, transformation from the β- to the γ-modification will not occur if certain extraneous oxides are present [27, 37]. A large number of oxide impurities will dissolve at high temperatures when the α- or α'-phases are present and form solid solutions. Upon cooling, these impurities help to stabilize the β-C_2S [12]. An excess of dissolved CaO in the crystal can also stabilize the polymorph. Additionally, smaller C_2S crystals are less prone to transform to the y-modification and β-C_2S remains

preserved in a 'metastable' state, since they can be cooled faster across their diameter and have a larger surface area to volume ratio [33, 38].

The α' (orthorhombic) and β (monoclinic) modifications in particular favor the incorporation of impurities [29]. The C_2S in industrial clinkers can contain up to 4-6 wt.% of foreign ions. Most commonly Al^{3+} and Fe^{3+} are observed, with S^{6+}, Mg^{2+} and K^+ being occasionally found [24]. While less common in industrial clinkers, P_2O_5 and B_2O_3 have proven to be successful stabilizers as well. These two compounds are more commonly discussed in the context of stabilizing pure C_2S, often on the laboratory scale.

Under the same sintering conditions, different polymorphs can be formed dependent upon the particular foreign ion(s) incorporated and the content. Benarchid et al. found that β-, α'- and α-C_2S polymorphs could all be formed when less than 9.5 wt. % of Fe_2O_3 and 8.45 wt. % of P_2O_5 was added to the raw feed before samples were fired at 1400°C and then cooled to room temperature [39]. According to Matković et al. only the addition of 1.42-2.27 wt.% P_2O_5 is necessary to stabilize β- and α'-polymorphs [40]. The addition of Fe_2O_3 results in only the development of β-C_2S because the presence of Fe_2O_3 inhibits the stabilizing effect of P_2O_5 on the α'-C_2S formation [41]. Wesselsky and Jensen found that β -C_2S was best stabilized with B_2O_3, whereas α'-C_2S required Na_2O in addition to the B_2O_3 [42]. The effects of previous transformations, cooling kinetics, the microstructure, and amorphous phases all affect the stabilization of β-C_2S against the transformation to the γ-phase [34].

The β-polymorph predominates industrial clinkers, and is considered to be the hydraulically important C_2S polymorph [12, 37]; however, α-modifications can also be found and are of no detriment to the clinker [23]. α-C_2S is not normally present simply because it is the highest temperature polymorph and stabilizing at room temperature is difficult; however, the α'-C_2S modifications are more reactive than β-C_2S thus their presence is acceptable when it does occur.

2.2.2 Belite Structure

All of the belite polymorphs are built upon the same free SiO_4 tetrahedra linked together by calcium ions, but, alterations in the reciprocal arrangement of tetrahedral and calcium coordination leads to different polymorphs [43]. The α'_H and α'_L structures are generally believed to be fairly complex superstructures of the α' structure [26]. With weak displacive transformations, α'_H and α'_L are very similar in structure [44]. The coordination of the Ca-ions is eightfold in α'-C_2S and sixfold in γ- C_2S [31]. In the β-modification the coordination number is different for both of the Ca ions, one being eight and the other being between six and nine [31, 45]. Similarities among the β- and α'-structures explain why the β-C_2S develops from the α'- C_2S upon cooling, despite γ- C_2S being more stable [31]. A change in coordination of the Ca and an accompanying rotation of the SiO_4 tetrahedra result in the transition from the γ → α' and the β → γ phases. The sixfold Ca coordination in γ-C_2S accounts for the larger molecular volume [31]. These small changes lead to differences in reactivity of the individual polymorphs.

Differences in the calcium coordination have been used to explain differences in reactivity among the polymorphs. The total strength of the bonds around an ion must equal its formal charge; for oxygen this is two units. Since one of the units of bond strength is allocated to a Si-O bond, the other is divided amongst the n Ca ions to which the oxygen is coordinated. N is equal to either 3 or 4 in the case of β-C_2S, so relative to γ-C_2S the length of some Ca-O bonds is greater and correspondingly the strength is less. This makes it easier for the hydrogen ion to split a Ca-O bond in the β-modification [31]. However, more recently this explanation has met criticism since it would indicate that both high pressure pseudowollastonite and β-C_2S would react faster than C_3S, which is not the case [27]. Alternatively, it has been proposed that the mean distance is more important than the shortest regarding reactivity with water. Accordingly, the mean Ca-Ca distance in the hydraulically active β-C_2S is distinctly shorter than in γ-C_2S.

The type of connection of the CaO polyhedral is also of importance for reactivity. Connection of CaO polyhedral by common faces is only found in active silicate compounds. The hydraulic activity of calcium silicate is possibly dependent upon many short Ca-Ca distances, and the connection of the CaO polyhedral is dependent on common faces [27]. Alternatively, it has been suggested that the hydraulic activity of a binder is correlated to the degree of disorder in the crystal lattice of the mineral components. Generally the high temperature modification of a mineral displays a higher degree of disorder than the lower temperature modifications [46]. Regardless of the reason, in the case of C_2S, reactivity is agreed to follow the following ranking α-C_2S > α'-C_2S > β-C_2S >> γ-C_2S.

2.2.3 Belite Identification

In pure calcium silicate, the identification of β-C_2S by XRD poses no problems. Identification of β-C_2S can be made using the peak at 31° and a much weaker peak at 35.2° [23]. To find a good match for the α'_H-C_2S or α'_L-C_2S is much more difficult, as there are no single patterns that cover all encountered peaks. It is necessary to exclude all other possible modifications by first trying to match their corresponding patterns: β-C_2S, C_3S and CaO, and potentially also γ- and α-C_2S.

Identification of belite polymorphs can be difficult because often multiple modifications exist in the same sample [37]. As was the case for C_3S, in the context of clinker analysis, identification of the C_2S minerals becomes even more complex due to the presence of other phases. Multiple phases create a composite pattern with most of the strong diffraction peaks overlapping, thus identifications are often made using the weaker peaks [45]. The belite content must be over 12% in order to characterize using the weaker peaks [24, 47]. Characterization can be very difficult for the individual phases but it becomes even more complicated when multiple phases in various modifications are present in one sample, which is the case in clinker.

2.3 OPC Requirements and Production

Across the world, different standards define cement and dictate its required composition. Most notably are the European Standard ENV 197-1 for common cements and the American society for testing and materials (ASTM) C 150-95. Cement conforming to the European standard ENV 197-1 (called CEM) must be composed of more than 50 M.-% of the sum of reactive calcium oxide and reactive silicon dioxides [12]. ASTM C 150 dictates an optional maximum of 35% for tricalcium silicate and 7% tricalcium aluminate, however dicalcium silicate must be in excess of 40% [12]. Furthermore, in Portland cement clinker, the total sum of calcium silicates (C_3S and C_2S), should be at least two thirds by mass.

In order to achieve these compositions, there are chemical constraints on raw materials used to produce clinker. In the production of OPC, the raw meal is composed of a calcareous material (most commonly limestone) and a smaller amount of an argillaceous one (generally clay or shale) [12]. Often additional raw materials are needed to achieve the desired chemical composition and consequently iron ore, bauxite or sand may be incorporated. These supplementary materials also add aluminum oxide and iron oxide to the mixture, which then function as mineralizers and facilitate the formation of calcium silicates at reduced temperatures. Either through the raw meal or the fuel, additional elements can enter the system. While some of them are inert, others must be monitored because even in small quantities they can have negative impacts on the production of the clinker or the performance of the clinker.

Limestone consists mainly of calcium carbonate typically in the polymorphic form of calcite. This is the primary source of calcium for the production of clinker minerals, however limestone can also deliver relevant quantities of minor components. These compounds can be present in the limestone as accessory phases or as substituents in calcite. The concentration and type of minor components needs to be monitored because they have the potential to be deleterious to clinker production or the durability of concrete [5]. The main constituents of both shales and clays is aluminium silicates which

also containe some combined iron and free silica as quartz [12]. SiO_2 generally only comprises 55-60 wt.% of these argillaceous materials. The rest is divided mostly between Al_2O_3 and Fe_2O_3, but also smaller amounts of MgO, alkalis and H_2O.

In order to achieve the primary objectives, the clinker should not contain significant amounts (normally over 3%) of free calcium oxide or excessive amounts (not more than 5-6%) of magnesium oxide. It should also contain very little moisture or combined carbon dioxide in order to ensure the full strength-giving potential. When magnesium oxide is present in the raw meal, it will lower the viscosity in the kiln. However, when it is present in amounts in excess of 5.0M.-%, it can crystalize out from the flux and form periclase. Periclase is associated with long term unsoundness (especially in slowly cooled clinkers) and should be avoided.

The fuel used to reach the sintering temperatures can also impact the clinker composition, especially in the case of coal or lignite. The combustion of these two fuels produce significant quantities of ash which are compositionally quite similar but not identical to the argillaceous components. On account of the similarities, the coal ash is often incorporated into the feed materials, resulting in changes to the clinker composition since the incorporation of 2% coal ash can lower the C_3S content from 76% to 64%. Oil can be problematic due to the contribution of sulfur. The contribution differs based on the exact conditions but it can be up to 4 M.-% [5, 12]. Conversely, natural gas is the least invasive fuel to use. This fuel introduces no components which are capable of interfering with the clinker chemistry.

One of the most important minor constituents to monitor and avoid is the alkalis, which includes both potassium and sodium [5]. In the presence of moisture, alkalis can react with certain aggregates (known as the alkali silica reaction) to produce a gel. The expansive property of this gel induces cracking of the concrete or mortar. The alkali content is measured in terms of the sodium oxide equivalent where the sum of Na_2O and 65.8% of the K_2O content is taken. To avoid the adverse effects of an alkali silica reaction, a sodium oxide equivalent less than 0.6% is recommended [12]. In addition to the alkali concentration, it is important to monitor the sulfate content in conjuncture with alkalis. Sulfates have the advantage of maintaining the alkalis as their sulfates. Given sufficient sulfate concentrations in the clinker, alkalis are typically present as K_2SO_4, Na_2SO_4, apthitalite or calcium langbeinite. This inhibits the Na_2O from entering the C_3A where it would otherwise increase the reactivity leading to setting problems. Similarly, the presence of sulphate occupies the potassium, so K_2O is unable to enter the C_2S and inhibits its conversion to C_3S. Alkalis present as their sulfates also decrease the viscosity of the flux, thereby promoting the formation of C_3S. However, if the alkali sulfate content is too high it can increase the crystal size of the C_3S to a point where its hydraulic activity is reduced. Furthermore, to avoid corrosion of the reinforcement, the chloride content in Portland cement is restricted to 0.10M.-% in most standards. After alkalis, sulfur, and chloride, fluorine is the minor element that is most important to be aware of. Fluorine has served as a mineralizer in the past and was added in the form of calcium fluoride (at about 1 M.-%) to enhance the C_2S content and promote C_3S formation at lower firing temperatures. However, Fluorine contents exceeding 0.2 M.-% tend to lower the strength, as well as delay setting and hardening at lower temperatures.

Other oxides such as manganese oxide, titanium oxide, vanadium oxide, and zinc oxide are less common but should also be avoided because they can create problems during burning and degrade the overall quality of the cement produced [5, 12, 48]. Substituting for ferric oxide in the flux, manganese reduces the viscosity. This results in the formation of larger C_3S crystals which reduce strength development. For this reason, the manganese content should not exceed 0.5 M.-%. Titanium oxide has the potential to inhibit strength development in the first two days but improve strengths after 3 days. It is believed to act as a mineralizer because it increases C_3S crystal sizes. Vanadium present in the raw meal at 0.2 M.-% increases the crystal size which is most likely responsible for a

corresponding 10% drop in the 28 day strength. When Zinc is present at 0.2 M.-% there is an increase in the reactivity of C_3A, which can cause problems with accelerated setting times.

In addition to the problems that they cause for the performance of clinker, minor oxides can be detrimental to both the formation of clinker minerals as well as the integrity of the kilns used to produce the clinker. While alkalis present as their sulphates promote the formation of C_3S, the low viscosity that causes this effect also leads to more dust being formed in the burning zone of the kiln. Furthermore, alkalis can be disruptive to the system when they are not discharged with the clinker since they volatilize in the higher temperature zones and then condense in the cooler zones. This phenomenon leads to blockages in the heat exchange systems. Oxidizing conditions in the kiln help to maintain sulfur in the clinker which can then combine with the alkalis. For the kiln system, it is also important to distinguish between sulfur which enters the system in the form of sulfates (such as calcium sulfate) and that which enters as sulfides (such as pyrite, marcasite and organic sulfides). Sulfides can oxidize through an exothermic reaction at 400-600°C. In this temperature range, there is less calcium oxide available to bond with the sulfides resulting in the emission of SO_2 which can be hazardous to the kiln. Calcium sulfates only decompose at 900-1000°C, so the oxides of sulphur produced have more opportunity to react with the alkalis and the CaO. Chlorides enter the system with the fuel (when coal is used) and the raw meal (when clays from marine environments are used). They can also be disruptive to the kiln system since they readily volatilize in the burning zone and condense in the heat exchanger to combine with alkalis and sulfates to form low melting point mixtures. For this reason, maximum chloride content acceptable from coal is 0.18M.-% and from the raw meal is 0.015M.-%. When fluorine is used as a mineralizer, it can lead to build up of excessive coating in the kiln. This is the result of the formation of added spurrite; it can be avoided by increasing the silica content or decreasing the Al_2O_3 and Fe_2O_3 content. When the P_2O_5 exceeds 1M.-% the amount of C_3S formed is reduced since P_2O_5 helps to stabilize the C_2S inhibiting the conversion to C_3S. Up to 0.5M.-% P_2O_5 can be incorporated in the structure of C_3S. At higher phosphate levels it will decompose to give a solid solution of C_2S, phosphate and free lime which have less ideal cementing properties. The presence of elevated concentrations of phosphates can alter the kinetics of C_3S hydration and cause a retardation [12]. When phosphorus is present in cement clinker in percentages lower than 1.1m.-% it has been shown to have no significant influence on the reactivity or the compressive strength[49]. Strontium in larger concentrations inhibits the reduction of free lime because C_3S is converted to $(CSr)_2S$ and free lime. As such SrO should be limited to 2.5%.

Not only is the chemical composition of the raw materials vital, but the physical form plays an important part in both the quality of the product and the production process [12]. For example, the hardness of these materials differs which means that not all materials achieve the same level of fineness during grinding. Feedstocks can have the same overall chemical composition but due to the different size fractions of the components, they can require different firing temperatures. Thus, to achieve the lowest possible temperature in the burning zone of the rotary kiln, and through this a lower fuel consumption, an adequate and consistent fineness is critical [12].

After material selection, the feed is prepared so that it is best suited for chemical reactions that will take place during thermal processing. This is done to not only insure the quality of the final product but also reduce the amount of materials and energy invested in the production. The raw materials first go through a sequence of intimate mixing. Subsequently, the feedstock is exposed to a series of thermal treatments. Thermal steps include drying (100°C), preheating (100-500°C), calcination (550-1200°C), sintering/clinkering (1350-1500°C), and cooling, all of which are conducted in succession with heat exchangers to conserve energy. Drying and pre-heating take place in external chambers before the materials are fed into the rotary kiln. Once in the kiln, the feedstock tumbles down, as the long drum rotates. This motion provides mixing of the feedstock as the material reaches higher temperature zones. Different reactions take place throughout this thermal gradient. Based on the CaO to SiO_2 ratio of the feedstock, different minerals will be formed at different stages in the rotary kiln, a diagram of this can be seen in Figure 5.

Of the principal reactions taking place, production can be divided into three categories: reactions during temperature increase up to 1300°C, reactions between 1300-1450°C and reactions during cooling. The reactions up to 1300°C include the decomposition of calcite, or calcination, the decomposition of clay minerals, and the reaction of lime with quartz that creates belite, aluminate and ferrite. The majority of the mix is still solid at this stage. At the end of this stage, the major phases present are belite, lime, aluminate and ferrite. The reactions at 1300-1450°C are known as clinkering. Here a partial melt is formed, induced by the aluminate and ferrite, where 20-30% of the mix is liquid. Much of the belite and the remaining lime react in the presence of the melt to produce alite. As the material flows and tumbles down the rotary kiln, it nodulizes to form clinker.

At this point, the mix has reached its maximum temperature and reactions associated with cooling can be observed. The cooling method and speed greatly affect the functional quality of the produced minerals. The liquid crystallizes, producing mainly aluminate and ferrite. Additionally, polymorphic transitions of the C_3S and C_2S occur whereby the minerals invert to their lower temperature forms [5]. Reactivity of the minerals is highly dependent upon the polymorph type. As explained above, in the case of C_2S there are 5 different polymorphs (Figure 4). The β polymorph is considerably more reactive with water than γ-C_2S, so care must be taken upon cooling to not revert to the γ-form. In the case of C_3S there are 6 different polymorphs where the lower temperature polymorphs can be considered distortions of the rhombohedral phase (R). The triclinic (T1-3) and monoclinic (M1-2) forms are similar to the rhombohedral despite their different crystallographic symmetry [12]. In clinker production, C_3S crystals grow as C_2S incorporates free lime. However, C_3S can be unstable and under certain cooling conditions can revert back to C_2S and free lime. Slow cooling can induce the lime to be extracted from the C_3S surface leaving a C_2S layer [50].

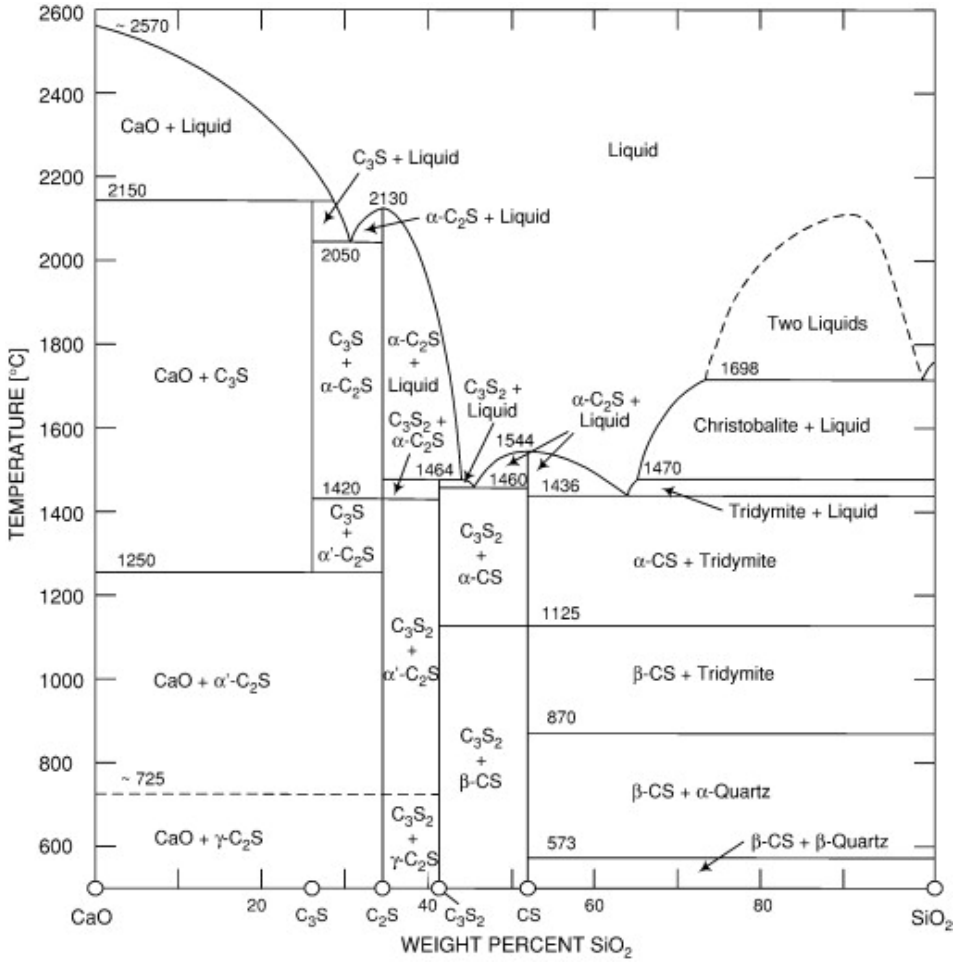

Figure 5: Phase diagram with mineral formation based on CaO and SiO_2 ratio and temperature [12, 51].

3 Converting Biomass to Energy

The concept of using biomass to provide energy is certainly not new; it could even be argued that this is the first energy source that mankind learned how to harness and control. Early humans used the combustion of wood to provide heat and light, allowing them to thrive as a species. Fossil fuel, in the form of coal, has been used since 1000 B.C. but it was not until the arrival of the industrial revolution that coal overtook biomass as the primary energy source [52]. Having a higher caloric value per kilogram than biomass, coal could provide more energy for longer periods of time. The higher heating value of biomass tends to fall in the range of 17-21 MJ/kg whereas anthracite coal has a higher heating value of 32.5 MJ/kg [53]. The decreasing forest area in England around this time contrasted with the abundance of coal available which helped to shift the energy demand away from biomass. As the industrial revolution proceeded, the development of fossil fuel technology grew. At this point, biomass combustion technology began to suffer from what would later be called the carbon lock-in [54]. Through a process of technological and institutional co-evolution, coal benefited from the development of high efficiency, low costs, optimal institutional arrangements, and many vested interests. Long periods of experience for fossil fuel technology resulted in the hindrance of the renewable energy market and locked industrial economies into fossil fuel-based energy systems. As a result society is currently heavily dependent on fossil fuels [55].

In recent decades, the political, economic, and environmental climate has encouraged a shift in focus towards renewable energies and spurred a renewed interest in their development. Mostly pushed by government initiatives, the development of renewable energy technology has begun to bloom. In addition to solar, wind and hydro energy, biomass is considered a main renewable energy source in the EU[56]. Biomass offers more flexibility, since unlike the other forms, humans have more influence over location and utilization. In an ideal 100% renewable energy scenario, all the energy sources function together. When the solar and wind energy supply is low, biomass can fill in as an adjustable and controlled energy source [57].

There are additional advantages to biomass, including its availability. Unlike coal, oil, and natural gas, biomass can be produced all over the earth making it a locally available resource. This has the advantage of lowering the capital investment costs associated with conversion into secondary energy carriers [57]. Furthermore, being locally available makes biomass an indigenous energy source for most countries. This has the advantage of reducing the dependency on imported oil and coal [58] [59]. These political and economic advantages can have a profound impact on developed countries and those in the process of developing.

Environmentally, the utilization of biomass for energy production provides additional advantages. When produced and utilized sustainably, biomass energy has the potential to help reduce greenhouse gas emissions [58]. Unlike fossil fuel, biomass can be replanted and replaced. During its growth phase the new biomass will absorb the CO_2, offsetting the CO_2 emitted in the combustion of its precursor. This creates a CO_2 balance where the net CO_2 emission is zero. This short CO_2 cycle replaces the combustion of fossil fuel, which has a long CO_2 cycle. The combustion of fossil fuel releases CO_2 that has been stored for millions of years and will not have the ability to be easily captured and returned to the earth's crust. Thereby, the use of biomass for energy offsets fossil fuel greenhouse gas emission [60] [61].

In addition to the reduction of CO_2 emissions, fine dust and both SOx and NOx emissions could potentially be reduced. In the case of co-firing, biomass can help to reduce the net SO_2 emissions since the biomass-derived alkaline ash has the ability to capture SO_2 produced by coal during combustion. Furthermore, most biomass has a lower nitrogen content than coal and can be converted to ammonia during the pyrolysis stage of combustion [62]. The reduction of CO_2, SOx and NOx emissions has a positive impact on combating the greenhouse-effect and/or acid rain [63] [64].

The combustion of biomass is also environmentally advantageous in that it offers waste disposal solutions [65]. The combustion of agricultural waste and residual biomass materials not only lowers the CO_2 emissions but it also decreases the material volume helping to solve the waste disposal problem. These ashes can be returned to the soil and have a positive effect on degraded land by returning nutrients.

For biomass, as a renewable energy, to take on a larger share of the total global energy consumption the noteworthy challenges need to be addressed. Negating cost and logistical problems, the most prominent issues are related to the thermal conversion process and environmental management [62] [66]. In the thermo-chemical conversion of biomass, problems arise with slagging and fouling. These can be detrimental to the functioning and life span of the furnace. Operating conditions, such as temperature, influence the degree of slagging and fouling in the furnace or boiler. Due to the relatively low melting temperatures of biomass ashes this can cause problems. In terms of environmental management, the ash produced must be better understood. Currently, most biomass ash is either disposed of in landfilling or recycled on agriculture fields or in forests. This transpires with very little formal control and guidelines. But as the amount of ashes produced increases along with the cost of disposal, sustainable ash management solutions become more important [67, 68]. The quantity and quality of ashes produced is heavily dependent on the biomass used and the conversion processes. Care must be taken to avoid environmental problems such as the leaching of ecological relevant heavy metals (such as Zn, Cd, Pb and Hg) which can be present in these ashes. Since the ash composition varies so widely, it is currently difficult to predict the ecological impact and identify an alternative application.

Today, biomass contributes more than 10-15% to the world energy supply and ranks as the fourth source of energy in the world [69]. On average, in the industrialized countries biomass contributes some 9–14% to the total energy supplies, but in developing countries this is as high as 20-33% [62]. Considered to be a promising alternative to replace fossil fuels due to its renewable nature and abundance, cleanly combusted biomass should contribute more to the world energy supply in the future.

3.1 Methods of Biomass Conversion

There are four different approaches to thermochemical conversion technologies of biomass: pyrolysis, gasification, direct combustion, and liquefaction. All of these technologies are at different stages of development. At the moment, combustion technology is the most advanced and most applied, but gasification and pyrolysis are increasing in importance. These technologies produce energy carriers (like charcoal, oil, gas or heat) as primary products. Energy carriers can subsequently be transformed through additional processing to secondary products.

There are a number of physical and chemical steps involved in biomass conversion but the process can be broken down into drying, pyrolysis, gasification, combustion and liquefaction. In the drying stage, moisture is removed at temperatures below 100°C. Removing the moisture at this stage creates a more efficient combustion process in subsequent steps since less energy is required to evaporate the contained moisture and heat the water vapor. In Pyrolysis, the biomass undergoes thermal degradation (or devolatilization) in the absence of an oxidizing agent. This process produces tar, carbonaceous charcoal, bio-oil and low molecular weight gasses such as H_2 as well as CO and CO_2. These products can be used in an assortment of ways; carbonaceous charcoal can be upgraded to active carbon and pyrolysis gas can be used for power generation. In the process of gasification, the biomass is again thermally degraded but in the presence of an externally supplied oxidizing agent. This process produces a mix of combustible gases, such as carbon monoxide and hydrogen [63]. Depending on the oxidizing agent, the calorific value of the gas can range from low to medium. This gas can be upgraded to methanol, burned externally in a boiler to produce steam, in a gas turbine to produce electricity, or in an internal combustion engine. Then there is combustion, the classical way

to convert biomass into energy, where the fuel is completely oxidized [63]. This produces hot gases which can be used to heat water in a boiler and produce electricity, as a process heat, or for water heating in central heating units. Liquefaction is the thermochemical conversion to the liquid phase at low temperatures and high pressures. Relative to pyrolysis, it produces more liquid and one with a higher calorific value and lower oxygen content.

Over the years, different methods of biomass thermal combustion have been developed and they can be distinguished by the following categories of techniques: Grate Stoker Combustion (GS), Fluidised Bed Combustion (FB) and Pulverised Fuel Combustion (PF). In a GS reactor, the fuel is fed onto a grate which rotates through the reactor as primary air passes through. The fuel is dried, carbonised and then burnt out on the grate. The combustible gases produced are burned after secondary air injection, usually in a separate combustion zone. The operational temperature is between 1000-1200°C [70]. GS is appropriate for firing fuels with large particle sizes, and relative high moisture contents (up to 65%). Combustion of blended biomass fuels, where multiple varieties of plant based organic matter are present, is not commonly practiced. In FB, the reactor usually consists of a vertical steel vessel containing a bed of granular material such as silica sand, limestone, dolomite, alumina or ceramic material. The bed material is supported by a perforated grid in order to allow air to be injected through diffusers, causing the bed to expand and become fluid. The constant moving action of the fluidized bed causes quick uniform mixing of fuel and bed material, resulting in good combustion conditions and relative high heat transfer rates. All three processes of drying, carbonisation, and burn out occur in the same volume. Distinctions can be made between bubbling fluidized bed (BFB) and circulating fluidized bed (CFB). In BFB the bed's particle size is between 0.5-1mm and the air injection velocity is moderate (1-2m/s). This combination of bed particle size and air velocity causes the bed to stay in place in the furnace. In a CFB, a bed material with smaller particle size between 0.2-0.4mm is employed along with faster air injection velocity of around 5 to 10m/s allowing both the bed material and the fuel to leave the furnace. The bed material is then collected and recirculated into the furnace. Typical operational temperatures are between 800 and 900°C. FB combustion is capable of converting a wide spectrum of biomass and mixtures of them. In PF, the fuel and primary air are introduced into the boiler and the combustion of the fuel occurs while it is suspended in air. The injection of secondary air helps to burn the combustion gases [70]. The operational temperature is normally between 1300 and 1700°C. This technology is limited to fuels with particle sizes <2mm that can be mixed with air and sprayed into the furnace.

3.2 Biomass Derived Ash

The recent growth of biomass utilization for energy production has increased interest in biomass ash residues and their potential applications; however, the implementation of biomass derived ash as a raw material for industrial purposes depends upon parameters such as the chemical and mineralogical composition and physical characteristics of the ash itself. Not only does biomass derived ash differ from coal derived ash, but it also shows greater variability in its properties, making suitable applications on a broad scale difficult to ascertain. Sometimes biomass ash is used as fertilizer or to return nutrients to the soil; more often, countries resort to landfilling as the only disposal option [71]. Landfilling is not seen as a long term nor a sustainable solution since it can cause problems with air and water pollution. The fine nature of the particles allows for easy dispersal with wind. Also when the disposal occurs with insufficient isolation and percolation, ground water and soil contamination is a possibility due to the leaching of heavy metals from the ashes. These forms of pollution have implications far beyond the immediate area and should be prevented. In order to avoid landfilling, alternative low-cost applications must be explored; more research is necessary to specifically address the chemical and mineralogical composition and physical characteristics of biomass ash streams [72]. There are a few factors which have a profound effect on the composition and properties of the resulting biomass derived ash, namely the biomass source, the thermal conversion system and the type of ash, or ash collection.

Most fundamentally, the biomass source impacts the composition of the resulting ash [72]. It is the inorganic fraction of the biomass that constitutes the ash after combustion. Thus, the inorganic fraction of the biomass has a major role in determining the total ash content and the composition of the ash. Furthermore, the particular ash forming elements impact the release of inorganics into the gas phase, so while the inorganic fraction provides the elements from which the ash can be composed it does not completely dictate the exact elemental composition. There are different ways in which the inorganic fraction is incorporated into biomass. Within biomass, the inorganic matter can be organically associated, present in the form of soluble ions or as included minerals. Additionally, the inorganic matter can also be introduced during harvesting, fuel preparation and processing [73]. Not only do different biomass sources have different inorganic matter present, and in different quantities, but they can also have the inorganic fraction present in different forms. All of these factors result in variations in ash composition and properties based on biomass sources. Biomass itself already shows a lot of diversity. The term "biomass" encompasses any source of organic carbon that is quickly renewed within the carbon cycle. All living organisms are biomass, including animals, plants, trees, crops and algae [74]. With the exception of animals, all of these are regularly used as biofuels, thereby making biomass derived ash just as broad a category as biomass. Classification of biomass can be simplified by grouping different types based on similar properties, structures and compositions. One of the most common and prevalent methods of classifying biomass for energy purposes is the division between 1st generation and 2nd generation biofuels. First generation biofuels are made from the sugars and oils extracted from arable crops while second generation biofuels are technologically more complex and utilize lignocellulosic biomass (or woody crops), agricultural residues or waste. While well-established, this classification has its limitations; it is temporal and groups biofuels based on technological developments rather than intrinsic biomass characteristics. By grouping biomass based on similar structures they tend to have a similar biology which begets a similar elemental composition. Biomass feedstocks for the purpose of energy production can be divided into the following categories: agricultural residues, dedicated energy crops, forestry, industry, parks and gardens, waste and others [75].

In addition to the biomass fed into the reactor, different thermal conversion systems can impact the resulting ash. To a certain degree the biomass can dictate the type of thermal conversion system necessary since not all biomass can be converted to energy under the same conditions. The conversion system dictates the operation parameters, within a particular range. Biomass combustion follows the following sequence of reactions: heating and drying, devolatilization, combustion of gas phase, and combustion of char [76]. In general terms, during the devolatilization phase loosely bound free ions, salts, and organically associated ash elements will be released. During the char combustion phase, the stronger bonded alkalis and part of alkaline earth metals will be released. In this regard, the conversion system impacts the composition of the resulting ash.

Generally, two types of ashes are produced during biomass combustion: bottom ash (BA) and fly ash (FA). When the ash is collected from the discharging point placed at the low end of the furnace, it is referred to as bottom ash (BA). The fraction that is entrained with the flue gas and collected afterwards in the installation is classified as fly ash (FA). Fly ash may be coarse or fine and it will be collected at different points of the installation by different gas cleaning techniques. Normally coarse fly ash is collected early in the installation during the passage through the boiler unit before getting to the gas cleaning system. The finest part will be collected by the flue gas cleaning system before the gas is expelled from the chimney. This process is also known as de-dusting and the residue from this operation is often referred as Air Pollution Control residue (APC). Both ash fractions are mainly composed of the non-combustible inorganic part present in the fuels and by the organic fraction that might be still present in the ash depending on the efficiency of combustion. Despite coming from the same source material, BA and FA can have drastically different compositions. Bottom ash tends to be composed of more silicate minerals while fly ash is dominated by calcium minerals [77].

Several types of equipment are commonly used during the gas cleaning [70]. Cyclones or multi-cyclones (cyclones placed in parallel) expose the flue gas to a centrifugal force. With this method, the particles hit the wall of the cyclone and precipitate into a container. Another method utilizes an Electrostatic Precipitator (ESP), where the flue gas particles are electrically charged and then exposed to an electric field. This attracts the particles to an electrode and removes those which are below 1 μm with a high efficiency. Additionally, there are baghouse filters where the flue gas passes through a filter (textile or ceramic) trapping the particles, allowing for the collection of very fine particles. Scrubbers are used to remove flue gas particles though collisions with water droplets. This procedure also allows for the absorption of SO_2, NO_2 and HCl to the water. The discharged water has to be treated afterwards by a wastewater treatment plant where the ash components are extracted as sludge. Furthermore, NO_x and SO_x reduction measures are necessary. In installations where biomass is combusted, NO_x reductions involves the injection of a reducing agent (such as ammonia or urea). These agents reduce NO_x to N_2. This redox reaction can be a selective catalytic reaction (SCR) if assisted by a catalyst, or selective non catalytic reduction (SNCR) if not. SO_x reduction methods rely on the reaction with lime or limestone. This reaction converts the SO_x into $CaSO_4$ (Anhydrite) which can be easily removed from the flue gas. Naturally all of these cleaning methods affect the composition of the resulting ash and must be acknowledged when ash utilization is an objective.

4 Waste Produced in The Netherlands

Using biomass waste streams for energy production can provide an environmentally friendly and economically attractive alternative. Utilizing the energetic potential of biomass wastes and residues can contribute to a reduction in CO_2 emissions by replacing the combustion of fossil fuel and combusting the waste more efficiently than mass burning. Investigation of waste streams can aid in the quantification of available waste biomass that could potentially be used for energy production. This must be done on a local level, as results will be different based on region. This report will focus on the specific situation of The Netherlands.

Unsustainable farming practices has many negative impacts on the environment, including eutrophication, nitrogen leaching, soil degradation, dehydration and dispersion of agrochemicals [78]. Less intensive farming and integrated farming practices can negate these consequences; however, these solutions will require more land. Since sustainable farming practices should be encouraged, the production of biomass for the solitary goal of energy production should be discouraged. Thus, energy crops are not a viable option for biomass sources to produce energy.

Biomass can still be used for energy production; however, it should stem from waste streams or by-products. Many human activities lead to the production of supplemental biomass. Most supplementary biomass is produced in forestry and agricultural practices as well as in the maintenance of nature areas and public parks [78, 79]. Other supplementary biomass streams include organic domestic waste, sludges and industry wastes. Specifically in The Netherlands, wood thinnings, straw, verge grass, crop residues and greenhouse waste represent primary types of biomass waste [63, 79].

Figure 6 represents the total waste produced in The Netherlands in 2012 according to the classification of the European legislation concerning waste statistics in the System of Environmental-Economic Accounting (SEEA) [80]. Waste is divided amongst the categories: chemical waste, recyclable waste, discarded materials, animal and vegetable waste, mixed waste, sludge and mineral waste.

Chemical waste includes sludge from industrial processes; used solvents; acid, base and salt waste materials; used oils; paint waste, ink and glue, and health care waste. Discarded materials are comprised of discarded vehicles, batteries, electronics, and machine components. Animal and vegetable waste is specific to waste coming from the preparation or production of foods; green waste, and manure. Mixed waste covers waste flows from households, industry, packaging and other streams.

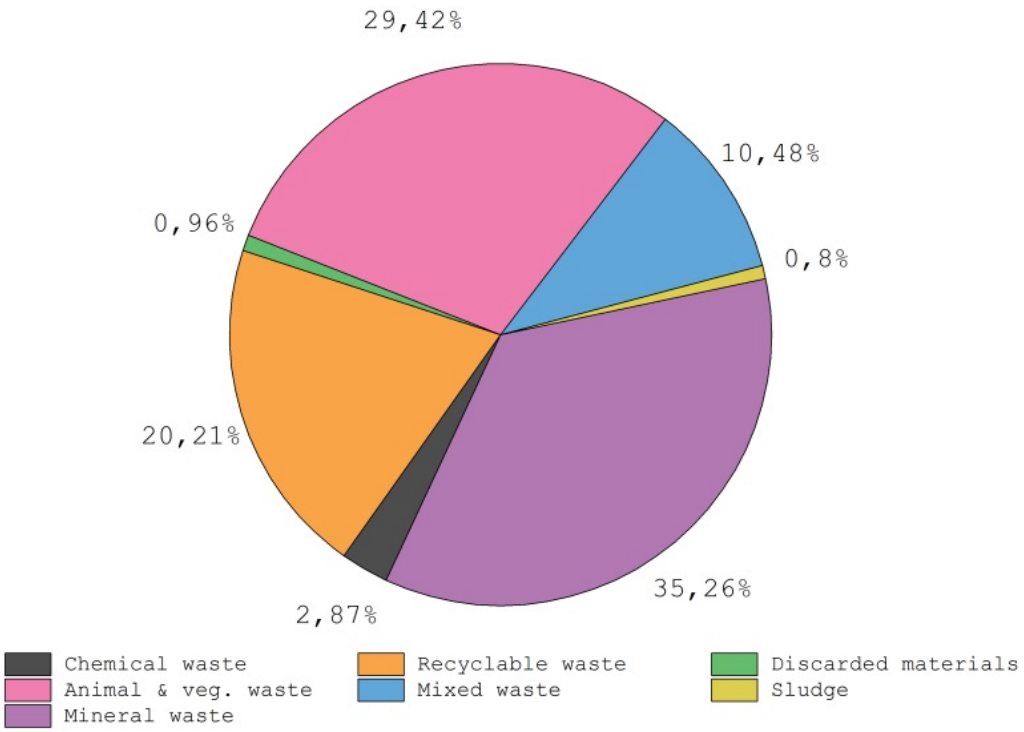

Figure 6: Division of the total Dutch waste in 2012 (80641000 tons). Data obtained from[81].

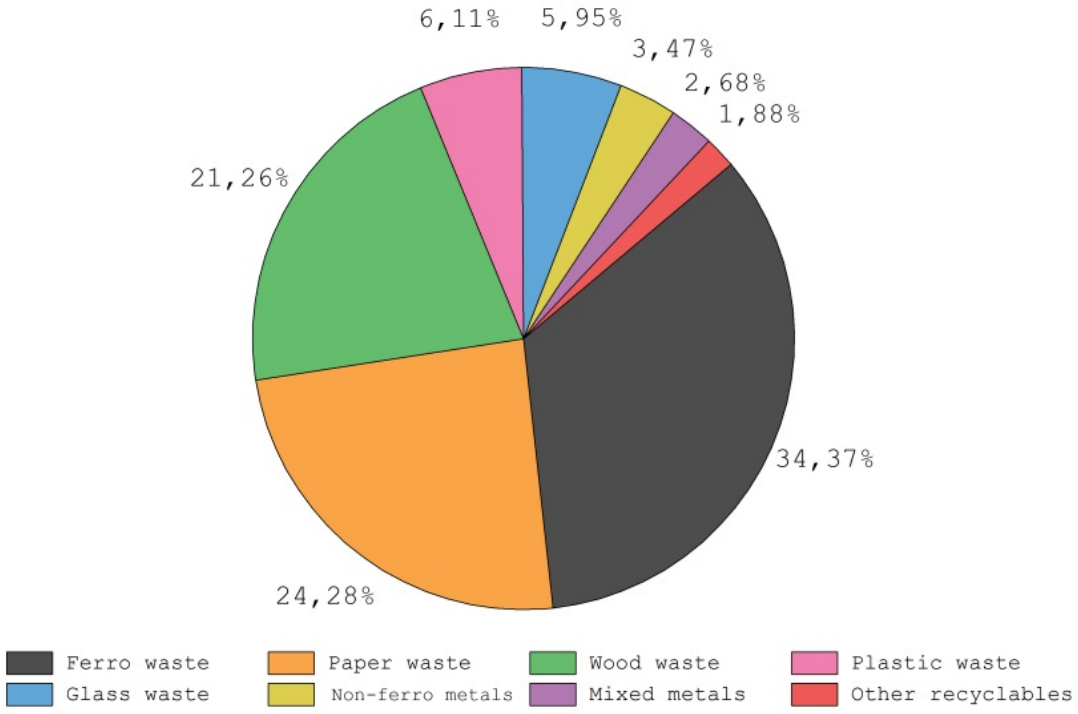

Figure 7: Division of recyclable waste in The Netherlands in 2012 (16298000 tons). Almost 4 million tons of paper waste and 3.5 million tons of wood waste were produced that year. Data obtained from [81].

Mineral waste is composed of concrete, stone and gypsum waste; waste of natural and artificial minerals; asbestos; combustion waste; waste of refractory materials, and contaminated soil and dredged material. Sludge refers to unhardened solid substances which are carried by water or are put down by water. This includes sewage sludge, sludge of drinking-water, not contaminated dredged material and the contents of septic tanks.

While there are numerous resources included in these categories that are currently deemed waste but have potential to be a primary resource in another industry, they are not biomass and not applicable in this project. However, by looking at the subgroups that comprise the recyclable waste category, some biomass derived streams can be identified (Figure 7). Paper waste is typically recycled and reused in the production of new paper. This process can only be repeated so many times before the fibres degrade too much and the quality of the paper is too low. At this point the paper is still suitable for combustion and since the original material was biomass, it is still considered biomass combustion.

4.1 Land Use in The Netherlands

In order to identify and cultivate additional biomass streams that could be used sustainably for energy production, it is advantageous to look beyond existing waste streams and investigate the divisions of land use. Various activities result in the consumption of biomass but also produce biomass waste streams. An investigation into land usage can help to identify exactly where those biomass waste streams exist and just how large they are.

Total land area in The Netherlands is 41543 km^2. The division of land based on functions for The Netherlands in 2010 can be seen in Figure 8. Distinctions are based on the following categories: transport, built-up area, semi built up area, recreation, agriculture, woodland/nature and water. All of these categories have the potential for the producing biomass waste streams that can be utilized for energy production to varying degrees.

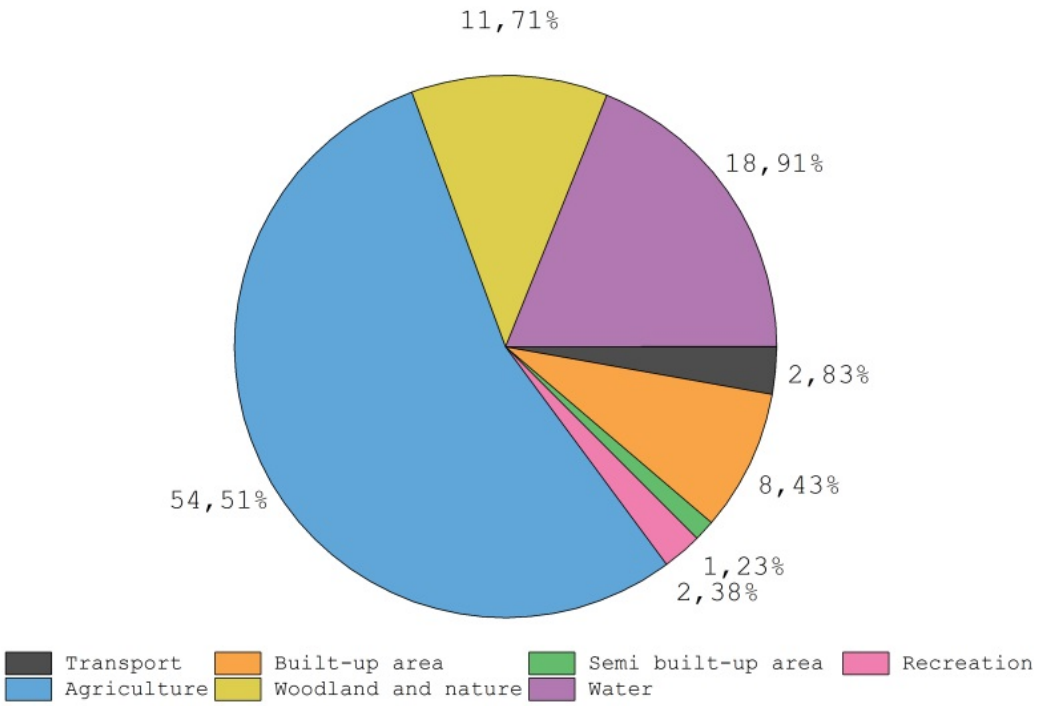

Figure 8: Division of land in the NL as of 2010 as seen as percentages of the total land area (data obtained from[81]).

Attention will be given to those land usages which produce biomass waste streams: built-up areas, woodland and nature, recreation and transport areas, and agricultural areas. In the following sections, these functions will be deeper investigated to find the exact biomass sources. A closer look into the individual land usages will identify phytomass streams with the potential to be applied in energy production.

4.1.1 Built-Up Areas

Built-up areas consist of land used for residents, work, shopping, cultural facilities and public amenities. This includes areas devoted to housing, local shops, schools, local offices, streets and local parking areas, courtyards, gardens, playing grounds, businesses, public institutions, hospitals, museums, theatre, cinema, community centers and many more. All of these functions typically include green areas, which require maintenance and can thereby produce surplus phytomass.

Organic waste, or biomass released after material use (i.e. municipal solid waste), also stems from these functions. Quantities depend on economic development, consumption pattern and the fraction of biomass material in total waste production [60]. Industry has the potential to produce significant quantities of organic waste depending on the exact source. Construction and demolition activities are one example; they have the potential to produce significant amounts of wood waste annually. This phytomass stream can range from clean wood to heavily contaminated (i.e. impregnated) wood. Since the stream is heavily tied to variables like economic development, its quantities can fluctuate significantly from year to year. However, since it is already in a dry state (significantly more so than forest thinnings), it is an ideal fuel so long as the contamination is below a certain threshold [63]. Several studies have estimated that 75% of the produced organic urban refuse is available for energy use [82] [83].

4.1.2 Woodland & Nature, Recreation and Transport Areas

Woodland and nature describes areas with forests, natural open area, and nature conservations. This also includes areas with trees for wood production. Areas used for recreation encompasses public spaces intended for relaxation like parks and sports grounds. This category also covers spaces like zoos, camping grounds, and open-air museums. Transport designates areas in use for traffic and transport by roads, railways, and air. While roads, railways, and airports themselves do not include biomass, this category also covers the greenery in connection with transport systems that is smaller than 1 ha. To varying extents, all of these functions include natural biomass which needs to be maintained on a regular basis.

To maintain healthy forest and wooded areas, thinning and pruning activities are carried out frequently. While a fraction of the debris should remain on the forest ground to recycle minerals, significant quantities of biomass could be available for other applications [78] [84]. The maintenance of natural areas in The Netherlands can result in the harvesting of turf from heather covered areas, willow cuttings, reed, hay, and thinnings [78]. Additionally, the production of timber involves clearcutting wooded areas and results in surplus phytomass. Logging residues as well as mill and manufacturing residues can be recoverable for energy use [85-87]

As can be seen in Figure 9, main roads (including the road-side verges) make up the majority of transportation area. Verges of roads must be maintained by regular mowing, producing verge grass. In The Netherlands, verge grass is typically deposited to waste landfill or composted, both of which are done at a cost. However, verge grass has the potential to serve as a biomass fuel [78, 88] [63]. Similarly, recreational areas need regular pruning and care. This results in a mixture of biomass sources including wood waste and grasses.

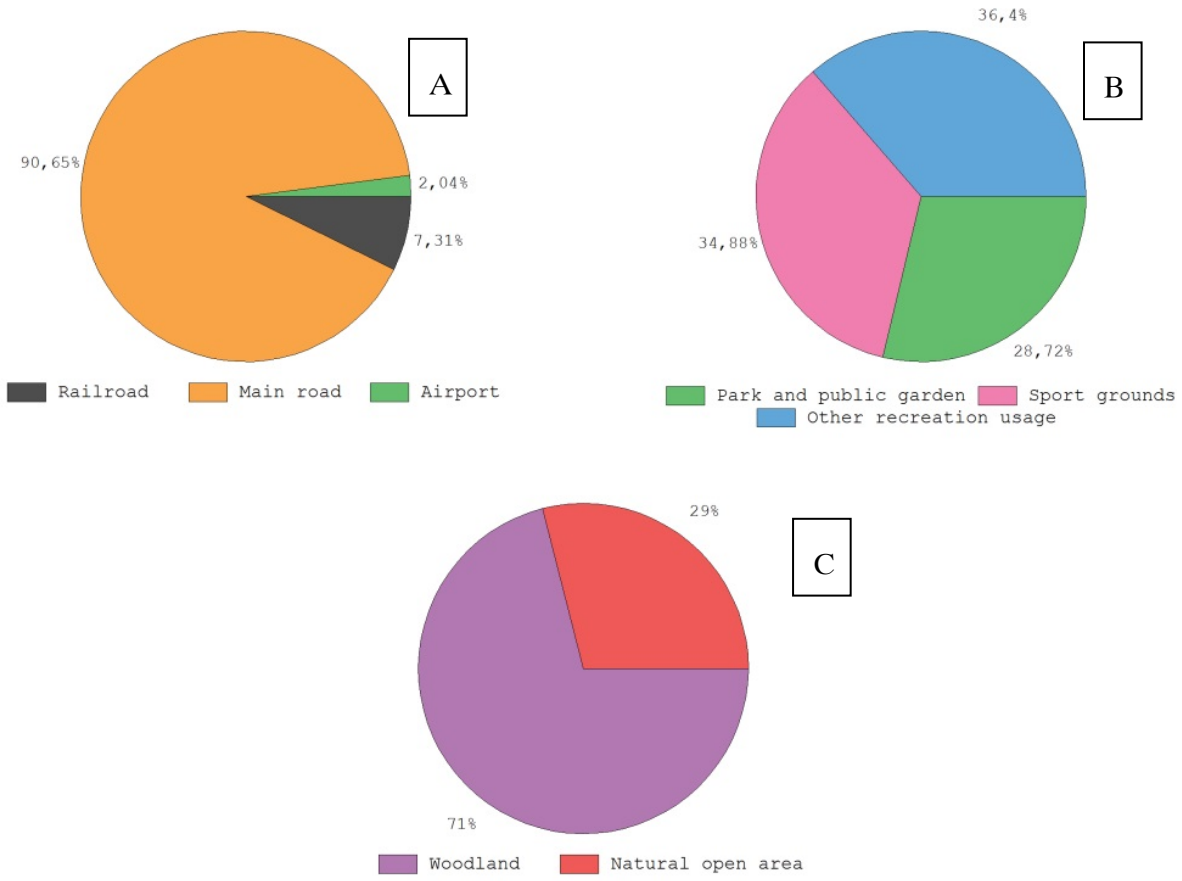

Figure 9: Division of land within the categories transport (A), recreation (B) and woodland & nature (C) in NL as of 2010 (data obtained from[81]).

4.1.3 Agriculture

The largest area in The Netherlands is used for agricultural purposes, 22644 km^2 to be exact. Agriculture is economically very important to The Netherlands and total agricultural exports amount to 75 billion euros [89]. Agricultural land has the potential to create large quantities of supplementary biomass streams, however the availability of these residues is dependent upon food and fodder production. Surplus biomass can be generated in the fields (primary residues) or during processing(secondary residues). The quantity of primary residues depends upon the ratio of the crop yield to the total above ground phytomass, known as the harvest index. A low harvest index indicates large quantities of residue biomass. The potential amount of surplus biomass depends on the amount of area cultivated, the gross yield per hectare and the harvest index of the particular crop, as well as utilization for fertilizer and fodder. To further investigate the potential in The Netherlands, the agricultural data from 2014 and 2015 will be viewed in more depth.

4.2 Divisions of Agricultural Land Use

The division of agricultural lands gives information on the exact crops which are being cultivated as well as their potential supplementary biomass streams. Quantification of the land area helps to calculate the size of the waste stream. With this information, the potential for an energy stream and yield of biomass derived ash has more validity.

While agricultural land is generally associated with farming, not all agricultural land is used to cultivate biomass (i.e. plants and animals). Distinctions can be made between utilized agricultural

area and other land. Utilized agricultural area (UAA) is land that is permanently or temporarily part of a holding and is mainly used for the production of agricultural goods (crops, livestock), including fallow land and (temporary) grassland. UAA includes arable land, horticulture in the open, horticulture under glass, grassland, and green fodder crops. Other land refers to unutilized agricultural land, wooded area, and other land (e.g. buildings, farmyard, ponds, nature reserves). In 2014 there was a total of 20010 km2, 91.9% was UAA and 8.1% fell into others [81]. A breakdown of the 18390 km2 that is utilized can be seen in Figure 10.

The majority of agricultural land in The Netherlands is devoted to grasslands and forage plants; of the 12251 km^2 devoted to these functions 81.15% is occupied by grasslands and 18.85% is occupied by forage plants [89]. Grass is the most significant crop in The Netherlands because it is used for dairy production (and to a lesser extent sheep, beef cattle and horses) [89]. The high output dairy system in The Netherlands places very specific demands on the land, namely the large production of high quality fodder. Output and input are directly related: the higher the output, the higher the required input (i.e. fodder, land). As dairy demand has increased, there has been a push towards sustainable intensification (eco-friendly farms) where yields increase with minimum use of resources and minimum effect on the environment. Any surplus of phytomass produced in the grasslands and forage plants is either stored in bales or sent to drying plants. This allows for a stockpile of fodder which can be used in subsequent seasons [89]. As a result, there is no phytomass remaining which can be used in the production of energy.

Next to grassland and forage plants, arable land comprises the largest agricultural land area, specifically 5173 km^2. Arable crops take up a significant area and produce surplus biomass. Horticulture in the open includes 871 km^2 and is devoted to vegetables, flower bulbs, fruit, nurseries and perennial plants, and floricultural crops. Horticulture under glass covers 94 km^2 and is utilized for vegetables, floricultural crops, nurseries and perennial plants, and fruit [81] . These two only comprise a small fraction of the utilized agricultural land.

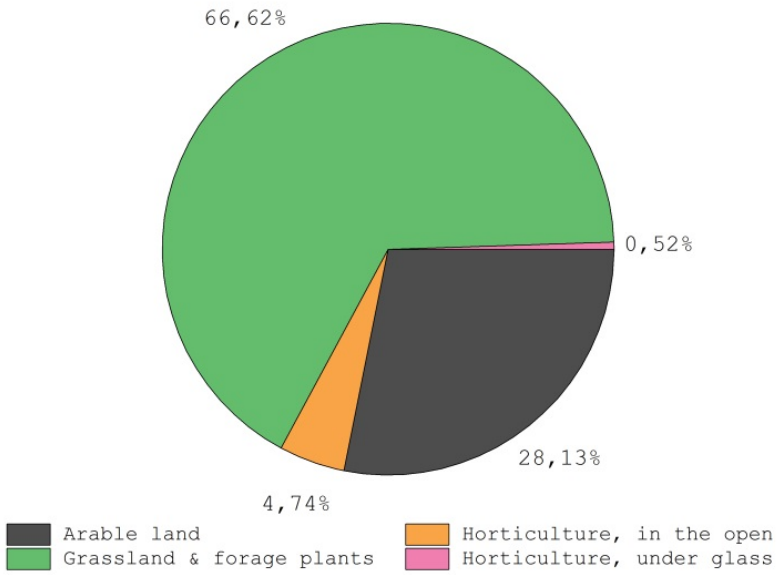

Figure 10: Division of utilized agricultural area (UAA) in The Netherlands in 2014 (data obtained from[81]).

4.2.1 Agricultural Production and Residues

For the arable crops, there is data available from 2015. The arable crops in The Netherlands in 2015 were divided in to the following groups (and subgroups): wheat, barley, other cereals (rye, oats, triticale), green fodder crops (grain maize, green maize, corn cob mix), pulses (red kidney beans), industrial crops (rape, fibre flax, linseed, chicory for inulin, hemp), potatoes, beets, seed onions. A breakdown of the specific area that each of these crops occupies can be seen in Figure 11.

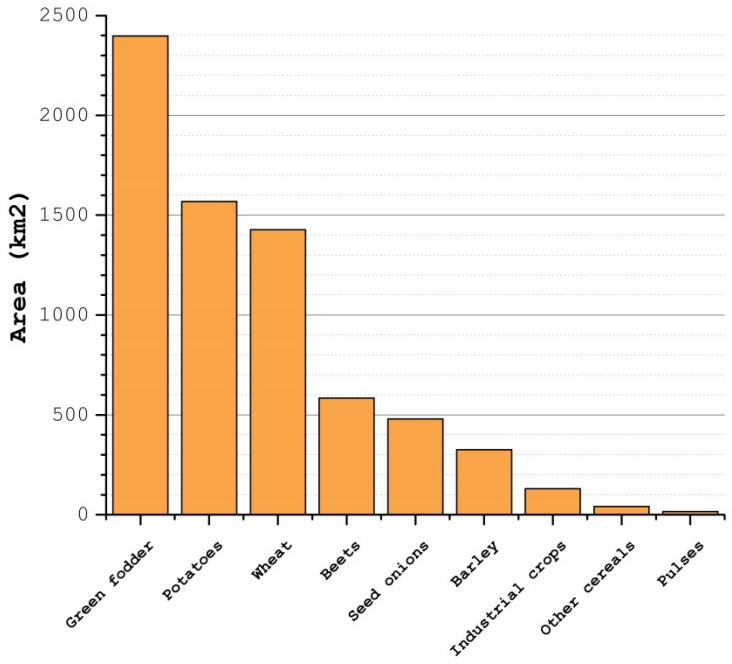

Figure 11: Distribution of the specific area that arable crops (green fodder, potatoes, wheat, beets, seed onions, barley, industrial crops other cereals and pulses) occupy (data obtained from[81]).

The edible portions of biomass (i.e. food, fibre and animal feed) comprise a small fraction of the harvested agricultural phytomass. Crop residues constitute a larger portion of the annually harvested phytomass [90] but limited statistics exist on their quantities and destinies. However, using data on crop yields, cultivated area and harvest intensity, it is possible to calculate the available crop residues. The harvest index is an agricultural value used to quantify the yield of a crop species versus the total amount of biomass produced. Or rather the harvest index is the ratio of yield to total plant biomass. Harvest index varies by crop species and characteristics averages and documented for different crops. Quantities of biomass residues in The Netherlands in 2015 can be seen in Table 2. Estimating residual biomass quantities is a complex exercise, relying on a number of assumptions and thus results should be taken as approximations.

From this data, it is clear that large quantities of crop residues are produced in the harvesting of seed onions and green fodder. However, potatoes, beets, wheat and industrial crops also offer relevant quantities. The combined potential of these biomass waste stream is encouraging in the argument for their combustion as an energy source and the utilization of the derived ashes as a ternary product.

Table 2: Calculated crop residues for the arable crops in The Netherlands based on the crop yield (CY) and harvest index (HI) and the amount of resulting ash (assuming an average ash content of 9.35% for agricultural and horticultural waste [91].

	CY [ton]	(HI)	Crop residue [ton]	Ash [ton]
Green fodder	1500.5	0.52	1385.1	129.5
Potatoes	706.1	0.82	155.0	14.5
Beets	478.5	0.50	478.5	44.5
Seed onions	270.7	0.08	3113.1	291.1
Wheat	141.3	0.55	115.6	10.8
Industrial crops	78.5	0.20	314.0	29.4
Barley	52.7	0.55	43.1	4.0
Other cereals	7.4	0.55	6.1	0.6
Pulses	0.6	0.25	1.8	0.2

5 CONCLUSIONS

- The global average gross CO_2 emissions per ton of clinker is over 850 kg. While the cement industry has made strides in reducing emissions, further actions still need to be taken to reduce the overall CO_2 production associated with clinker production to reach the Climate Change and Energy Sustainability target of the Europe 2020 program. Since the aim is to reduce greenhouse gas emissions to 20% lower than the levels in 1990, obtain 20% of energy from renewable resources, and increase energy efficiency by 20%, offsetting some of the 5-8% human atmospheric CO_2 emissions from clinker production while encouraging renewable energy would help to achieve that goal.
- Due to political, economic, and environmental incentives the utilization of biomass as an energy source is experiencing a renaissance in development. Today, biomass contributes more than 10-15% to the world energy supply.
- Numerous biomass waste streams are available in The Netherlands specifically, which have the potential to act as a source of energy and thereby potentially produce a valuable ash which can function as a binder in construction applications. In particular verge grass, forestry thinnings and agricultural wastes deserve further investigation into their suitability as an energy source and a valuable ash.
- The production of energy from biomass results in biomass derived ash which has the potential to be used as a valuable raw material for industrial purposes, including clinker production. The chemical and mineralogical composition and physical characteristics of the derived ash are decisive for where and how these ashes can be best used and will be further characterized and better understood.

6 REFERENCES

1. Taylor, M., C. Tam, and D. Gielen, *Energy efficiency and CO2 emissions from the global cement industry.* Korea, 2006. **50**(2.2): p. 61.7.
2. Oss, H.G.v., *US Geological Survey (USGS) Cement - 2007.*
3. Worrell, E., et al., *Carbon dioxide emissions from the global cement industry.* Annual Review of Energy and the Environment, 2001. **26**: p. 303-329.
4. WBCSD/IEA, *Cement Technology Roadmap 2009-Carbon emissions reductions up to 2050, in, International Energy Agency [IEA].* World Business Council for Sustainable Development [WBCSD], Paris, France, 2009.
5. Taylor, H.F.W., *Cement chemistry*. 1997: Thomas Telford Services Ltd.
6. Initiative, C.S., *Cement industry energy and CO2 performance: getting the numbers right*. 2009, Geneva: World Business Council for Sustainable Development.
7. Scrivener, K.L. and R.J. Kirkpatrick, *Innovation in use and research on cementitious material.* Cement and Concrete Research, 2008. **38**(2): p. 128-136.
8. Hendriks, C.A., et al. *Emission reduction of greenhouse gases from the cement industry.* in *Proceedings of the Fourth International Conference on Greenhouse Gas Control Technologies*. 1998.
9. Gartner, E., *Industrially interesting approaches to "low-CO2" cements.* Cement and Concrete Research, 2004. **34**(9): p. 1489-1498.
10. Worrell, E., et al. *International comparison of energy efficiency improvement in the cement industry.* in *proceedings ACEEE*. 1995.
11. Dunstetter, F., M.N. de Noirfontaine, and M. Courtial, *Polymorphism of tricalcium silicate, the major compound of Portland cement clinker: 1. Structural data: review and unified analysis.* Cement and Concrete Research, 2006. **36**(1): p. 39-53.
12. Hewlett, P.C., *Lea's chemistry of cement and concrete*. 2004: A Butterworth-Heinemann Title.
13. Maki, I. and S. Chromý, *Microscopic study on the polymorphism of Ca 3 SiO 5.* Cement and Concrete Research, 1978. **8**(4): p. 407-414.
14. Peterson, V.K., *A Rietveld refinement investigation of a Mg-stabilized triclinic tricalcium silicate using synchrotron X-ray powder diffraction data.* Powder Diffraction, 2004. **19**(04): p. 356-358.
15. Stephan, D. and S. Wistuba, *Crystal structure refinement and hydration behaviour of 3CaO· SiO 2 solid solutions with MgO, Al 2 O 3 and Fe 2 O 3.* Journal of the European Ceramic Society, 2006. **26**(1): p. 141-148.
16. Woermann, E., W. Eysel, and T. Hahn, *Chemical and structual investigations of solid solutions of tricalcium silicate.* Zement-Kalk-Gips, 1968.
17. Neubauer, J., *Quantitative röntgenographische Phasenanalyse an Portlandzementklinkern: Grundlagen und Anwendung*. 1998.
18. Stanek, T. and P. Sulovsky, *The influence of the alite polymorphism on the strength of the Portland cement.* Cement and Concrete Research, 2002. **32**(7): p. 1169-1175.
19. Harada, M.O. and S. Takagi, *Effect of Polymorphism of Tricalcium Silicate on Structure and Strength Characteristics of Hardened Cement Paste.* Rev. Gen. Meet., Tech. Sess.–Cem. Assoc. Jpn, 1977. **31**: p. 31-33.
20. Mascolo, G., et al., *Influence of polymorphism and stabilizing ions on the strength of alite.* Journal of the American Ceramic Society, 1973. **56**(4): p. 222-223.
21. Bigare, M., et al., *Polymorphism of tricalcium silicate and its solid solutions.* Journal of the American Ceramic Society, 1967. **50**(11): p. 609-619.

22. Guinier, A. and M. Regourd. *Structure of Portland cement minerals*. in *Proceedings of the 5th International Symposium on the Chemistry of Cement*. 1968. Tokyo, Japan.

23. Stutzman, P.E., *Guide for X-ray powder diffraction analysis of Portland cement and clinker*. 1996: US Department of Commerce, Technology Administration, National Institute of Standards and Technology, Office of Applied Economics, Building and Fire Research Laboratory.

24. Kristmann, M., *Portland cement clinker: Mineralogical and chemical investigations: Part I Microscopy, X-ray fluorescence and X-ray diffraction.* Cement and Concrete Research, 1977. **7**(6): p. 649-658.

25. Bredig, M.A., *Polymorphism of Calcium Orthosilicate.* Journal of the American Ceramic Society, 1950. **33**(6): p. 188-192.

26. Barbier, J. and B. Hyde, *The structures of the polymorphs of dicalcium silicate, Ca2SiO4.* Acta Crystallographica Section B: Structural Science, 1985. **41**(6): p. 383-390.

27. Jost, K., B. Ziemer, and R. Seydel, *Redetermination of the structure of-dicalcium silicate.* Acta Crystallographica Section B: Structural Crystallography and Crystal Chemistry, 1977. **33**(6): p. 1696-1700.

28. Mumme, W., et al., *Rietveld crystal structure refinements, crystal chemistry and calculated powder diffraction data for the polymorphs of dicalcium silicate and related phases.* Neues Jahrb. Mineral. Abh, 1995. **169**: p. 35-68.

29. Lehmann, H., K. Niesei, and P. Thormann, *The stability ranges of the dicalcium silicates.* Tonindustrie Zeitung, 1969. **93**(6): p. 197-209.

30. Pimraksa, K., S. Hanjitsuwan, and P. Chindaprasirt, *Synthesis of belite cement from lignite fly ash.* Ceramics International, 2009. **35**(6): p. 2415-2425.

31. Smith, D.K., A. Majumdar, and F. Ordway, *The crystal structure of γ-dicalcium silicate.* Acta Crystallographica, 1965. **18**(4): p. 787-795.

32. Zhao, M. *Quantitative Control of C2S Crystal Transformation*. in *Applied Mechanics and Materials*. 2012. Trans Tech Publ.

33. Odler, I., *Special inorganic cements, modern concrete technology, series 8.* E & Fn Spon, New York, 2000.

34. Chan, C.J., W.M. Kriven, and J.F. Young, *Physical stabilization of the $\beta \rightarrow \gamma$ transformation in dicalcium silicate.* Journal of the American Ceramic Society, 1992. **75**(6): p. 1621-1627.

35. Bensted, J., *δ-dicalcium silicate and its hydraulicity.* Cement and Concrete Research, 1978. **8**(1): p. 73-76.

36. Popescu, C.D., M. Muntean, and J.H. Sharp, *Industrial trial production of low energy belite cement.* Cement and Concrete Composites, 2003. **25**(7): p. 689-693.

37. Jost, K.H., et al., *Phasenbestand und Hydraulische Aktivität von Belitklinkern.* Silikattechnik, 1985. **36**(12).

38. Yannaquis, N. and A. Guinier, *The polymorphic $\beta \rightarrow \gamma$ transformation of calcium orthosilicate.* Bull. Soc. Fr. Mineral. Crystallogr., 1959. **82**: p. 126-136.

39. Benarchid, M.Y., et al., *Hydration of iron–phosphorus doped dicalcium silicate phase.* Materials Chemistry and Physics, 2005. **94**(2): p. 190-194.

40. Matković, B., et al., *Phases in the System Ba2SiO4 - Ca2SiO4.* Journal of the American Ceramic Society, 1986. **69**(2): p. 132-134.

41. Lai, G.-C., T. Nojiri, and K.-i. Nakano, *Studies of the stability of β-Ca 2 SiO 4 doped by minor ions.* Cement and Concrete Research, 1992. **22**(5): p. 743-754.

42. Wesselsky, A. and O.M. Jensen, *Synthesis of pure Portland cement phases.* Cement and Concrete Research, 2009. **39**(11): p. 973-980.

43. Ghosh, S., *Cement and Concrete Science and Technology*. Vol. 1. 1991: Thomas Telford.

44. Eysel, W. and T. Hahn, *Polymorphism and solid solution of Ca2GeO4 and Ca2SiO4.* Zeitschrift für Kristallographie-Crystalline Materials, 1970. **131**(1-6): p. 322-341.

45. Midgley, H., *A compilation of X-ray powder diffraction data of cement minerals*.* Magazine of Concrete Research, 1957. **9**(25): p. 17-24.

46. Stark, J., et al., *Existence conditions of hydraulically active belite cement*. 1981, Zement-Kalk-Gips.

47. Regourd, M. and A. Guinier, *Cristallochimie des constituants du clinker de ciment Portland.* Revue des matériaux de construction, 1975(695).

48. Bogue, R.H., *The Chemistry of Portland Cement*. 2nd ed. 1955, New York: Reinhold Publishing Corporation.

49. Boughanmi, S., et al., *Does phosphorus affect the industrial Portland cement reactivity?* Construction and Building Materials, 2018. **188**: p. 599-606.

50. Peray, K.E. and J.J. Waddell, *The rotary cement kiln*. 1986: Edward Arnold.

51. Taylor, J.R. and A.T. Dinsdale, *Thermodynamic and phase diagram data for the CaO-SiO2 system.* Calphad, 1990. **14**(1): p. 71-88.

52. Calarco, V., *Coal's long term future in world energy.* 1992.

53. Demirbaş, A., *Calculation of higher heating values of biomass fuels.* Fuel, 1997. **76**(5): p. 431-434.

54. Unruh, G.C., *Understanding carbon lock-in.* Energy Policy, 2000. **28**(12): p. 817-830.

55. Negro, S.O., R.A.A. Suurs, and M.P. Hekkert, *The bumpy road of biomass gasification in The Netherlands: Explaining the rise and fall of an emerging innovation system.* Technological Forecasting and Social Change, 2008. **75**(1): p. 57-77.

56. Haas, R., et al., *A historical review of promotion strategies for electricity from renewable energy sources in EU countries.* Renewable and sustainable energy reviews, 2011. **15**(2): p. 1003-1034.

57. Heidenreich, S. and P.U. Foscolo, *New concepts in biomass gasification.* Progress in Energy and Combustion Science, 2015. **46**: p. 72-95.

58. Faaij, A., et al., *Externalities of biomass based electricity production compared with power generation from coal in The Netherlands.* Biomass and Bioenergy, 1998. **14**(2): p. 125-147.

59. Koppejan, J. and S. Van Loo, *The handbook of biomass combustion and co-firing*. 2012: Routledge.

60. Hoogwijk, M., et al., *Exploration of the ranges of the global potential of biomass for energy.* Biomass and Bioenergy, 2003. **25**(2): p. 119-133.

61. Spliethoff, H. and K.R.G. Hein, *Effect of co-combustion of biomass on emissions in pulverized fuel furnaces.* Fuel Processing Technology, 1998. **54**(1–3): p. 189-205.

62. Khan, A.A., et al., *Biomass combustion in fluidized bed boilers: Potential problems and remedies.* Fuel Processing Technology, 2009. **90**(1): p. 21-50.

63. Stassen, I.H.E.M., *Biogas and biomass technology: Energy generation from biomass and waste in the Netherlands.* Renewable Energy, 1994. **5**(5–8): p. 819-823.

64. Knoef, H.A.M. and H.E.M. Stassen, *Energy generation from biomass and waste in The Netherlands: A brief overview and perspective.* Renewable Energy, 1995. **6**(3): p. 329-334.

65. McKendry, P., *Energy production from biomass (part 3): gasification technologies.* Bioresource technology, 2002. **83**(1): p. 55-63.

66. Rajamma, R., et al., *Characterisation and use of biomass fly ash in cement-based materials.* Journal of Hazardous Materials, 2009. **172**(2): p. 1049-1060.

67. Pels, J.R., D.S. de Nie, and J.H. Kiel. *Utilization of ashes from biomass combustion and gasification*. in *14th European Biomass Conference & Exhibition*. 2005.

68. James, A., et al., *Ash management review—applications of biomass bottom ash.* Energies, 2012. **5**(10): p. 3856-3873.

69. Saidur, R., et al., *A review on biomass as a fuel for boilers.* Renewable and Sustainable Energy Reviews, 2011. **15**(5): p. 2262-2289.

70. Van Loo, S. and J. Koppejan, *Biomass combustion and co-firing.* Earthscan, London/Sterling, 2008.

71. Van Eijk, R., I. Obernberger, and K. Supancic. *Options for increased utilization of ash from biomass combustion and co-firing.* in *IEA bioenergy task*. 2012.

72. Olanders, B. and B.-M. Steenari, *Characterization of ashes from wood and straw.* Biomass and Bioenergy, 1995. **8**(2): p. 105-115.

73. Zevenhoven-Onderwater, M., *Ash-forming matter in biomass fuels*. 2001: Åbo Akademi Åbo/Turku, Finland.

74. Werkelin, J., et al., *Chemical forms of ash-forming elements in woody biomass fuels.* Fuel, 2010. **89**(2): p. 481-493.

75. Tumuluru, J.S., et al. *A review on biomass classification and composition, co-firing issues and pretreatment methods*. in *Proceedings of the American Society of Agricultural and Biological Engineers Annual International Meeting*. 2011. Citeseer.

76. Han, J., et al., *Fluidized bed combustion of some woody biomass fuels.* Energy Sources, Part A: Recovery, Utilization and Environmental Effects, 2008. **30**(19): p. 1820-1829.

77. Dahl, O., et al., *Comparison of the characteristics of bottom ash and fly ash from a medium-size (32 MW) municipal district heating plant incinerating forest residues and peat in a fluidized-bed boiler.* Fuel Processing Technology, 2009. **90**(7–8): p. 871-878.

78. Faaij, A., et al., *Exploration of the land potential for the production of biomass for energy in The Netherlands.* Biomass and Bioenergy, 1998. **14**(5–6): p. 439-456.

79. Rabou, L., et al., *Biomass in the Dutch energy infrastructure in 2030*. 2006, Wageningen UR.

80. Nations, U., *System of Environmental-Economic Accounting 2012*. 2014, The World Bank.

81. Netherlands, S. *CBS statline*. Accessed online, April 4th 2008 [cited 2014 January]; Available from: https://www.cbs.nl/en-gb.

82. Johansson, T.B., et al., *Renewable fuels and electricity for a growing world economy: defining and achieving the potential.* Renewable Energy. Sources for Fuels and Electricity. Island Press, Washington DC, 1993.

83. Williams, R., *Variants of a low CO2-emitting energy supply system (LESS) for the world-prepared for the IPCC Second Assessment Report Working Group IIa.* Pacific Northwest Laboratories, 1995. **39**.

84. Faaij, A., et al., *Gasification of biomass wastes and residues for electricity production.* Biomass and Bioenergy, 1997. **12**(6): p. 387-407.

85. Yamamoto, H., J. Fujino, and K. Yamaji, *Evaluation of bioenergy potential with a multi-regional global-land-use-and-energy model.* Biomass and Bioenergy, 2001. **21**(3): p. 185-203.

86. Yamamoto, H., K. Yamaji, and J. Fujino, *Evaluation of bioenergy resources with a global land use and energy model formulated with SD technique.* Applied Energy, 1999. **63**(2): p. 101-113.

87. Hall, D.O., *Biomass energy in industrialised countries—a view of the future.* Forest Ecology and Management, 1997. **91**(1): p. 17-45.

88. Voinov, A., et al., *Estimating the potential of roadside vegetation for bioenergy production.* Journal of Cleaner Production, 2015.

89. Dijk, H.v., et al. *Fifty years of forage supply on dairy farms in The Netherlands.* in *Grassland and forages in high output dairy farming systems. Proceedings of the 18th Symposium of the European Grassland Federation, Wageningen, The Netherlands, 15-17 June 2015.* 2015. Wageningen Academic Publishers.

90. Smil, V., *Crop Residues: Agriculture's Largest Harvest Crop residues incorporate more than half of the world's agricultural phytomass.* Bioscience, 1999. **49**(4): p. 299-308.

91. Phyllis, E., *Database for biomass and waste.* Energy Research Centre of The Netherlands, 2012.

CHAPTER 3

CHARACTERIZATION OF CURRENTLY AVAILABLE BIOMASS DERIVED ASHES FOR APPLICATION AS A CEMENT REPLACEMENT

ABSTRACT

Biomass combustion has longer served as a source of energy and due to environmental concerns, its utilization is on the rise. The global combustion of biomass results in ash which is projected to reach 476 million tonnes annually. Currently there are limited applications for these biomass-derived ashes. A better understanding of the ash properties as well as the effects of biomass source and conversion technology on those ash properties is needed to ascertain applications.

This work identifies biomass derived ashes featuring hydraulic properties, or alternatively, those which can potentially be further processed to yield hydraulic minerals. The investigation focused on data from the Phyllis 2 database, the ALLASKA database, and experimentally derived results: commonalities were found between the ashes analysed in the lab and the conclusions drawn from the databases. To judge the potential suitability of an ash, the composition (both chemical and mineralogical) and physical properties (particle size and distribution) were evaluated based on the original biomass source and the implemented conversion technology. The objective of this study was to identify calcium and silicon rich biomass ashes that could potentially contain calcium silicate based hydraulic minerals or have the chemical composition necessary to form them. Thus, ashes were sought with CaO concentrations of 61-69M.-% and SiO_2 concentrations of 15-20M.-%.

Organic residues and contaminated biomass (OR-CB) and herbaceous and agricultural biomass (HAB) were found to contain SiO_2 with averages of 29.3 and 42.2 M.-% respectively. CaO was more difficult to find in abundance but wood and woody biomass (WWB) showed a concentration up to 65.0 M.-% and an average of 39.8 M.-%. The subcategories of bark and hardwood were rich in CaO with averages of 39.8 and 34.5 M.-% respectively. Ashes derived from the OR-CB category paper sludge showed the potential to provide both CaO and SiO_2 in the necessary quantises to either contain clinker minerals or potentially form them. The type of combustion technique used impacts the ash quality. circulating fluidized beds and bubbling fluidized beds where shown to produce ashes that on average have higher contents of these CaO and SiO_2.

1 INTRODUCTION

Biomass' stake in the production of energy has been on the rise in recent decades. In a recent study, it was estimated that biomass provides about 8% of the world energy supply for heat, electricity and transportation fuels. Predictions assert that biomass use could grow to 33-50% by 2050. Of the total biomass derived energy, 95-98% stems from direct combustion[1]. The production of energy from biomass also means the production of ash. If the biomass derived energy were to grow to the predicted range, approximately 476 million tonnes of biomass ash would be produced annually (assuming 7 billion tonnes of biomass combusted with a 6.8% ash yield). The substitution of coal with biomass in energy production has positive environmental impacts [2] but possibly negative impacts for the cement and concrete industry and therefore a few challenges must be addressed; namely the replacement of coal-derived fly ashes now suitable for the cement and concrete industry for biomass derived ashes with at least similar performance characteristics and quantitative ordinary Portland cement replacement potential.

At the moment, there are few available applications for biomass derived ashes. While this is a minor problem given the small quantities currently produced, it will only grow in the future as more biomass is combusted. By comparison, coal-derived fly ash has been suitable to replace part of ordinary Portland cement (OPC) in concrete applications for decades. Coal-derived fly ash is allowed to be incorporated into concrete as dictated by the EN-450 European standard. Under this standard, acceptable compositions are made explicit, resulting in the limitation of usable fly ash to those derived from solely coal combustion or co-combustion of coal and biomass with biomass being capped at 40 M.-% or 50 M.-% if the biomass is only green wood. Co-combustion at these percentages result in a fly ash whose properties and composition are heavily dominated by coal-ash; the maximum proportion of ash derived from the co-combustion material (i.e. biomass) cannot 30 M.-%. As such, the fly ash is safe to use under the same application as a pure coal fly ash. Biomass that is heavily contaminated or has a high ash content has the ability to produce a greater impact on the resulting ash which is why the only 40 M.-% of biomass is tolerated. Currently there is no acceptance of pure biomass derived ash in blended cements under the European standards.

When used to partially replace cement, coal-derived fly ash has the advantage of conserving energy, resources, and cost while at the same time potentially improving the durability of the resulting concrete [3]. The recent growth of biomass utilization for energy production has raised interest on biomass ash residue and its utilization in cement and concrete applications. Regarding composition, biomass derived ash can differ from coal-derived ash particularly in the high content of alkali metals and chlorides. These elements make biomass ash less attractive for cement applications due to the durability decreasing effects they can promote in concrete.

Although not acceptable according to EN-450, researchers have investigated the utilization of pure biomass derived ash for its suitability to partial replace cement in concrete applications. A few particular biomass ashes have been found to be advantageous as partial cement replacement in concrete. One such ash is rice husk ash, which due to its high contents of amorphous silica has the ability to improve the strength and durability of concrete due to its pozzolanic reactivity [4-10]. It has been found that when rice husk ash with a particle size of 6-10 μm is used to replace 10 M.-% of OPC, a concrete with a stronger interfacial transition zone and a lower permeability (more dense microstructure) is formed [4, 11]. Rice husk ash is produced predominantly in south east Asia, where agricultural waste (particularly the rice husks) in the production of rice is burnt in open fields. This method of combustion gives little control over the combustion efficiency and as such not all ashes are advantageous. A similar agricultural waste is sugar cane bagasse ash. Produced primarily in South America, the ash is created when the waste from the sugar cane bagasse is combusted to provide heat and power for the processing of the sugar cane [12-15]. Due to the more controlled combustion conditions, a higher level of consistency is reached with the ash. It has been found that replacing 20% of OPC with sugar cane bagasse ash improves the early strength as well as increases density of the

concrete microstructure which results in reduced water permeability and chloride penetration [16] [17].

In addition to specific biomass types, different biomass sources can be combined before combustion to produce a specifically functional ash. In Thailand, large quantities of both sugar and rice are produced each year. These crops result in the annual production of roughly 66 million tonnes of sugarcane bagasse and 10 million tons of rice husk. A combination of 82.5% bagasse, 15% rice husk, and 2.5% chop wood are combusted in small power plants to produce electricity for the sugar mills. Most of the bagasse-rice-husk-wood ash is disposed of through landfilling which results in environmental problems [3], however these ashes can also be incorporated into concrete mixtures to solve the disposal problem and also provide advantages to the concrete mixture [18].

In addition to these agricultural waste crops, research has been conducted on the application of woody biomass derived ash as a cement replacement. Unlike rice husk ash and sugar cane bagasse ash, the incorporation of wood ash as a partial cement replacement has been found on average to reduce the compressive, flexural, and tensile strength of concrete. When the SiO_2 content within the ash is high enough, strength increases with longer hydration times [19]. Rajamma et al. [20] found that although the replacement of OPC with 10% wood ash could produce a mortar with acceptable strength properties, the chemical and physical properties of woody ash vary so greatly that their effect cannot be predicted. In order to understand and predict how a cement and biomass derived mixture will behave during hydration and perform as concrete, more must be known about the particular ash being utilized. Thus, such broad generalizations on the effects of woody ash have no validity since they are not applicable for all scenarios.

The objective of the study described in this chapter is the identification of biomass derived ash with hydraulic properties or routes to obtain hydraulic properties from biomass derived ash. These ashes will be assessed on their ability to act as a cement replacement or raw material replacement based on their composition (both chemical and mineralogical) physical properties (particle size and distribution). These properties will be examined as a result of the original biomass source and the implemented conversion technology. This investigation will cover the current ash production chain from biomass selection through combustion technology. Parameters (such as the input biomass and conversion technology) which presumably have an advantageous influence on the biomass ash composition will be identified and the extent to which they can be manipulated in order to obtain an ash with high potential for application to (partial) replace cement will be assessed. The investigation will be divided into three different sections based on distinct sources of information; the Phyllis 2 database, the ALLASKA database, and experimentally derived results.

The first section will review the Phyllis 2 database [21] as an exploration of currently available biomass streams. The objective of this section is to better understand the effects of the biomass species on the chemical and physical properties of the derived ash. The chemical analysis will focus on those oxides which are of particular concern to clinker production: namely CaO, SiO_2 Al_2O_3 and Fe_2O_3. The presence of Al_2O_3 and Fe_2O_3 is significantly less critical than CaO and SiO_2 since hydration characteristics of the clinker minerals they form (C_3A and C_4AF) are significantly lower. Additionally, the oxide concentrations will be visualized as ternary diagrams to map the relative concentrations and observe trends per species. A traditional ternary diagram for cement chemistry with the corners represented by CaO, SiO_2 and Al_2O_3 + Fe_2O_3 will be evaluated. However, since biomass derived ashes have a more variable composition than limestone and clay the ternary diagram will be expanded and modified. Based on the ASTM specification C-618 for the identification of different classes of fly ash (C vs. F) a ternary diagram with one of the three glass science categories: glass formers (SiO_2 + Al_2O_3 + Fe_2O_3), alkali modifiers (Na_2O + K_2O) and alkali-earth (CaO + MgO), representing each of the corners will be depicted [22]. The alkali-earth oxides are grouped together because not only does MgO act as a stabilizing agent in alite but can also act as a replacement for CaO. Mg^{2+} is known to substitute directly for Ca^{2+} in the C_3S lattice due to the similarity in their ionic radii [23]. The atomic

radii and the preferred coordination determine the type of substitution. While alkali modifiers are typically not present in clinker raw materials they tend to be present in biomass derived ashes. Since these oxides can have a negative impact on clinker formation, the concentrations of Na_2O and K_2O are important to note. Lastly this section will review biomass properties that are critical for conversion, namely the ash content (A) the moisture content (MC) and the higher heating value (HHV), as they relate to the biomass source. The HHV signifies the amount of heat released during the combustion of a specified amount of biomass. This section will evaluate the potential suitability of an ash to act as a potential precursor for clinker minerals based on trends in chemical and physical properties for different biomasses sources.

The second section will include a review of the ALLASKA database [24] with respect to the oxide composition of biomass derived ashes (CaO, SiO_2, Al_2O_3, Fe_2O_3, Na_2O, K_2O, Cl, S and P_2O_5) and how they relate to the thermo-conversion technology and parameters (information not contained within the ALLASKA database. The third section covers an experimental investigation, which was part of this study, in which the chemical composition, mineral composition and particle size distribution for various biomass derived ashes was determined with respect to biomass source and applied conversion technology. These are the ashes which are available for subsequent application in the following chapters. The ashes will be evaluated as to how they compare to the data obtained from the Phyllis 2 and ALLASKA databases and based on the information gathered specific ashes will be selected for later research.

The data obtained from the three sections will be evaluated in order to identify potential routes for the production of biomass derived ash featuring hydraulic properties, or alternatively, for the production of ashes which can potentially be further processed to yield hydraulic minerals which can be used as cement replacement. Here it is thus hypothesized that presence of specific oxides (specifically CaO and SiO_2) will potentially result in hydraulic properties of the ash. The quantities of these oxides are significant because that can indicate whether the clinker minerals are already present or if the ash has the potential for the production of clinker minerals if further thermally processed. Based on the comparison of the samples which have been experimentally characterized with the observations made from the two databases, ashes with the most potential for hydraulic properties will be selected for further investigation in subsequent chapters.

2 Materials and Methods

2.1 Sample Types and Origin

The investigations will be based on two existing databases as well as experimental work in the framework of this study on a variety of biomass derived ashes as detailed below.

2.1.1 Biomass Ash Data Derived from Databases

Developed within the PHYDADES European project [25], the Phyllis2 database is intended to provide the public with reliable information on biomass fuels and biomass ashes. The database contains almost 3000 data records of individual batches of biomass or waste materials and is accessible in three different classifications schemes. For the purpose of this investigation, the ECN Phyllis scheme was used. This scheme groups biomass batches into 16 different classes based on practicality and plant physiology. The classes are: algae, biochar, char, fossil fuel, grass/plant, husk/shell/pit, manure, non-organic residue, organic residue/product, others, municipal solid waste (MSW) and refuse derived fuel (RDF), sludge, straw (stalk/cob/ear), torrefied material, treated wood and untreated wood. For the sake of this study, algae, biochar, char, fossil fuel, manure, non-organic residue/product and others will be omitted since they do not fit into the confines of the investigation. The remaining nine classes can be categorized amongst three distinct categories: wood and woody

biomass (WWB), herbaceous and agricultural biomass (HAB) and organic residues and contaminated biomass (OR-CB). Segregation of the data into these categories allows for easier interpretation of the data and the ability to draw conclusions on the composition of biomass derived ashes based on biomass type. Due to a lack of information on the ashes within the category of torrefied material, this data will not be included in the WWB and HAB categories despite containing those biomass sources.

WWB will be limited to the class untreated wood. Untreated wood encompasses all fresh wood including park wood waste and wood from saw mills. Both hardwoods and softwoods are included in this category and within those two divisions, data from numerous individual tree species can be found (such as beech, birch, oak, pine, poplar and willow). This category also includes different tree parts, including bark, cork, leaves and needles. The biomass that comprises the HAB group is a little more diverse but similar in properties. HAB includes plants, grass, straw and some organic residues (namely residues from agriculture and horticulture as well as husk shells and pits). The group plants is composed of fruits, vegetables and flowers/garden plants. Grass encompasses verge grass, which is a mixture of different (unidentified) grass species as well as subgroups like hemp, jute and kenaf. While straw and grass are physiologically not very different, here straw is in reference to the dry stalks of cereal plants, after the grain and chaff have been removed; this includes wheat, barley, rice and maize. The OR-CB group is even more diverse. It includes many types of organic residues such as waste paper, residues from the food industry, and the organic fraction from domestic waste (all organic residue that is not a direct residue from agriculture and horticulture). This group also includes municipal solid waste (MSW) and refuse derived fuel (RDF). Furthermore, the data from sludge is included here; together sludge from sewage water treatment, sludge from the paper industry, waste water treatment, and sludge from the food processing industry. Lastly OR-CB includes treated wood, which contains composted wood, demolition wood, preserved wood and particle board.

The ALLASKA database was built under the ash program at Värmeforsk (Thermal Engineering Research Association) with the intention of promoting the environmentally responsible utilisation of ashes [24]. The database is a collection of quantitative information on the properties of residues from combustion processes in Swedish power plants. As an association for the energy, processing, and manufacturing industries, Värmeforsk's primary goal is to solve problems related to heat and power production. The ALLASKA database contains information on geotechnical data, leaching properties, chemical composition, particle size and organic contents of ash residues coming from the combustion of biomass and waste materials in different types of boilers. The results can be filtered according to different parameters such as fuel, ash types, and combustion systems. This section will evaluate biomass derived ashes based on the reactor in which they were generated, i.e. in a pulverised fuel reactor (PF), grate stoker furnace (GSF), circulating fluidized bed (CFB) or a bubbling fluidized bed (BFB). In this study, the ALLASKA database analysis was limited to biomass based fuels. The utilization of MSW, undefined industrial waste and coal fuels were therefore excluded from the database analysis of this study.

2.1.2 Biomass Derived Samples Experimentally Analysed in this Study

Additionally, ashes were provided by the Energy council of The Netherlands (ECN) for direct investigation. A variety of pure biomass-derived ashes were examined as well as a couple of ashes from co-combustion, one sewage sludge- and one municipal solid waste derived ash. A table with the biomass source as well as the known locations can be found in Table 3 where the samples are also divided into the same classification categories as from the databases. In this, both fly ashes and bottom ashes were examined. In addition to stemming from a variety of biomass streams and locations, these biomass types were converted in a variety of different installation types. A table containing the thermal conversion data can be found in Table 4.

Table 3: Original biomass source and harvest location prior to thermal conversion divided into the four categories wood and woody biomass (WWB), herbaceous and agricultural biomass (HAB) organic residues and contaminated biomass (OR-CB) and coal and co-combustion (COAL & CO).

		Biomass source	Harvest location
WWB	WBFA-1	Wood pellets	Canada/USA
	WBFA-2	Mixed clean biomass	The Netherlands
	WBFA-3	Clean wood	Unknown
	WBBA-1	Clean wood, beech	The Netherlands
	WBBA-2	Clean wood, beech	The Netherlands
HAB	HAFA-1	Wheat straw	Unknown
	HAFA-2	Wheat straw	Unknown
	HAFA-3	Rice straw	Unknown
	HAFA-4	Rice straw	Unknown
	HAFA-5	Mixed green waste	province Limburg (NL)
OR-CB	PSFA	De-inking sludge + demolition wood	Sweden
	PSBA	De-inking sludge + demolition wood	Sweden
	ORFA-1	Industry waste wood (sawmills and processing)	Finland
	ORFA-2	Sewage sludge	The Netherlands
	ORBA-3	Municipal solid waste	The Netherlands
COAL & CO	CFA-1	Coal	Unknown
	CFA-2	Co-fired (coal/woody biomass)	Canada/USA

Table 4: Information on the conversion parameters (Reactor, MW(th), and temperature) of the biomass derived ash analysed in this study. See Table 1 for type and source of respective ash samples.

		Ash Type	Reactor type	MW(th)	Location	Temp
WWB	WBFA-1	Fly ash	Pulverized Fuel combustion	180 MW	Gent	
	WBFA-2	Fly ash	Bubbling fluidized bed combustor	80 MW	Cuijk	650-900
	WBFA-3	Fly ash	Pulverized Fuel combustion	Unknown	Unknown	
	WBBA-1	Bottom ash (olivine bed material)	Lab scale Fluidized bed gasification	25 kW (th)	ECN, Petten	850
	WBBA-2	Bottom ash (olivine bed material)	Lab scale Fluidized bed gasification	25 kW (th)	ECN, Petten	850
HAB	HAFA-1	Fly ash	Bubbling fluidized bed combustor	lab-scale FB	ECN, Petten	750
	HAFA-2	Fly ash	Bubbling fluidized bed combustor	lab-scale FB	ECN, Petten	750-950
	HAFA-3	Fly ash	Bubbling fluidized bed combustor	lab-scale FB	ECN, Petten	750
	HAFA-4	Fly ash	Bubbling fluidized bed combustor	lab-scale FB	ECN, Petten	750-860
	HAFA-5	Fly ash	Unknown	10 MWth	Geleen	
OR-CB	PSFA	Fly ash mixed with air pollution control	Bubbling fluidized bed combustor	75 MW(fuel)	Sweden	850
	PSBA	Bottom ash	Bubbling fluidized bed combustor	75 MW(fuel)	Sweden	850
	ORFA-1	Fly ash	Integrated gasification and combustion system	lab-scale	Finland	
	ORFA-2	Fly ash	Fluidized bed	N.A.	Moerdijk	
	ORBA-3	Bottom ash	Grate stoker	unknown	Netherlands	
COAL	CFA-1	Fly ash	Pulverized Fuel combustion	690 MW	Mehrum	
& CO	CFA-2	Fly ash	Pulverized Fuel combustion	180 MW	Gent	

2.2 Methods of Chemical Analyses

The data from the two different databases was statistically analysed based on the aforementioned groups and their chemical compositions. Particular attention was given to the clinker mineral forming elements (Ca, Si, Al and Fe) and notice was taken of those which can have adverse effects on clinker production and cement hydration (alkalis and phosphorous). As this specific study fits into a larger research project aimed at replacing 100% Portland cement with biomass ash, the main objective was to find biomass-derived ashes that 1: feature hydraulic properties and can act directly as a clinker replacement or 2: have the necessary composition to act as a clinker raw material replacement. Therefore, the focus of this specific study was on calcium and silicon rich biomass ashes that could potentially contain calcium silicate based hydraulic minerals such as alite (C_3S) and belite (C_2S) or form them. Ashes were sought with CaO concentrations of 61-69M.-% and SiO_2 concentrations of 15-20M.-%.

The ashes obtained from samples analysed in this study were subjected to chemical and mineralogical analysis. X-ray fluorescence was used to determine the elemental composition using a Panalytical Epsilon 3XL XRF. The loss on ignition (LOI) was determined according to ASTM D 7348-08 using a one gram sample and 950°C. X-ray diffraction was performed on the ashes to obtain a qualitative mineralogical analysis of the crystalline phases using a Philips PW 3020 X'Pert Diffractometer. The

energy source was CoKα (1.789Å) and the tube settings were 45 kV and 30 mA. Step scans were performed from 5-70° 2θ at 0.03° 2θ steps and at a rate of 3.0 seconds per step. Diffraction patterns were analysed using Qual X software. The particle size and particle size distribution was measured using a laser beam particle size analyzer (Mastersizer S Ver. 2.19, Malvern Instruments Ltd., Malvern, U.K.). Particles between 0.1μm and 1000μm were measured as an aqueous suspension of dispersed particles passed through a laser beam and the angle of diffraction was measured.

3 RESULTS

3.1 Phyllis Database

3.1.1 Clinker Forming Oxides

To determine a relationship between element composition in the form of major element oxides present and the biomass source, data from the Phyllis database was first grouped into three distinct categories. Subsequently the concentrations of the 4 main clinker mineral forming oxides were examined per category. Figure 12 depicts the SiO_2 fractions for the averaged WWB, HAB and OR-CB categorized samples relative to one another.

In view of a composition that could either contain or produce clinker minerals, the SiO_2 fraction of the raw feed should be around 15-20M.-%. With respect to the previous, it appears that WWB falls short in terms of the theoretically favourable SiO_2 content showing a range of 0 to 57.2% with an average of 12.3 M.-%. In contrast, the SiO_2 content of the OR-CB samples fall within the theoretically favoured range, if not slightly above it with the middle 50% of samples having contents ranging from 22.5 to 39.7 M.-%. Although the standard deviation is large, the median content is at the upper limit (34.2 M.-%) and the lower quartile lies squarely in the theoretical optimum range. Close examination of sample sub-categories indicates that the composition range is populated by waste paper-, treated wood- and RDF + plastic derived ash samples. Paper sludge ash also resides partially in this region but also extends into higher contents. HAB samples show high SiO_2 contents with the standard deviation stretching from 0 to 95.6M.-%. The middle 50% of samples had contents ranging from 12.8 to 61.8M.-%. In order to draw conclusion on the potential applicability of HAB ash as a cement raw feed with regard to SiO_2 content, the sub-categories must be examined independently. As can be seen in Figure 13, a few sub-categories fall directly in the desired SiO_2 range, namely husk shell pits and agricultural residues.

With respect to CaO content, theoretical optimal content of biomass derived ashes should be in the range of 61-69M.-%. In Figure 14, it can be seen that the average CaO content in WWB (29.8M.-%) samples falls closest to what would be required of cement raw feed. There is, however, a large variability in this category and the CaO content of the lower 50% (1.3 to 28.8M.-%) does apparently not contain enough CaO to be of value as cement raw feed. In Figure 15 it can be seen that both bark and hardwoods feature the highest CaO content, close to the theoretically required content for clinker production. In the case of bark, 50% of the samples had a CaO content over 39.2 M.% and 25% of the samples had a content over 45.8 M.%. Considering the CaO content of the particular hardwoods, no clear trends could be identified. While samples of oak, poplar willow and birch ashes were all found amongst the 25% with the highest CaO content, they also amounted to the 25% with the lowest. There is no information as to which part of the trees the samples originated from and as a result, different tree sections could provide the explanation for the high distribution. Tropical hardwood and softwood derived ashes tend to have lower contents of CaO and as such appear not suitable for clinker production. Figure 14 also shows that the average CaO content in HAB (10.2 M.-%) ashes falls far below the theoretically required value. However, one specific sample derived from rape straw contained 66.0 M.% CaO and the next highest value (50.3 M.% CaO) also originated from rape straw. While rape straw could potentially provide enough CaO, the remaining biomass sources in the HAB

category cannot. OR-CB ashes also exhibited a low average CaO content (18.9M.-%). However, the variability in CaO content of OR-CB ashes appeared large, as reflected by a range of 0.2 to 60.4M% and a standard deviation of 13.3. Looking deeper at the individual sub-categories, OR-CB derived ashes show a specific trend (Figure 16). One waste paper ash and one treated wood sample ash were outliers and contained substantial CaO, however, all other samples in these two categories fell short of the desired 61-69% range. None of the RDF WSM or sewage sludge derived ashes contained quantities of CaO near the theoretically required amount. However, RDF mixed with plastic and paper sludge ashes did have a few samples with substantial CaO (albeit closer to 61%, the lower limit).

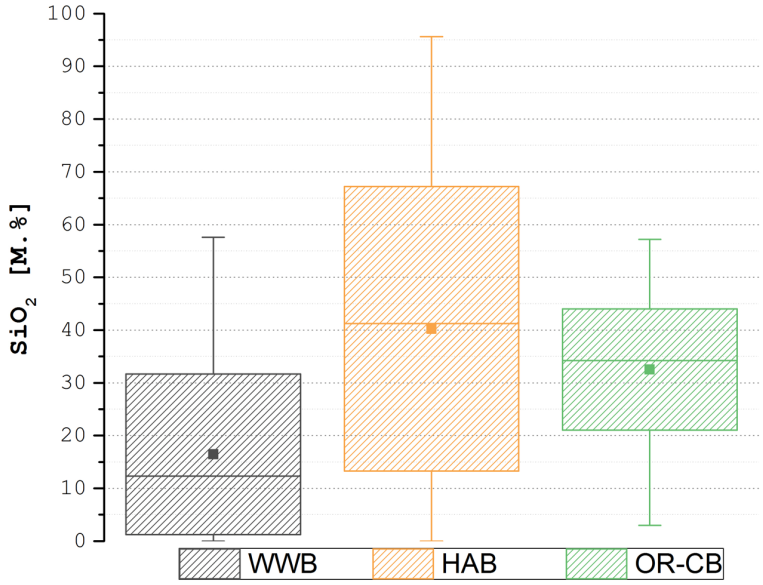

Figure 12: SiO_2 contents of biomass ash samples from the Phyllis database [21] for the categories wood and woody biomass (WWB), herbaceous and agricultural biomass (HAB) and organic residues and contaminated biomass (OR-CB). Target SiO_2 concentration is 15-20 M%.

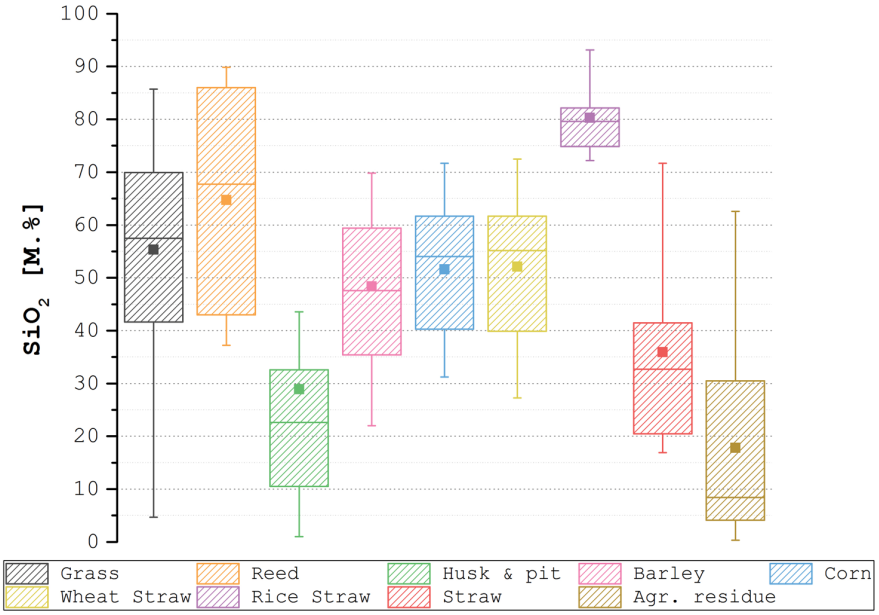

Figure 13: SiO_2 concentration within the herbaceous and agricultural biomass (HAB) sub-categories: grass, reed, husk & pit, barley, corn, wheat straw, rice straw, straw, and agricultural residues from the Phyllis database [21]. Target SiO2 concentration is 15-20 M%.

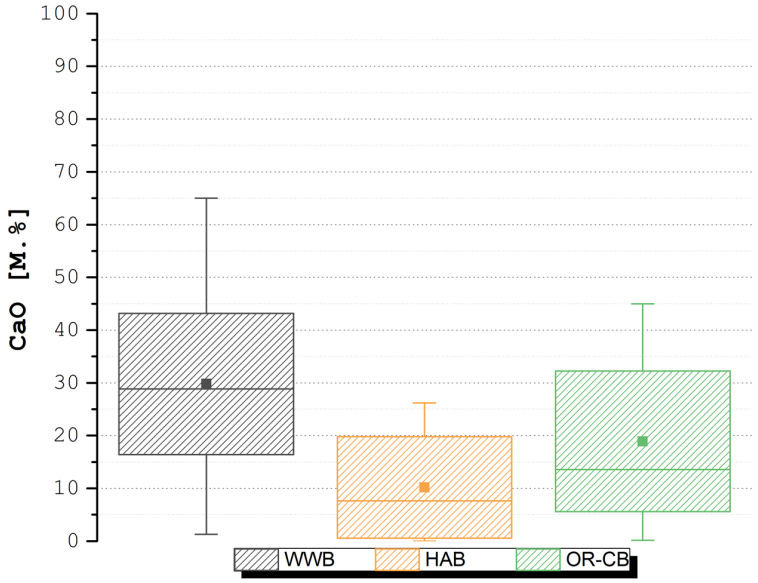

Figure 14: CaO concentration of biomass ash samples from the Phyllis database [21] for the categories wood and woody biomass (WWB), herbaceous and agricultural biomass (HAB) and organic residues and contaminated biomass (OR-CB). Target CaO concentration is 61-69 M%.

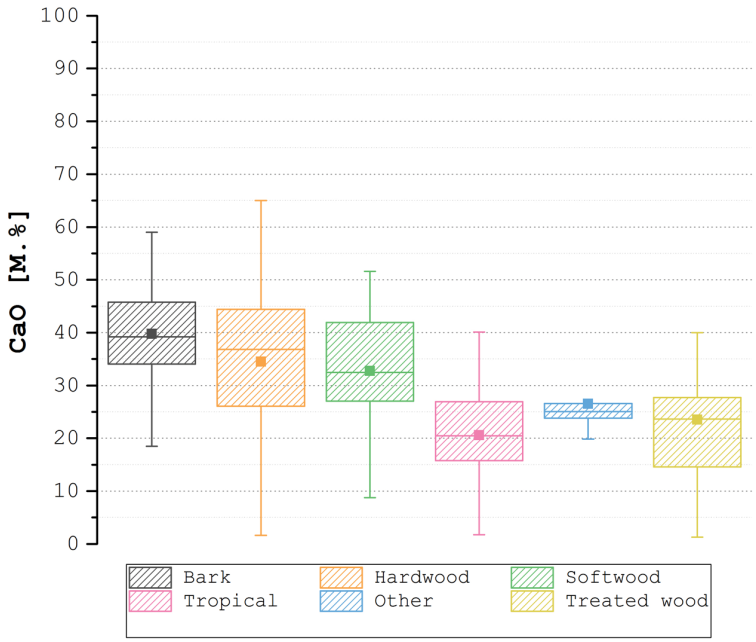

Figure 15: CaO content for individual wood and woody biomass (WWB) derived sub-catagories: Bark, hardwood, softwood, tropical, other and treated wood from the Phyllis database [21]. Target CaO concentration is 61-69 M%.

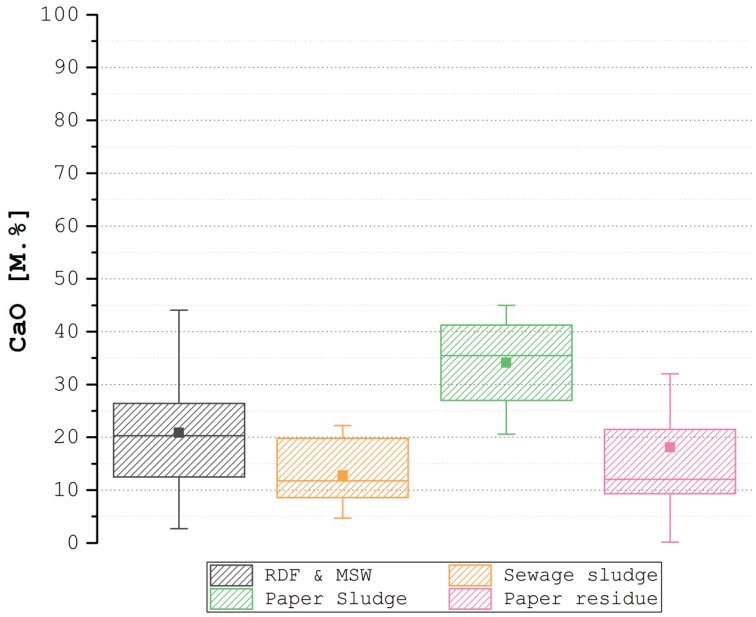

Figure 16: CaO concentration in OR-BD broken down into sub-categories: RDF & MSW, sewage sludge, paper sludge, paper residue from the Phyllis database [21]. Target CaO concentration is 61-69 M%.

In addition to CaO and SiO_2, both Al_2O_3 and Fe_2O_3 should be present in the biomass derived ash if it is to be used as a clinker replacement or raw feed for clinker production. Theoretically the ash should therefore contain between 3 and 5 M.-% of each. Concerning the 3 biomass stream categories

investigated, the vast majority of all samples fell in the desired range, however some subcategories were prone to elevated contents of one or both of these oxides. Paper, RDF and MSW derived ashes, for example, tended to have higher contents of Al_2O_3, often in the range exceeding 15M.%. Also, sewage sludge ash was generally too high in both Al_2O_3 and Fe_2O_3. Similar elevated contents of Al_2O_3 and Fe_2O_3 were found in ashes of treated woods.

3.1.2 Ternary Diagrams

The identification of the individual oxides is useful; however, the biomass source needs to provide a balance of multiple oxides in order to be used as single raw material for clinker production or replacement of clinker. Therefor it is useful to view the composition of the different biomass derived ashes in a ternary diagram like the one shown Figure 17. Each point in the plot represents the composition of a single sample. With the main clinker forming oxides normalized to 100% and the samples of the three biomass categories distinguished by colour, trends can be identified and those samples which fall in the desired region can be selected. While all three categories are represented within the semi-circle that encompasses the desired composition, HAB appears to be the most recurrent. The OR-CB samples appear to be the most disordered while both WWB and HAB showing strong tendency to contain more SiO_2. Alongside the higher SiO_2 concentration WWB also show a preference for higher CaO concentrations. Conversely HAB showed lower concentrations of CaO.

While Figure 17 shows the ternary diagram that includes the oxides necessary for clinker production, in the case of biomass derived ash it is more informative to expand the oxides depicted because the alkali oxides can be critical to clinker mineral formation. Therefore, for better visualization of the oxide proportions present, the ash compositions are plotted in a ternary diagram composed of the three glass science categories in Figure 18. The majority of the samples did not fall into the desired range with the exception of a few. Only two HAB samples were found in this section since the majority of them were richer in $SiO_2+Fe_2O_3+Al_2O_3$ and had low levels of CaO+MgO. From Figure 17 it can be seen that it is mostly SiO_2 that comprises the HAB samples. A few more OR-CB samples were detected in these composition ranges, however, in general they also tended to be richer in $SiO_2+Fe_2O_3+Al_2O_3$. WWB had the most biomass samples falling in the desired range. Woody biomass tends to be richer in CaO and since larger quantities of CaO are necessary for clinker this appears a more promising biomass source.

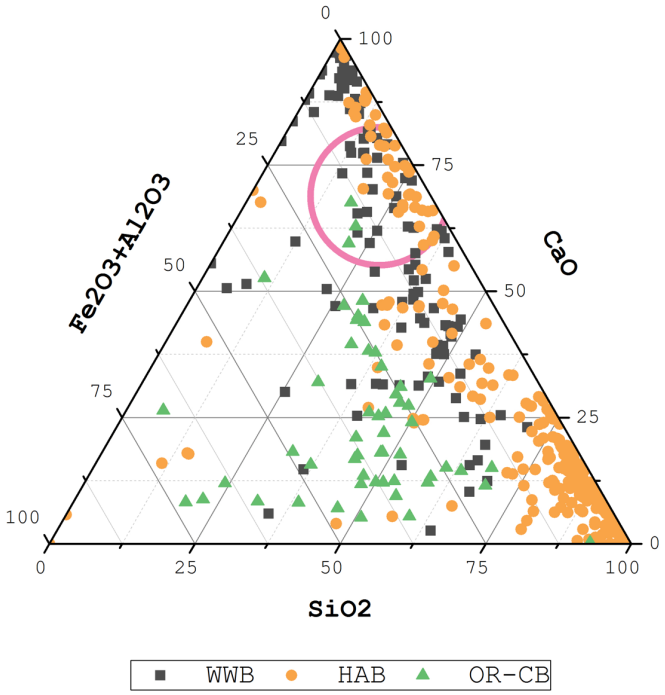

Figure 17: Ternary diagram with the main clinker forming oxides normalized to 100% with the three biomass categories (WWB, HAB and OR_CB) distinguished by colour. The semi-circle represents the area of desired composition and HAB appears to be the most recurrent biomass type in this range.

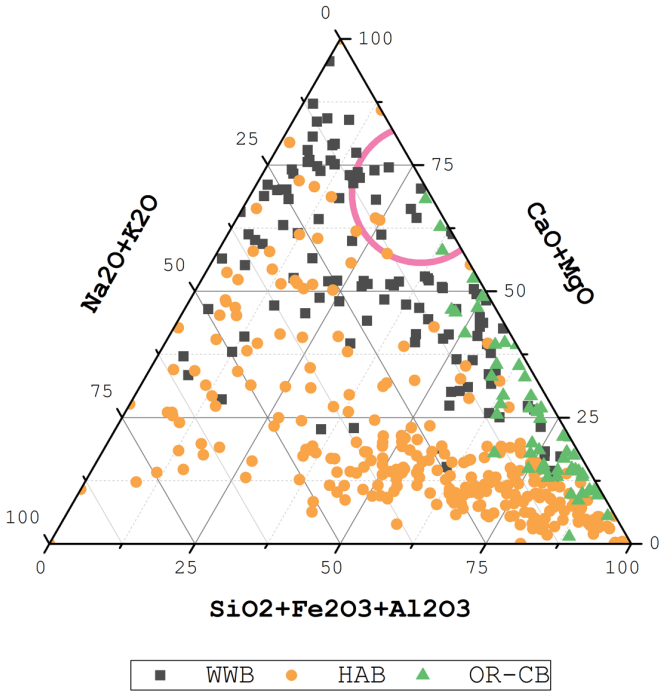

Figure 18: Ternary diagram with the most abundant oxides grouped based on function in clinkering and normalized to 100% for the three biomass categories (WWB, HAB and OR_CB) as distinguished by colour. The semi-circle represents the area of desired composition and WWB appears to be the most recurrent biomass type in this range.

3.1.3 Physical Properties (A, MC & HHV)

In addition to the chemical composition of the ash, another important characteristic dependant on the biomass source is the ash content. In order to make use of the biomass ash after biomass combustion there has to be a significant amount of material available. The Phyllis 2 database provides the ash content from most of the material entries. As depicted in Figure 19, the mean ash content of samples grouped in the WWB, HAB and OR-CB categories are 2.4% 6.4% and 9.5% respectively. Although OR-CB showed the highest average ash content it also showed the largest standard deviation.

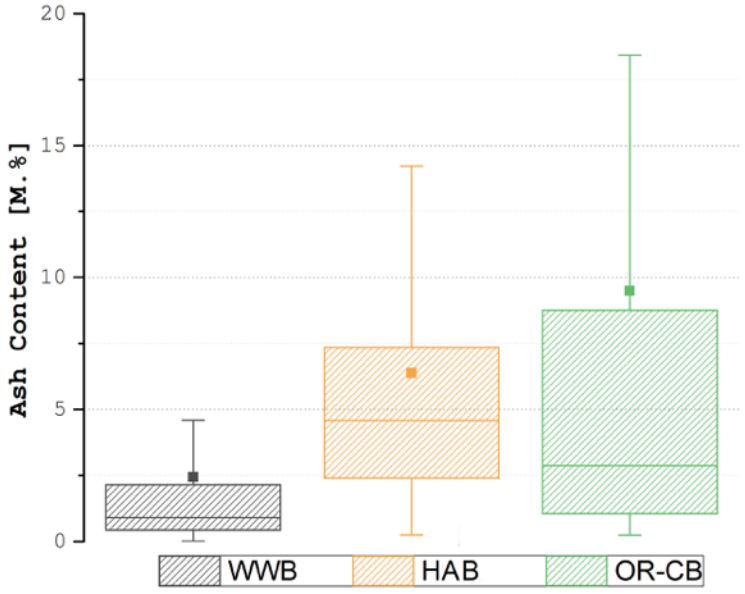

Figure 19: Ash content as a mass percentage of the total biomass mass for the categories wood and woody biomass (WWB), herbaceous and agricultural biomass (HAB) and organic residues and contaminated biomass (OR-CB). OR-CB results in the most ash and WWB the least.

The moisture content (MC) and higher heating value (HHV) for the 3 categories were also evaluated. Moisture is important to quantify because it lowers the weight specific caloric value of biomass. If the MC is too high, combustion can take more energy than it produces. The HHV is indicative for the biomass' potential as a fuel source. While not decisive for the application of the ash as a cement replacement, it is nonetheless critical because if the HHV is too low, the biomass has no potential application as a fuel. There appeared no substantial difference between the three categories of biomass types for either of these parameters. The average MCs for WWB, HAB and OR-CB were 15.0, 19.3 and 12.5 respectively. These numbers are almost identical in their respective 3rd quartile (Q3 75% and less) with the marginal differences being the result of a few outliers. The median values were 8.0, 9.7, and 6.8 for WWB, HAB and OR-CB respectively, all of which are acceptable moisture contents. The average HHVs for WWB, HAB and OR-CB were 15.0, 14.4 and 15.5 respectively. No significant differences in MC or HHV were therefore found amongst the 3 biomass categories.

3.2 ALLASKA Database: Effect of Conversion Technology on Ash Composition

In addition to the biomass source, the conversion technology also affects the composition of the resulting ash. Conversion technology can be grouped together by reactor types, however there can

still be differences based on operational parameters (i.e. changes in firing temperature). For any given reactor type, the general process is consistent. In this section, the average composition of biomass derived ashes which have been produced in a pulverised fuel reactor (PF), grate stoker furnace (GSF), circulating fluidized bed (CFB) and bubbling fluidized bed (BFB) will be evaluated. The biomass selection was limited to wood and woody biomass since (as seen in the previous section) this category showed the smallest most accurate range in the contents of the major oxides with the average CaO content being 29.8 M.-% and the average SiO_2 content being 16.5 M.-%. Furthermore, there is an abundance of data on woody biomass available in the ALLASKA database.

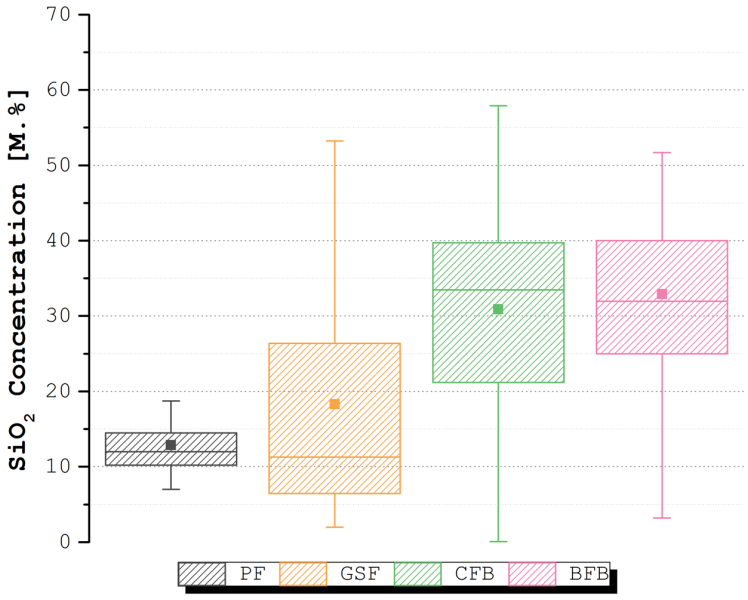

Figure 20: SiO_2 content in woody biomass ash after thermal conversion in 4 different boilers; pulverised fuel reactor (PF), grate stoker furnace (GSF), circulating fluidized bed (CFB) and bubbling fluidized bed (BFB). Target SiO_2 concentration is 15-20 M.-%.

Statistical representations of the SiO_2 and CaO contents for ashes produced in a PF, GSF, CFB and BFB can be seen in Figure 20 and Figure 21 respectively. After conversion in a pulverised fuel boiler, significantly lower quantities of SiO_2 are present relative to the other boilers. Half of the samples had contents between 10.2 and 14.5 M.-%. While lower, this is not far below the 15-20 M% range which is theoretically required in raw feed for the production of OPC. The CaO content in the ash produced in a PF is on par with the other technologies, in fact the second highest amount. It is interesting to note that the PF ash had a significantly smaller content range for both CaO and SiO_2, suggesting more consistency in the composition of the resulting ash. Conversely, GSF derived ashes showed a very wide range for both SiO_2 and CaO contents. While the average SiO_2 content falls directly in the theoretically required range, the distribution appeared too large and the average CaO content falls far below what is theoretically required. Based on these characteristics GSF technology appears less suitable for producing ash useful as raw material for production of OPC.

The CFB and BFB derived ashes had remarkably similar SiO_2 and CaO contents with the average SiO_2 concentration for BFB falling slightly above that of CFC and the average CaO content for BFB falling slightly below that of CFB. However, the whole distribution was remarkably similar, as was the

range and standard deviation. The relatively small differences observed are likely due to the similarities in the combustion technologies between these two methods. In terms of SiO_2 and CaO content, these data suggest that both BFB and CFB techniques are suitable for converting biomass into energy while still resulting in ash with potentially suitable qualities for OPC production.

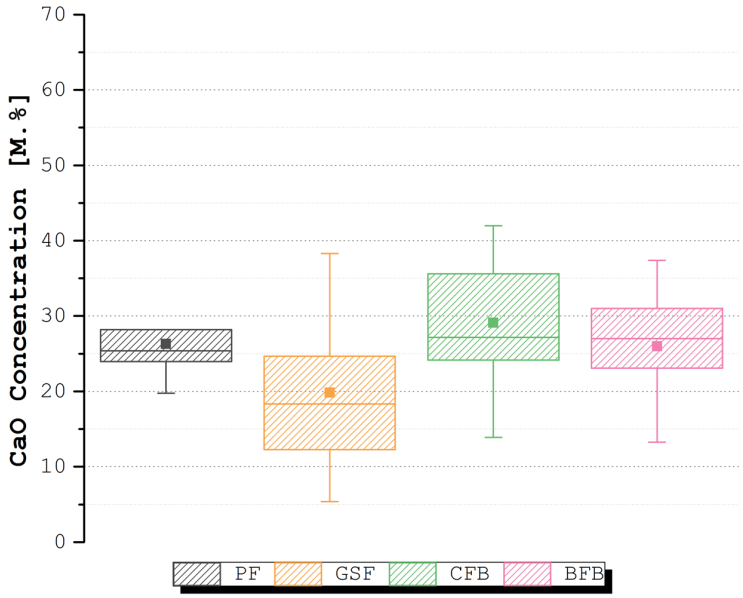

Figure 21: CaO content in woody biomass ash after thermal conversion in 4 different boilers; pulverised fuel reactor (PF), grate stoker furnace (GSF), circulating fluidized bed (CFB) and bubbling fluidized bed (BFB). Target CaO concentration is 61-69 M.-%.

Concerning the oxides of elements that are present in smaller quantities, less distinct trends could be observed based on the combustion system involved. In Figure 22, the average concentration of oxides (Al, Fe, Mg and K) in the range of 2-10 M.-% can be seen and in Figure 23, the minor oxides, i.e. those accounting for less than 2 M.-% on average (Na, Mo, P and Ti) can be seen for each of the 4 conversion systems. Concerning the minor oxides, there are very few differences and it can be concluded that the conversion system has little to no effect on the presence of minor oxides in the resulting ash. Some variation in the oxides present in slightly larger quantities can be observed. In particular, the ash resulting from both BFB and CFB had higher average contents of Al_2O_3 (9.4 and 10.4 M.-%) in comparison to GSF and PF (3.3 and 2.3 M.-% respectively). GSF and PF resulted in ashes that contained higher amounts of K_2O than either BFB or CFB (5.7 and 10.5 vs 4.1 and 3.4 M.-%).

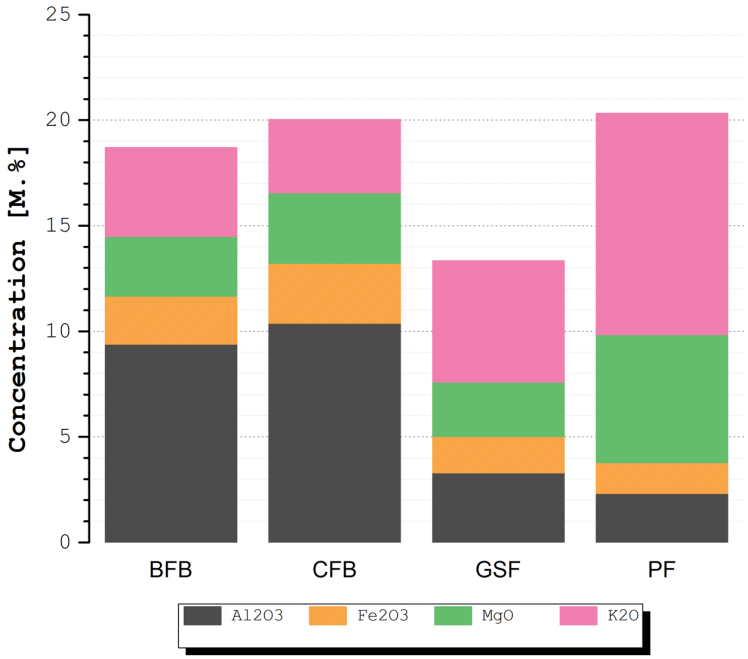

Figure 22: Distribution of oxides in woody biomass ash after thermal conversion in 4 different boilers (BFB and CFB had higher average contents of Al_2O_3).

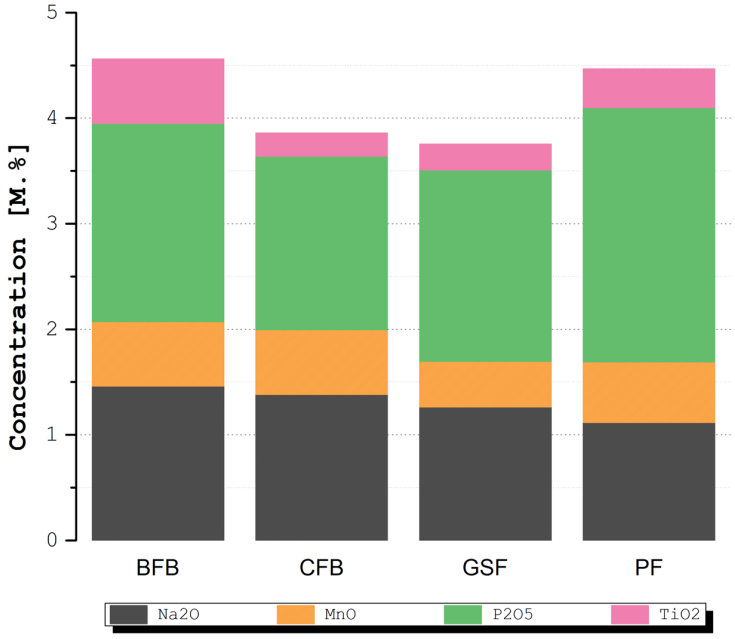

Figure 23: Distribution of minor oxides (i.e. < 2 M.-%) in woody biomass ash after thermal conversion in 4 different boilers (the conversion system has little to no effect on the presence of these minor oxides).

3.3 Fly Ashes Chemically Characterized in this Study

3.3.1 Composition

The elemental analysis of the fly ashes chemically characterized in this study can be found in Table 5, where all of the elements present in quantities greater the 2 M.% are depicted. Due to the presence of different trace elements for each sample and the resulting abundance of data, a full elemental analysis is not included in this report. All of the ashes under investigation had significant quantities of either Ca, Si or both. Again, the samples have been grouped in the following categories: wood and woody biomass (WWB), herbaceous and agricultural biomass (HAB) and organic residues and contaminated biomass (OR-CB). For the sake of comparison, the composition of two (partially) coal-derived fly ashes are included in this analysis and are classified as COAL. CFA-1 stems from the combustion of pure coal and CFA-2 stems from the combustion of 50% coal and 50% woody biomass.

In terms of the concentration of Si, WWB had the lowest average value of (4.5M.-%) and also the smallest range (3.5 M.-%). The highest average Si content was found in the HAB group (17.3 M.-%) and this is also the group that contained the overall highest Si containing sample, HAFA-3, with 24.9M.-%. The second highest Si average was for the group COAL (12.8 M.-%). OR-CB had an average Si concentration of 9.48 M.-% however the range here is 11.4 M.-% indicating high variability for relatively lower Si concentrations.

The OR-CB category showed the highest average Ca content (22.0 M.-%) but it also showed the largest range in concentrations (34.6 M.-%). Paper sludge fly ash (PSFA) which fits within the OR-CB category, had the highest Ca concentration of all the samples tested (44.2 M.-%). Additionally, the WWB group had a high average Ca content (19.26 M.-%) but also had a high range (23.8 M.-%). On Average both HAB and COAL samples had the lowest Ca concentrations. The 100% coal-derived fly ash, CFA-1 had the lowest Ca content (1.6M.-%).

Regarding the minor elements OR-CB had average Al and Fe near the quantities necessary for clinker minerals (3.0 and 6.4 respectively). Both WWB and HAB stand out for higher average K concentrations (4.64 and 5.14 M.-% respectively) however they also showed a substantial range in concentrations (10 and 5.8 M.-% respectively). Additionally, WWB had one sample with a Mg concentration of 10.1 M.-% while the other WWB samples averaged 2.0 M.-%. OR-CB had one sample with a significant concentration of P. Since this ash was derived from sewage sludge, the high P content is expected [26, 27]. All other samples showed P within an acceptable range.

It is interesting to note that CFA-2, the co-combustion ash, is far more similar in composition to CFA-1, the coal-derived ash, than the fly ashes stemming from woody biomass in the category WWB. Due to the fact that woody biomass has a small ash content (approximately 2.4 M.% on average as seen above) and coal has a much larger ash content (around 10 M.%) the resulting composition is dominated by the coal elements.

Table 5: Elemental composition derived from XRF (for the detectable elements that exceeded 2 M.-%) for ashes within the categories wood and woody biomass (WWB), herbaceous and agricultural biomass (HAB), organic residues and contaminated biomass (OR-CB) and coal or partially coal-derived (COAL). The highest average Si content was found in the HAB group (17.3 M.-%). The OR-CB category showed the highest average Ca content (22.0 M.-%).

		Ca	Si	Al	Fe	K	Mg	P	S	Cl
WWB	WBFA-1	30.1	2.9	0.5	2.8	10.3	0.8	0.4	1.5	0.9
	WBFA-2	22.7	5.1	0.7	1.7	4.9	1.2	1.3	2.0	0.1
	WBFA-3	20.9	4.7	0.8	2.5	6.7	1.6	0.7	1.8	0.1
	WBBA-1	16.3	3.2	0.1	13.8	1.0	4.2	0.2	0.0	0.0
	WBBA-2	6.3	6.4	0.1	12.2	0.3	10.1	0.1	0.0	0.0
HAB	HAFA-1	24.2	13.1	1.5	3.3	3.0	0.3	0.8	0.7	0.6
	HAFA-2	25.3	12.0	1.5	3.2	3.2	0.4	0.8	0.9	0.8
	HAFA-3	6.2	24.9	0.6	1.3	8.8	1.3	0.4	0.6	5.6
	HAFA-4	5.5	23.0	0.4	1.0	7.4	1.1	0.4	2.0	4.1
	HAFA-5	9.2	13.5	2.4	3.0	3.3	0.6	0.8	2.3	0.2
OR-CB	PSFA	44.2	3.4	1.5	1.2	0.4	0.4	0.0	0.3	0.3
	PSBA	9.6	14.8	2.9	8.5	0.9	0.2	0.1	0.1	0.1
	ORFA-1	22.3	7.6	3.4	7.9	1.0	1.6	0.4	1.0	0.4
	ORFA-2	16.3	7.8	5.7	13.1	0.8	0.9	8.7	2.7	0.0
	ORBA-3	17.7	13.8	1.7	1.5	1.5	0.1	0.0	0.0	0.2
COAL	CFA-1	1.6	22.7	11.7	5.3	2.9	0.5	0.2	0.5	0.0
	CFA-2	9.7	15.6	6.0	5.9	3.8	0.5	0.3	0.6	0.0

3.3.2 Mineralogical Characterization

The mineralogical composition of the ashes as determined by XRD can be found in Table 6. The compositions of the individual ashes are derived from the relative intensities of the different components, thus relative quantities can be determined making the stated compositions semi-quantitative. Similar compositions can be found within the different biomass categories. In the case of WWB, all the fly ash samples had quartz followed by calcite as the most abundant phases. In the case of the two bottom ashes (WBBA-1 and WBBA-2), Mg-containing phases were found to be the most prevalent, followed by calcite. Interestingly enough, quartz was not detected in the bottom ash samples at all, unlike all of the other ashes which had quartz as the most abundant phase (except PSFA where it was second). Forsterite or a combination of periclase and forsterite were detected in the bottom ashes. The elevated concentrations of Mg and Fe in the two ashes apparently result in the formation of forsterite. Since Mg was even more abundant in WBBA-2, periclase formed in addition to forsterite. In addition to quartz and calcite, the three fly ashes also contained arcanite (K_2SO_4). The sample WBFA-2 was found to have more Ca containing phases than the other WWB samples, namely portlandite and lime.

The HAB ashes were all dominated by quartz. Despite being identical in biomass source and almost identical in conversion parameters and elemental composition, the two wheat straw based ashes (HAFA-1 and 2) had slightly different mineralogical compositions; both ashes contained quartz, calcite and anorthite ($CaAl_2Si_2O_8$). However, HAFA-1 contained portlandite while HAFA-2 had a sulphur containing calcium phase, namely anhydrite. Both HAFA-3 and 4 contained potassium chloride as the second most abundant phase. Next to quartz this was the only phase present which excludes their ability to exclusively replace the raw feed since no calcium phases were present. HAFA-5 differed from the other HAB ashes in its composition and appeared more in line with the WWB category. Despite the lower values of Ca, the elemental composition was not very different and the elements formed similar minerals in comparison to WWB ashes.

Just as with the elemental composition, the mineralogical composition of OR-CB samples showed high variability. PSFA contained a clinker mineral, namely C_2S. In addition to C_2S, there was still lime and quartz. Gehlenite and portlandite were also present. Despite being a calcium silicate, gehlenite's reactivity is so low that it is often considered to be non-hydraulic. The corresponding bottom ash sample, PSBA, featured a singular crystalline phase, quartz. However, the diffraction pattern for this phase also showed a hump that is characteristic of amorphous materials. In addition to quartz, ORFA-1 contained anorthite and $Ca_8Si_5O_{18}$. These two calcium-containing phases may have hydraulic potential. Anorthite, discussed above, was also found in the WWB fly ashes. $Ca_8Si_5O_{18}$ is another calcium silicate that was only found to be present in ORFA-1. ORFA-2 was composed of quartz, calcite, anhydrite and calcium iron phosphate while ORFA-3 was composed of quartz, anorthite and lime. The crystalline fraction of the two coal-derived fly ahses where composed of quartz and mullite. In addition to these two phases, the co-combustion ash also had anhydrite present.

Table 6: XRD derived semi-quantitative mineralogical composition for the ashes characterized in this study (including the most abundant phases) in decreasing quantities.

WWB	WBFA-1	Quartz	Calcite	Arcanite		
	WBFA-2	Quartz	Calcite	Arcanite	Portlandite	Lime
	WBFA-3	Quartz	Calcite	Arcanite		
	WBBA-1	Forsterite	Calcite			
	WBBA-2	Periclase	Forsterite	Calcite		
HAB	HAFA-1	Quartz	Calcite	Portlandite	Anorthite	
	HAFA-2	Quartz	Anorthite	Calcite	Anhydrite	
	HAFA-3	Quartz	Potassium			
	HAFA-4	Quartz	Potassium			
	HAFA-5	Quartz	Calcite	Lime	Arcanite	
OR-CB	PSFA	Lime	Quartz	C_2S	Gehlenite	Portlandite
	PSBA	Quartz				
	ORFA-1	Quartz	Anorthite	$Ca_8Si_5O_{18}$		
	ORFA-2	Quartz	Calcite	Anhydrite	Calcium Iron Phosphate	
	ORBA-3	Quartz	Anorthite	Lime		
COAL & CO	CFA-1	Quartz	Mullite			
	CFA-2	Quartz	Mullite	Anhydrite		

3.3.3 Particle Size of Biomass Derived Ashes

Unlike the chemical and mineralogical composition, the particle size of biomass derived ash is related more to the type of ash and conversion technology than the biomass source. As can be seen from Figure 24, bottom ash tends to have larger particles than fly ash across the whole distribution. The diameters at which 10%, 50% and 90% of a sample's particles are smaller (based on volume) are commonly used to represent the midpoint and range of the particle sizes of a given ash. Furthermore, they serve as values of comparison to relate and evaluate the different ashes. These values are referred to as the D(10), D(50) and D(90). There is also significantly less variability in the D(10) D(50) and D(90) values for bottom ash than there is for fly ash as can be seen from the smaller standard deviation. The large spread in standard distribution for fly ash particles invites the further division of these ashes based on conversion technology in the attempt to identify implications of reactors on the resultant ash size.

Bottom ash is formed when the bed material of the furnace interacts with the ash through physical collision and chemical reactions. The collisions result in the attachment of ash particles on the bed particles resulting in the formation of a porous ash layer on the surface of the bed sand particles. Given that a BFB bed's particle size is between 0.5-1 mm and a CFB bed's particle size is between 0.2-0.4 mm, the observed bottom ash D(50) ranging from 70 to 100µm is smaller than would be expected. These values are most likely the result of a small sample size (i.e. 4) and half of the furnaces being lab scale.

Dividing the fly ash into those samples produced in a BFB and those from a PF provides additional information as can be seen in Figure 25. Fly ashes stemming from a PF tend to be larger than those from a BFB. While the two reactors produce similar sized particles on the smaller end of the spectrum (i.e. D(10)), the disparity in particle size grows as the cumulative undersize approaches 100%. The BFB ashes still show the large standard deviation that was apparent for all fly ashes, however this large variance is not present in the PF samples. In addition to ash type and reactor, there is apparently something else affecting the particle size, particularly in the case of BFB.

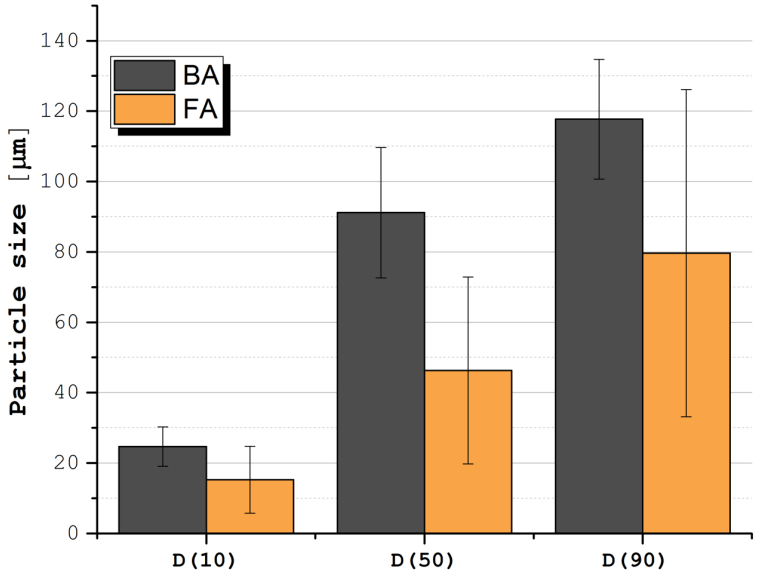

Figure 24: Particle size distribution as shown through the mean D(10) D(50) and D(90) for bottom ash (BA) and fly ash (FA) samples (refer to Table 4 for specific ash groups). BA constantly contains larger particles relative to FA.

There were two ashes included in this study, which were not combusted in either a BFB or PF despite being fly ashes. ORFA-1, originating from industry waste wood produced in an integrated gasification and combustion system, appeared most similar to the woody biomass sample from fluidized bed

(WBFA-2). This indicates that integrated gas and combustion resulted in an ash more like a combustion. The type of reactor which was used to produce HAFA-5 was unknown and it came from a biomass stream that was different from all the rest (mixed green waste). As was the case with the elemental and mineral composition, the particle size distribution of this ash was significantly different from the majority of the others. HAFA-5 was only similar to PSFA which was an outlier regarding particle size. It is suspected that PSFA had particles that were significantly larger due to the processing involved in de-inking the sludge, namely the addition of lime. The fly ash produced in BFB showed a large standard deviation, (Figure 26).

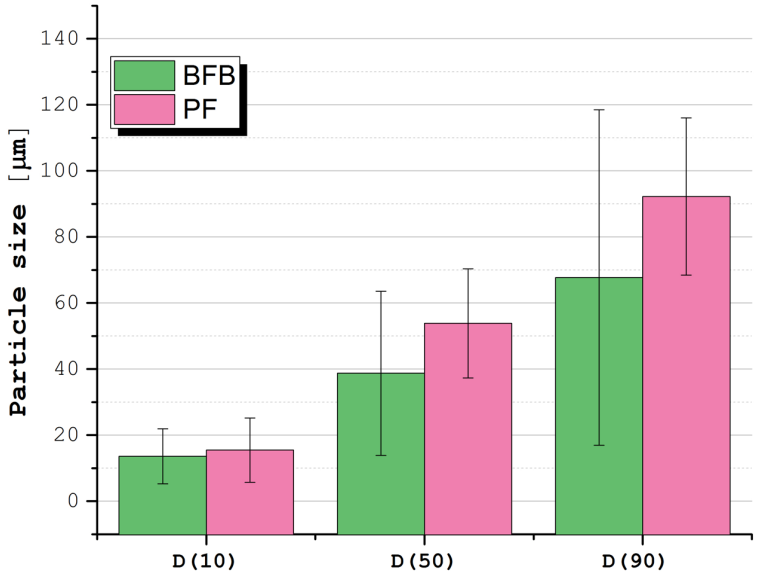

Figure 25: Mean D(10) D(50) and D(90) for fly ash produced in a BBF (Bubbling fluidized bed combustor) and in a PF (Pulverized Fuel combustion). The smaller end of the spectrum both BFB and PF produce similar sized particles but as the cumulative undersize approaches 100% PF produces larger particles.

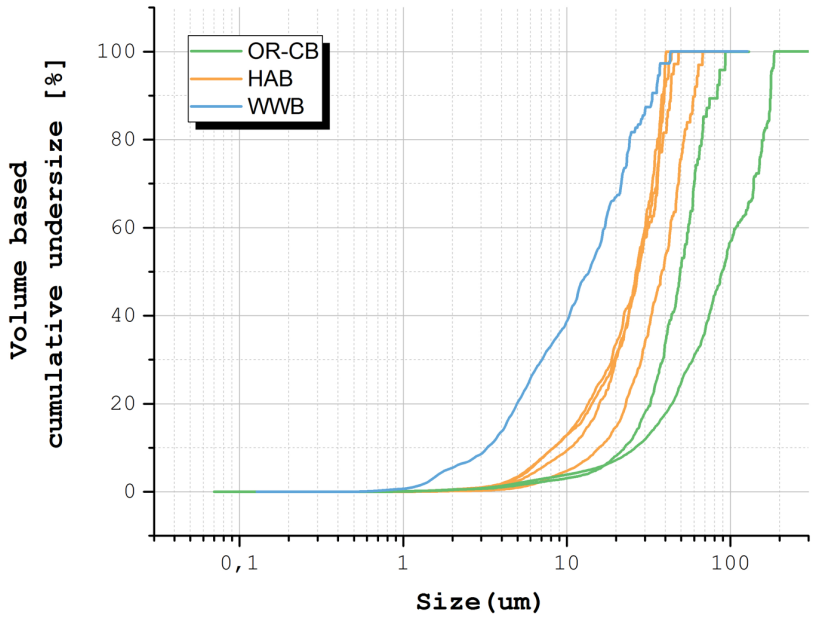

Figure 26: Particle size distribution for the fly ashes produced in BFB grouped by biomass source category. WWB had the smallest particles and OR-CB had the biggest.

4 Discussion

4.1 Phyllis Database

4.1.1 Clinker Forming Oxides

Based on the analysis of the biomass sources and the ash composition of samples within the Phyllis 2 database, it can be concluded that particular biomass waste streams appear more suitable than others as either a clinker replacement or as an alternative raw feed for clinker production. While some streams showed abundant concentrations of either SiO_2 or CaO, a few sources had the potential to provide all the necessary elements in roughly the theoretically appropriate quantities (i.e. 61-69 M.-% of CaO and 15-20 M.-% of SiO_2).

It was apparent that within the WWB category both bark and hardwood had the potential to provide relevant contents of CaO (average of 39.8 and 34.5 M.-% respectively). While some samples within these two subgroups fell below the required amounts, the majority provided ample CaO required for the formation of hydraulic clinker minerals. In addition, from the OR-CB category, paper sludge was found to contain CaO in amounts that are on the lower limit of what is required and therefore still show potential as source of CaO for formation of hydraulic clinker minerals.

Sufficient potential sources of SiO_2 were more abundant, however, the content of most sources exceeded the theoretically required SiO_2 threshold (20 M.-%). Although all WWB samples fell short of what was necessary, some sub-categories from the groups OR-CB and HAB fell in the desired range. Particularly waste paper, treated wood and, to some extent, paper sludge provided potentially sufficient SiO_2 without being in excess (22.5 to 39.7 M.-%). RDF + Plastic derived ashes appeared also as optional SiO_2 source but these are considered less desirable because they are not biomass based and the combustion of plastic (even as a waste treatment solution) should be avoided. From

HAB, it was the husk/shells/pits and the organic waste (or more specifically agricultural waste) derived ashes that offered SiO_2 (28.9M.-% and 18.3M.-%) in the potentially desired amounts.

Generalizations are difficult to make for the SiO_2 and CaO composition of sewage sludge ash because there appeared to be high variability [28]. Considered to be a semi-biomass, the element composition can be more variable than natural biomass due to processing and the origin of materials [1]. In a survey of 42 different studies Cry et. al found that the mean content was 36.1 M.-% for SiO_2, 14.8 M.-% for CaO, 14.2 M.-% for Al_2O_3, 9.2 M.-% for Fe_2O_3, 11.6 M.-% for P_2O_5 and 2.8M.-% for SO_3. Therefore, due to the high variability of its composition and high concentration of P_2O_5, sewage sludge ash appears not to be a favourable source for clinker replacement or as an alternative raw feed for clinker production.

Regarding the elevated concentrations of Al_2O_3 and/or Fe_2O_3 detected in the subcategories paper, RDF and MSW, sewage sludge and treated wood ash, all of these biomass streams had undergone additional processing prior to combustion and this could have been most likely the source of Al_2O_3 and Fe_2O_3. Rarely does a pure biomass stream show an excess of either of these two oxides, indicating that their presence stems more from the processing and human intervention than the actual biomass.

OR-CB appears to be the best biomass derived ash source for potential cement replacement since it provides both Ca and Si (22.0 and 9.48 M.-% respectively) while also having the highest ash content (9.5M.-%). Wood ash also has potential given that particular samples were on the higher side of both Ca and Si (19.3 and 4.5 M.-% respectively) content for all biomass derived ash samples investigated. Since Ca is the element that needs to be present in the largest quantities, WWB also makes a viable option, given that the particular sample analysed has sufficient Si as well. Furthermore, WWB showed the lowest deviations in element contents, reflecting a higher degree of consistency in the composition of the waste stream.

In addition to the chemical composition of the ash, another important characteristic dependant on the biomass source is the ash content. The ash content is a critical parameter since it dictates the volume of material derived from the different types of biomass. WWB had the lowest ash content (2.4 M.-%) while OR-CB had the highest (9.5 M.-%) and the largest range. The OR-CB group includes all organic residue that is not a direct residue from agriculture and horticulture (waste paper, residues from the food industry, domestic waste municipal solid waste and refuse derived fuel). The higher ash content and broader range are most likely the result of the diversity of the category. Furthermore, OR-CB includes treated organic residues like sewage water sludge, paper industry sludge, food industry sludge, composted wood, demolition wood, preserved wood and particle board. The processes of these materials prior to combustion introduces external compounds which adds to the ash fraction. When these external compounds are inorganic they can have a significant impact on the ash fraction, which is not always ideal.

4.2 ALLASKA Database

Based on the analysis of the conversion technology and ash composition extracted from the data within the ALLASKA database, it can be concluded that particular conversion technologies are more beneficial than others as the resulting ash can potentially act as either a clinker replacement or as source for the production of an alternative raw feed for clinker. It was observed that both CFB and BFB produce ashes that, on average, have higher contents of the desired oxides CaO and SiO_2. Also, these two types of conversion systems showed higher consistency in ash composition as variability in range was small. These two types of fluidized beds also provided ash with more desirable values with respect to minor element oxides. The samples produced in these reactors had more Al_2O_3 and less K_2O on average. In terms of the data extracted from the ALLASKA database, both a BFB and CFB are best for converting woody biomass into energy while producing an ash with the potentially right elemental make up for clinker. GSF has less value for producing an ash that can be suitable for OPC production as can be concluded based on the large variability of SiO_2 and CaO concentrations and

the undesirable CaO contents of the produced ash. PF showed more consistency in ash composition and acceptable concentrations of SiO_2 and CaO. However, the excessive amounts of K_2O reported in the PF produced ash make it inapplicable as a clinker substitute.

Furthermore, it can be concluded that way of processing of the biomass and the thermal conversion parameters involved can be very influential with respect to the final composition of the derived ash. In the case of pelletized fuel, increases in the Ca content were detected in the fly ash. Additionally, the bed material in fluidized beds can greatly affect the composition of the bottom ash. These parameters can therefore be used to alter the content of particular elemental oxides to benefit most of what is present in the biomass.

4.3 Experimentally Derived Results

In terms of ash composition there were ample results from the experimental investigation. These results corroborated the conclusions drawn from the two databases. On average the WWB ashes were higher in CaO while the HAB ashes provided more SiO_2. Fly ash derived from paper sludge not only provided sufficient CaO and SiO_2 but also already contained calcium silicate, potentially making it an ideal clinker replacement or raw feed replacement.

For the experimentally obtained results, similarities can be found amongst ashes in the distinct categories (WWB, HAB, OR-CB and Coal), for example the WWB show higher contents of Ca than all other elements; the only exception to this being WBBA-2 which despite a similar biomass source and conversion technology had lower quantities of Ca and elevated Mg and Fe concentrations. This is the result of the ash being a bottom ash sample and in this particular case the bed material was composed of olivine, $(Mg^{+2}, Fe^{+2})_2SiO_4$. The other bottom ash, WBBA-1, also showed higher concentrations of Fe. Similar to WBBA-2, WBBA-1 was also a bottom ash sample retrieved from a lab scale Fluidized bed gasifier where olivine composed the bed material. It is interesting to note that these two samples had the lowest amounts of Ca present but also the highest amounts of Mg and Fe. Since the composition of olivine is $(Mg^{+2}, Fe^{+2})_2SiO_4$ and elevated concentrations of Mg and Fe are generally not found in WWB, it can be concluded that significant quantities of the bed material were incorporated into the bottom ash indicating that the bed material is decisive in the composition of bottom ash [29]. While both had olivine as a bed material, the exact composition of the olivine was most likely different with the olivine used in the conversion of WBBA-2 having a higher fraction of Mg. Both WBFA-1 and WBFA-3 were produced in pulverized Fuel combustion, however in the case of WBFA-1 the biomass was pelletized prior to combustion. These two ashes have similar compositions, however WBFA-1 has significantly more Ca. This is most likely the result of the pelletization process, where lime is used as a binder. The elevated concentration of Ca makes it attractive as a potential clinker feed material, however caution must be given to the potassium content and the potentially too low SiO_2 content. WBFA-2 showed the second highest content of Ca. The fuel for the bubbling fluidized bed combustor that produced WBFA-2 is predominantly clean woody biomass from the maintenance of parks and roads, however small amounts of cacao husks, molasses and other clean biomass waste material are also used. Despite the difference in fuel/biomass source, there are few significant differences to the composition. Compared to the other WBFA samples WBFA-2 has the highest concentration of Si, which is most likely the result of the bed material in the bubbling fluidized bed being quartz sand.

The HAB samples also followed the trends that were observed from the database analysis, namely the samples showed elevated contents of SiO_2. HAFA-1 and 2 were produced from the same biomass source (wheat straw) as were HAFA-3 and 4 (rice straw). The impact of the biomass source on the resulting composition is strong, given how similar the pairs are to themselves but different to each other. All four samples were produced in a bubbling fluidized bed combustor (at the lab scale), however HBFA-2 and HBFA-4 operated at higher temperatures than their counterparts (namely 750-950°C). There does not seem to be a correlation between operating temperature and concentrations,

just a clear difference in the more prominent elements. In the case of HBFA-1 and HBFA-2, all the elements present in lower concentrations only differed by 0.2 M.% with a change in temperature. The difference for Ca and Si was each 1.1 M% with Ca being higher at higher temperatures and Si being lower at higher temperatures. While the difference is larger in the case of Ca and Si, relative to the concentration is it lower than some of the less present elements. HAFA-3 and 4 showed slightly larger differences in concentration for the two operating conditions but nothing significant and no clear correlations between temperature can be made. It should be noted though that both rice straw samples had high concentrations of Cl, making them unattractive options for clinker production. This could potentially come from the biomass itself or possibly from some processing in the cultivation and harvesting of the crop. HAFA-5 shows a significantly different composition that the other samples in the HAB group. Most notably there is a distinct lack of Ca without the compensation of an elevation in Si content. This ash was produced from mixed green waste and confirms the proposition that a clearly defined biomass stream is necessary in the production of ashes that can function as either clinker or a raw feed for clinker production. The lack of information on this sample makes it of little use.

The commonalities among the ash compositions of the OR-CB category are less apparent than those of WWB and HAB, however they are still dominated by either Ca, Si or both. The lesser degree of similarity is logical given the larger differences in biomass sources and routes to combustion. Both PSFA and PSBA stem from the same source and conversion system, however PSFA is the fly ash extracted from the BFB while PSBA is the bottom ash. While the fly ash is remarkably rich in Ca, there are not too many other elements present. The bottom ash has a lower concentration of Ca but is rich in Si, Al and Fe. While neither of these two ashes has the ideal composition alone, a mixture of the two could provide an ideal raw feed composition. ORFA-1 has a composition similar to the fly ashes in the WWB category, with the noted exception of elevated concentrations of Al and Fe. The only difference between the biomass source is that the wood combusted in ORFA-1 is considered industry waste wood and is thus considered contaminated. There are no elevated concentrations of adverse elements and there is even a reduction in potassium, making this ash even more suited for clinker than the non-contaminated woods. The remaining two ashes in this category stem from severely unstable streams, namely sewage sludge and municipal solid waste, neither of which shows a particularly desirable composition since the Ca content for both is far below what is required of clinker raw feed.

Interesting observations can also be made from the mineralogical compositions of the experimentally tested ashes. $Ca_8Si_5O_{18}$ (which was found in ORBA-1) is not well documented, however its structure is believed to be related to kilchoanite and γ-C_2S [30]. Rarely occurring in nature, $Ca_8Si_5O_{18}$ can be found in autoclaved building materials [31]. $Ca_8Si_5O_{18}$ (or Ca_8Si_5) was first obtained and documented in 1966 during the hydrothermal treatment of mixtures containing γ-Ca_2SiO_4 and quartz; Bennett found $Ca_8Si_5O_{18}$ to form from starting materials with a Ca/Si ratio between 1.5 and 1.75 under temperatures ranging from 180 to 600°C [32]. Alongside $Ca_8Si_5O_{18}$, Bennett found other phases after hydrothermal treatment including hydrated γ-C_2S (or γ-C_2SH). However, Speakman found that γ-C_2SH decomposes to give $Ca_8Si_5O_{18}$ (as well as poorly crystallized reinhardbraunsite) [33]. When the reaction proceeded for 1 day, small amounts of $Ca_8Si_5O_{18}$ decomposed to from Kilchanite. Unlike traditional hydration products, hydrothermal processing produces crystalline compounds with well-defined structures [31]. However in the case of $Ca_8Si_5O_{18}$, its XRD pattern is poorly crystalline compared to other hydroceramics phases [30]. Misidentification over the years has been attributed to this. This phase could have hydraulic properties or be a precursor to the formation of reactive calcium silicates.

Furthermore, the similarities between the mineralogical composition of HAFA-5 and the WWB category indicates that the mixed green waste samples may in fact have contained woody biomass or something similar. Further reinforcing the fact that proper documentation is necessary to identify and

then utilize biomass waste streams to their fullest potential (i.e. more than just combustion but ash utilization as well).

Additionally, it can be said that both coal and co-fired fly ash do not have the potential to serve as a clinker replacement or raw feed replacement based on the chemical analysis of the ash. The lack of calcium results in no hydraulic minerals and no potential for hydraulic minerals with additional heat treatment.

5 CONCLUSIONS

- Conclusions on composition: A potentially ideal ash for OPC replacement or clinker production can be achieved based on the ashes of particular biomass streams. SiO_2 can be obtained from OR-CB (organic residues and contaminated biomass) or possibly HBA (herbaceous and agricultural biomass) but then from the sub categories husk shell pits or organic resides. CaO can be obtained from WWB (wood and woody biomass) bark and hardwood specifically. Ashes derived from the OR-CB category paper sludge showed the potential to provide both CaO and SiO_2 however the extent of their reactivity remains to be investigated. Excessive levels of phosphorous were detected in sewage sludge derived ash and excessive levels of chlorine were detected in rice straw.
- Conclusions on ash properties: In general, OR-CB provided the highest average ash content.
- Conclusions on conversion system: circulating fluidized beds (CFB) and bubbling fluidized beds (BFB) produce ashes that on average have higher contents of the desired oxides CaO and SiO_2 with a smaller deviation range, and are also more desirable concerning minor elemental oxides since they had more Al_2O_3 and less K_2O (compared to pulverized fuel reactors and grate stoker furnaces).
- Most suitable ashes for further investigations:
    - WBFA-1 (wood pellets, pulverized fuel combustion, 180 MW, fly ash) should be used for further investigations due to the highest amount of Ca present for all WWB ashes.
    - WBFA-2 (mixed clean biomass, bubbling fluidized bed combustor, 80 MW, fly ash) should also be further investigated due to the higher Si content with coexistent significant Ca content.
    - PSFA (de-inking sludge + demolition wood, bubbling fluidized bed combustor, 75 MW(fuel), fly ash) should also be subjected to further investigation due to the presence of calcium silicate in the derived ash.
- Least suitable ashes for further investigations:
    - Excessive levels of phosphorous were detected in sewage sludge derived ash (ORFA-2)
    - Excessive levels of chlorine were detected in rice straw (HAFA-3 and HAFA-4)
- Recommendations for combustion: To achieve the best suited ash for clinker replacement, pelletized wood should be combusted in a fluidized bed with quartz sand as bed material. The derived fly ash should have the potential to act as clinker due to the enhance calcium content introduced in the pelletization process and the enhanced silica content introduced from the bed material. Furthermore, due to the variable nature and broad category of biomass, one or more clearly defined biomass stream (with an elemental composition that fits within an explicitly defined range) is necessary for the production of ashes that can function directly as either clinker replacement or indirectly as a raw feed for clinker production.

6 REFERENCES

1. Vassilev, S.V., et al., *An overview of the composition and application of biomass ash. Part 1. Phase–mineral and chemical composition and classification.* Fuel, 2013. **105**(0): p. 40-76.
2. Demirbas, A., *Combustion characteristics of different biomass fuels.* Progress in energy and combustion science, 2004. **30**(2): p. 219-230.
3. Mehta, P.K. and P.J.M. Monteiro, *Concrete: microstructure, properties and materials*. 2006: McGraw-Hill.
4. Hwang, C.-L., B.L. Anh-Tuan, and C. Chun-Tsun, *Effect of rice husk ash on the strength and durability characteristics of concrete.* Construction and Building Materials, 2011. **25**(9): p. 3768-3772.
5. Zain, M.F.M., et al., *Production of rice husk ash for use in concrete as a supplementary cementitious material.* Construction and Building Materials, 2011. **25**(2): p. 798-805.
6. Mehta, P.K. *Properties of blended cements made from rice husk ash*. 1977. ACI.
7. Cook, D.J., R.P. Pama, and B.K. Paul, *Rice husk ash-lime-cement mixes for use in masonry units.* Building and Environment, 1977. **12**(4): p. 281-288.
8. Govindarao, V.M.H., *UTILIZATION OF RICE HUSK - A PRELIMINARY-ANALYSIS.* Journal of Scientific & Industrial Research, 1980. **39**(9): p. 495-515.
9. Al-Khalaf, M.N. and H.A. Yousif, *Use of rice husk ash in concrete.* International Journal of Cement Composites and Lightweight Concrete, 1984. **6**(4): p. 241-248.
10. Dass, A., *POZZOLANIC BEHAVIOUR OF RICE HUSK-ASH.* 1984.
11. Della, V., I. Kühn, and D. Hotza, *Rice husk ash as an alternate source for active silica production.* Materials Letters, 2002. **57**(4): p. 818-821.
12. Amin, N., *Use of Bagasse Ash in Concrete and Its Impact on the Strength and Chloride Resistivity.* Journal of Materials in Civil Engineering, 2011. **23**: p. 717.
13. Batra, V.S., S. Urbonaite, and G. Svensson, *Characterization of unburned carbon in bagasse fly ash.* Fuel, 2008. **87**(13–14): p. 2972-2976.
14. Chusilp, N., C. Jaturapitakkul, and K. Kiattikomol, *Utilization of bagasse ash as a pozzolanic material in concrete.* Construction and Building Materials, 2009. **23**(11): p. 3352-3358.
15. Frías, M., E. Villar, and H. Savastano, *Brazilian sugar cane bagasse ashes from the cogeneration industry as active pozzolans for cement manufacture.* Cement and Concrete Composites, 2011. **33**(4): p. 490-496.
16. Bui, D.D., J. Hu, and P. Stroeven, *Particle size effect on the strength of rice husk ash blended gap-graded Portland cement concrete.* Cement and Concrete Composites, 2005. **27**(3): p. 357-366.
17. Cordeiro, G.C., et al., *Influence of particle size and specific surface area on the pozzolanic activity of residual rice husk ash.* Cement and Concrete Composites, 2011. **33**(5): p. 529-534.
18. Horsakulthai, V., S. Phiuvanna, and W. Kaenbud, *Investigation on the corrosion resistance of bagasse-rice husk-wood ash blended cement concrete by impressed voltage.* Construction and Building Materials, 2011. **25**(1): p. 54-60.
19. Siddique, R. and M.I. Khan, *Supplementary cementing materials*. Vol. 37. 2011: Springer Science & Business Media.
20. Rajamma, R., et al., *Characterisation and use of biomass fly ash in cement-based materials.* Journal of Hazardous Materials, 2009. **172**(2): p. 1049-1060.
21. ECN. *Phyllis2, Database for Biomass and Waste*. 2012 [cited 2013; Available from: http://www.ecn.nl/phyllis2.
22. Hewlett, P., *Lea's chemistry of cement and concrete*. 2003: Elsevier.

23. Woermann, E., W. Eysel, and T. Hahn, *Chemical and structual investigations of solid solutions of tricalcium silicate.* Zement-Kalk-Gips, 1968.

24. AB, Å.C. *ALLASKA, Environmentally correct utilisation of ashes*. 2014; The purpose of this database is to collect quantitative information on the properties of residues from combustion. These ashes were produced at Swedish combustion plants.]. Available from: http://www.varmeforsk.se/allaska-en.

25. *Phyllis Database Dissemination, Education and Standardisation*. [cited 2016; Available from: http://www.phydades.info/

26. Cieślik, B.M., J. Namieśnik, and P. Konieczka, *Review of sewage sludge management: standards, regulations and analytical methods.* Journal of Cleaner Production, 2015. **90**: p. 1-15.

27. Adam, C., et al., *Thermochemical treatment of sewage sludge ashes for phosphorus recovery.* Waste management, 2009. **29**(3): p. 1122-1128.

28. Cyr, M., M. Coutand, and P. Clastres, *Technological and environmental behavior of sewage sludge ash (SSA) in cement-based materials.* Cement and Concrete Research, 2007. **37**(8): p. 1278-1289.

29. Marinkovic, J., *Choice of bed material: a critical parameter in the optimization of dual fluidized bed systems*. 2016: Chalmers University of Technology.

30. Meller, N., K. Kyritsis, and C. Hall, *The mineralogy of the CaO–Al2O3–SiO2–H2O (CASH) hydroceramic system from 200 to 350 °C.* Cement and Concrete Research, 2009. **39**(1): p. 45-53.

31. Hu, X., et al., *Effects of hydrothermal process on formation of calcium silicate hydrates at 250 C.* Journal of the Society of Inorganic Materials, Japan, 2006. **13**(320): p. 32-39.

32. Bennett, J., et al., *Ca8Si5O18 and the Nature of "γ-Dicalcium Silicate Hydrate".* 1966.

33. Speakman, K., et al., *Hydrothermal reactions of γ-dicalcium silicate.* Journal of the Chemical Society A: Inorganic, Physical, Theoretical, 1967: p. 1052-1060.

CHAPTER 4

USE OF CURRENTLY AVAILABLE BIOMASS DERIVED ASH FOR CEMENT REPLACEMENT AS SECONDARY CEMENTING MATERIALS (BIOSCM)

ABSTRACT

The replacement of a percentage of cement with secondary cementitious materials (SCM) is commonly employed to reduce the high CO_2 emissions associated with concrete production. Typically, these SCMs are industrial by-products such as fly ash or blast furnace slag. Currently the application of biomass derived ashes is not tolerated under EN-450. This work explores the functionality of utilizing woody biomass derived ashes as a SCM at lower (20 and 40%) and higher replacement rates (60% and 80%) selectively. This chapter explores the extent to which biomass derived ashes obtained in the production of energy (in the form of heat and electricity) can currently replace ordinary Portland cement (OPC).

Here it is shown that three types of woody biomass derived ashes are capable of contributing to strength development when used to partially replace OPC. Unlike previous investigations into biomass derived ashes which focus on pozzolanic properties, this investigation sought ashes that would function hydraulically. It was found that paper sludge fly ash (PSFA) performed better than the other two investigated ashes at later ages (28 days and beyond). When PSFA ash was used to replace 20% OPC a compressive strength of 94% the strength of the 100% OPC reference was obtained. Alternatively, one of the other two investigated woody biomass derived fly ashes (WBFA-2) showed increased strength development at early ages when used to replace 20% OPC; these samples reached 109% and 104% of the OPC control at 3 and 7 days respectively. At 28 days, the strength of the sample with WBFA-2 replacing 20% OPC was still 96% of the 100% OPC reference. PSFS is presumed to perform better than WBFA due to the presence of reactive calcium silicates, namely belite.

Woody biomass derived ashes are therefore considered potentially capable of functioning as a SCM (or BioSCM), however a more comprehensive understanding of the relationship between biomass, conversion technology and the effectiveness of a specific woody biomass derived ash to function as a BioSCM is needed as distinct functional differences were found between the three ashes investigated in this study. The implementation of woody biomass derived fly ash as a BioSCM provides a solution for ash utilization. Furthermore, it has the potential to reduce global CO_2 emissions since the production of clinker could be reduced.

1 INTRODUCTION

Since the production of clinker is the most energy intensive step in the making of concrete structures, simply replacing a portion of the clinker with alternative materials can have a drastic effect on the overall CO_2 emissions. These materials can be mineral admixtures which themselves have either cementitious or functional properties, or simply be fillers. Secondary cementing materials (SCMs) contribute to the strength of cementitious products either hydraulically or pozzolanically [1]. Fillers are natural or artificial inorganic minerals which improve the physical properties of cements due to their particle size distribution. They can be inert or even mildly contribute to strength development through hydraulic or pozzolanic properties [2]. Additionally, fillers can provide nucleation sites, to promote the hydration of cement.

The different binding mechanisms can be distinguished as hydraulic, latent hydraulic or pozzolanic [3]. Hydraulic binders are binders that set and harden through a chemical interaction with water. They are capable of doing so under water. OPC is an example of a hydraulic binder. Latent-hydraulic binders are hydraulic binders that act through the addition of an activator (usually lime and water). A common example of a latent hydraulic binder is granulated blast furnace slag which possesses hydraulic properties when suitably activated. Pozzolanic materials are silico-aluminous or silico-calcareous materials and when they are ground to a sufficient fineness and mixed with water they will react with dissolved calcium hydroxide to form calcium silicate hydrates (CSH). A common example is fly ash, which when blended with cement will react with the calcium hydroxide produced in the hydration of the cement to form additional CSH. Silico-aluminous materials do not harden independently however silico-calcareous materials may have some hydraulic properties.

The use of alternative binders is not a new concept; long before the idea of secondary cementitious materials existed, the Romans incorporated (volcanic) tuffs in their binders. These are a type of natural pozzolans which are generally of volcanic origin or sedimentary rocks. While natural pozzolans are still used in selective areas of the world, industrial by-products are more commonly applied as mineral admixtures in concrete [1].

Millions of tonnes of industrial by-products are produced each year and, aside from low value applications like road construction, there are few applications that take full advantage of their pozzolanic or cementitious potential. Mineral admixture in concrete is one area where their full potential can be realized. The most common industrial by-products to be blended with clinker are fly ash, blast furnace slag and silica fume. Fly ash is a residue from coal combustion in modern power plants. Volatile matter and carbon are burned off as the coal passes through the furnace while the mineral impurities melt and fuse together. This material solidifies into glassy spherical particles when it reaches lower temperature zones. The fine particles, or fly ash, fly out with the flue gas stream and are removed from the gas by cyclone separation, electrostatic precipitation and bag-house filtration. According to EN 197-1 fly ash can be either silico-aluminous or silico-calcareous: ASTM standard C 618-85 specifies these as class F fly ash and class C fly ash respectively. The difference in composition (namely SiO_2 and CaO concentrations) is a result of different types of coal being combusted: anthracite or bituminous coal produces a more silica rich ash and lignite or sub-bituminous coal produces a fly ash with less silica and more calcium oxide. Fly ash functions well as a cement replacement due to the pozzolanic reaction incited when the amorphous SiO_2 of the fly ash comes in contact with the $Ca(OH)_2$ produced during cement hydration resulting in the formation of calcium-silicate-hydrates (CSH). In addition to the pozzolanic properties, calcareous fly ash can also have hydraulic properties [2] [3]. Blast furnace slag is a residue from the production of cast iron. Slow cooling of the slag produces relatively inert minerals, however when ground to fine particles, the powder becomes reactive. Alternatively, if the slag is rapidly quenched, the constituents are kept in an amorphous state and are already reactive. According to EN 197-1 granulated blast furnace slag is a latent hydraulic material and when activated properly has hydraulic properties. Silica fume (or microsilica) is a by-product in the silicon metal and ferrosilicon alloy industries. When quartz is

reduced to silica in an induction arc furnace, SiO_2 vapours are produced. These vapours oxidize and condense when they reach lower temperatures and transform into tiny amorphous spherical silica particles. Their small size and rich SiO_2 content make these particles highly pozzolanic.

In addition to the industrially produced mineral secondary cementitious materials, some biomass derived mineral ashes exist. Often these natural alternatives are produced in the combustion of agricultural waste streams such as rice husk or sugar cane bagasse. During the harvesting of agricultural crops, a lot of biomass waste is produced. Often these organic side products are combusted to provide heat and energy for the production process. Each tonne of paddy rice results in approximately 200 kg of husk and after combustion about 40 kg of ash remains [1]. When the combustion is controlled and the ash remains amorphous, a highly pozzolanic material is produced which behaves similarly to silica fume [4]. In Thailand, an agriculturally based society, roughly 10 million tonnes of rice husk and 66 million tonnes of sugarcane bagasse are produced annually [5]. Together with wood chips, these waste streams are combusted to produce electricity in biomass power plants and result in about 17 million tonnes of bagasse rice husk wood ash (BRWA) [5]. Disposal generally constitutes of landfilling. While some ash is used as fertilizer to return nutrients to the soil, large quantities are often landfilled. This environmentally unsound disposal can cause problems with air and water pollution. The fine particles are easily dispersed through the air creating health and safety issues. Ground water contamination is also a potential problem due to the leaching of heavy metals from the ashes.

Similar to the industrial by-products, the functionality of a biomass-derived ash as a cement replacement depends on its chemical and mineralogical composition and physical characteristics. Again, the ash can contribute to strength development through a few distinct ways, namely via a hydraulic reaction, a pozzolanic reaction, and/or the introduction of nucleation points. If inert, an ash still has the ability to contribute to the end strength. In this scenario, it can act as a filler and its functionality is dependent on the particle size and distribution; it can increase the packing density resulting in a denser matrix. A few factors have a profound influence on chemical composition and physical characteristics of the biomass-derived ash: biomass feedstock, conversion technology (i.e. furnace/boiler type) and thermal conversion parameters (residency time, temperature) [6]. Thermochemical conversion technologies for biomass are either direct-fired or gasification systems and can range in scale from open field burning (relatively low temperatures) to fluidized bed gasifiers (high temperatures). The conversion technology used dictates biomass selection or conversely available biomass will dictate the conversion technology on smaller scales. In the case of large-scale installations, it is common to see the utilization of specifically grown energy crops, which have been pelletized and sometimes shipped long distances. Open field burning is generally used to dispose of local agricultural waste and provided heat or power for agricultural processes. Between these two extremes, there are various levels of biomass preparation and conversion technologies of varying complexity. The conversion parameters are dependent upon both the biomass type and conversion technology.

The combustion of biomass for the purpose of energy production is becoming a more attractive option as society pushes towards energy produced from renewable sources. This results in the production of biomass derived ash, which at the moment has few applications. One option for biomass-derived ash disposal is to incorporate it into concrete much like coal derived fly ash. However at the moment, there is no tolerance for the use of any material not derived (at least mainly) from coal combustion in the standards [7]. The potential for larger scale incorporation exists as more power plants convert to biomass options and the available biomass derived ash stream incresses. Therefore, it is crucial to explore the potential of biomass derived ashes as supplementary cementing materials to prove their viability and gain acceptance in the standards.

The increase in biomass combustion for the sake of energy production naturally means an increase in biomass derived ash production. Environmentally friendly disposal options need to be explored. It has

been suggested that the disposal of biomass derived fly ash could be problematic in agricultural or industrial applications due to the higher leachability of heavy metals relative to coal derived fly ash [8]. This makes their use in concrete all the more attractive.

This work explores the use of three woody biomass derived ashes to replace cement or alternatively provide filler material for concrete production with the aim to lower CO_2 emissions associated with concrete production. As this specific study fits into a larger research project aimed at replacing 100% Portland cement with biomass ash, the main objective is to obtain biomass-derived ash featuring hydraulic properties. Unlike previous investigations into biomass derived ashes, which have focused more on ashes which contain significant quantities of SiO_2 (like rice husks and sugar cane bagasse ashes), this investigation sought ashes that would function hydraulically. A high calcium to silicate ratio (as in OPC) was preferred since this is required for the presence of hydraulic calcium silicate minerals. A pozzolanic reaction would not be ideal since that can only take place in the presence of hydrating clinker producing alkalinity or an alkali activator. Therefore, the focus of this specific study was on calcium rich biomass ash that could potentially contain minerals such as alite (C_3S) and belite (C_2S). Since biomass derived ash is commonly produced at relatively low combustion temperatures (depending on the combustion technique applied from 650 up to 900 °C) it is hypothesized in this study that belite-like minerals rather than alite-like minerals can be expected as alite requires higher combustion temperatures (1350-1450°C) [9, 10]. In this regard, the selected biomass derived ashes will likely perform more in line with class C fly ashes.

The benefit of replacing OPC with three different types of woody biomass derived ashes obtained in the production of energy (in the form of heat and electricity) is investigated. The goal is to replace the largest quantity possible and still achieve compressive strengths of mortars comparable to those produced with pure OPC. It is hypothesized that the ash with the highest calcium to silica ratio (i.e. the highest calcium content) has the largest probability of containing belite and will thus perform the best.

2 Materials and Methods

2.1 Materials: Biomass Derived Fly Ashes

In this specific study, three different types of biomass-derived ash were examined. All of these ashes were produced with woody biomass as a raw material. Woody biomass was specifically chosen due to the elevated concentrations of calcium often found in the resulting ash (see Chapter 3). The Energy research Centre of The Netherlands (ECN) provided all of the ashes used in this specific study.

The first ash, Paper Sludge Fly Ash (PSFA) originated from the Swedish incineration plant, Hylte Stora Enso. Using virgin wood and recycled paper, the plant produces pulp, which is used to make the paper for newspaper production. Hylte Stora Enso has 4 thermal installations for heat recovery and energy production. The fly ash was sampled from the bubbling fluidized bed incinerator that is fed by fuel consisting of a mixture of waste paper sludge and recovered waste wood. The cleaning system of the flue gas which is generated during the biomass incineration process includes an electrostatic filter, a textile bag filter and a scrubber intended to remove dust, dioxins, and other pollutants. The investigated ash is composed of fly ash collected from the electrostatic filter (90% by mass) and the textile bag filter (10% by mass).

The second ash (WBFA-1 - Woody Biomass Fly Ash) comes from the combustion of wood pellets in Rodenhuize power station which is an 180MW pulverized fuel combustion plant dedicated to biomass combustion in Ghent, Belgium. One third of the wood pellets comes from Canada and 45% from the United States of America.

Finally, the third ash (WBFA-2) is derived from a mixed clean biomass from the biomass power plant in Cuijk, The Netherlands. This is an 80 MW(th) bubbling fluidized bed combustor. It burns only clean biomass, but of a large variety. The bulk of the fuel is woody biomass from maintenance of parks and roads. Occasionally it utilizes cacao husks, molasses or any other waste material that is also considered as clean biomass.

While this specific study focuses only on woody biomass sources (albeit with three individual ash compositions and two different conversion technologies) the methodology can be applied in other regions to any biomass or conversation technology available. Importance must be given to the consistency (element composition) of ash streams or rather biomass input. Material quantity and consistency are important factors when replacing the relatively well defined OPC, and as a consequence of these criteria, many biomass- and waste product sources might not be suitable due to high variability in element composition and quantity available. Ashes must therefore be characterized first.

2.2 Methods: Ash Characterization

Initial information on the ashes (and the biomass categories they fit into) is presented in chapter 3, however a more in-depth analysis of these individual ashes is presented here. X-ray fluorescence (XRF) was used to determine the elemental composition using a Panalytical Epsilon 3XL XRF. The corresponding oxide composition was calculated from the elemental composition using the cement oxide method.

X-ray diffraction was performed on the ashes to obtain a qualitative mineralogical analysis of the crystalline phases using a Philips PW 3020 X'Pert Diffractometer. The energy source was CuKα (1.789Å) and the tube settings were 45 kV and 30 mA. Step scans were performed from 5-70° 2θ at 0.03° 2θ steps and at a rate of 3.0 seconds per step. Diffraction patterns were analysed using Qual X software.

The particle size and particle size distribution of ashes was measured using a laser beam particle size analyzer (Mastersizer S Ver. 2.19, Malvern Instruments Ltd., Malvern, U.K.). Particles between 0.1μm and 1000μm were measured as an aqueous suspension of dispersed particles passed through a laser beam and the angle of diffraction was measured. Additionally, the diameters at which 10, 50 and 90% of the particles were smaller than (i.e. D(10) D(50) and D(90)) were determined and compared to that of a CEM I 42.5 N [ENCI], to evaluate the particle size distribution.

Table 7: Mixture proportions of ash blended cement mortars [grams].

	Ash	CEM I	Fly Ash	Sand	Water	Super
OPC	0%	1800	0	5400	900	-
OPC +SP	0%	1800	0	5400	900	22.5
40% WBFA-1	40%	1080	720	5400	900	-
20% WBFA-1	20%	1440	360	5400	900	-
40% WBFA-2	40%	1080	720	5400	900	-
20% WBFA-2	20%	1440	360	5400	900	-
80% PSFA +SP	80%	360	1440	5400	900	22.5
60% PSFA +SP	60%	720	1080	5400	900	22.5
40% PSFA	40%	1080	720	5400	900	-
20% PSFA	20%	1440	360	5400	900	-

Water to binder ratio (OPC + Ash) 0.50; Binder to sand ratio 1:3

2.3 Methods: Preparation of Mortar Specimens

Initially the ashes were used to replace 20 and 40M.-% OPC in a standard mortar mixture based on EN 196-1. These "lower" replacement rates were tested for all three ashes to determine how they function as a supplementary cementing material. Performance was evaluated based on the compressive strength development of the samples compared to that of a 100% OPC control. Additionally, replacement rates of 60 and 80 M.-% were tested with PSFA, which performed best at 20 and 40M.-% replacement rates of the three ashes investigated. The mortar mixture proportions are given in Table 7. The water to binder ratio (i.e OPC + Ash) was set at 0.50 and the binder to sand ratio was set at 1:3. For each mixture and testing day, 6 specimen were made. In order to achieve a functional workability, super plasticizer was required for the 60 and 80% replacements. For this reason, two different controls of 100% OPC were made, one with super plasticizer and one without. OPC denotes the control mortar made with pure Portland cement and OPC+SP denotes the pure Portland mortar control with super plasticizer. The flexural and compressive strengths of mortar prisms were tested after 3, 7, 28 and 90days curing.

3 RESULTS

3.1 Ash Analysis

3.1.1 Elemental Composition

The elemental composition of the three types of ashes investigated is listed in Table 8 for the major compounds (i.e. elements exceeding 0.15% mass of the sample). The corresponding oxide composition, calculated using the cement oxide method, can be found in Table 9.

Table 8: Elemental composition of three types of biomass derived fly ashes determined by X-ray fluorescence [M.-%].

Compound	Ca	Si	Al	Fe	Ti	Mg	Zn	K	S	Cl
PSFA	44.24	3.39	1.52	1.20	0.58	0.41	0.37	0.36	0.34	0.32
WBFA-1	30.11	2.94	0.47	2.80	0.22	0.81	0.19	10.27	1.49	0.86
WBFA-2	22.69	5.13	0.71	1.68	0.14	1.16	0.30	4.91	1.97	0.10

Table 9: Calculated oxide composition of the biomass derived ashes as determined using the cement oxide method [M.-%].

Compound	CaO	SiO_2	Al_2O_3	Fe_2O_3	SO_3	TiO_2	MgO	K_2O	ZnO	LOI 950 °C
PSFA	74.00	10.46	4.20	1.84	1.19	1.04	0.99	0.56	0.49	3.99
WBFA-1	42.21	11.83	1.93	3.41	3.72	0.28	4.57	11.79	0.18	15.29
WBFA-2	40.71	17.94	2.24	2.75	7.47	0.27	3.29	8.23	0.42	10.26

The element composition of the three types of woody biomass derived fly ashes appears to be different as can be concluded from Table 8 and Table 9. It can be immediately concluded that PSFA is rich in Ca (74% calculated CaO) while WBFA-1 and -2 contents are substantially lower (42 and 41%

calculated CaO respectively). To be a potentially suitable fly ash for cement replacement according to EN 450 [7], the content of reactive calcium oxide should not exceed 10.0 % by mass. All of the ashes under investigation exceed this amount based on the calculations however the calcium may be present in minerals other than calcium oxide. In the case that the calcium is present as a calcium silicate, then the ash is more applicable as a hydraulic binder or a latent hydraulic binder and less as a pozzolanic filler.

The calculated SiO_2 quantities on the other hand are relatively low (10 to 18% SiO_2) for the three analysed ashes in comparison to both OPC and fly ash. For application as a fly ash, the amount of reactive SiO_2 should exceed 25 M.-%, since the fly ash should function pozzolanically (however this is not the objective of this work). Furthermore, to be classified as a Class C fly ash the $SiO_2+Al_2O_3+Fe_2O_3$ content must exceed 50% and to be classified as a Class F fly ash the $SiO_2+Al_2O_3+Fe_2O_3$ content must exceed 70%. In the case of PSFA, WBFA-1 and WBFA-2 this sum fell below the stipulated amount with 16.5, 17.2 and 23.0 M.-% respectively.

Additionally, the adverse oxides known to correlate to poor field performance of concrete products are also regulated and limited for fly ashes according to EN 450. The SO_3 content for fly ash must not exceed 3 M.-%, which only PSFA satisfies. WBFA-1 and WBFA-2 exceed this threshold with contents of 3.7% and 7.5 M.-% respectively. Fly ash obtained from the combustion of pulverised coal is typically low in MgO however the combustion of biomass can introduce magnesium oxide into the ash. Since EN 450 allows for the usage of co-combustion ash, the maximum MgO content is stipulated. Only WBFA-1 exceeds the 4.0 M.-% tolerance. Furthermore, the alkali content of fly ash is particularly noteworthy since excessive amounts can cause efflorescence in concrete or reduce the mitigation of an alkali-silica reaction [11]. Higher MgO contents are more typical of granulated blast furnace slag where contents can range from 8-13 M.-% and still provide sufficient strength development in the presence of an alkaline activator [12].

Cement producers take extreme measures to control alkali content of cement within specific ranges by controlling raw materials and manufacturing processes. Alternatively, fly ash is a by-product and as such no actions are taken to limit the alkali content beyond the selection of the coal to be combusted. In order to be acceptable under EN 450, the total content of alkalis (Na_2O_{eq}) should not exceed 5.0 M.-%. Since Na_2O_{eq} is equal to the sum of Na_2O and 0.658 x K_2O only PSFA satisfies this requirement. Both WBFA-1 and WBFA-2 exceed the Na_2O_{eq} limit based on the high K_2O values alone (11.8 and 8.2 M.-% respectively)

3.1.2 Mineral Composition of Biomass Derived Fly Ashes

X-ray diffraction (XRD) was performed to obtain a qualitative mineralogical analysis of the crystalline phases. As can be seen in Figure 27, PSFA consists mainly of CaO (lime) and SiO_2 (quartz). However, calcium silicate and gehlenite ($Ca_2Al(AlSiO_7)$), were also present. Trace amounts of portlandite were detected, as they were for all of the ashes; this is most likely the result of poor storing conditions which allowed ambient H_2O to interact with calcium oxide and form $Ca(OH)_2$. The occurrence of the elements calcium, silica and oxygen present in these minerals corresponds well to the XRF results. The two WBFAs showed significantly higher levels of SiO_2 than PSFA as can be seen in the relative intensity of the quartz peaks. For both of these ashes, quartz had the most intense peak. In WBFA-1 SiO_2 was followed closely by calcite indicating that this mineral also represents a significant portion of the crystalline fraction. However, in the case of WBFA-2 there is a significant difference in the intensity of the SiO_2 peak and those of all the remaining phases. Both of these ashes also showed arcanite (K_2SO_4) to be present, which agrees well to the detection of potassium in the XRF (a higher percentage being found in WBFA-1 relative to WBFA-2 mirroring higher relative intensities of arcanite peaks in the XRD graph of WBFA-1).

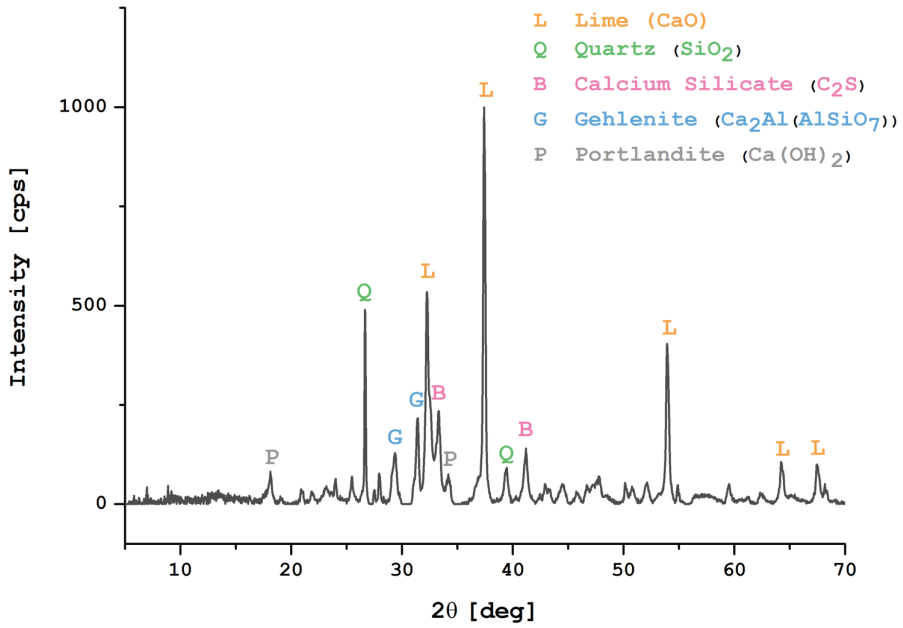

Figure 27: Typical example of and XRD graph of a paper sludge derived fly ash (PSFA) sample showing distinct peaks of crystalline lime, quartz, calcium silicate, gehlenite and portlandite minerals.

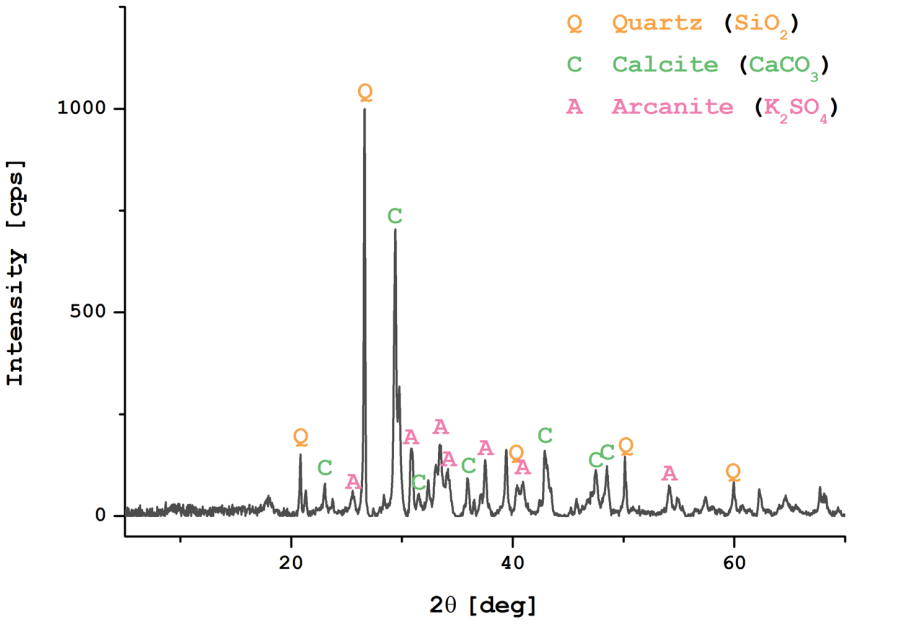

Figure 28: Typical example of and XRD graph of a woody biomass derived fly ash (WBFA-1) sample showing distinct peaks of quartz, calcite and arcanite minerals.

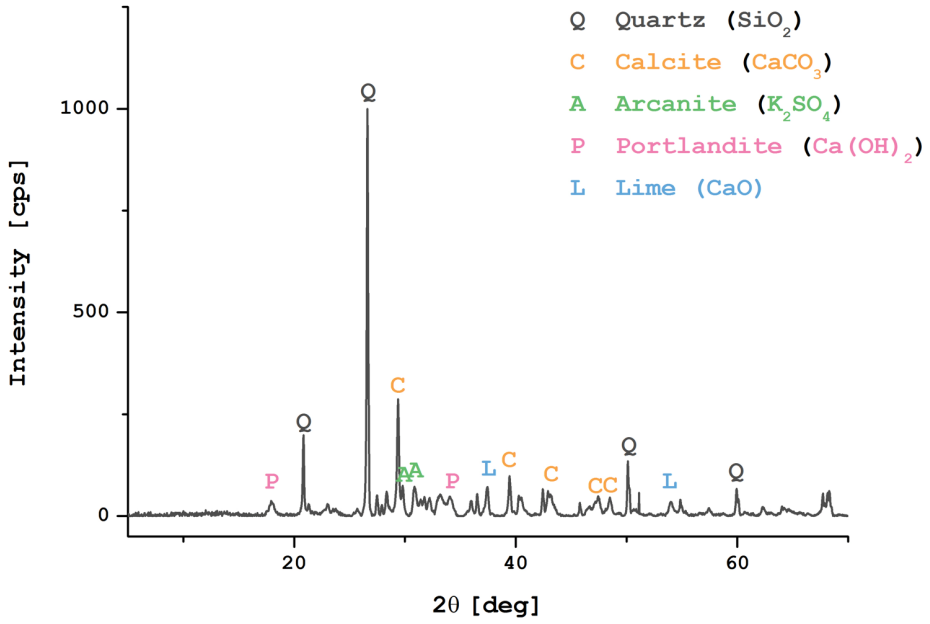

Figure 29: Typical example of and XRD graph of a woody biomass derived fly ash (WBFA-2) sample showing distinct peaks of quartz, calcite, arcanite, portlandite and lime minerals.

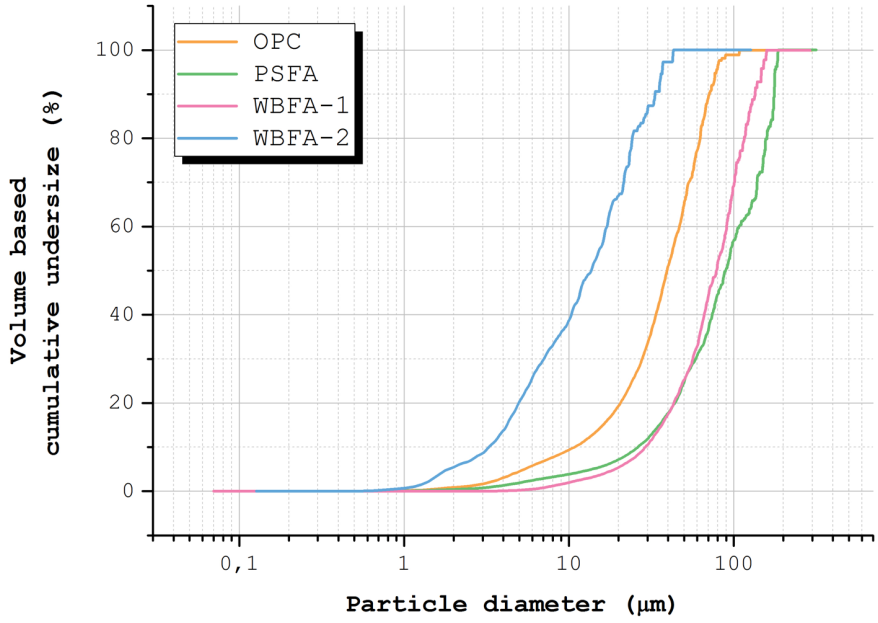

Figure 30: Particle size distribution depicted though volume based cumulative undersize for OPC, PSFA, WBFA-1 and WBFA -2. The three ashes appear to have similar particle size distributions to OPC; however, WBFA-2 particle size appears smaller on average while the PSFA and WBFA-1 appear larger.

3.1.3 Particle Size and Distribution

The particle size distributions for the OPC as well as the ashes PSFA, WBFA-1 and WBFA-2 can be viewed in Figure 30 as traditional S-curves for cumulative volume based diameter-undersize. This diagram shows that the three ashes have similar distributions to OPC, however, the WBFA-2 ash particle size was smaller on average while the PSFA and WBFA-1 ashes were larger.

The intercepts of the curves at 10%, 50% and 90% are commonly used to represent the midpoint and range of the particle sizes of a given ash. Furthermore, they serve as values of comparison to relate and evaluate the different ashes. These values are referred to as the D(10), D(50) and D(90), where D(10) is the diameter at which 10% of a sample's volume is comprised of smaller particles. Similarly D(50) is the diameter at which 50% of a sample's volume is comprised of smaller particles and D(90) is the diameter at which 90% of a sample's volume is comprised of smaller particles. The D(10), D(50) and D(90) can be viewed in Table 10. WBFA-2 was the smallest ash with the D(90) being closer to the D(50) of CEM I and D(10) of PSFA and WBFA-1. Both PSFA and WBFA-1 had the largest D(10) D(50) and D(90).

Table 10: Diameter for which 10% 50% and 90% of the ash particles sizes are smaller, for CEM I, PSFA, WBFA-1 and WBFA-2. WBFA-2 particles are substantially smaller while both PSFA and WBFA-1 particles are substantially larger than CEMI particles [μm].

	D(10)	D(50)	D(90)
CEM I	10.84	39.26	71.28
PSFA	26.29	89.13	175.96
WBFA-1	29.18	78.54	126.31
WBFA-2	3.34	13.71	33.34

3.2 Compressive Strength of Mortar Specimens

The main objective of testing the biomass derived fly ashes as supplementary cementing materials was to see the extent to which they could replace OPC and still achieve an acceptable compressive strength. Their results are viewed in relation to a 100% OPC control. Description is split into two groups: the lower replacement rates (20 and 40 M.-%) for all of the ashes, and the entire suite of PSFA which includes replacement rates 20, 40, 60, and 80 M.-%.

3.2.1 Lower Replacement Rates

In Figure 31, the compressive strength of mortar samples for all three ashes at the lower replacement rates can be seen. It is immediately apparent that all ashes performed very differently, however they did follow similar trends. The 40% replacement specimen achieved lower strength than the 20% replacement specimen across all ashes. While none reached the strength of the control CEM I specimen, some difference in performance for the three different types of ashes was observed. Among the specimens with 40% replacement, PSFA achieved the highest strength at older ages (> 28 days) while the WBFA-1 performed the worst. In fact, the PSFA 40% replacement had a higher strength than the WBFA-1 20% replacement at later age (≥28 days). WBFA-2 ≥ 28 days at 40% replacement's performance fell between the other PSFA. The WBFA-2 specimen at 3, 7 and 28 days at 20% replacement achieved higher strength than PSFA at 20% replacement but at 90 days the PSFA performed better. Both PSFA and WBFA-2 at 20% replacement did not reach the strength of the control CEM I specimen at 28 days however they did exceed the required 42.5 MPa for 28 days old

specimen. WBFA-1 at 20% replacement did not reach the required 42.5 MPa at 28 days nor at 90 days.

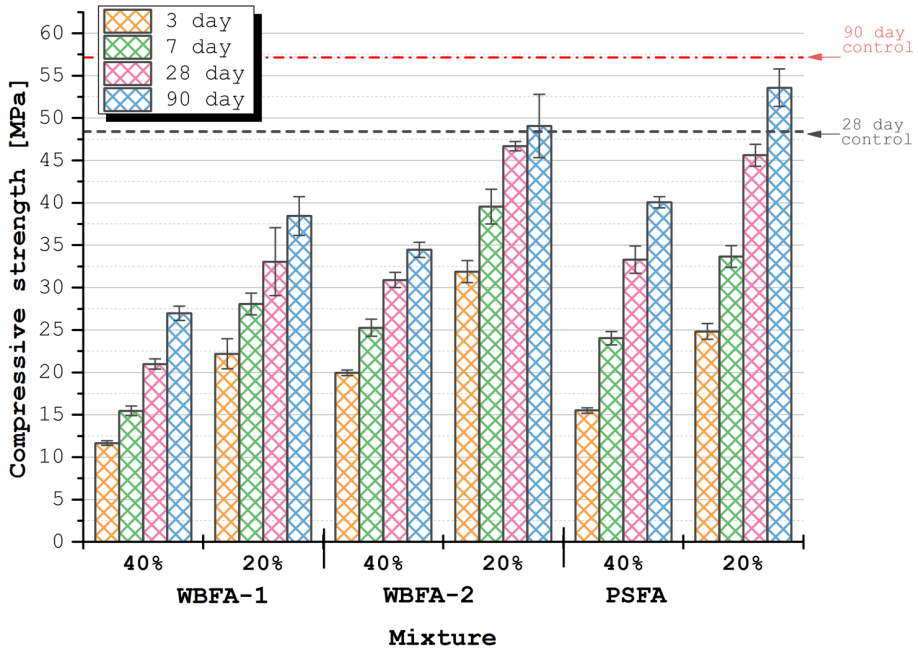

Figure 31: Compressive strengths after 3, 7, 28 and 90 days for mixes with 40 and 20 M-% OPC replacement with WBFA-1, WBFA-2 and PSFA relative the 100% OPC control at 28 and 90 days (dotted lines). Both WBFA-2 and PSFA based specimen at 20% OPC replacement reached the minimally required 42,5 MPa strength at 28 days.

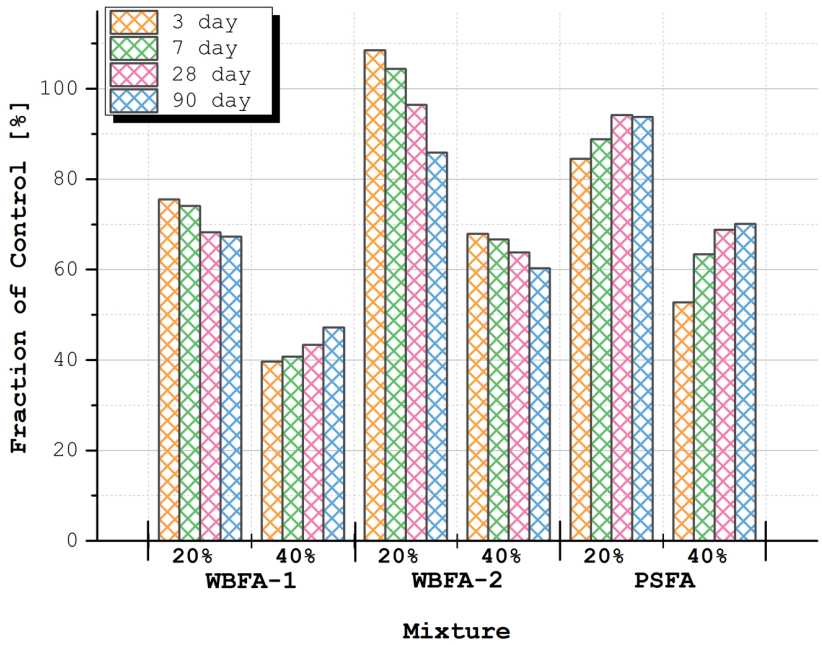

Figure 32: Compressive strengths shown as a percentage of the control for 20 and 40 M.-% replacement OPC with WBFA-1, WBFA-2 and PSFA at 3, 7, 28 and 90 days.

Considering the strengths as percentage of the control specimen compressive strength (Figure 32) at all specimen ages, some specific trends appear. From this perspective, it is apparent that WBFA-1 at 40% and PSFA at both replacement percentages relatively improve in strength with age in comparison to 100% OPC specimen, while the remaining ashes show a relative decrease in strength in time.

3.2.2 Higher Replacement Rates

Based on the results of the lower replacement rates, PSFA was selected to be tested at higher replacement rates. Since the main objective of this research is to replace as much OPC with biomass derived materials as possible, while keeping the energy investment as low as possible (thereby limiting the total CO_2 emissions), it is important to test the extent to which biomass derived ash can replace OPC. It is also interesting to note what strengths are achievable because, while they may fall below what is dictated by the standards, they could still be useful for specific (e.g. low strength) applications.

The pure OPC samples gained the highest strengths and as can be seen in Figure 33, and strengths decreased with increasing replacement rates. It is interesting to note that the 100% OPC mixture had a higher compressive strength than 100% OPC with super plasticizer. This is due to the large superplasticizer dosage that was necessary to accommodate the mixture of 20% OPC and 80% paper sludge derived fly ash and was therefore also applied as extra control for the 100% OPC specimen. The large particle size and the porous structure of the fly ash particles would have otherwise demanded a higher water content to achieve a functional workability. The superplasticizer dosage was based on the water content (since the cement value varied with replacement) and was kept at 2.5 M.-%. For the mixture containing 60% PSFA and 40% OPC this provided a good workability. However, the dosage was not optimal for the 20% (plus 80% PSFA) or 100% OPC. The 20% OPC was still stiff with 2.5% super plasticizer but was able to be compacted into the form with no extra vibration. The 100% OPC mixture blend when poured into the mould, indicating too high of a super plasticizer dosage. Despite these undesirable characteristics, the super plasticizer dosage was still kept constant in order to achieve results that could be compared.

A closer examination of the 90 day compressive strengths is shown in Figure 34. The 100% OPC samples had an average compressive strength of 57 MPa whereas the 100% OPC + SP sample had a compressive strength of 51 MPa; these two values serve as the controls. The 20% PSFA reached 53 MPa which is 94 % of the control sample. The 40% PSFA sample reached 40 MPa which is 70% of the control. The 80% PSFA and 60% PSFA samples are compared to the 100% OPC+SP samples since they also contain super plasticizer. After 90 days, the 80% reached 11 MPa and the 60% reached 31 MPa which are 22% and 61 % of the control respectively.

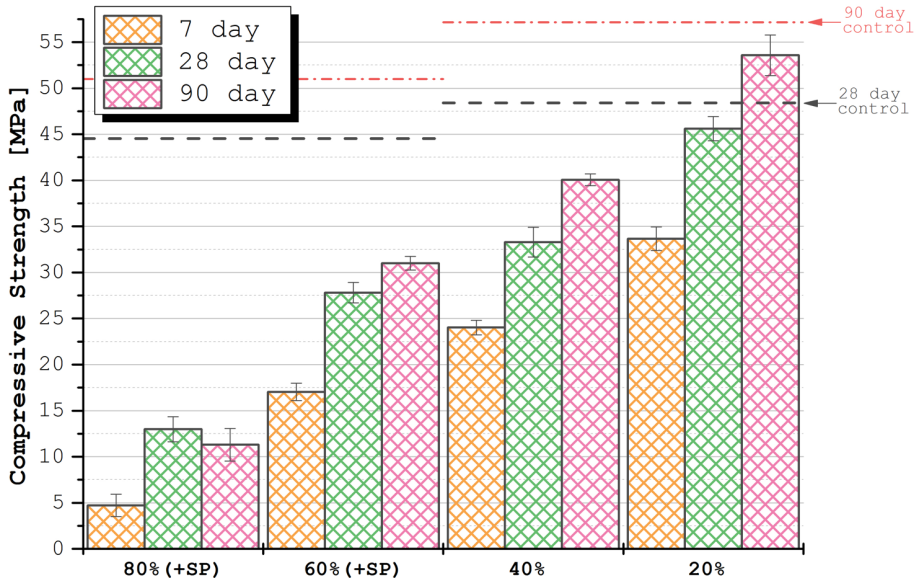

Figure 33: Compressive strengths after 7, 28 and 90 days for mixes with 20, 40, 60, 80 M.-% PSFA. The 80% and 60% mixtures contained super plasticizer (+SP).

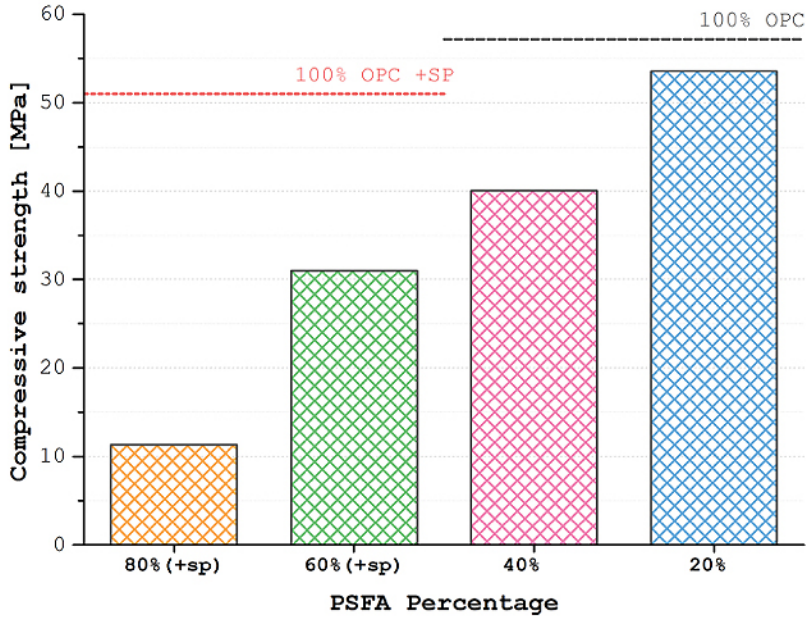

Figure 34: 90 day compressive strength values of 80, 60, 40 and 20% PSFA relative to the two controls (100% OPC and 100% OPC with super plasticizer).

4 DISCUSSION

4.1 Ash Analysis

4.1.1 Composition of Biomass Derived Fly Ashes

As reported in literature considering the heterogeneity of the element composition of woody biomass derived ashes, not only are the wood species and tree parts (roots, bark, leaves, branches, limbs, trunks and vines) influencing factors, but also the growing conditions and the application of the material prior to utilization as an energy source play a role [13]. In addition to pulp and paper mills and demolition wood, woody biomass can stem from numerous sources including: logging residues, forestry thinnings, sawmill residues, urban waste wood, trimmings from parks and road maintenance, and trees grown specifically as energy crops.

The three ashes used in this study were selected based on the results of a previous study (Chapter 2). Based on the analysis of different biomass sources these ashes were chosen because their CaO and SiO_2 contents were expected to be close to the range required for OPC raw feed. Typically calcium, silicon, aluminium, potassium and magnesium dominate wood ash composition [13] [14]. As expected, elevated concentrations of CaO were found in the ashes but the content in PSFA was higher than the rest (74.0 M.-%). This is most likely due to the lime used in the paper de-inking process. Additionally, the CaO oxide content is calculated from the elemental composition and does not account for Ca incorporated into other minerals. As shown in the mineralogical analysis Ca was present in not only CaO but also portlandite, C_2S and gehlenite (the latter two being calcium silicates).

To be a suitable fly ash for cement replacement EN-450 suggest that the amount of free lime present be limited to 1.5 M.-% to avoid problems with volume stability otherwise the ash must be tested for conformity to the requirements for soundness. The amount of reactive calcium oxide cannot exceed 10 M.-%. Based on the XRD results, PSFA definitely exceeded this threshold. The two WBFA ashes also had significant quantities of calcite present. Calcite can function as an active participant in the hydration process or as an inert filler [15]. While the reaction of calcite can result in volume changes they are not necessarily associated with changes to the external dimensions. However calcite is known to affect both the porosity and permeability of Portland cement pastes, although no consistent patterns seem to emerge [16-19]. Furthermore, in the three analyzed ashes SiO_2, Al_2O_3 and Fe_2O_3 were present, however the total of these oxides fell below the required amount necessary to be applicable as a fly ash (50 or 70 M.-%). Therefore, their performance as OPC replacements was expected to rely on hydraulic minerals instead of a pozzolanic reaction. Thus, comparisons to the composition of cement is of more interest than comparisons to the composition of fly ash. With the objective applying a secondary thermal treatment (see chapter 6) or altering the initial thermal conversion parameters, then comparisons to the composition of cement raw meal is also of interest. PSFA is distinct in that it is the only ash which already contained clinker minerals, namely C_2S (Figure 27).

Additionally, to be applicable as a cement raw material the SiO_2 content should fall between 18.6 and 23.4 M.-%, Al_2O_3 content should fall between 2.4 and 6.3 M.-% (PSFA and WBFA-2 satisfy) and the Fe_2O_3 content should fall between 1.3 and 6.1 M.-%. PSFA had sufficient Al_2O_3 and Fe_2O_3, however the SiO_2 content was only 56% of the desired amount. WBFA-1 only had sufficient amounts of Fe_2O_3. WBFA-2 had sufficient Al_2O_3 and Fe_2O_3 concentrations and the SiO_2 content was 96% of the desired amount [20].

The intention behind a chloride limit is to reduce the risk of corrosion of embedded reinforcement. For all cement types and strength classes the chloride content should be below 0.1 M.-% [2]. The same threshold exists for fly ashes [7]. While all three ashes contained less than 1.0 M.-% Cl, only WBFA-2 meet the requirement of less than 0.1 M.-%.

None of the investigated ashes contained P_2O_5 above 0.15 M.%. Since this is below the threshold of concern they should be no adverse effects on the reaction mechanism or performance as a result of phosphorous. Both WBFA-1 and WBFA-2 had significant quantities of alkalis present in the form of potassium (11.79 and 8.23 M.-% respectively). The potassium was determined in the XRD to be present in both ashes as arcanite (K_2SO_4). Arcanite can affect the strength development through an increase in the alkalinity of the pore fluid. This is associated with accelerated alite hydration and higher earlier strengths [21]. Higher early strengths were observed for the 20% replacement with WBFA-2.

Based on the compositions of the biomass derived ashes it can be concluded that none of the ashes are directly applicable as a cement replacement or cement raw material replacement. Of the investigated ashes, PSFA had the most ideal composition for potentially replacing cement raw material due to the existing presence of C_2S and the high CaO concentrations. Given alternative thermal treatments (either during the initial combustion of the biomass or a secondary heat treatment of the ash) the CaO and SiO_2 can form additional C_2S or new C_3S.

4.1.2 Particle Size and Distribution

Since the particles are aimed to replace OPC, a similar or smaller size and distribution to that of OPC was sought after. The particle size is important to keep in mind when analyzing the compressive strengths of mortar samples because certain advantages are associated with smaller particles that can be reflected in strength gain. For example, smaller particles have a larger surface area providing more area to react for a particular amount. An increase in surface area also offers more nucleation sites. Additionally, smaller particles can contribute to the filler effect.

Since both PSFA and WBFA-1 were larger (D(50) = 89.13 and 78.54 μm respectively) than CEM I (D(50) = 39.26 μm), it can be expected that they are less effective at contributing to strength development than WBFA-2 which was smaller (D(50) = 13.71 μm) assuming the same reactivity. Overall WBFA-1 had the lowest strength performance. At 20% replacement, WBFA-1 did not reach either the range of the control or the goal of 42.5 MPa. This could be a result of the larger particle size and distribution observed. In its unaltered state, WBFA-1, provides significantly less strength development at 20% replacement or beyond. Reducing the particle size could enhance the reactivity and packing density which would be reflected in a higher strength development.

Despite the larger particle size PSFA showed higher strength development than WBFA-2 at later ages. This is possibly due to the chemical properties of the ash being more critical than the physical properties, supporting the hypothesis that PSFA contains reactive calcium silicates. Since PSFA was chemically more reactive, it did not just depend on the advantages of an optimized packing density and increased nucleation sites, whereas WBFA-2 benefited from these physical features at early ages.

4.2 Mortar Compressive Strength

4.2.1 Lower Replacement Rates

Relative strength decrease in comparison to control specimens indicates a decreased cement hydration probably meaning that the fly ashes mainly function as filler and over time provide no chemical reaction to contribute to strength development. What is most striking (see figure 6) is that the WBFA-2 at 20% replacement actually achieves strengths above the control at 3 and 7 days. This advantage decreases over time but, as indicated before, at 28 days it still remains close to the 100% OPC strength. This could be result of the finer particles enhancing the packing density as well as promoting the early hydration of OPC through the introduction of nucleation points. Alternatively, it could be the presence of arcanite increasing the reaction rate of alite. These results can also be viewed as the development of strength over time (as shown in Figure 35). All three ashes followed a similar

curve for both of their replacement percentages. The rates of strength development for the PSFA mixtures were significantly higher at early ages and did not level off to the same degree as the other mixtures by 90 days. Despite an initially lower compressive strength, the PSFA 20% replacement gained on the strength relative to WBFA-2 20% replacement after 90 days curing. This is also roughly the time that the PSFA 40% outperformed the WBFA-1 20% too. PSFA 40% had already developed a higher strength than WBFA-2 40% by 28 days. While not initially performing the best, replacement with PSFA eventually reached the highest strength per replacement percentage and improved at the fastest rate. These results can be seen as an indication of a pozzolanic reaction of PSFA, i.e. it is providing a cementing reaction that is dependent upon the hydration of the OPC and concomitant $Ca(OH)_2$ production (activator for pozzolanic activity) and cannot fully contribute to strength development without the progression of that reaction. Alternatively, the observed (delayed) strength increase over time could also be the result of belite (C_2S) being present specifically in the PSFA ash. Belite is known to react slower than alite and by replacing the OPC with PSFA, the alite fraction is reduced, while the belite fraction is relatively increased. Since there was both SiO_2 and C_2S present in the ash it is likely that the observed delayed strength development is the result of a combination of the two. Since the WBFA-2 (at both replacement rates) initially achieved relatively good compressive strengths but levelled off relatively quickly, and did not contain C_2S, it can be assumed that this specific ash contributes to optical particle packing and hydration enhancement due to its fine particle size.

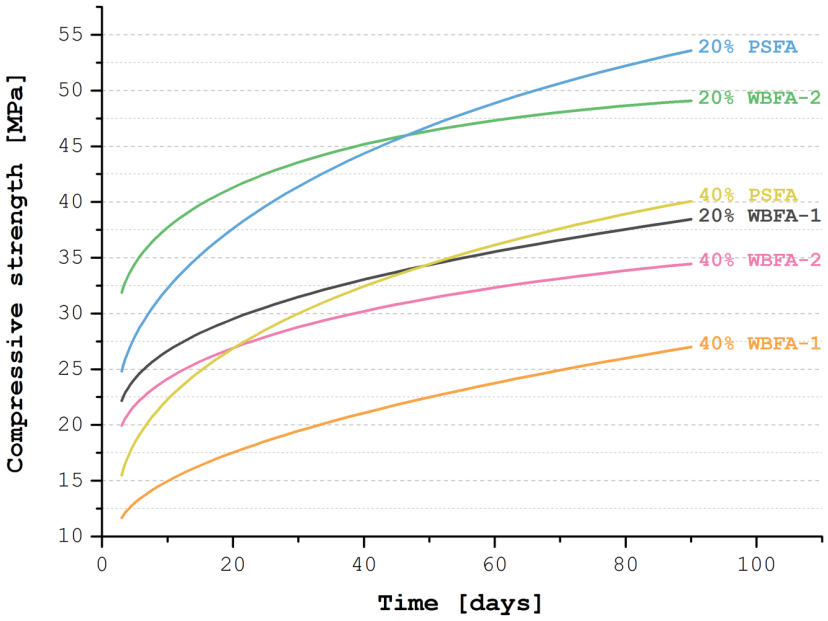

Figure 35: The development of compressive strength between 7 and 90 days PSFA WBFA-1 and WBFA-2 at 20% and 40% replacement of cement.

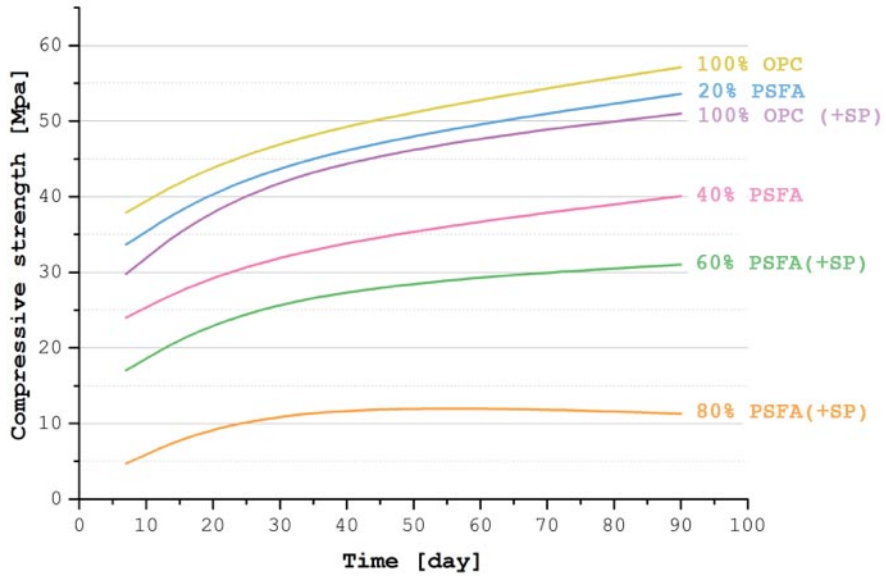

Figure 36: The development of compressive strength of mortar samples based on 100% OPC binder or OPC being partially replaced for paper sludge derived fly ash (PSFA) (% indicates amount of OPC).

4.2.2 Higher Replacement Rates

Since the 80% PSFA sample only reached 22% of the control it can be assumed that there is little to no binding effect of the fly ash. Relative to the control, the 60% PSFA performed the best since it achieved 61% of the strength. A look at the strength development over time (as in Figure 36) can also give valuable information. After 28 days, typically only 30% of the present C_2S will potentially have reacted whereas 70% of the C_3S will have reacted. However within 1 year, 90% of the C_2S will have hydrated [9]. Since the development of compressive strengths is corresponding to the chemical cementitious reactions, an increase or decrease in the rate of hydration could indicate which type of cementitious minerals are present. Replacing a fraction of the cement with fly ash means a dilution of the four main cement minerals (C_3S, C_2S, C_3A and C_4AF) with the minerals present in the ash. From the XRD (see Figure 27), it is known that the specific paper sludge derived fly ash is mostly composed of lime and quartz. However, there is some belite present, as well as gehlenite. These two minerals can contribute to strength development at later ages, as these are typically slow reacting minerals. Quartz is also present in the ash but it is not known how reactive this form of SiO_2 actually is. In terms of pozzolanic reaction, a more amorphous SiO_2 will display higher reactivity, while the crystalline form of quartz provides little strength development.

When looking at the slopes of the curves in Figure 36, reflecting the rate of cementitious reactions, there are two segments which immediately stand out; the first being the 100% OPC + SP mixture between 7 and 28 days, as it shows a higher rate of hydration in comparison to the other mixtures. The second most apparent segment is for 80% PSFA between 28 and 90 days, which shows a lack of strength increase. This is most likely the result of the overall low hydraulic activity of the mixture. Aside from these two occurrences, the rates of strength development are fairly similar with a slight tendency for a faster rate for lower replacement rates (i.e. more OPC). It is interesting to note that the 20% PSFA mixture had an apparent higher rate of hydration than the 100% OPC control between 7 and 28 days, only to fall to approximately the same rate between 28 and 90 days. This indicates the presence of an early reacting mineral in the fly ash. However, for the 40% PSFA sample, there is a reduction in the rate of strength development for the first-time segment. This is probably the result of too high of a dilution of the cement minerals despite the early reactivity of some specific mineral present in the fly ash.

Based on these observations it can be concluded that this particular paper sludge derived fly ash is suitable for replacing 20% of OPC, as it still achieves the target compressive strength after 28 and 90 days hydration. Higher replacement (40%) rates are possible however the compressive strength was only 78% of the targeted 42.5 MPa after 28 days. Higher strengths could possibly be achieved at these higher replacement rates if the ashes would be pretreated prior to application, e.g. by grinding as this would increase the specific reactive surface area, or by thermal treatment as this could possibly increase amount and types of specific cementing minerals such as belite or alite. This would however require additional energy, and thus CO_2 emissions, and potential gain in economic and environmental benefit would need to be quantified.

5 CONCLUSIONS

- All biomass derived ashes achieved lower compressive strengths than that of pure OPC. Replacement of 20% OPC with the woody biomass and paper sludge-derived ashes WBFA-2 and PSFA respectively provided sufficient strength to satisfy the 42.5 MPa standard. The strength with 20% replacement using WBFA-1 however fell short of this goal. At 40% replacement, the PSFA mixture still achieved a relatively high strength (40.1 MPa) by 90 days. PSFA performed presumably better than both the WBFA ashes due to the presence of reactive calcium silicates.
- Both WBFA-1 and WBFA-2 contributed more to early strength development whereas the positive effect of PSFA increased with time. At 3 and 7 days WBFA-2 even provided strengths higher than pure OPC when used to replace 20%. Since WBFA-2 was the only ash to have a particle size distribution smaller than OPC it is assumed that this is the result of increased nucleation sites and particle packing.
- Methods of upgrading the biomass derived ash (i.e. alterations to the particle size and distribution) to improve their performance as a BioSCM need to be further explored.
- Biomass derived ash is applicable in OPC replacement for applications where lower or slower hydration is desired.
- To replace traditional OPC with biomass derived ashes, the effect on the overall CO_2 emissions must be quantified to justify the lower strengths and ascertain the usefulness of such objectives.

6 REFERENCES

1. Mehta, P.K. and P.J.M. Monteiro, *Concrete: microstructure, properties and materials*. 2006: McGraw-Hill.
2. EN-197-1, *Cement - Part 1: Composition, specifications and conformity criteria for common cements* 2011. p. 1-39.
3. Hewlett, P.C., *Lea's chemistry of cement and concrete*. 2004: A Butterworth-Heinemann Title.
4. Zhang, M.H. and V.M. Malhotra, *High-performance concrete incorporating rice husk ash as a supplementary cementing material.* Aci Materials Journal, 1996. **93**(6): p. 629-636.
5. Horsakulthai, V., S. Phiuvanna, and W. Kaenbud, *Investigation on the corrosion resistance of bagasse-rice husk-wood ash blended cement concrete by impressed voltage.* Construction and Building Materials, 2011. **25**(1): p. 54-60.
6. Giron, R.P., et al., *Fly Ash from the Combustion of Forest Biomass (Eucalyptus globulus Bark): Composition and Physicochemical Properties.* Energy & Fuels, 2012. **26**(3): p. 1540-1556.
7. EN-450-1, *Fly ash for concrete - Part 1: Definition, specifications and conformity criteria*. 2012. p. 1-34.
8. Berra, M., T. Mangialardi, and A.E. Paolini, *Reuse of woody biomass fly ash in cement-based materials.* Construction and Building Materials, 2015. **76**: p. 286-296.
9. Taylor, H.F.W., *Cement chemistry*. 1997: Thomas Telford Services Ltd.
10. Koppejan, J. and S. Van Loo, *The handbook of biomass combustion and co-firing*. 2012: Routledge.
11. Schlorholtz, S.M., *Alkali Content of Fly Ash–Measuring and Testing Strategies for Compliance.* 2015.
12. Erdoğdu, K. and P. Türker, *Effects of fly ash particle size on strength of Portland cement fly ash mortars.* Cement and Concrete Research, 1998. **28**(9): p. 1217-1222.
13. Olanders, B. and B.-M. Steenari, *Characterization of ashes from wood and straw.* Biomass and Bioenergy, 1995. **8**(2): p. 105-115.
14. Etiégni, L. and A.G. Campbell, *Physical and chemical characteristics of wood ash.* Bioresource Technology, 1991. **37**(2): p. 173-178.
15. Matschei, T., B. Lothenbach, and F.P. Glasser, *The role of calcium carbonate in cement hydration.* Cement and Concrete Research, 2007. **37**(4): p. 551-558.
16. Ingram, K.D. and K.E. Daugherty, *A review of limestone additions to Portland cement and concrete.* Cement and concrete composites, 1991. **13**(3): p. 165-170.
17. Vuk, T., et al., *The effects of limestone addition, clinker type and fineness on properties of Portland cement.* Cement and concrete Research, 2001. **31**(1): p. 135-139.
18. Tsivilis, S., et al., *Properties and behavior of limestone cement concrete and mortar.* Cement and Concrete Research, 2000. **30**(10): p. 1679-1683.
19. Voglis, N., et al., *Portland-limestone cements. Their properties and hydration compared to those of other composite cements.* Cement and Concrete Composites, 2005. **27**(2): p. 191-196.
20. Kosmatka, S.H., B. Kerkhoff, and W.C. Panarese, *Design and control of concrete mixtures*. 2011: Portland Cement Assoc.
21. Cieślik, B.M., J. Namieśnik, and P. Konieczka, *Review of sewage sludge management: standards, regulations and analytical methods.* Journal of Cleaner Production, 2015. **90**: p. 1-15.

CHAPTER 5

MODIFYING CURRENTLY AVAILABLE BIOMASS DERIVED ASH FOR APPLICATION AS SECONDARY CEMENTING MATERIALS (BIOSCMP)

ABSTRACT

Biomass derived ashes of various compositions stemming from woody biomass can function as a cement replacement. There are at least two ways in which biomass-derived fly ashes can potentially contribute to the compressive strength: either through the ideal particle size which facilitates a higher packing density as well as providing more nucleation sites or through a chemical reaction producing additional calcium silicate hydrate (CSH), either pozzolanically or hydraulically. To enhance the compressive strength of concrete made with biomass derived fly ash as a cement replacement (BioSCM), various processing techniques can be implemented on the raw fly ash to improve the way in which that particular ash contributes to strength, i.e. chemically or physically (BioSCMp). Ideally minor adaptations to the ash can improve the contribution to strength development such that higher replacement rates up to 40% can be implemented.

This work evaluates how the functional performance of two different ashes: paper sludge fly ash (PSFA) and woody biomass fly ash (WBFA-1) are effected by grinding and sieving respectively. PSFA was shown to be significantly course than OPC (D(90)=176.0 vs. D(90)=71.3 μm), so grinding to a particle size < 45μm was postulated to enhance the particle packing, increase nucleation sites and mechanically activate the particles. WBFA-1 was shown to have significantly different mineralogical compositions for different sieving fractions (<45, 45-125, >125μm) and it was hypothesized that the different compositions would offer different reaction mechanisms. Altered ashes were used to replace 40% OPC and the effects on the compressive strength relative to the unaltered ashes and pure OPC were evaluated.

Here it is shown that despite more favourable characteristics and compositions, no appreciable gain to the compressive strength was achieved at elevated replacement rates; in fact, lower strengths were observed. Ground PSFA showed 57.1% of the OPC compressive strength at 90 days where as the unground ash showed 70.1%. Furthermore, the three different sieving fractions of WBFA-1 developed between 30.3 32.3 and 29.8% of the OPC strength whereas the unsieved ash was 47.2 %. It is hypothesized that incomplete combustion leaves impurities (or inhibitory compounds) in the ash which are more accessible in the finer fractions. Thus, the modifications tested in this work did not upgrade the quality of the biomass derived ash in their ability to act as a cement replacement and it is suggested that thermal treatments of the ashes should be explored as a means to enhance functional performance with respect to OPC replacement potential.

7 INTRODUCTION

As seen in the previous chapter, biomass derived ashes of various compositions stemming from woody biomass can function as a cement replacement. The individual nature and composition of the ash potentially offers different advantages such as the improvement of early strength or contribution to the total strength development. However, for the three ashes tested in the previous chapter, benefits were only present at lower replacement rates (20 M.-%). For the samples with replacement rates of 40%, the compressive strength of the mortars was significantly lower than the Ordinary Portland Cement (OPC) control and the 42.5 MPa standard.

As a proposed solution to decrease the gap between the compressive strength of the OPC control and that of the samples with higher replacement rates, various processing techniques can be implemented on the raw fly ash to improve the way in which that particular ash contributes to strength (i.e. chemically or physically). Since the overall goal of this research is to replace as much OPC with biomass derived ashes as possible, while investing as little energy as possible (and thereby emitting as little CO2 as possible), it is noteworthy to determine if minor adaptations to the ash can improve the contribution to the strength at higher replacement rates.

As discussed in the previous chapter, there are at least two ways in which these particular biomass-derived fly ashes can potentially contribute to the compressive strength: either through the ideal particle size which facilitates a higher packing density as well as providing more nucleation sites or through a chemical reaction producing additional CSH (either pozzolanically or hydraulically). The incorporation of biomass derived ash in the concrete mixture alters the particle size distribution and is therefore expected to change the resulting compressive strength. For that reason, it is important to investigate the effect of the particle size distribution of the ashes relative to the cement on the resulting compressive strength. Chindaprasirt found that the compressive strength of cement paste blended with fly ash decreased with increasing cement replacement rates when the median particle size was 19.1 μm, yet cement pastes containing fly ash with a lower median particle size (6.4 μm) resulted in higher compressive strengths at higher replacement rates [1]. This result is attributed to the packing effect of fine fly ash. The small spherical fly ash particles are able to fill the voids and airspace between the larger particles, thereby increasing the density [2, 3]. Furthermore, since a smaller particle size means a higher surface area, the pozzolanic reaction of present amorphous SiO_2 and Al_2O_3 will be higher due to more exposed area for a reaction [4]. However, the positive effect of the packing density can only be utilized up to a certain replacement threshold (filling available pores). Moreover, there still needs to be enough alkalinity available for the pozzolanic reaction of the particles to contribute to the solid matrix. A larger content of smaller particles increases the specific surface area of the secondary cementing material (SCM) and provides more nucleation sites. An increase in nucleation sites provides more area to incite the reaction of the cement, thereby contributing functionally to strength development. The fly ash also alters the chemical composition of the blend through the introduction of minerals such as calcite and silica. Changes in the composition of the ash can influence the reactivity of the ash itself or with respect to the present cement. For example, an increase in the amorphous (reactive) SiO_2 fraction of the ash will elevate the ability to act as a pozzolanic material.

Past research has shown that in the case of coal derived fly ash, the granulometry of ash has a pronounced effect on mortar strength [5]. In the case of class F fly ash, it was found that when the smallest sized fraction (< 45 μm) was used to partially replace cement, the strength (at 2, 7 28 and 90 days) was higher than when the larger sized fractions (> 125 μm) were used. At 28 and 90 days the strength of the samples with smaller particle fly ash replacement exceeded that of the control mortar without replacement [6, 7]. Mehta [8] found that strength development with class C fly ash (i.e. high calcium) was less sensitive to particle size distribution than with class F (i.e. low calcium). When low calcium fly ashes were used, the reactivity was directly proportional to the number of particles <10 μm and inversely proportional to particles >45 μm. Mehta speculated that for high calcium fly ashes

the rates of reactivity were less affected by the particle size distribution due to the already high reactivity of both the crystalline and the amorphous phases. Superior reactivity of the crystalline phase is associated with the presence of reactive compounds like C3A. Both low and high calcium fly ashes contain aluminosilicate glass, however the high calcium fly ash contains enough calcium ions to enhance the reactivity of the aluminosilicate glass. Furthermore, Mehta discovered that when the particle size was less than 10 μm there was more contribution to early strength (i.e. up to 28 days) and when the particle size was 10-45 μm a larger contribution to later strength was observed [9]. These investigations, however, are limited in that they did not examine the composition of the individual particle sized fractions and considered solely on the composition of the ash as a whole. Since it is potentially possible for the minerals present in an ash to concentrate in particular fraction sizes, the information gained from the latter study is incomplete. What can however be concluded from these reports is that the particle size of the ash can impact the strength development. Furthermore, there is reason to believe that the mineral composition of ashes may also play a role in strength development.

One method to alter the particle size of obtained ash before use as cement replacement is by sieving it into distinct size groups. While this introduces an extra step in SCM production that is coupled with an energy demand, it can still be advantageous if there is a significant gain in strength. If the amount of energy invested in sieving the ash is less than the amount of energy spent to compensate for strength loss, then it can be assumed that net energy will be saved. Sieving is one of the less energy intensive methods of obtaining smaller particles and can also be used to alter the chemical and mineralogical distribution of the ash (when different minerals concentrate in particular fraction sizes). Thus, sieving can be used to selectively change mineralogical composition and upgrade the quality of the SCM.

A more energy intensive approach to reducing the particle size is through grinding. Contrary to sieving, grinding does not alter the mineralogical composition of the resulting ash fractions. Nevertheless, the utilization of grinding still provides the ability to improve the reactivity of the ash. This is achieved through mechanical activation, or more specifically, enhancing the reactivity through the combined effects of increasing the reactive surface area and inducing physicochemical changes [10]. Mechanical activation allows for bulk changes through the creation of structural defects, structural rearrangements and phase transformation, all of which lead to a more reactive particle [11-13]. Additionally, the creation of new surfaces and surface modifications can significantly alter the reactivity of particles [10]. Kumar found that the mechanical activation of fly ash lead to significantly less unreacted fly ash and when used to replace clinker, mechanically activated fly ash also led to a denser microstructure coupled with increased early strength. 50–60% mechanically activated fly ash could be used to replace clinker and strengths higher or comparable to commercial cement could be obtained [10]. However, it is unclear and not entirely proven how mechanical activation deviates from simply enhancing reactivity through reduction of particle size.

Using isothermal calorimetry Kumar claimed that the mechanical activation of fly ash has an indirect bearing on the hydration of cement derived tricalcium silicate and tricalcium aluminate. This was reflected by a change in the maximum hydration rate of the phases and the time at which the maximum hydration rate occurs, which was also correlated with an increase in early compressive strength. While it is not completely understood why this happens, Kumar states that the effect of mechanical activation of fly ash on strength results from the formation of a more compact microstructure which is the result of mechanical activation creating a higher reactivity of the lime present which in turn effects the hydration of the clinker phases. Mechanical activation allows the lime to be more available and the interaction of the Ca ions on the surface of C_3A and C_3S particles encourages hydration. Though, Kumar does not explain how this effect is different from increasing nucleation points and his explanation sounds remarkably similar.

This work explores the effects of upgrading two woody biomass derived ashes (PSFA and WBFA-1), which are used to replace OPC at a replacement rate of 40%. Upgrading methods include grinding and sieving the biomass-derived ashes to alter their particle size distribution and potentially the

chemical composition of the different specific size fractions. The particular method of upgrading is determined for the two specific ashes investigated. After determining the best method for each individual ash, the ashes are used to replace OPC in a standard mortar mixture and allowed to hydrate for 3, 7, 28 and 90 days at which point the compressive strength is determined and compared to that of the unaltered biomass-derived ash used at the same replacement rate, and pure OPC control specimens. The goal is to achieve no loss of compressive strengths at elevated replacement rates through the investment of minimal energy in the ash pre-treatment.

8 Materials and Methods

8.1 Raw Ash Composition

As a continuation of the previous chapter, two ashes were selected for further experiments. Paper sludge fly ash (PSFA) was chosen because of its superior performance (relative to other biomass derived ashes investigated in chapter 4) particularly at higher replacement rates: at 90 days 40% replacement with PSFA had reached a compressive strength of 40 MPa, which was 70% of the pure OPC's strength. Woody biomass fly ash (WBFA-1) was chosen due to its poor performance at higher replacement rates: at 90 days 40% replacement with WBFA-1 had reached a compressive strength of 27 MPa, which was only 47% of the control OPC's strength. Of all the ashes tested, it showed the lowest contribution to strength development, allowing for significant room for improvement. A detailed description of the ashes can be found in chapter 4, a recap of the compositions (elemental and oxide) can be found in Table 11 and Table 12 respectively.

Table 11: Elemental composition of biomass derived fly ash as determined by XRF [M.-%].

Compound	Ca	Si	Al	Fe	Ti	Mg	Zn	K	S	Cl
PSFA	44.2	3.4	1.5	1.2	0.6	0.4	0.4	0.4	0.3	0.3
WBFA-1	30.1	2.9	0.5	2.8	0.2	0.8	0.2	10.3	1.5	0.9

Table 12: Oxide composition of biomass derived ash as determined using the cement oxide method [M.-%].

Compound	CaO	SiO2	Al2O3	Fe2O3	SO3	TiO2	MgO	K2O	ZnO	LOI 950 °C
PSFA	74.0	10.5	4.2	1.8	1.2	1.0	1.0	0.6	0.5	4.0
WBFA-1	42.2	11.8	1.9	3.4	3.7	0.3	4.6	11.8	0.2	15.3

8.1.1 Ash Particle Size Distribution

Using laser analysis (Donner Technologies DIPA-2000), the particle size distribution of the ashes as well as the D(10) D(50) and D(90) were determined and compared to that of CEM I 42.5 N (more details in chapter 4). Since the particles are replacing OPC a similar size and distribution was sought.

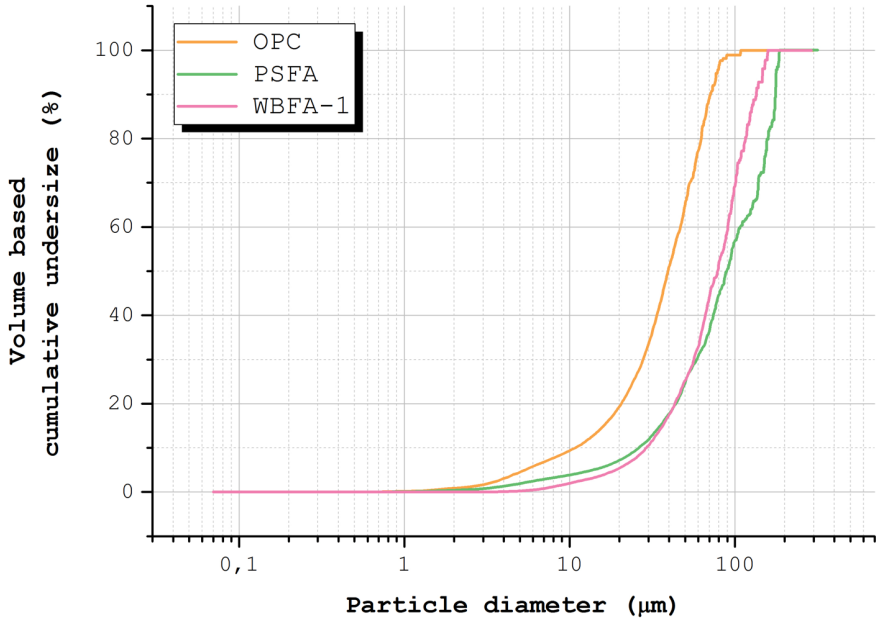

Figure 37: Particle size distribution depicted though volume based cumulative undersize for OPC, PSFA and WBFA-1. The Latter two appear much courser and particularly low in the 0-45 um particle size fraction in comparison to OPC.

8.2 Grinding and Sieving of Ashes

The objective of improving the ashes' functionality was tested through altering the particle size distribution and potentially concurrently the mineralogical composition through division into the respective particle size classes. Two techniques were utilized to achieve these adaptations: sieving and grinding. Using a horizontal sieve shaker, the ashes were sieved into distinct particle size classes. Both fly ashes were sieved to the fraction sizes: 0-45 μm, 45-63 μm, 63-90 μm, 90-125 μm and 125+ μm. After sieving, the ashes were again examined by XRD and ESEM (with EDX). In addition, the particle size of PSFA was reduced to < 45µm using a Retsch MM200 Mixer Mill. After grinding the particle size was again determined.

Treatments of the ashes were selected based on the results of the preliminary investigations. When the treatments showed promising changes in either mineralogical composition or particle size, they were performed on larger quantities of the ashes to produce enough ash for cement replacement. As before CEM I 42.5 N was used to produce mortar specimens according to EN 196-1, see chapter 4 for details. In this series, 40% cement replacement was tested for all the modified ashes since the focus here is achieving higher replacement rates. The flexural and compressive strengths of mortar specimens were tested on 6 specimens after 3, 7, 28 and 90 days. The results of the 40% replacement were again compared to a 100% OPC control and the results of the 40% replacement with the unprocessed ash obtained in the previous chapter.

9 RESULTS

9.1 Ash Particle Size Distribution

The particle size distribution of the ash in relation to that of CEM I is of importance since it impacts reactivity and the packing density. The distributions can be seen in Figure 37 and the D(10) D(50) and D(90) can be seen in Table 13. As evident from the diagram, the distribution of all three powders show similar curves, however the cement curve is skewed to the left and more compact. 90% of the cement particles had a diameter smaller than 71 μm whereas 90% of PSFA was smaller than 176 μm; 90% of WBFA-1 was smaller than 126 μm. A similar staggering can be found for 50% of the particles: CEM I had a D(50) of 39 μm while PSFA had 89 μm and WBFA-1 had 79 μm. The difference in the D(10) was less pronounced however still noticeable: CEM I had a D(10) of 11 μm while PSFA had 26 μm and WBFA-1 had 29 μm. PSFA had a smaller D(10) than WBFA-1 despite being larger at all other percentages. PSFA had the largest spread in particle distribution.

Table 13: Diameter in μm for which 10%, 50% and 90% (D(10), D(50) and D(90))of the ash particles are smaller for CEM I, PSFA and WBFA-1.

	D(10)	D(50)	D(90)
CEM I	10.8	39.3	71.3
PSFA	26.3	89.1	176.0
WBFA-1	29.2	78.5	126.3

9.2 Determination of Treatment Effect Per Ash

9.2.1 Paper Sludge Derived Fly Ash (PSFA)

The crystalline fraction of the unsieved, i.e. complete ash, for PSFA was composed of lime (CaO), quartz, C2S, gehlenite and portlandite (see results section of chapter 4). After dividing the ash in various size classes, all the different sieving fractions showed similar mineralogical compositions as can be seen in Figure 38. Lime remained the most abundant phase detected and in similar quantities for all size fractions; this is evident from the most prominent peak located at 37.42 2θ having roughly the same intensity for all size fractions. Minor alterations in the content of quartz can be observed based on fraction size. The most intense quartz peak lies at 26.64 2θ and can be observed in the 125+ µm, 90-125 µm and 63-90 µm fractions. For the smaller particle sizes the peak is still present but at a slight decrease in intensity. Similar observations can be made for the mineral gehlenite, however to an even smaller degree.

Since there were remarkable similarities in mineral composition amongst the sieving fractions, this approach to altering the performance of the ash as a BioSCMp with respect to chemical reactivity appears not to be useful. However, there are other ways to potentially increase the functionality of PSFA. Relative to OPC, PSFA has a larger average particle size distribution as can be seen by the entire distribution being shifted to the right (Figure 37). Mechanical grinding has the potential to improve the reactivity of PSFA through the introduction of more nucleation points, increasing the specific surface area and improving the packing density.

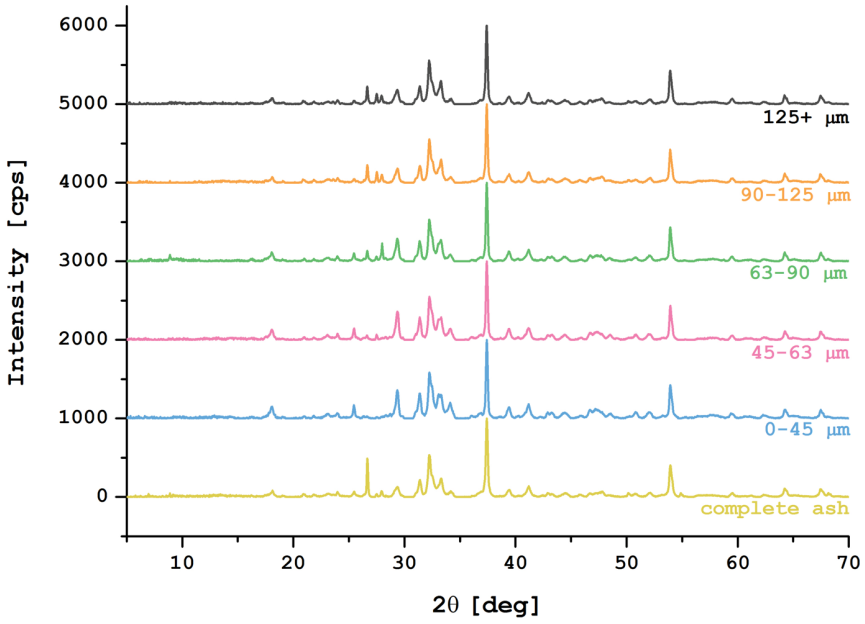

Figure 38: XRD of the different sieved PSFA size fractions showing only minor differences in compound composition.

Grinding the ash to a particle size smaller than OPC will allow for a better particle packing and thereby increasing the density of the mortar as a whole. Furthermore, smaller particle sizes will offer a larger specific surface area that enhances the nucleation effect of PSFA. While grinding is a particularly energy intensive procedure (resulting in higher costs and emissions) it could still be advantageous if the contribution to the quality or durability of the hydrated product is sufficiently beneficial. To achieve mechanical activation, the ash was ground to a particle size < 45µm and then used as a partial replacement for OPC.

9.2.2 Woody Biomass Derived Fly Ash (WBFA)-1

The unsieved WBFA-1 ash was composed of quartz, calcite, and arcanite (see chapter 4 for details). After dividing the ash based on particle size, the different sieving fractions showed significantly different mineralogical compositions as shown in Figure 39. The same peaks are present in all of the samples but the intensity changes drastically, particularly for the two extreme size fractions. In fact, there appears to be gradual progressions and digressions in peak intensities from the smallest particle size group to the largest. The three minerals that make up the complete ash continue to comprise the different size fractions; however, they are present in varying proportions.

From these observations, it can be generalized that quartz dominates the larger fraction sizes (as seen by the most intense peak at 26.64 2θ) and its content decreases in favour of calcium based compounds as the particle size decreases. Between the different size fractions, there is a pronounced difference in the quartz intensities indicating a large difference in the abundance of quartz. The abundance of quartz ranges from barely detectable to practically the only phase present.

A similar propensity for minerals to concentrate in different particle sizes can be observed for calcite and arcanite (K2SO4); however, both of these phases dominate the smaller particle sizes. As seen from their most intense peaks (29.41 and 30.80 2θ respectively), their concentrations decrease as the particle size increases. This trend is more distinct for calcite with 0-45 µm showing the highest calcite concentrations and 125+ µm showing the least. As the least abundant phase in the complete ash, arcanite peaks have the lowest intensities. For arcanite, the different size fractions do not show substantial differences either. The only significant observation is that the 125+ µm has very small arcanite peaks indicating that this phase is barely present.

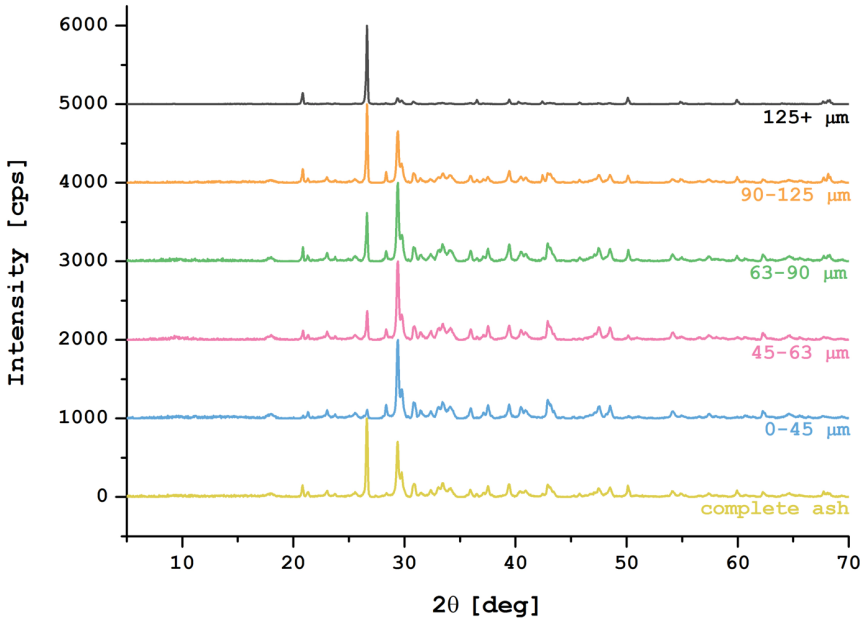

Figure 39: XRD of the different sieved WBFA-1 size fractions showing decrease in quartz (peak at 26.64 2θ) but increase in calcite and arcanite (peaks at 29.41 and 30.80 2θ respectively) with decreasing size fraction.

Since there are such distinct differences in the chemical composition based on particle size, sieving can potentially be used as a method of upgrading the quality of the ash as a BioSCMp. Based on the analysis of the different sieving fractions, dividing them into three groups (0-45, 45-125 and 125+ µm) will provide three distinctly different compositions, which can then substitute for a fraction of OPC and tested for their strength development. This will allow for an analysis of the chemical compositions and particle sizes impact on the functionality of the ash.

9.3 Compressive Strength Tests Per Ash

9.3.1 PSFA

The compressive strengths of the samples with 40% cement replacement with ground PSFA (<45µm) and 40% cement replacement with the unaltered PSFA (D(90)=176.0µm) was tested at 3, 7, 28 and 90 days and can be seen in Figure 40. It is apparent that the ground ash did not perform as well as the unaltered ash; furthermore, the differences in strength development of the two mixtures also increased with time.

An examination of the performance of both the ground ash and the unaltered ash relative to the strength achieved by the pure OPC control shows that not only was the performance of the ground ash inferior, but it did not even achieve 60% of the strength of OPC despite containing 60% of the cement. As can be seen from Figure 41, the unaltered ash gained strength relative to the pure OPC and by 90 days had stabilized at 70.1% of the strength. However, when the ash was ground, its percentage of OPC strength peaked at 28 days, and at 90 days it showed a slightly lower percentage. This indicates that while the OPC and the unground PSFA continued to contribute to hydration at later ages, the ground ash has no significant contribution.

This result indicates that, merely grinding the ash to a particle size of 45 µm and smaller does not improve the strength achieved and is an unnecessary step in BioSCMp preparation. Since it costs energy and brings no benefit, grinding alone (i.e. a smaller particle size alone) is not sufficient to increase the replacement rate up to 40%).

When unaltered, PSFA was able to reach 93.8% and 70.1% the strength of OPC after 90 days hydration at replacement rates of 20 and 40 M.-% respectively (see chapter 4). In the case of 40% replacement, this equates to a strength of 40.1 MPa, which falls short of the target 42.5 MPa but, although not allowed according to prescribed norms, could still deliver sufficient strength for nonstructural applications.

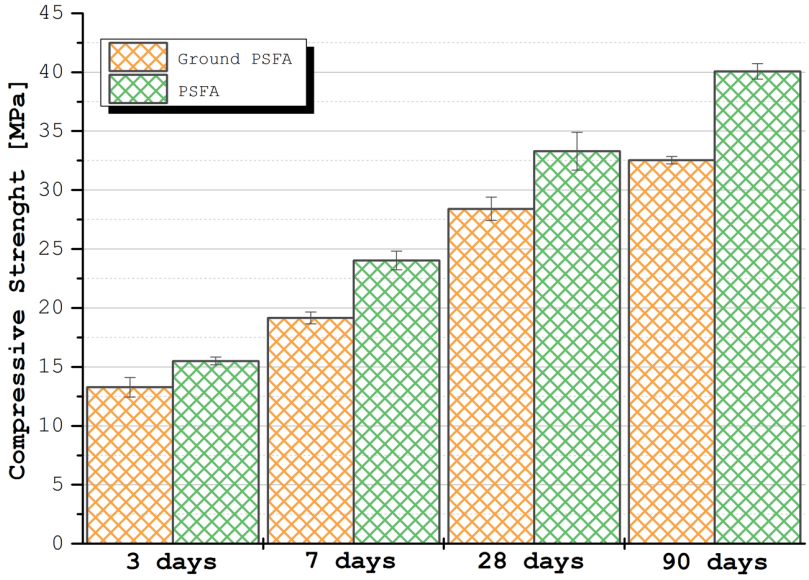

Figure 40: Compressive strength for samples with 40% cement replacement with PSFA ground to <45µm and relative to 40% replacement with unaltered ash.

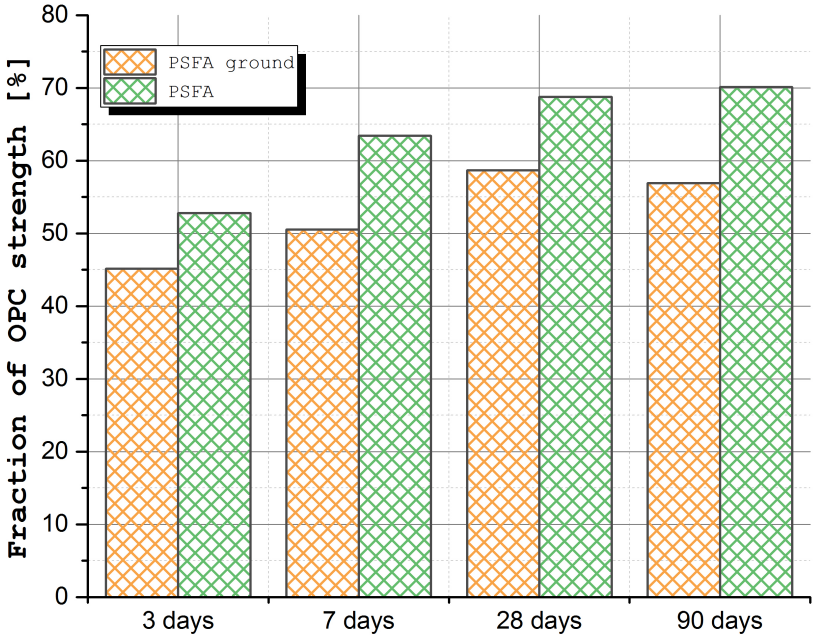

Figure 41: Percentage of OPC strength achieved for 40% replacement with PSFA <45µm and PSFA unaltered.

9.3.2 WBFA-1

The compressive strength results for the three different WBFA-1 particle size fractions used to replace 40% OPC can be seen alongside 40% replacement with the unaltered ash in Figure 42. Not only did all of the sieving fractions result in a concrete of lower strength but also, they significantly underperformed the unsieved ash at later stages of hydration. After 3 days hydration, all of the samples had similar compressive strengths, but by 7 days and after, the unsieved ash contributed significantly more to strength development. The 3 different sieving fractions performed remarkably similar in strength development, with the strengths of the samples containing 45-125 μm and 125+ μm being closer in range and typically higher than the 0-45 μm fraction.

In Figure 43 the strengths of the different mixtures seen as fractions of the OPC control strength are displayed for the various hydration times. The unsieved ash itself did not perform all that well relative to pure OPC, which is why it was chosen for upgrading. However, despite the poor performance of the unsieved ash, all of the modified ashes performed even worse. Over time, the complete ash was able to gain strength relative to the OPC strength indicating a contribution to strength development; the only sieving fraction to do that was 0-45 μm. At 3 days, the 0-45μm sample had 27.2% of the OPC strength and that grew to 30.3% by 90 days. While this is not as large as the increase from 39.6% to 47.2% that the complete ash provided, it is nonetheless significant because the other two sieving fractions provided a reduction in the relative compressive strength with time. This indicates that both 45-125 μm and 125+ μm contributed less to the strength development over time.

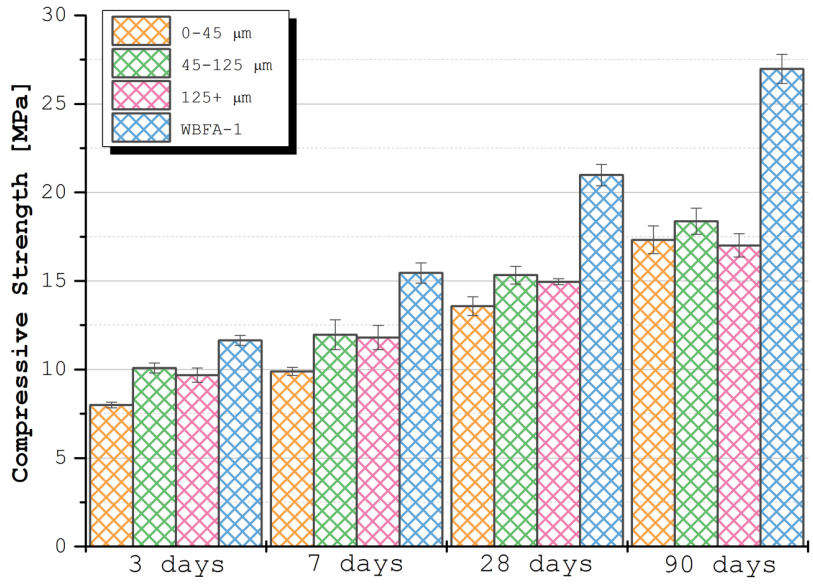

Figure 42: Compressive strength with 40% replacement of cement with WBFA-1 and three sieving fractions thereof.

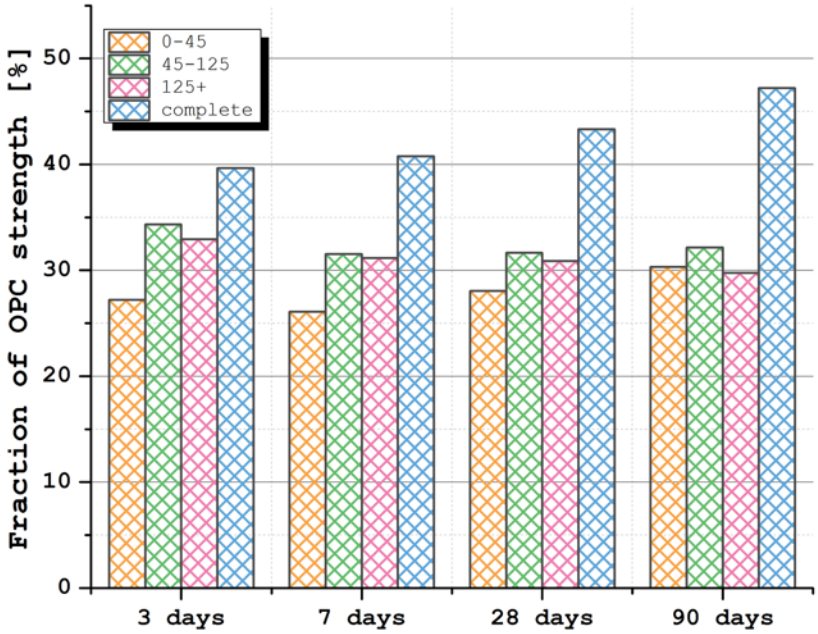

Figure 43: Percentage of OPC strength achieved for 40% replacement of cement with WBFA-1 and the three sieving fractions.

10 DISCUSSION

It was discovered in this work that the particular steps to upgrade the quality of the biomass derived ashes regarding their performance as a BioSCMp was actually detrimental to its ability to contribute to strength development. In the case of both ashes, the unaltered fly ash showed significantly higher compressive strengths when used to replace 40% cement in a standard mortar mixture after 28 days of hydration and beyond.

PSFA was ground to a particle size smaller than 45μm and its performance was compared to the unaltered ash when they were used to replace 40% cement in a standard mortar. Grinding of the ash was intended to mechanically activate it (i.e. induce reactivity through mechanical intervention), however it was discovered that this modification resulted in lower compressive strengths being achieved at all ages. The reduction in strength could be the result of a reduction in reactivity due to the presence of lignosulfonate. Calcium or sodium lignosulfonates are by-products from the manufacture of wood pulp resulting from the breakdown of lignin in the sulfite wood pulping process [14, 15]. Incomplete combustion of wood pulp ash contains lignosulfonates. PSFA had a LOI of 4.0M-%, thus Lignosulfonate could be present in large quantities. In their crude form, lignosulfonates contain many impurities such as hexose sugars which are powerful retarders [15]. While they are commonly used as a water reducing admixture, lignosulfonates can also result in air entrainment, strength loss and set retarding [9]. Here it is speculated that the grinding the PSFA ash either released lignosulfonate or made them more accessible (i.e. leachable) from the individual ash particles.

Alternatively, the high content of calcium could be responsible for the observed phenomenon where the larger particle sizes acted as a superior BioSCMp. In an investigation on coal derived fly ash, Mehta asserts that in the case of high calcium fly ash, the rate of reactivity is less affected by the particle size, whereas low calcium fly ash had reactivity directly proportional to the number of particles less than 10 μm and inversely proportional to the number of particles greater than 45 μm. The lack of a correlation between reactivity and particle size in the case of high calcium fly ash is attributed to the already higher reactivity of the crystalline and glassy phases in the high calcium fly ash. Mehta claimed that the calcium content controls the mineralogy, or more specifically the composition of the crystalline minerals and the amount of glass present. A higher calcium content corresponded to more reactive crystalline compounds like C_3A being present and a more active calcium aluminosilicate glass; thus the ash is already of a superior reactivity and measures such as grinding did not prove much benefit [8]. These observations can be extrapolated to PSFA; while no C_3A was present some other reactive compounds such as C_2S were (see chapter 4). It must be remembered that Mehta's conclusions are drawn from coal-derived fly ashes and while there are similarities in the composition, PSFA has significantly more CaO and different minerals present. However, this could serve as an explanation as to why grinding the ash did not produce a superior BioSCMp.

Not only did the unground PSFA perform better than the ground PSFA, its percentage of OPC strength also continued to grow with time. The ground PSFA's percentage of OPC strength only increased at early ages and then lessened to a smaller degree. It is recognized that very fine particles of reactive materials are responsible for early age strength development [9]. Thus, the ground PSFA was able to provide more strength before 28 days, but the effect diminished with time. The unground ash was able to continue increasing its strength relative to that of the control because possibly once the fine particles were consumed, the coarse particles began to participate in the continuation of the strength development [7].

Similar to the situation with PSFA, it was discovered that the presumable upgrading of WBFA-1 actually had an adverse effect on strength development. Sieving of WBFA-1 resulted in size fractions with different chemical compositions. The size fraction 0-45μm consisted mainly of calcite while 125+ consisted mainly of quartz; these two minerals have distinctly different reaction mechanisms [15]. The unsieved ash itself did not perform well relative to pure OPC control and it was therefore selected for

upgrading for this very reason. However, it was observed that the sieved fractions performed even worse. These results defied expectations, particularly in the case of the 125+ μm fraction since it was composed mainly of quartz, which is known to have a delayed contribution to strength due to the pozzolanic reaction. It is however possible that the quartz present in this size fraction was too large to be significantly reactive [16]. Replacement with the size fraction 0-45 μm (which contained the least amount of SiO_2 and no belite which also contributes to delayed hydration) managed to achieve a larger contribution to strength development at later stages. However, it was expected that the 0-45 μm would contribute to early strength, if at all. The smaller particle sizes offering a larger specific surface area and providing more nucleation points was anticipated to be 0-45 μm fraction's main contribution. Nevertheless, the calcite rich ash did contribute to strength development. Again, it could be that more or different inhibitory compounds were leachable from the different size fractions. WBFA-1 had a particularly high LOI (15.3M.-%) indicating the possible presence of organics such as wood derived sugars, proteins or humic acids which are known to retard or even prevent the normal setting and hardening of cement [15, 17]. More research needs to be conducted to determine exactly what is going on here. In the comparison of a high calcium fly ash to a low calcium fly ash used to partially replace cement, Erdogde found that the high calcium fly ash resulted in a higher strength than the low calcium fly ash [7]. This was attributed to the presence of higher reactive calcium-containing minerals in the high calcium fly ash. However regardless of the calcium content, he found that the finer the size fraction used, the higher the compressive strengths were.

Based on the observations on the two biomass-derived fly ashes studied in the investigation, upgrading the functionality of the ash through grinding and sieving to increase the compressive strengths at higher replacement rates is not recommended. The mixtures made with modified ash have strengths below that of the OPC control and lower than the untreated replacements at all ages. Therefore, the investment of energy necessary to achieve the modifications is of no benefit.

11 CONCLUSION

- Replacement of cement with biomass derived ash in the range of 40% is more applicable for low strength applications like non-structural concrete.
- When biomass derived ash is used in higher replacements (i.e. 40%), then modifications to the particle size or composition through grinding or sieving are not effective measures to enhance the strength development.
- For these experiments, it is recommended that the ashes be used as-is to replace minor parts (up to 20%) of OPC.
- Other options to possibly improve ash functionality such as secondary temperature treatment of the primary ashes to increase content of hydraulic or pozzolanic minerals will be investigated in chapter 6.

12 REFERENCES

1. Chindaprasirt, P., C. Jaturapitakkul, and T. Sinsiri, *Effect of fly ash fineness on compressive strength and pore size of blended cement paste.* Cement and Concrete Composites, 2005. **27**(4): p. 425-428.
2. Gopalan, M., *Nucleation and pozzolanic factors in strength development of class fly ash concrete.* Materials Journal, 1993. **90**(2): p. 117-121.
3. Isaia, G.C., A.L.G. Gastaldini, and R. Moraes, *Physical and pozzolanic action of mineral additions on the mechanical strength of high-performance concrete.* Cement and Concrete Composites, 2003. **25**(1): p. 69-76.
4. Slanička, Š., *The influence of fly ash fineness on the strength of concrete.* Cement and Concrete Research, 1991. **21**(2-3): p. 285-296.
5. Monzo, J., J. Paya, and E. Peris-Mora, *A preliminary study of fly ash granulometric influence on mortar strength.* Cement and concrete research, 1994. **24**(4): p. 791-796.
6. Giergiczny, Z. and A. Werynsk, *Influence of fineness of fly ashes on their hydraulic activity.* Special Publication, 1989. **114**: p. 97-116.
7. Erdoğdu, K. and P. Türker, *Effects of fly ash particle size on strength of portland cement fly ash mortars.* Cement and Concrete Research, 1998. **28**(9): p. 1217-1222.
8. Mehta, P.K., *Influence of fly ash characteristics on the strength of portland-fly ash mixtures.* Cement and Concrete Research, 1985. **15**(4): p. 669-674.
9. Mehta, P.K. and P.J.M. Monteiro, *Concrete: microstructure, properties and materials*. 2006: McGraw-Hill.
10. Kumar, R., S. Kumar, and S. Mehrotra, *Towards sustainable solutions for fly ash through mechanical activation.* Resources, Conservation and Recycling, 2007. **52**(2): p. 157-179.
11. Boldyrev, V.V., *Mechanochemistry and mechanical activation of solids.* Russian Chemical Reviews, 2006. **75**(3): p. 177.
12. Fernández-Bertran, J.F., *Mechanochemistry: an overview.* Pure and applied chemistry, 1999. **71**(4): p. 581-586.
13. Juhasz, A. and L. Opoczky, *Mechanical activation of Minerals by Grinding: Pulverizing and Morphology of Particles, 1994.* Akadémiai Kiadó and Ellis Horwood, Budapest, Hungary, and Chichester, UK.
14. Taylor, H.F., *Cement chemistry*. 1997: Thomas Telford.
15. Hewlett, P., *Lea's chemistry of cement and concrete*. 2003: Elsevier.
16. Benezet, J. and A. Benhassaine, *The influence of particle size on the pozzolanic reactivity of quartz powder.* Powder Technology, 1999. **103**(1): p. 26-29.
17. Shirley, D., *Impurities in concreting aggregates.* Slough, UK: Cement and Concrete Association, 1981.

CHAPTER 6

DEVELOPING METHODS OF PROCESSING AND SECONDARY THERMAL TREATMENTS TO OBTAIN HYDRAULIC MINERALS FROM BIOMASS DERIVED ASHES (SST ASH)

ABSTRACT

Biomass derived ash has the ability to replace ordinary Portland cement (OPC) for the production of concrete and given sufficient functional minerals, replacement rates could reach 100%. The intent of this research project is the development of the scientific basis for methodologies that enable the production of renewable sustainable cement (i.e. BioCement) based on ashes derived from the conversion of agricultural biomass residues with the intention of replacing as much ordinary Portland cement as possible, to reduce the CO_2 emissions associated with the cement and concrete industry. In order to increase the replacement rates, various methods intended to increase the content of functional (i.e. hydraulic) minerals within the biomass derived ash were explored. In this chapter, secondary thermal treatments (STT) were investigated. Modifications in hydraulic mineral production methods focused on pre-treatments, firing regimes and post-treatments. Success was analysed through the creation, type, and quantity of hydraulic minerals as determined by XRD. The ultimate goal was to form the highest concentration of cementing minerals with the least amount of process and energy (heat) invested. Ideally these production methods would be incorporated into future industrial biomass-to-energy conversion processes, thereby producing two valuable products: renewable energy and cementitious ash.

In this investigation, it was determined that hydraulic minerals could be formed from biomass derived ash and the treatment methods steer the quantity and quality of the hydraulic minerals produced. When paper sludge fly ash (PSFA) was subjected to a STT at 1238°C the composition of the ash converted from lime, quartz, β-C_2S, gehlenite and portlandite into SST PSFA composed of α'H-C_2S, β-C_2S and gehlenite. When woody biomass fly ash-1 (WBFA-1) was subjected to a STT at 1214°C the composition of the ash converted from quartz, calcite and arcanite into SST WBFA-1 composed of merwinite, akermanite and α-C_2S. When woody biomass fly ash-2 (WBFA-2) was subjected to a STT at 1210°C the composition of the ash converted from quartz, calcite, arcanite, portlandite and lime into SST WBFA-2 composed of wollastonite and pseudowollastonite.

It was found to be beneficial to promote the ash particle interaction through compaction and, in the case of PSFA and WBFA-1, a reduction in particle size below 45 μm prior to STTs. Longer firing times improved the quantity and the crystallinity of the hydraulic minerals. Staged heating and a ramping rate of 10°C/min were beneficial in the production of the most hydraulic minerals (i.e. the best STT ash). Furthermore, the retention of high temperature polymorphs through quenching was observed.

1 INTRODUCTION

Before establishing the potential of biomass derived ashes to replace Ordinary Portland Cement (OPC), it is important to understand exactly which OPC minerals are significant and how they are made. More specifically, the formation of the particular minerals which give cement its hydraulic reactivity should be understood. Furthermore, an understanding of additional functional minerals which could potentially be created (given the chemical composition of the biomass derived ash) is an advantage. This knowledge can be applied to current biomass ash production processes to obtain ashes featuring OPC mineral properties.

As described in detail in Chapter 2, C_3S and C_2S are the most important phases since they contribute the most to the sought after hydraulic properties and subsequent strength. These two phases are not stoichiometricly pure compounds but rather solid-solutions which incorporate additional oxides. The two calcium aluminate compounds (calcium aluminate and calcium alumino ferrite) are interstitial phases between the larger crystals of the silicates [1]. The exact individual phase compositions of these four main minerals are dependent on the production process and the chemical makeup of the raw feed. Minor phases, such as periclase, calcium oxide and alkali sulfates can also be found in commercial OPCs. However, within the range of a standard raw material chemical composition, many more mineral phases are possible.

1.1 CaO-SiO_2 System

High temperature phase equilibria diagrams can be used to simplify the understanding of the complex reactions between the starting minerals and determine the phase composition of the resulting material after thermal treatment. The CaO-SiO_2 system (see Figure 44) focuses on the phase formation under increasing temperatures for different CaO to SiO_2 ratios. It has four binary compounds C_3S (alite) C_2S (belite), C_3S_2 (rankinite) and CS (wollastonite).

C_3S_2 is commonly known by its mineral name, rankinite. Three modifications exist for CS: pseudowollastonite (α-CS), parawollastonite (β-CS) and wollastonite (β-CS). Pseudowollastonite is the high temperature modification and occurs rarely in nature. Parawollastonite and wollastonite, in contrast, are reasonably common. Both CS or C_3S_2 are less common in clinker. Unlike C_2S and C_3S neither CS or C_3S_2 are appreciably hydraulic under ordinary conditions, therefore their formation is avoided in clinker production and as a consequence higher CaO/SiO2 ratios of the raw feed are required

The applicability of binary phase diagrams to the interpretation of cement production reactions is limited since numerous other elements are present. Ternary diagrams provide a closer approximation to the relevant chemistry through the addition of an extra component.

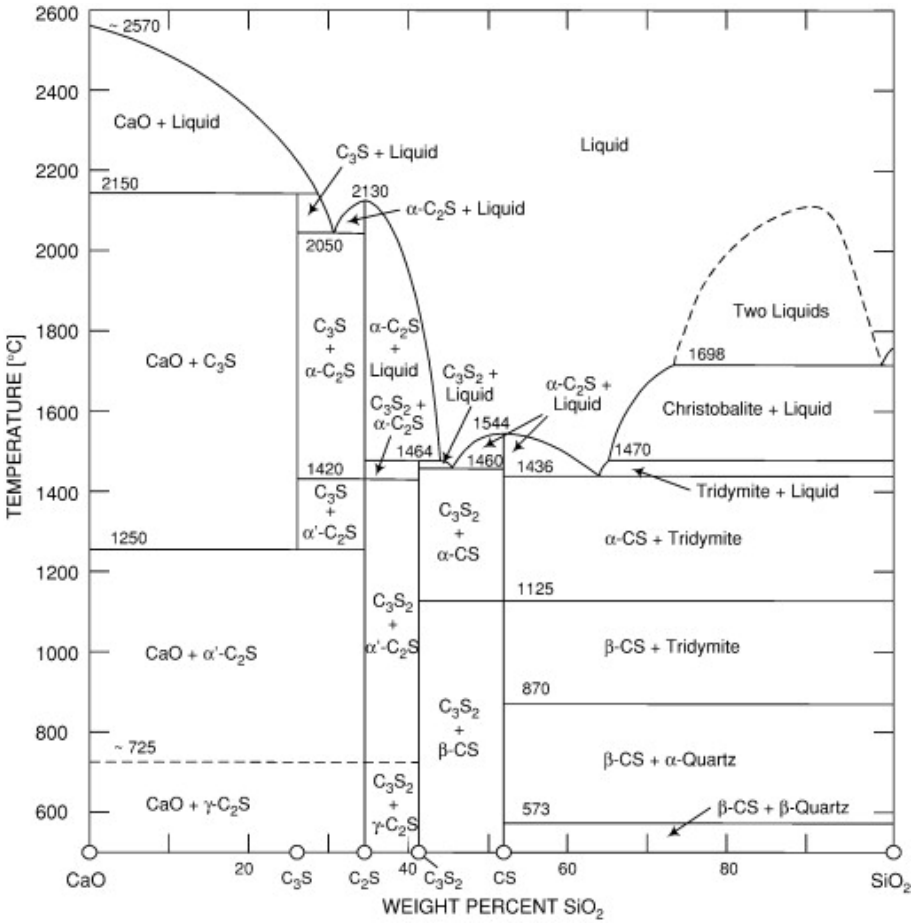

Figure 44: The CaO-SiO_2 phase system (excluding the polymorphism of C_3S and the distinction between α'_H-α'_L-C_2S [2].

1.2 The CaO-SiO_2-Al_2O_3 System

With the introduction of Al_2O_3, the three most important oxide components in OPC clinker are represented in the system. This ternary CaO-Al_2O_3-SiO_2 diagram facilitates a preliminary understanding of the chemistry underlying the formation of Portland cement clinker. In this diagram, it is assumed that equilibrium is achieved at 1500°C despite the fact that cement manufacturing takes place in the temperature range of 1400-1450°C. In order to reach the partially molten state of clinkering temperatures, a mixture in the pure CaO-Al_2O_3-SiO_2 system requires a higher temperature. The CaO-Al_2O_3-SiO_2 diagram can be used to predict which solid phases will potentially be present for various chemical compositions. However, the final phase assemblage after cooling may be more complex due to fractionation. The slow rate of reaction between solid and liquid phases promotes non-equilibrium conditions. As the clinker is rapidly cooled, high temperature assemblages are locked in. Additionally, metastable phases are not adequately represented in the diagram [3].

In addition to the above mentioned CaO-rich binary phases which make up over 90% of OPC, there are a few ternary phases of interest. Gehlenite (C_2AS), one such phase, belongs to the melilite family. It forms as an intermediate compound in the manufacture of OPC clinker but does not occur in the final product. Gehlenite can be found in some low energy cements (such as calcium aluminate cements). [4] found that gehlenite, in a fly ash belite cement, began hydration after an induction period of 28 days and by 200 days it had reached a hydration degree of 65%. The rate of hydration for gehlenite is considerably slower than C_2S and is not considered appreciably hydraulic. However, the hydration kinetics and mechanism of gehlenite have only recently been intensely investigated and it was found that after long hydration times, high-alumina cements and granulated blast furnace slag

mixtures have shown improved mechanical properties [5]. The explanation for this enhancement is due to the presence of granulated blast furnace slag in which a gehlenite hydrate forms instead of calcium aluminate hydrate [6] [7]. Furthermore, gehlenite when prepared by the sol-gel process was found by [8] to have an increased hydraulic reactivity. Gehlenite forms extensive solid-solutions, e.g. in akermanite, a member of the gehlenite family ($Ca_2MgSi_2O_7$), but not within the CaO Al_2O_3 SiO_2 system [9]. Thus, an understanding of MgO's influence on mineral formation is also advantageous.

1.3 Influence of MgO on the CaO-SiO_2-Al_2O_3 System

Binary, ternary and quaternary phases containing MgO all exist in the CaO-SiO_2-Al_2O_3 system. Phases containing magnesium in solid solution and free MgO are significant in terms of clinker quality. Free MgO exhibits slower hydration kinetics and a deleterious expansion in the hardened paste and therefore should be monitored and limited. However, MgO can also have inconsequential effects on clinker minerals or even provide some minor advantages. Limited quantities of MgO are taken up by all four of the major clinker phases (around 0.5-2.0% for C_3S, 0.5% for C_2S, 1.4% for the C_3A and 3.0% for C_4AF). Additionally, MgO has the ability to stabilize particular alite polymorphs [3]. Due to the similar structure of MgO and CaO, Mg ions can replace exclusively the Ca-sites in alite [9]. Increasing the MgO content in clinker promotes the growth stability of alite crystals close to the equilibrium conditions. It also favours the occurrence of the M3 polymorph and can be considered essential to its occurrence [10].

Significant MgO containing phases can be found in the melilite mineral group, which in addition to gehlenite, includes merwinite and akermanite. The akermanite-gehlenite solid solution is continuous between the two end members, which have the formulas $Ca_2MgSi_2O_7$ and $Ca_2Al_2SiO_7$ respectively [11]. Due to their occurrence in blast furnace slags (BFS) and BFS's incorporation in slag cement, these minerals have been studied for their reactive properties. As a latent-hydraulic materials, the activation of slag relies on the high alkalinity created when calcium silicate hydrates to produce $Ca(OH)_2$ and on the heat liberated in C_3S and C_3A hydration [12]. Historically, slag was considered to be only mildly reactive in water and without cement it was not capable of producing enough hydrated phases to provide the mechanical strength comparable to pure OPC [13-15]. However, the understanding of the hydraulic activity is beginning to change, as more research is being done on properties and compositions of different types of slags. Following the reactions of slag–lime suspensions with time (as an accelerated chemical method), Mostafa found that quickly and slowly cooled slags were hydraulically active [16]. While the exact hydration product formed is dependent upon the CaO concentration, the cooling rate did have bearing on the resulting reactivity.

In terms of slag, the chemical composition and thermal history determine the phase composition and structure; in turn, this controls the hydraulic activity. Stainless steel slags may contain a high magnesium content, so in addition to γ-C_2S, common phases include merwinite[1], bredigite[2] and periclase[3] [17]. Merwinite is an intermediate orthosilicate with a monoclinic structure that forms in the temperature range 800-1430°C [18].

The composition of blast furnace slag also makes it an interesting material to substitute for raw materials in cement manufacturing. While the chemical composition of slag can be somewhat similar to that of the clinker, in terms of mineral composition, it is significant different due to the different production temperatures and processes. However, a similar chemical composition makes slag a promising raw feed. The study conducted by [19] revealed that incorporation of slag into the raw material had a positive effect on the properties the cement produced. Therefore, in analogy to slag, it

[1] $Ca_3Mg(SiO_4)_2$
[2] $Ca_7Mg(SiO_4)_4$
[3] MgO

appears important not only to consider the biomass-based ash element composition but also the firing and quenching regime in order to obtain functional hydraulic minerals.

1.4 Study Objective

The objective of the study described in this chapter was therefore to determine the best practices to produce the largest content of the most hydraulic (or functional) minerals for three distinct ashes. It is expected that a secondary thermal treatment (STT) can enhance the reactivity of these ashes, and while they may not possess the exact same mineral composition as OPC, they could potentially contain hydraulic and functional minerals. Since the chemical composition of the ashes is fixed, it is presumed that whatever minerals can be formed will be formed with alterations in firing temperatures. The pre- and post-treatment, as well as the particulars of the firing regime, should serve to change the quantity and quality of the desired phases or stabilize metastable minerals or polymorphs.

The experiments will be broken down into 4 categories: preliminary thermal analysis, pre-treatment methods, firing regime and post-treatment cooling techniques. In each category, different objectives will be investigated, different information will be gained, and different goals will be realised.

I. Preliminary thermal analysis: In this study, it is hypothesized that required firing temperatures for achieving hydraulic minerals will differ from the 1450°C range used in traditional production methods due to the differences in chemical composition between biomass derived raw ashes and OPC feed stocks. The presence of different foreign ions can possibly lower the sintering temperature by acting as fluxing agents. The incorporation of iron and alumina in traditional raw feed helps to keep the sintering temperature below 1600°C. In the case of the three types of biomass-derived ashes, the amounts of iron and alumina are not so high, but there are alkalis present; they are known to reduce sintering temperatures. Since the three ashes also have different chemical compositions, the optimal firing temperature for STT for each individual ash will need to be determined.

II. Pre-treatment: The intimate contact between traditional OPC raw feed particles as they tumble through the rotary kiln encourages the formation of new phases. In contrast, the biomass derived ash particles will be static in the laboratory oven. This intimate contact will need to be achieved by other means; pre-treatment methods are therefore expected to be required. To increase particle interaction, experiments were done to evaluate two different particle sizes (as received and D(90) >45 μm) as well as four different feed forms (tablets, nodules, compacted powder and loose powder).

III. Firing regime: Methods of firing were also investigated to verify the best approach to the formation of hydraulic minerals. Investigations focused on the dwelling time at the maximum temperature, the rate at which the temperature of the furnace increased, and plateaus at critical temperature points.

IV. Post treatment: The rate at which the samples cool is critical to the final polymorph obtained; this is decisive for the overall reactivity. To determine the best method to rapidly cool the samples in order to retain C_3S and β-C_2S while avoiding the transition to γ-C_2S, various quenching methods were explored. These methods included cooling the nodules by submerging the crucible in water bath, allowing the nodule to cool in the ambient environment, directly spraying the nodule with water, and spraying the nodule with compressed air. All samples were directly removed from the oven at the target temperature and subjected to the quenching methods.

Within the four categories, the main objective for all of the different investigations was to produce the largest quantity of the highest quality hydraulic minerals, while investing the use of the lowest amount of energy.

2 MATERIALS AND METHODS

2.1 Materials

As a continuation of the previous chapters, the investigations focus on the same three biomass-derived ashes. All of these ashes were produced with woody biomass as a raw material. Woody biomass was specifically chosen due to the elevated concentrations of calcium found in the derived ash. X-ray fluorescence (XRF) was used to determine the elemental compositions using a Panalytical Epsilon 3XL XRF. The corresponding oxide compositions, calculated using the cement oxide method, can be found in Table 12.

Table 14: Calculated oxide composition of biomass derived ash as determined using the cement oxide method [M.-%] PSFA: paper sludge fly ash; WBFA-1 and 2: woody biomass fly ashes.

Compound	CaO	SiO_2	Al_2O_3	Fe_2O_3	SO_3	TiO_2	MgO	K2O	ZnO	LOI 950 °C
PSFA	74.00	10.46	4.20	1.84	1.19	1.04	0.99	0.56	0.49	3.99
WBFA-1	42.21	11.83	1.93	3.41	3.72	0.28	4.57	11.79	0.18	15.29
WBFA-2	40.71	17.94	2.24	2.75	7.47	0.27	3.29	8.23	0.42	10.26

2.2 Methods

In this study, production practices from traditional OPC manufacturing were simulated in the laboratory to investigate the formation of hydraulic clinker minerals from the biomass-derived ashes. Under the 4 categories; preliminary thermal analysis, pre-treatment, firing regime and post-treatment, different influencing factors in the production of hydraulic minerals were evaluated. For all of the experiments, X-ray diffraction (XRD) analysis was used to identify the minerals present and their changes with the different treatments as a means of determining optimal production methods yielding functional hydraulic minerals.

2.2.1 Preliminary Thermal Analysis

The first objective in this section was to determine potentially significant firing temperatures for all three ashes using thermal analysis. Thermal analysis was used to detect minor chemical changes and provide analytical information on individual cement phases. Digital scanning calorimetry coupled with thermogravic analysis (DSC/TGA) provides data on the heat flow between the sample and a reference crucible vs. temperature, as well as the corresponding weight loss. The ashes were initially analysed with DSC/TGA to determine the temperatures at which chemical reactions and mineralogical transformations occurred. Temperature points for further investigation were selected based on peaks in the DSC curve which correlated to exothermic and endothermic reactions. For each ash 6 temperatures were identified for further investigation.

To achieve the STT, the samples were placed in a Carbolite furnace and fired to the discrete temperatures identified. Using XRD, the minerals formed at each target temperature were identified. For each ash, the ideal composition was determined based on which of the mineral compositions for the different firing temperatures contains the largest quantity of the most hydraulic minerals. This temperature was then considered to be the best firing temperature and was used for all subsequent tests.

Finally, this section also includes the specification of the mineral composition for all three ashes which have been thermally treated at their specified best firing temperature. This composition will serve as the comparison for the subsequent treatments. Based on the changes in the quantity of hydraulic minerals, or the particular minerals identified, each method can be judged as either an improvement or an impairment to the production process.

2.2.2 Pre-Treatment

In the evaluation of particle size, the "as received" particle size was evaluated as well as when the ash was ground to D(90) < 45 μm. To achieve the alternate particle size, the biomass derived ashes (PSFA, WBFA-1, and WBFA-2) were ground in a Retsch mill in an acetone suspension (ratio ash to acetone was 3:1) at 30 oscillations per second for 2 minutes.

Various feed preparations were also explored. The ash was mechanically compressed into tablets, compressed into nodules by hand, compacted directly into a platinum crucible, or left loose in a platinum crucible. Tablets were made using a single piston tabletting machine. The nodules were roughly 2 cm in diameter and made by compressing a biomass acetone paste into spheres by hand. Additionally, samples were compacted directly into a platinum crucible, or left loose in a platinum crucible.

For the most sustainable production, ideally hydraulic minerals would form independently from pre-treatment procedures, thus reducing the energy investment and CO_2 production. However, minor pre-treatments could potentially also reduce the firing time and temperature, resulting in higher energy savings.

2.2.3 Firing Regime

Investigations in the firing regime focused on the dwelling time at the maximum temperature, the rate at which the temperature of the furnace increased, and plateaus at critical temperatures (i.e. temperatures where mineralogical transformations transpire).

Dwelling times of 1, 2, 4 and 6 hours were all investigated. Ideally the lower the necessary dwelling time, the more energy would be saved; however, the desired minerals must still be produced in this time frame. Energy investment can also be cut with the ramping rate of the oven; if optimized so that the higher ramping rate does not deplete more energy, a faster ramping rate could reduce the overall firing time resulting in a reduction in the energy investment. Both a ramping rate of 10°C/min and 5°C/min were investigated. While a 10°C/min rate saves time and energy versus a 5°C/min rate, it needed to be confirmed that the rate would still allow enough time for the necessary reactions to proceed. Staged heating was conducted with the first temperature plateau at 450°C where the sample was held 1 hour, then the next plateau at 810°C where the sample was held two hours and the final plateau at the target temperature where, again, the samples were held for two hours. The plateau temperatures were chosen based on de-hydroxylation and de-carbonation points. In traditional cement production, the calcination zone is significant since it governs the subsequent reactions in the burning zone. If the ash enters the burning zone before all the CO_2 has been removed, it becomes difficult for sintering to take place [20]. For the staged heating experiments a ramping rate of 25°C/min was used to first heat the sample to 450°C where it was held for 1 hour, then the temperature was increased to 850°C where it was held for another hour, then the sample was heated up to its target temperature and held at that temperature for 2 hours.

The different firing regimes were examined not only in an attempt to produce the best ash possible (i.e. ash containing more hydraulic minerals), but also to produce it in the most efficient way possible (i.e. saving time and energy).

2.2.4 Post-Treatment

Four different quenching methods were evaluated. Samples were quickly submerged in a water bath, allowed to cool in the ambient air, sprayed directly with water and sprayed directly with compressed air. All samples were removed from the oven at the target temperature and subjected to the quenching methods. Quenching continued until the samples were under the 100°C threshold and no polymorph transformations could transpire.

3 Results

3.1 Preliminary Thermal Assessment

The ashes were analysed with DSC/TGA to determine the temperatures at which chemical reactions and mineralogical transformations occurred and helped to identify the optimal firing temperatures for the production of hydraulic minerals. The results of the DSC/TGA for WBFA-2 can be seen in Figure 45. This curve is representative of all three ashes; they followed a similar path regarding weight loss and heat flow under increasing temperatures.

A few endothermic peaks occur in the DSC below 1000°C; these are attributed to thermally induced decompositions of the initial minerals. The first endothermic peak occurs between room temperature and 125°C, and is the result of dehydration. As such, the peak is coupled with a gradual progression in weight loss; in the case of WBFA-2 and PSFA this weight loss is approximately equal to 0,5 M.-%. WBFA-1 showed a slightly higher mass loss (2.5 M.-%) and a sharper endotherminc peak at 162°C. This second peak is more in line with the water loss observed in the thermal analysis of samples containing CSH. According to Bhatty and Lindberg et al. C_3S and C_2S pastes have endothermic peaks around 180°C as a result of dehydration reactions due to the loss of water from CSH [21, 22]. This indicates the potential presence of hydrated minerals in the WBFA-1, which, due to their amorphous nature, were not detected by X-ray diffraction. The presence of hydrated minerals implies that after the initial thermal treatment during energy production hydraulic minerals were present. In the course of storage, they became exposed to water. Around 400°C the next peak occurs, which corresponds to the dehydroxylation of another hydration product, portlandite ($Ca(OH)_2$). Portlandite was detected in both PSFA and WBFA-2 and as such, they both have prominent peaks here. WBFA-1, however contained no portlandite. Between 780 and 1000°C, decarbonation of calcium carbonate occurs and is again indicated through the appearance of an endothermic peak. This transition is often coupled with other possible solid-solid phase transitions [22].

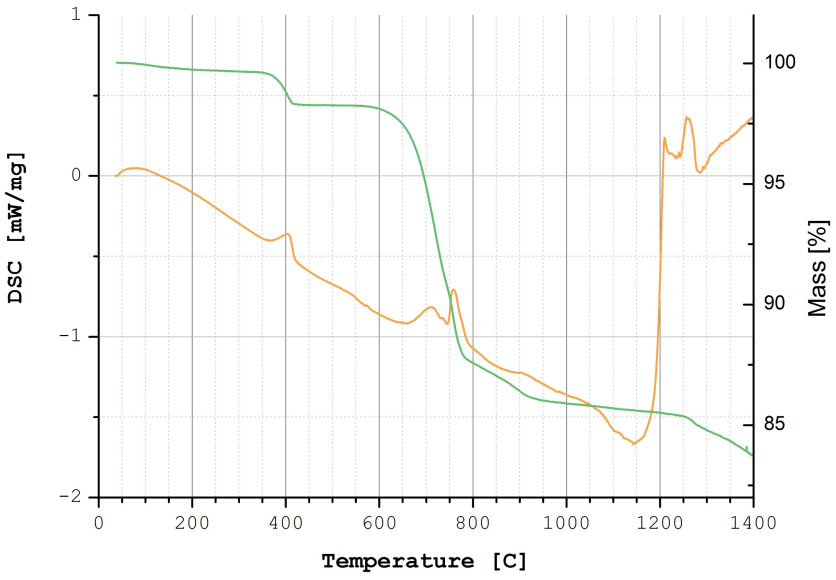

Figure 45: DSC (orange) and TGA (green) curves for WBFA-2 between room temperature and 1400°C.

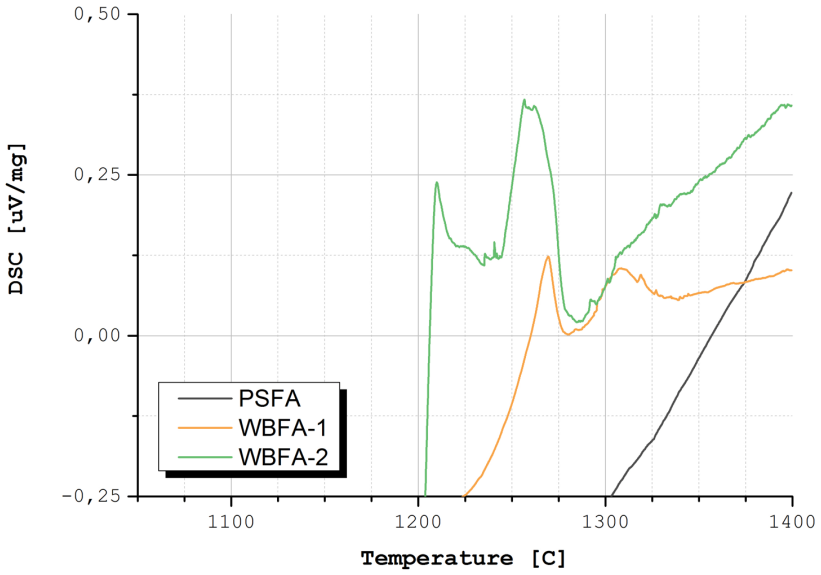

Figure 46: DSC pattern for the three biomass derived ashes in the high temperature range between 1150 and 1400°C.

At the higher temperatures, the formation of clinker minerals transpires and therefore this range is of more interest in determining the optimum firing temperature (Figure 46). As the temperature increases, the curves for the different ashes continue to follow the same trends, only at different temparatures. They all reach a depression between 1000 and 1200°C, followed by a sharp increase in heat flow and a couple peaks and valleys. This is the temperature range at which melting begins to occur and sintering reactions can transpire. Temperatures were selected for each particular ash based

on these points in the DSC curve to be investigated for the mineral composition of the ash after heat treatment. Based on the compositions, it was possible to choose an ash specific optimal firing temperature. Optimal was defined as the temperature where the resulting ash had the largest quantity of the most hydraulic minerals with the lowest heat investment. For all subsequent investigations, the temperature determined to be the optimum was used as the default temperature for STT. Based on the individual DSC/TGA curves, the target temperatures listed in Table 15 were selected for mineralogical characterization.

Table 15: Selected target temperatures for PSFA, WBFA-1 and WBFA-2 based on individual DSC curves.

	Temp 1	Temp 2	Temp 3	Temp 4	Temp 5	Temp 6
PSFA	1100°C	1238°C	1266°C	1287°C	1342°C	1418°C
WBFA-1	1074°C	1172°C	1214°C	1250°C	1269°C	1279°C
WBFA-2	1143°C	1210°C	1220°C	1235°C	1256°C	1286°C

3.1.1 Determination of Optimal Firing Temperature

The mineral composition of the three ashes were qualified after thermal treatments to determine the optimum firing temperature for the STT of each ash. The optimum temperature was decided based on the formation of the largest quantity of the most hydraulically active minerals that had the lowest heat investment.

3.1.1.1 PSFA

Individual PSFA samples were fired to 1100°C, 1238°C, 1266°C, 1287°C, 1342°C, and 1418°C and then analysed. After firing to 1100°C the nodule had not changed much in appearance to that of the raw fly ash. The colour was light and even, like the ash, and it crumbled easily, indicating that it was not a solid mass. However, at 1238°C (Figure 47) there was some indication of a reaction having taken place; the nodule had become harder and more porous looking. Moreover, the colour became uneven with a light bluish-green hue and speckled with light brown spots. The nodules fired to 1266°C and 1287°C looked very similar to that at 1238°C but where harder to the touch. At 1342°C (Figure 47) the colour had become significantly darker and it remained that way at 1418°C. The sample fired to 1418°C looked like a rock; it still had pores but they were significantly smaller.

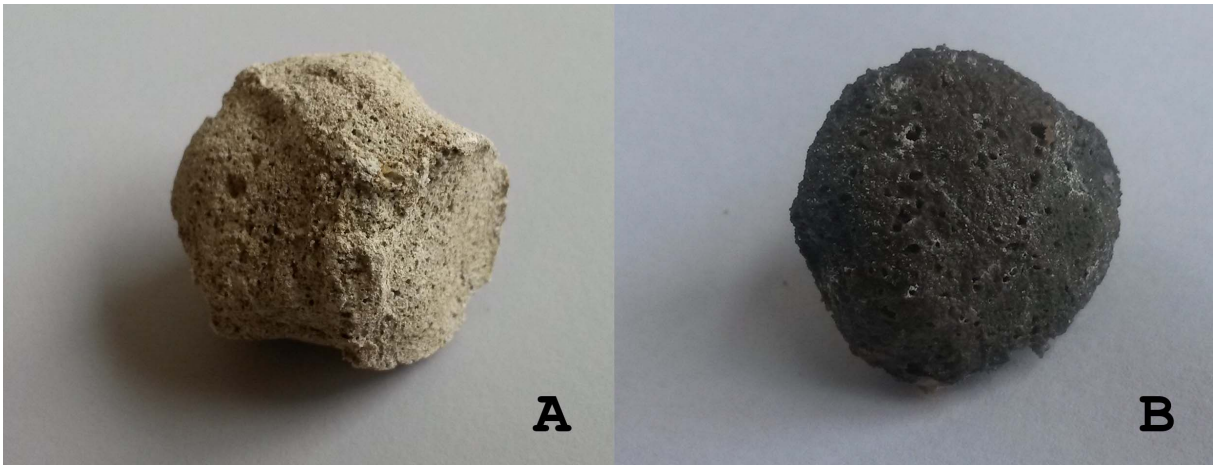

Figure 47: STT PSFA nodules after firing at 1238°C (A) and 1342°C (B).

Results of XRD analyses revealed that PSFA prior to the STT consisted mainly of lime and quartz, however gehlenite, portlandite, and calcium silicate were also present. An increase of exposure temperature resulted in changes in the XRD peak position and intensity, indicating that changes in mineral composition took place. There appeared a gradual shift from one XRD pattern to that of the next temperature.

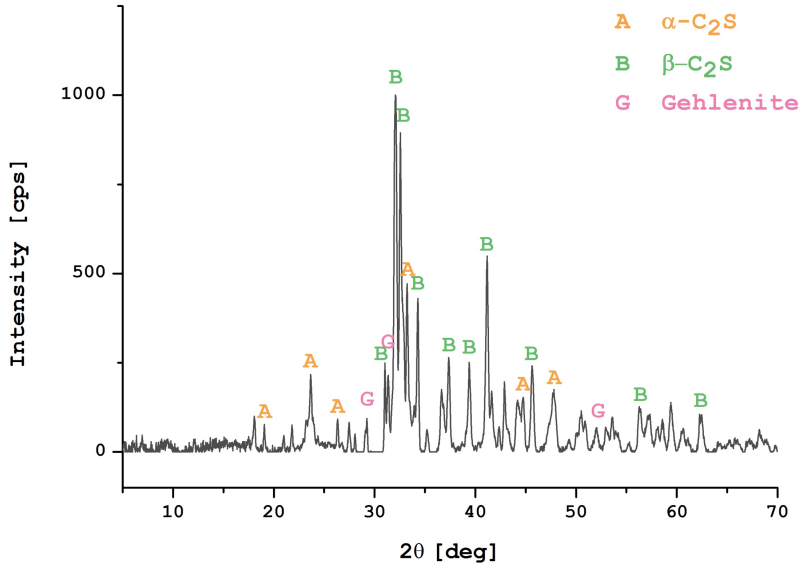

Figure 48: XRD pattern for STT PSFA fired at 1238°C showing a sample composed of β-C_2S α'_H-C_2S and gehlenite.

Lime was the most prevalent crystalline phase detected in the raw STT PSFA, and when the sample was heated to 1100°C, the peaks corresponding to lime were still present at a reduced intensity. For the STT samples fired at 1238°C and higher, lime was no longer detected (see Figure 48). The next most prominent phase in the raw fly ash was quartz, which was still minutely present in the STT sample heated up to 1100°C. However, similar to lime, quartz was no longer detected in the STT samples fired at 1238°C and higher. Both lime and quartz had been converted into other minerals by 1238°C. In the STT PSFA samples fired at 1238, 1266 and 1287°C, gehlenite was still detected. Since this is a relative unreactive form of calcium silicate it is not a desirable mineral, however it shows that calcium silicates can be formed in this temperature range and other alterations to the feed (most notable in the elemental composition) could potentially produce more reactive calcium silicates, like C_2S and C_3S. Portlandite was only detected in the raw fly ash and not in the STT ashes. This is expected because portlandite should not exist in samples heated above 450°C due to the dehydroxylation of $Ca(OH)_2$. However, free CaO in the samples can react with moisture in the ambient environment or be exposed during cooling and revert to $Ca(OH)_2$.

The identification and temperature dependent alterations of the calcium silicate phases are more difficult to detect than the previously described minerals. This is due to the many different polymorphs of calcium silicate and to the fact that all of the respective reflection patterns are very similar, with only minute alterations in peak position and intensity. Furthermore, C_2S is not stoichiometricly fixed and allows for substitution of calcium ions or inclusion of foreign ions. This flexibility in composition results in multiple reflections patterns corresponding to each polymorph. All of the different target temperatures showed C_2S to be present, however which particular patterns they aligned with, changed with thermal treatments. α'_H-C_2S was most discernible in the raw fly ash sample and also clearly

present in the STT PSFA specimens fired at 1100, 1238, 1266 and 1287°C. β-C_2S was present in the samples fired at 1100, 1238, 1266, and 1287°C. However, another pattern for β-C_2S was additionally found which appeared the most pronounced in samples fired at the highest temperatures, 1342 and 1418°C.

3.1.1.2 WBFA-1

WBFA-1 was thermally treated at 1074°C, 1172°C, 1214°C, 1250°C, 1269°C, and 1279°C. The sample fired at 1074°C already showed changes in its appearance, becoming a lighter grey than the raw fly ash. The colour was not consistent throughout and had a sandy appearance and texture. It had solidified somewhat, becoming harder than the raw fly ash however it could be easily broken with minimal force. The nodule also contained small pores which were not present in the unfired nodule. By 1172°C the colour had become darker and more brown than grey. The sample appeared to have further solidified but still maintained its porous structure. The sample had completely melted when fired at 1250°C. The colour became a lighter brown with a milky quality. Greenish yellow segregations could be found within. The samples fired at 1269°C and 1279°C showed the same characteristics as the 1250°C sample.

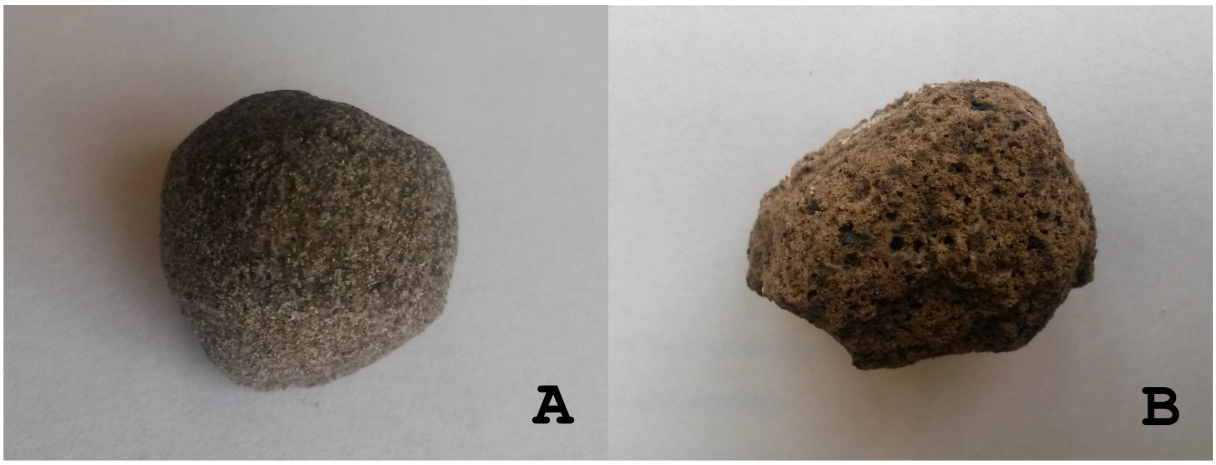

Figure 49: STT WBFA-1 nodules after firing at 1074°C (A) and 1172°C (B).

The raw fly ash was composed of quartz, calcite and arcanite. The calcite which was found in the raw fly ash is most likely due to storage conditions. Since the fly ash was produced at temperatures above 800˚C one would not expect to find any $CaCO_3$ remaining; it should have disassociated into CaO. However, storage of the fly ash post-combustion allowed for exposure to CO_2 in the air which over the course of time was absorbed by the lime. STT, even at the lowest temperatures, provided significant changes in the mineral composition. All of the quartz and calcite appeared gone when STTs were applied. Arcanite, however, remained in the samples that had undergone STT. There appeared two distinct groups of mineral composition after STT; the first including 1074°C 1172°C, and 1214°C, (the lower temperatures) and the second including 1250°C, 1269°C, and 1279°C (the higher temperatures).

Focusing on the first group, the appearance of new peaks at the sacrifice of those in the raw fly ash was clear. The mineral phase with the highest intensity in the three lowest temperature samples was calcium magnesium silicate in the form of akermanite. Additionally, α-C_2S was detected in these samples. The intensity of the α-C_2S peaks increased with higher firing temperatures. Smaller quantities of wollastonite and arcanite were also found in the low temperature samples, however their content decreased as the temperature increased. In the higher temperature group, akermanite was only present in the samples fired up to 1250°C, beyond that merwinite prevailed. While akermanite has the chemical formula of $Ca_2Mg(Si_2O_7)$ and was found in the lower temperature samples,

merwinite has a chemical formula of $Ca_3Mg(SiO_4)_2$ and was found to increase in proportion as the firing temperature increased. The formation of merwinite increased at the expense of akermanite.

In addition to the magnesium containing variants of calcium silicate, belite continued to be present in the higher temperature ashes. The α-C_2S that was detected in the lower thermally treated samples appeared to still exist but showed some pattern shifting.

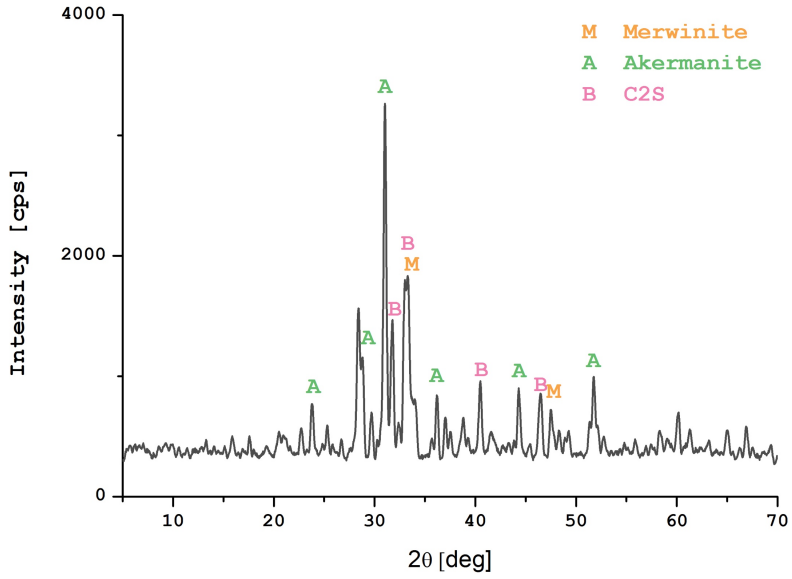

Figure 50: XRD pattern for STT WBFA-1 fired at 1214°C showing a sample composed of merwinite akermanite and β-C_2S.

3.1.1.3 WBFA-2

WBFA-2 was fired at 1143, 1210, 1220, 1235, 1256, and 1286°C. After the STT at 1143°C a slight colour change was perceptible. Instead of being a solid light brown, the nodule become specked with dark brown spots. By 1210°C softening had begun to occur and the bottom of the nodule had become flat, however it did not reach a full melt. The colour became a consistent dark brown and the nodule was somewhat shiny and perceptibly harder. For the sample fired at 1235°C and all those thereafter the nodule melted completely. The colour became a dark amber-brown and was semi-transparent.

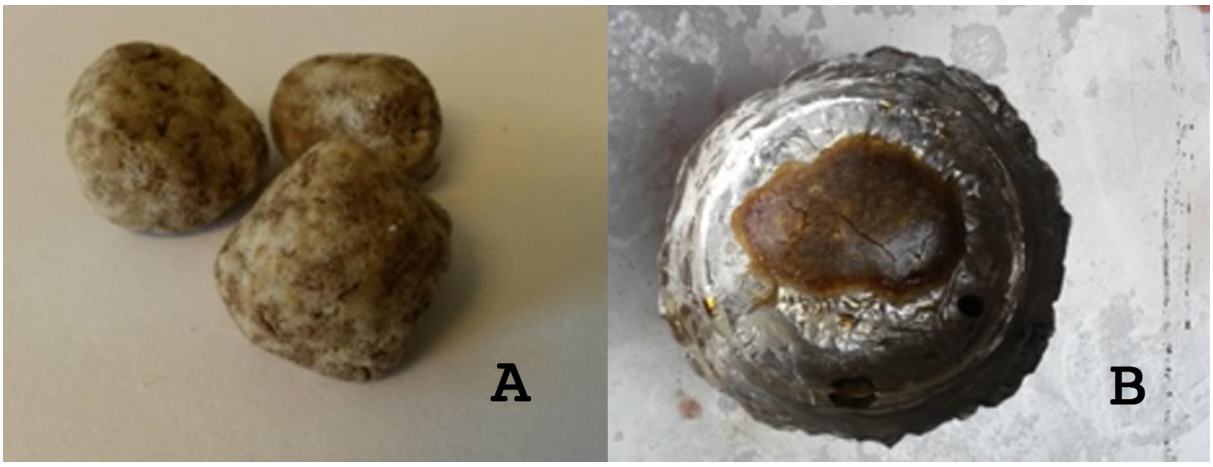

Figure 51: STT WBFA-2 nodules after firing at 1142°C (A) and 1235°C (B).

In the case of WBFA-2, the raw fly ash appeared also completely different from those thermally treated. The raw fly ash was composed of quartz, calcite, arcanite, portlandite and lime. Once heat was applied, similarities were found among neighbouring patterns and these could be grouped into three sets. The identified minerals appeared consistent for the low temperature (1143), medium temperatures (1210 and 1220) and high temperatures (1235, 1256, 1286). While there was some mineral overlap amongst the groups, their distinctions appeared more prominent.

The low temperature sample fired at 1143°C was predominantly composed of akermanite and wollastonite. For the samples fired beyond 1143°C, akermanite was no longer detected. Wollastonite however continued to be present in the medium temperature samples (1210 and 1220°C). In the medium temperature samples, the phase pseudowollastonite also appeared and continued to be present in all of the high temperature samples. With increasing temperature, the amount of pseudowollastonite appeared to increase at the expense of wollastonite. This is logical since pseudowollastonite is a high temperature phase of $CaSiO_3$ that is dimorphous with wollastonite. The samples fired at 1235°C and higher only contained pseudowollastonite. This indicates a dearth of calcium in the ash composition if Ca_2SiO_4 and Ca_3SiO_5 are to be achieved.

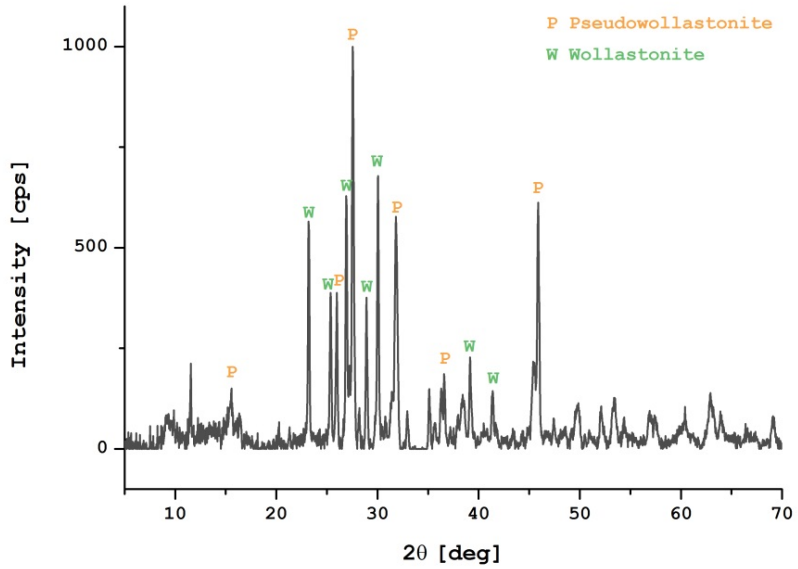

Figure 52: XRD pattern for STT WBFA-2 fired at 1210°C showing a sample composed of pseudowollastonite and wollastonite.

The intensity of peaks appeared to become reduced at the higher firing temperatures. A possible explanation for this is that the sample was less crystalline. An increase in the amorphous fraction of the sample will dwarf the intensity of the minerals present. Unfortunately, the amorphous fraction is hidden to XRD, so its composition could not be determined.

3.2 Pre-Treatment

The pre-treatment experiments evaluated the extent to which the size and form of the fired ashes influence the formation of hydraulic minerals. Each ash was subjected to the different pre-treatments and then fired to the ash specific optimum temperature. After STT, the mineralogy was determined with XRD. The phase composition was then compared to that without the pre-treatment and evaluated for its effectiveness.

3.2.1 Particle Size

The effect of particle size of the ash prior to STT was also evaluated based on changes to the mineralogical composition as determined by XRD. For all three ashes, the diffraction patterns of the original ash look remarkably similar to those of the ground ash. While most of the peaks are located

at the same positions, there are apparent differences in the intensity of the peaks as a result of particle size. This indicates that the same minerals are present; however, the quantities of those minerals apparently increased with smaller particle size of the ash.

In the case of PSFA for both the ground ash and the original ash (D(90) = 175.96), C_2S was the most prevalent mineral detected (see Figure 53). However, gehlenite was also identified and the content was higher in the as-is ash relative to the ground ash. Both C_2S and gehlenite are hydraulic minerals but C_2S is more reactive. In the case of PSFA grinding to D(90) < 45 μm prior to STT appeared advantageous.

In the case of WBFA-1 merwinite, akermanite and calcium silicate were detected in both samples. Merwinite and calcium silicate showed higher intensities in the ground samples where as akermanite was more prevalent in the as-is (D(90) = 126.31) sample. Thus in the case of WBFA-1, reducing the particle size to D(90) < 45 μm prior to STTs was preferred, as it promoted the content of more reactive minerals.

In the case of WBFA-2, one immediately notices distinct differences in the peak intensities shown in figure 9, but unlike the other two ashes, there appeared also different peaks present for the ground sample versus the as-is sample. Both contained wollastonite however pseudowollastonite was also detected in the as-is (D(90)=33.34) sample. Pseudowollastonite does not really have an advantage over wollastonite. Grinding thus appeared less important in the case of WBFA-2. Perhaps due to the already distinctively smaller particle size, grinding did not have such a big impact on the raw feed prior to STT. The difference between the D(90) before and after grinding was significantly smaller for WBFA-2 than for the other two ashes. This appears the most likely reason for the relatively small difference in minerals obtained after STT.

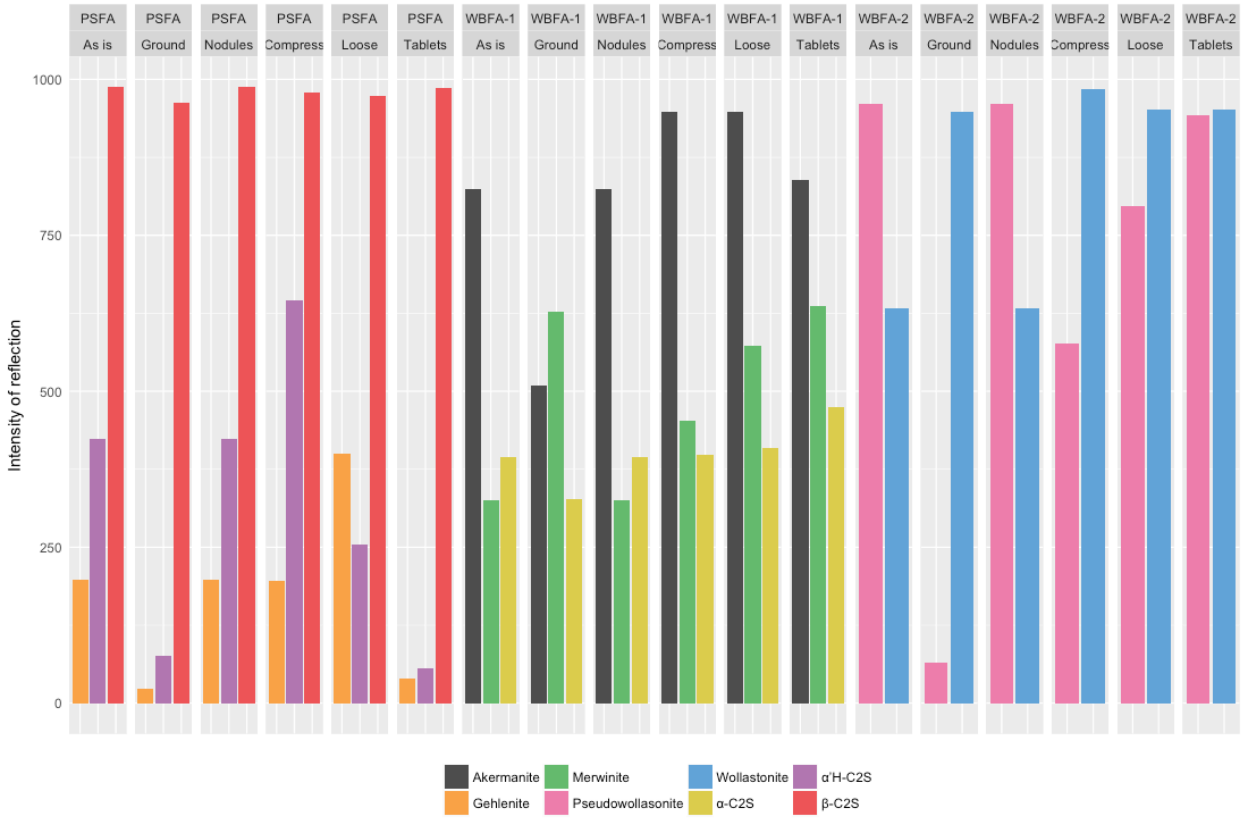

Figure 53: Relative Intensities of reflections for the most prominent minerals in STT PSFA, STT WBFA-1 and STT WBFA-1 after different pre-treatments.

3.2.2 Feed Form

Considering the XRD patterns of the different PSFA feed forms after STT, it appears that most of the peaks are located at the same 2θ position and that their intensities fall in the same general range. However, the tablet and the nodule sample reflection patterns appear more similar to each other but more distinct to those of the compacted and the loose sample reflection patterns (see Figure 53). The compacted sample showed the highest content of α'_H-C_2S while the tablets showed the lowest. All feed forms had the same intensity for β-C_2S indicating roughly the same quantity. The loose sample showed the highest intensity for gehlenite while compacted and nodules samples were slightly lower in gehlenite and tablet samples showed basically no gehlenite peak. Since the formation of gehlenite is often at the expense of calcium silicate, compaction of ash to tablets appears therefore a favourable treatment.

The WBFA-1 ash showed a very different pattern for the nodules than the rest of the feed forms. This diffraction pattern featured fewer peaks and a lower intensity. This was particularly the case for merwinite and calcium silicate. The tablets showed a slightly higher content of merwinite, but otherwise there appeared no discernible differences based on feed form for WBFA-1.

The XRD patterns of all the feed forms for WBFA-2 ash were the same in terms of peak position; however slight differences were apparent for their intensities. The nodules exhibited a slightly lower intensity for wollastonite and a slightly higher intensity for pseudowollastonite. To a lesser extent, this was also true for the tablets.

3.3 Firing Regime

The firing regime tests are divided into 3 subcategories: dwelling time, ramping rate, and staged heating. The "dwelling time" series of experiments explored the effects of holding the maximum temperature for 1, 2, 4 and 6 hours. Ramping rates of 5°C per minute and 10°C per minute were tested to determine effects on the mineral composition. Additionally, staged heating was explored to determine if there were any advantages to thermal plateaus in the temperature climb.

Each ash was subjected to the different dwell times, different ramping rates, and the staged heating before the mineralogy was characterized with XRD. The phase composition was then compared to that of the control and the firing regimes were evaluated for their effectiveness.

3.3.1 Dwell Time

For PSFA, there were no substantial changes to the quantity of β-C_2S detected in the samples exposed to different heating times (see Figure 54). All samples fired at 2-hour and longer had similar intensities for the α'_H-C_2S diffraction, however the sample fired for only one hour had a significantly lower α'_H-C_2S intensity. This indicates that a lower quantity of α'_H-C_2S was formed when the sample was not exposed to a sufficient firing time. Conversely, the content of gehlenite seemed to diminish with extended firing times.

WBFA-1 showed distinct difference in intensities based on the dwell time, most notably for the minerals merwinite and α-C_2S. For both of these minerals, the highest intensity was found for the samples that underwent a 1-hour dwell time. The second best performer was the sample that had a 6-hour dwell as intensity decreased with time. The 1-hour dwell time does not fit the pattern, and the elevated intensities could have resulted from difference in preparation. There were no substantial changes to the akermanite content.

For WBFA-2 there appeared clear variances in intensities based on the dwell time for the minerals wollastonite and pseudowollastonite. The longer the dwelling time the more pseudowollastonite was produced at the expense of wollastonite. Since pseudowollastonite is the high temperature polymorph, it follows that WBFA-2 benefits from longer dwelling times.

For all ashes, sharper peaks were observed for higher dwelling times. The broader peaks corresponding to the shorter dwelling times indicate that there was not enough time for the minerals to crystalize fully. Based on these observations, it is apparent that a 1 hour dwell time is not sufficient.

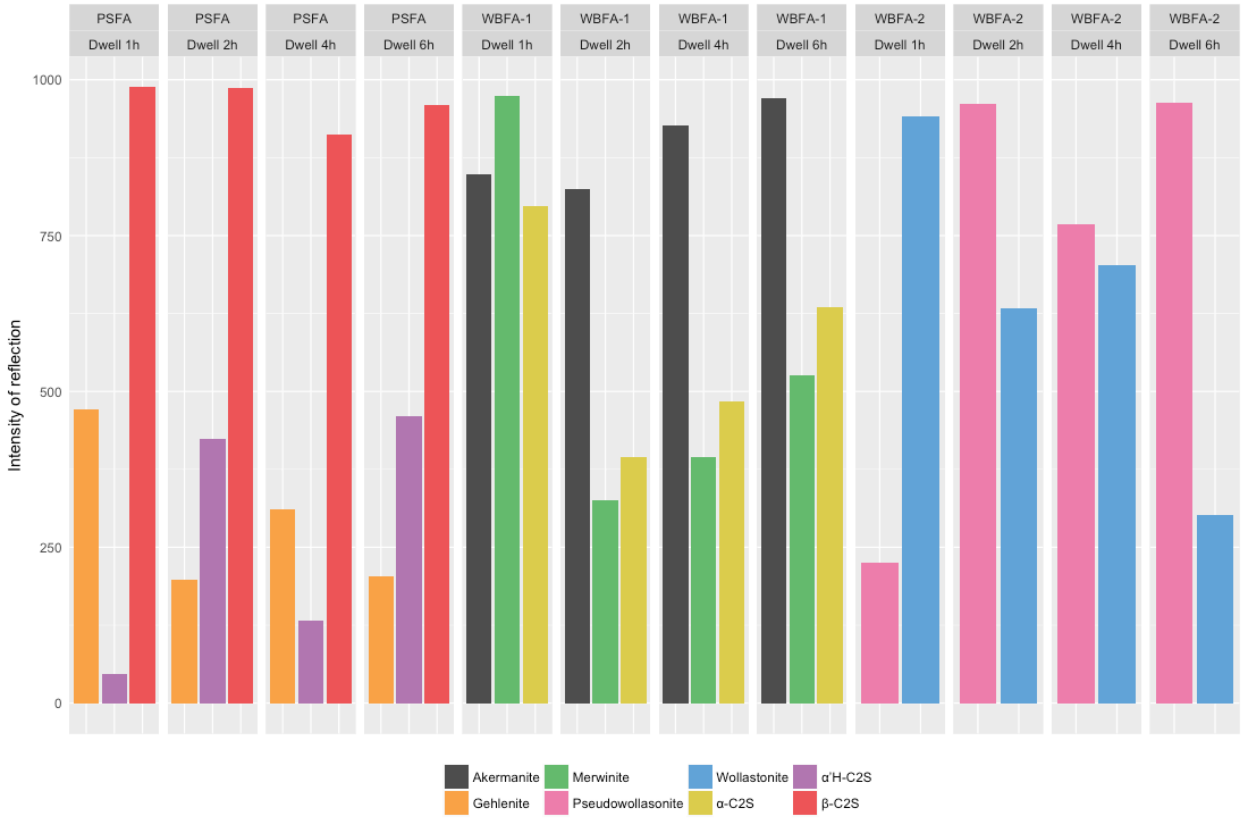

Figure 54: Relative Intensities of reflections for the most prominent minerals in STT PSFA, STT WBFA-1 and STT WBFA-1 after different dwelling times.

3.3.2 Ramping Rate

Both the ramping rates of 5°C/min and 10°C/min were investigated to see the effect on the mineral formation in the STT ash. Concerning PSFA, the sample that was heated at 10°C/min showed higher concentrations of α'_H-C2s (Figure 55). In terms of the other two relevant minerals, β-C_2S and gehlenite, there were no discernible differences in mineral formation based on the ramping rate. Since α'_H-C_2S is the most hydraulically active mineral it is the most desirable and as such a ramping rate of 10°C/min appears desirable.

For WBFA-1, the peaks associated with merwinite were the only ones to show changes in intensity based on the ramping rate. The sample that was heated at a rate of 10°C/min showed higher merwinite concentrations. Since this is the high temperature form of calcium magnesium silicate that incorporates and extra calcium atom, it would indicate that a ramping rate of 10°C/min is preferred.

For WBFA-2, in terms of the effect of the ramping rate, there appears to be little difference in mineral formation. For the peaks aligned with pseudowollastonite and wollastonite, there is no change in intensity based on ramping rate. As such, a ramping rate of 10°C/min should be selected since it optimizes the energy investment.

3.3.3 Staged Heating

Staged heating was performed to see if there were any advantages to mineral formation when dwelling in the temperature ranges where pertinent reactions take place. For PSFA, the staged heating pattern looks similar to that of the direct heating (see Figure 55). The only mineral differences were again with α'_H-C_2S where it can be seen that direct heating maintained more of the high temperature polymorph. In the case of PSFA, there appears therefore no advantage to staged heating.

WBFA-1, however, showed drastic differences in the peak intensities for the sample that was exposed to staged heating. Staged heating was more conducive to the formation of merwinite while direct heating produced significantly more akermanite. In terms of calcium silicate, there was less of a difference; however, the intensity of the staged sample was slightly higher. Since merwinite is more desirable than akermanite and there was a slight increase in calcium silicate, staged heating is advantageous for WBFA-1.

WBFA-2 exhibited a disappearance of peaks when exposed to stage heating. While the intensities of the peaks present look similar, wollastonite appeared only present when the sample was directly heated. While both samples contained pseudowollastonite, the staged heating sample was composed solely of pseudowollastonite. For WBFA-2 it also appears that staged heating has advantages.

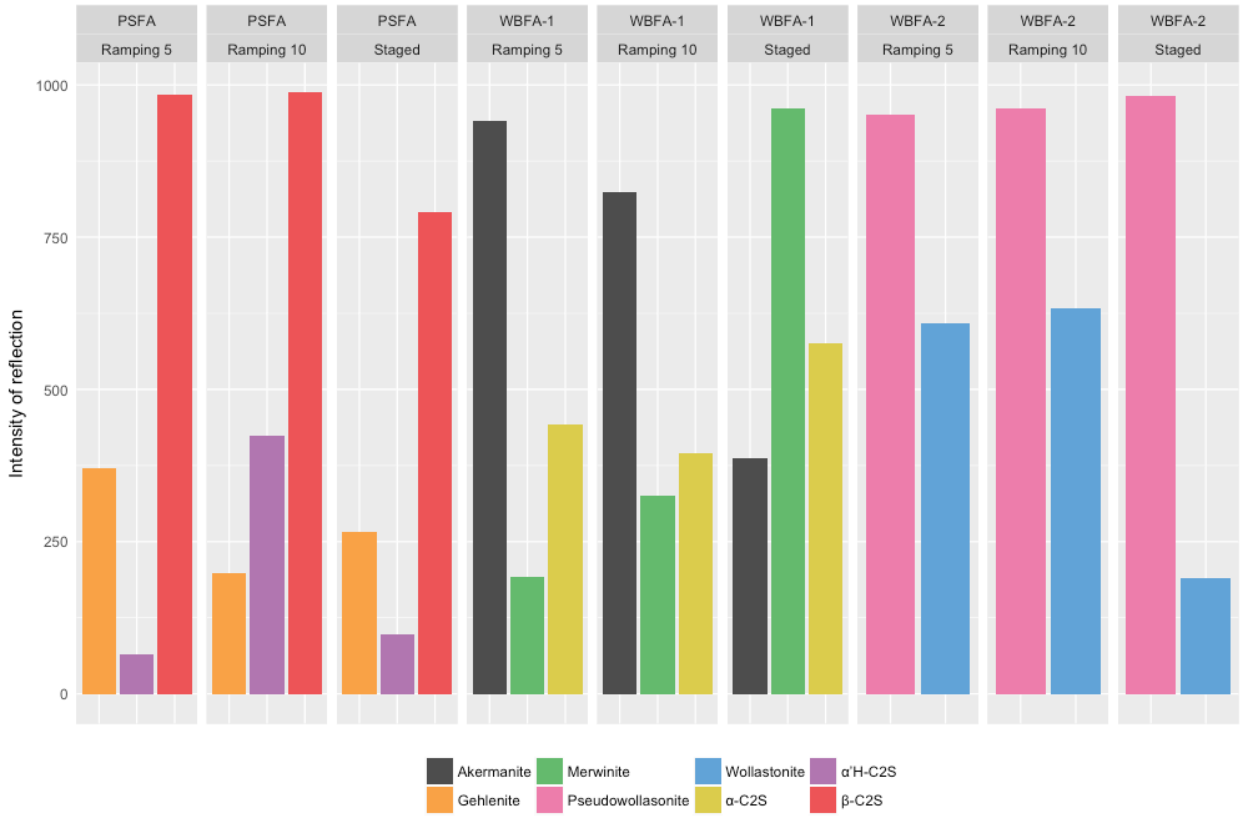

Figure 55: Relative Intensities of reflections for the most prominent minerals in STT PSFA, STT WBFA-1 and STT WBFA-1 after ramping rates of 5°C/min and 10°C/min and staged heating.

3.4 Post-Treatment

In order to determine the best way to preserve the minerals (and polymorphs) formed at higher temperatures, different methods of cooling were explored. The methods included slow cooling at the sample's own rate outside the of oven, quenching with compressed air, spraying with water, and emerging the crucible in a water bath.

For PSFA, the different cooling methods showed remarkably similar XRD patterns. Again, all of the samples were composed of predominately C_2S. For β-C_2S, there is some deviance in peak broadness for the samples cooled in the water bath and in the ambient, however higher intensities can also be seen (see Figure 56). This indicates that the minerals were less crystalline but present in higher quantities. Spraying the sample with water produced the highest intensity for the phase gehlenite. From this data, it would seem that cooling in the ambient or submerging the crucible in a water bath are the best methods to cool. However, cooling in the ambient may be somewhat misleading since the amount of total sample was not so large, and the diameter of the individual sample was limited to 2 cm. The smaller sizes correlate to a larger specific surface area which would expedite cooling. Both of these factors allow for a faster rate of cooling which may not be possible if the production quantity is increased.

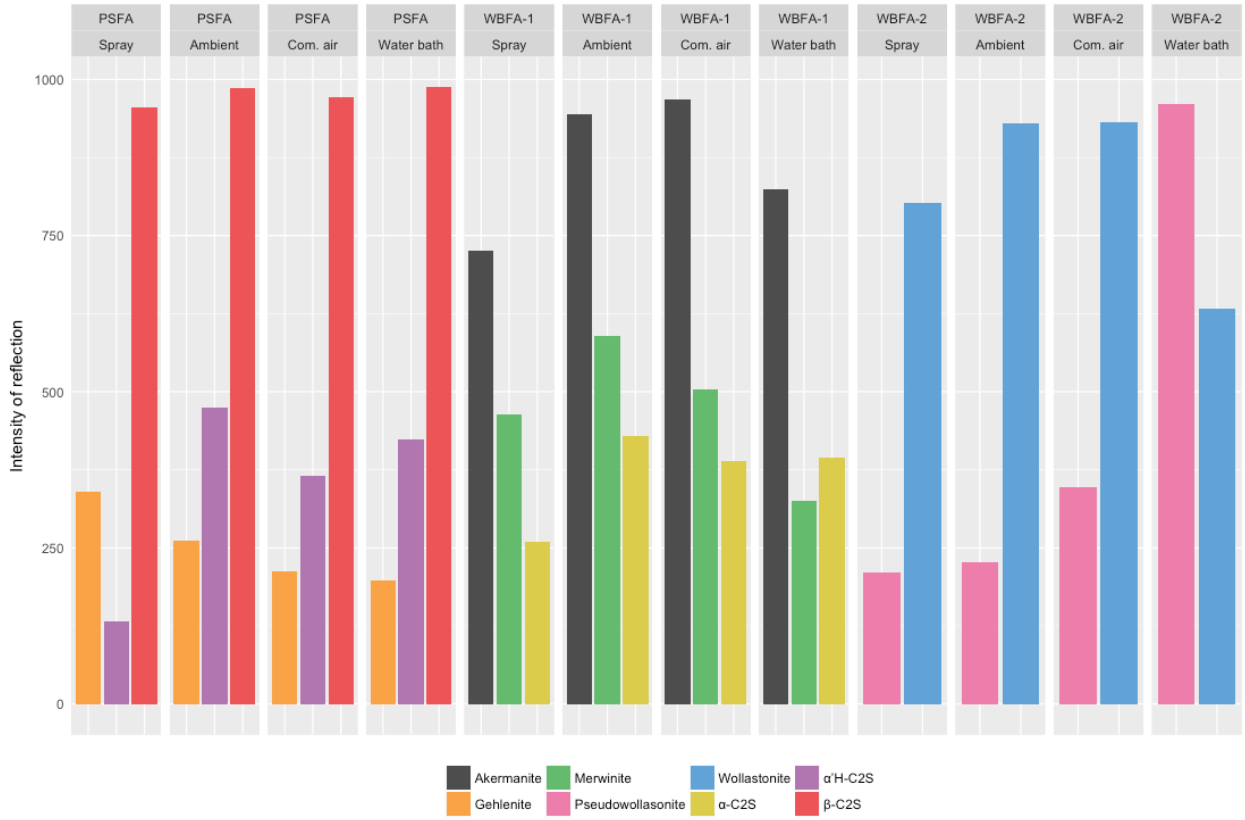

Figure 56: Relative Intensities of reflections for the most prominent minerals in STT PSFA, STT WBFA-1 and STT WBFA-1 after different post treatments.

The large effect of the cooling method on mineral formation in WBFA-1 can be seen through the extreme differences in peak intensities of the reflection patterns. Quenching through spraying water and compressed air showed the highest peak intensities for merwinite and α-C_2S. Submerging the crucible in a water bath showed intensities in a similar range, albeit slightly lower. Spraying the samples with water also produced a new phase, which was not present in any of the other samples. This phase is associated with a hydration product. While spraying with water may work on a large scale production level, laboratory size production is too susceptible to hydration. As such it is recommended to quench with compressed air or submerging the crucible in a water bath for WBFA-1.

The impact of the cooling method on the mineral formation in WBFA-2 was minimal for all quenching methods with the exception of submergence of the crucible in a water bath. While the other three patterns showed similar diffraction patterns, the water bath sample showed a markedly different pattern. The sample cooled in a water bath consistently showed the lowest intensity for all the

wollastonite peaks. However, the water bath sample produced the highest intensity for the high temperature modification, i.e. pseudowollastonite.

4 Discussion

The objective of this study was to thermally treat biomass derived ashes in order to obtain hydraulic minerals and determine the best modes of production, in general and particular to each ash. Methods which produced the largest quantity of apparently the most hydraulically reactive minerals in each type of ash were determined as the best production practices. It was hypothesized that all three ashes (PSFA, WBFA-1, and WBFA-2) could be thermally treated to produce a binder that contains hydraulic minerals, i.e. an STT ash that could be classified as a BioCement. In order to be classified as a BioCement, the described binder must be comprised of at least 50 M.-% belite (C_2S) and/or alite (C_3S) and originate from recent biomass. Based on the pre and post treatments as well as the firing regime, the relative content of the individual minerals changed, and this information can be used for selecting the ash-specific required treatment that results in the largest quantity of the most reactive minerals.

4.1 Optimum Firing Temperature

4.1.1 Ideal Element Composition of the Ashes

The raw PSFA fly ash was composed predominantly of lime and quartz with β-C_2S, gehlenite and portlandite present in smaller quantities (Table 16). After the first STT, i.e. firing the sample initially to 1100°C, it was found that lime and quartz were still present while at subsequently higher temperatures (1238-1418°C) lime and quartz were apparently converted to other minerals. At temperatures above 1100°C, the PSFA ash featured varying amounts of β-C_2S, α'$_H$-C_2S and gehlenite. Given the overabundance of CaO (see Table 12) in the raw ash, it was anticipated that C_3S would be formed in place of, or in addition to, the β-C_2S; however, this did not transpire. The occurrence of α'$_H$-C_2S in the STT PSFA shows the formation of new hydraulic minerals. Furthermore, α'$_H$-C_2S is the high temperature polymorph of C_2S and is a more reactive form [3]. Thus, for the optimum production of a hydraulic binder from PSFA, the formation of α'$_H$-C_2S in addition to β-C_2S and gehlenite appeared feasible when the raw ash is subjected to a STT at 1238°C. Based on semi-quantitative analysis derived from the relative intensities of β-C_2S and α'$_H$-C_2S, STT PSFA has over 50M.-% reactive calcium silicates and can be classified as a BioCement.

The raw WBFA-1 fly ash was composed predominantly of quartz, calcite and arcanite. It was found that after STT its composition changed to merwinite, akermanite and α-C_2S in varying amounts. Given the composition of the raw feed, the occurrence of merwinite and akermanite was not entirely unexpected as these are both calcium silicates that contain magnesium. However, it was unexpected that potassium did not occur in any of the mineral phases given the fact that it was as prevalent as SiO_2 in the raw ash. It is possible that the potassium was either present in an amorphous phase that is hidden to the XRD or that it was substituted for magnesium in the merwinite and akermanite crystal structure. Small amounts could also have stabilised C_2S and been included in its crystal structure (replacing calcium atoms). Alternatively, the lack of potassium could be the result of higher firing temperatures being used in the thermal treatment vs. the original biomass conversion temperatures. During the thermal conversion of biomass into energy, some potassium can be volatilized. Factors, such as association of the elements and combustion conditions, control the release of ash-forming matter. Potassium, which is present in certain silicate minerals, will not be volatilized as readily as organically-bound or dissolved alkali metals due to the different bonding of the elements [23]. In the case of potassium sulphate, vaporization is complex and a variety of condensed and vapour phase products can be produced [24]. For example, at temperatures in the range of 1000 – 1200 °C, potassium sulphate will sublimate [25]. Since potassium volatilization can cause an array of problems

in the reactors with deposit formation, it is generally avoided. This results in potassium acting as an ash-forming element and consequently is present in the derived ash. In the case of WBFA-1 raw ash, potassium was present in the mineral form of arcanite. However, there are no traces of potassium in the crystalline fraction of the STT, indicating that vaporization did transpire in the STT.

Since C_2S is the most hydraulic mineral present in WBFA-1, methods of production in the STT were evaluated based on the ability to increase the quantity of α-C_2S. If merwinite and akermanite continued to be present, then merwinite was preferred to akermanite. Due to its occurrence in blast-furnace slags, merwinite is not unknown to the cement chemist. Merwinite is an intermediate orthosilicate with a monoclinic structure that forms in the temperature range 800-1430°C [18]. Traditionally considered to be only mildly hydraulic, merwinite alone does not produce enough hydrated phases to provide the mechanical strength of OPC [13-15]. However limited merwinite's hydraulic behaviour is, it is still superior to akermanite in reactivity, so if the minerals persist after STT merwinite is preferred to akermanite.

Raw WBFA-2 was composed predominantly of quartz and calcite with portions of arcanite portlandite and lime. After STT, its composition changed to varying amounts of akermainte, wollastonite and pseudowollastonite. However, beyond 1143°C akermanite was no longer detected and only wollastonite and pseudowollastonite were present. Both of these minerals are modifications of calcium metasilica and have the chemical formula $CaSiO_3$. Despite the same chemical make-up, the crystal structures are markedly different. Neither one of these materials are appreciably hydraulic at ordinary temperatures [9]. Pseudowollastonite, however, is the higher temperature polymorph with the transition from wollastonite to pseudowollastonite occurring at 1125°C [3]. Pseudowollastonite's presence in the STT WBFA-2 indicates successful preservation of the higher temperature polymorphs with cooling. While the mineral itself is not particularly sought, is serves as an indication of methods to preserve the presences of other high temperature polymorphs like C_3S and α-C_2S which have a propensity to revert back to low temperature polymorphs. As such, the increased presence of pseudowollastonite is seen as desirable over wollastonite.

Table 16: Minerals present in the raw ash (PSFA, WBFA-1 and WBFA-2) and the minerals detected after secondary thermal treatment (STT).

	PSFA	WBFA-1	WBFA-2
Raw ash & BioSCM	lime	quartz	quartz
	quartz	calcite	calcit
	belite	arcanite	arcanite
	gehlenite		portlandite
	portlandite		lime
STT	α'H-C_2S	merwinite	wollastonite
	β-C_2S	akermanite	pseduowollasonite
	gehlenite	C_2S	

4.1.2 Target Temperatures

As hypothesized target temperatures were found to be very ash specific and varied between the ashes tested. Firing temperatures were individually assigned to each particular ash. It was found that the

target temperature at which most favourable hydraulic minerals were formed for PSFA was 1238°C, while for WBFA-1 it was 1214°C and for WBFA-2 it was 1210°C. All of these optimal temperatures are at least 200°C below traditional firing temperatures. However, none of the samples, even those which achieved a full melt, yielded any alite. Since both WBFA-1 and WBFA-2 reached a sintering temperature, it is therefore hypothesized that the lack of alite is the result of an unsuitable chemical composition of the raw ash or alternatively that upon cooling, the alite transitioned back to CaO and belite. In the case of PSFA, it is possible that firing temperatures were too low to form a sufficient melt and as a result alite did not form.

PSFA had the highest target firing temperature (1238°C) and the ash never reached a complete melt, even when fired at 1418°C. This is in contrast to the other two ashes which had already melted at 1250 and 1235°C. Both WBFA-1 and WBFA-2 contained high percentages of potassium (10.27 and 4.91 M.-% respectively) which is a fluxing agent. Fluxing agents promote reactions by increasing the quantity of liquid at a given temperature. When multiple fluxing agents are present, the effects become more complex, as is the case when both potassium and SO_3 are present. K_2O lowers the temperature of formation of the melt and in the absence of SO_3, it increases the melts viscosity [9]. However, when only SO_3 is present the viscosity can be decreased. The viscosity is decisive in the mineral formation. A low viscosity favours the formation of alite by accelerating the dissolution of lime and belite and the diffusion through the liquid. Even a small stoichiometric excess of alkali oxides over SO_3 has the potential to increase the viscosity [3] [9]. The stoichiometric ratio of alkali oxides (which for these ashes includes Na_2O and RB_2O) to SO_3, is 0.47 for PSFA, 3.11 for WBFA-1, and 1.11 for WBFA-2. So, due to the high concentrations of potassium in WBFA-1 and WBFA-2, a lower melting temperatures is expected. However due to an alkali oxide to SO_3 ratio of over 1, the viscosity of the melt was probably too high to allow formation of alite . In terms of alite formation WBFA-2 has therefore more potential than WBFA-1 considering that its alkali oxide to SO_3 ratio is significantly closer to 1. However, in comparison to the two WBFA ashes, PSFA has apparently a higher alite formation potential as the viscosity of its melt is probably low considering its low alkali oxide to SO_3 ratio (0.47).

In traditional cement raw feed, aluminium and iron are used to lower the melting point. PSFA contains a relevant quantity of Al (4.20 M.-% Al_2O_3) but that of the other two ashes is below desired levels (ideally 4-8% Al_2O_3 in the raw feed for OPC [3]). In the case of Fe, all the ashes contained an acceptable quantity (i.e. 1.5-4.5 M.-% Fe_2O_3)[3]. MgO also lowers the temperature at which the main melt begins to form and it can also slightly decrease the melt's viscosity [9]. Since PSFA contained very little, additional MgO could therefore potentially be used as a fluxing agent to lower its melting temperature resulting possibly in the promotion of the formation of alite. However, MgO in excess can cause other problems. For example, in the case of WBFA-1 where the calculated MgO content was 4.57M.-%, magnesium containing minerals were formed. If the magnesium concentration reaches the point that minerals such as akermanite or merwinite form at the expense of alite or belite, the advantage of the lower firing temperature is superseded by the disadvantage of formation of minerals which feature lower hydraulic functionality.

Alterations to the chemical composition of the ashes prior to refiring should therefore be explored, particularly in terms of balancing the quantities of elements which act as fluxing agents and/or affect formation of clinker minerals in the melt. The determined ideal target temperatures could possibly be further lowered by modifying the ash compositions. If the balance of specific elements are shifted, it might be possible to form more minerals and polymorphs of higher reactivity.

4.2 Pre-Treatment of the Raw Ash

4.2.1 Feed Form

Four different feed forms were investigated in this work including three different types of compaction (compressed into tablets, compressed into nodules or compacted directly into the crucible) and

leaving the ash lose in the crucible. It was hypothesized that higher degrees of compaction of the raw ash would promote the interaction of the individual elements and increase the sintering reactions. Tablets provide the highest level of particle compaction and were presumed to supply the highest level of particle interaction, thereby offering the most efficient production of new minerals. However, it was found that while compaction was important for all three different ash types, tablets did not always produce the best possible STT ash. In the case of WBFA-1 tablets proved to be the best form of compaction but for WBFA-2 handmade nodules provided best results. PSFA showed similar results for all the different types of compaction, however leaving the ash lose in the crucible formed an inadequate STT.

4.2.2 Particle Size

It was presumed that a reduction in particle size would promote the particle interaction and the formation of new minerals. For both PSFA and WBFA-1, it was found that grinding the ash prior to the thermal treatment produced a more desirable STT ash since higher quantities of C_2S were formed relative to the unground ash. This was however not true for WBFA-2, probably because its raw ash already had a significantly smaller particle size. In the case of WBFA-2, the smaller particle size many have even been detrimental because once ground, it produced more of the less hydraulic mineral wollastonite. It can therefore be concluded that D(90) < 45um is advantageous to the production of the more hydraulic minerals in PSFA and WBFA-1 but not in WBFA-2.

4.3 Fire Regime

4.3.1 Dwell Time And Ramping Rate

All of the ashes benefited from a longer dwelling time. There was no new mineral formation with a longer exposure time, however the quantity and the crystallinity of the desired minerals appeared to improve with firing time. It was also found that a ramping rate of 10°C/min was sufficient for all of the ashes since it produced the same mineral composition as the samples heated at 5°C/min.

4.3.2 Staged Heating

Staged heating was presumed to be advantageous in hydraulic mineral formation since it allows all of the volatile compounds to be removed from the ash before critical reactions transpire. The ashes showed different results for the effects of staged heating vs. direct heating. PSFA benefited from ramping the oven directly to the maximum temperature while WBFA-1 and WBFA-2 benefited from plateaus at 450°C and 810°C. In traditional cement production, the calcination zone is significant since it governs the subsequent reactions in the burning zone. If the ash enters the burning zone before all the CO_2 has been removed, it becomes difficult for sintering to take place [20]. The loss on ignition represents the reduction in mass as a result of heating a sample under specified conditions and is expressed as a weight percentage of the dry mass. The decrease in weight is attributed to the volatile substances that have escape the material. The loss on ignition is reported as part of an elemental or oxide analysis of a mineral. The volatile materials typically consist of hydrates, hydroxy-compounds, and carbon dioxide. Considering that the loss on ignition for WBFA-1 and WBFA-2 were 15.29 and 10.26 % respectively, while for PSFA it was only 3.99 %, it appears logical that the WBFA-1 and WBFA 2 could benefit from a staged heating since they contained significantly more volatile compounds which could be inhibiting the clinkering reactions.

4.4 Post-Treatment

Post-treatment focused on methods to cool the samples while maintaining functional minerals that were formed in the heat treatment. Exposure to water was never advantageous and in the case of WBFA-1 lead to the formation of hydration products. Given the small size of the samples being fired, exposure to water is not ideal; the smaller particles have less embodied heat meaning less energy has

to be removed. Furthermore, smaller particles have a larger specific surface area which allows for a larger ratio of areas exposed to water vs. areas not exposed. With exposure to water, there is the potential to apply too much water, in which case not all of it will evaporate fast enough resulting in unwanted premature hydration of the minerals.

In the case of PSFA and WBFA-2, submerging the crucible in a water bath was sufficient to quickly remove heat and lower the sample to a temperature range where the minerals are stable. Other researchers have found that after removing the sample from the furnace at the sintering temperature, simply pouring the materials into a bigger steel receptacle was sufficient to disseminate the heat quickly. Cooling could be further promoted with an air stream [26].

WBFA-1 maintained the functional minerals formed even with ambient temperature cooling. However, this is most likely a result of the mineral composition. WBFA-1 was composed of merwinite, akermanite and α-C_2S while a more ideal WBFA-1 composition would have been α-C_2S and merwinite, but not akermanite. While α-C_2S does have the tendency to revert back to a less reactive low temperature polymorph, upon slow cooling (like all of the mineral phases present in PSFA and WBFA-2), merwinite does not disintegrate upon cooling [27]. Fast cooling is less necessary for WBFA-1 given its particular mineral composition, however it is advantageous in the formation of the other (more hydraulic) minerals present in the three ashes.

5 CONCLUSION

From these experiments, it can be concluded that hydraulic minerals can be formed from biomass derived ashes when these are subjected to a secondary thermal treated. Furthermore, the specific minerals formed, as well as their quantity and quality, can be manipulated by specific pre-treatments (feed, form and firing regimes) and post-treatment firing regimes. From this work, the following conclusions can be made:

- Paper sludge fly ash (PSFA) which in its unaltered form consisted of lime, quartz, β-C_2S, gehlenite and portlandite could be converted into a SST ash composed of α'H-C_2S β-C_2S and gehlenite. Due to the prominence of the mineral phases β-C_2S and α'$_H$-C_2S, STT PSFA can be classified as a BioCement.
- Woody biomass fly ash-1 (WBFA-1) which in its unaltered form (BioSCM) consisted of quartz, calcite and arcanite could be converted into a SST ash composed of merwinite, akermanite and α-C_2S.
- Woody biomass fly ash-2(WBFA-2) which in its unaltered form consisted of quartz, calcite, arcanite, portlandite and lime could be converted into a SST ash composed of wollastonite and pseudowollastonite.
- The ash specific optimum firing temperatures to produce the largest quantity of hydraulic minerals were:
    - PSFA 1238°C
    - WBFA-1 1214°C
    - WBFA-2 1210°C
- High concentrations of potassium in the raw ash result in lower sintering temperature, however they may also inhibit the production of alite due to increase in viscosity of the melt.
- It is beneficial to promote the particle interaction through compaction and a reduction in particle size. Ideally, samples should be fired in tablet or compacted nodule form and the D(90) should be less than 45 μm.
- All of the ashes benefited from a longer dwelling time. There was no new mineral formation with a longer exposure time, however the quantity and the crystallinity of the desired minerals appeared to improve with firing time. It was also found that a ramping rate of 10°C/min was sufficient for all of the ashes since it produced the same mineral composition as the samples heated at 5°C/min.
- Staged heating is critical when the raw ashes contain significant contents of volatile compounds (i.e. hydroxides and carbonates) indicated by a higher loss on ignition.
- Fired samples should be rapidly cooled (submerged in their crucible in a water bath) to help expedite the removal of embodied heat as the minerals being formed are metastable and could revert back to less reactive low temperature polymorphs when not cooled sufficiently fast.

6 REFERENCES

1. Dunstetter, F., M.N. de Noirfontaine, and M. Courtial, *Polymorphism of tricalcium silicate, the major compound of Portland cement clinker: 1. Structural data: review and unified analysis.* Cement and Concrete Research, 2006. **36**(1): p. 39-53.
2. Welch, J. and W. Gutt, *Tricalcium Silicate and Its Stability Within the System CaO - SiO2.* Journal of the American Ceramic Society, 1959. **42**(1): p. 11-15.
3. Hewlett, P.C., *Lea's chemistry of cement and concrete*. 2004: A Butterworth-Heinemann Title.
4. Guerrero, A., et al., *Hydraulic activity and microstructural characterization of new fly ash-belite cements synthesized at different temperatures.* Journal of materials research, 1999. **14**(6): p. 2680-2687.
5. El-Didamony, H., K.A. Khalil, and M.S. El-Attar, *Physicochemical characteristics of fired clay-limestone mixes.* Cement and Concrete Research, 2000. **30**(1): p. 7-11.
6. Doval, M., M. Palou, and V. Kovar, *Hydration and microstructure of binder compounds containing C(2)AS and C2S synthesized by sol-gel method.* Ceramics-Silikaty, 2006. **50**(2): p. 106-114.
7. Asbridge, A., C. Page, and M. Page, *Effects of metakaolin, water/binder ratio and interfacial transition zones on the microhardness of cement mortars.* Cement and Concrete Research, 2002. **32**(9): p. 1365-1369.
8. Doval, M., M. Palou, and S. Mojumdar, *Hydration behavior of C2S and C2AS nanomaterials, synthetized by sol–gel method.* Journal of thermal analysis and calorimetry, 2006. **86**(3): p. 595-599.
9. Taylor, H.F.W., *Cement chemistry*. 1997: Thomas Telford Services Ltd.
10. Maki, I., et al., *Effect of MgO and SO_3 on the Impurity Concentration in Alite in Portland Cement Clinker.* Journal of the American Ceramic Society, 1992. **75**(11): p. 3163-3165.
11. Swainson, I.P., et al., *Neutron powder diffraction study of the åkermanite-gehlenite solid solution series.* Physics and Chemistry of Minerals, 1992. **19**(3): p. 185-195.
12. Moranville-Regourd, M. *Portland Cement–based Binders–Cements for the next millennium*. in *Creating with Concrete: International Conf.* 1999.
13. Venkateswaran, D., et al., *Treatment and characterisation of electric arc furnace (EAF) slag for its effective utilisation in cementitious products.* Global slag magazine, 2007: p. 21-25.
14. Kriskova, L., et al., *Hydraulic Behavior of Mechanically and Chemically Activated Synthetic Merwinite.* Journal of the American Ceramic Society, 2014. **97**(12): p. 3973-3981.
15. Wang, Q., P. Yan, and J. Feng, *A discussion on improving hydration activity of steel slag by altering its mineral compositions.* Journal of Hazardous Materials, 2011. **186**(2): p. 1070-1075.
16. Mostafa, N., et al., *Characterization and evaluation of the hydraulic activity of water-cooled slag and air-cooled slag.* Cement and Concrete Research, 2001. **31**(6): p. 899-904.
17. Kriskova, L., et al., *Effect of mechanical activation on the hydraulic properties of stainless steel slags.* Cement and Concrete Research, 2012. **42**(6): p. 778-788.
18. Kriskova, L., et al., *Effect of high cooling rates on the mineralogy and hydraulic properties of stainless steel slags.* Metallurgical and Materials Transactions B, 2013. **44**(5): p. 1173-1184.
19. Sáez-de-Guinoa Vilaplana, A., et al., *Utilization of Ladle Furnace slag from a steelwork for laboratory scale production of Portland cement.* Construction and Building Materials, 2015. **94**: p. 837-843.
20. Peray, K.E. and J.J. Waddell, *The rotary cement kiln*. 1986: Edward Arnold.
21. Sha, W., E.A. O'Neill, and Z. Guo, *Differential scanning calorimetry study of ordinary Portland cement.* Cement and Concrete Research, 1999. **29**(9): p. 1487-1489.
22. Bhatty, J.I., *A review of the application of thermal analysis to cement-admixture systems.* Thermochimica Acta, 1991. **189**(2): p. 313-350.

23. Lindberg, D., et al., *Towards a comprehensive thermodynamic database for ash-forming elements in biomass and waste combustion — Current situation and future developments.* Fuel Processing Technology, 2013. **105**: p. 129-141.

24. Lau, K., et al., *Studies of the vaporization/decomposition of alkali sulfates.* Journal of The Electrochemical Society, 1985. **132**(12): p. 3041-3048.

25. Armatys, K., M. Miller, and A. Wolter, *Thermochemical characterization of the gas circulation in the relevant cement industry processes.* ECS Transactions, 2013. **46**(1): p. 259-269.

26. Wesselsky, A. and O.M. Jensen, *Synthesis of pure Portland cement phases.* Cement and Concrete Research, 2009. **39**(11): p. 973-980.

27. Bowen, N., *Atomic Arrangement Of Merwinite, Ca3mg [Sio+] 2, An Unusual Dense-Packed Structure Of Geophysical Interest.* 1972.

CHAPTER 7

MODIFYING THE CHEMICAL COMPOSITION OF BIOMASS DERIVED ASH PRIOR TO SECONDARY THERMAL TREATMENT WITH THE INTENT TO UPGRADE THE QUALITY AND QUANTITY OF THE HYDRAULIC MINERALS FORMED (dSTT AND adSTT)

ABSTRACT

The intent of this research is to replace the largest fraction of ordinary Portland cement (OPC) with biomass derived-ash possible for the application of concrete. Based on the results obtained in Chapter 6, additional treatments are explored in an attempt to upgrade the quality of the secondary thermally treated ashes (STT) so that the resulting mineralogical composition is more similar to that of OPC. This set of experiments will again centre on the three biomass derived ashes used in the previous chapters: paper sludge derived Fly Ash (PSFA) and woody biomass derived fly ashes (WBFA-1 and WBFA-2).

Alterations to the chemical composition prior to thermal treatments will be explored primarily through the addition of specific mineral oxides. This will be referred to as doping. Doping plans are based on the chemical composition of the raw ash and the mineralogical composition of the STT ash. It is hypothesized that altering the raw ash's chemical composition so that it is more similar to traditional raw materials will result in a mineralogical composition that is more similar to OPC.

After the chemically altered ash undergoes a secondary thermal treatment it is considered doped secondary thermally treated ash (dSTT ash) and the composition is compared to that of the STT ash (as well as OPC) to determine if alterations to the chemical composition had a positive effect on the formation of alite and belite. Furthermore, this chapter explores the option of doping the ash with sieved fractions of the same ash in order to achieve the desired composition prior to secondary thermal treatment; this type of doping will be referred to as autogenous doping (adSTT).

In this investigation, it was determined that hydraulic minerals could be formed from biomass derived ash and that chemical alterations prior to a secondary thermal treatment steer the quantity and quality of the hydraulic minerals produced. In particular when doped with chemical grade SiO_2, dSTT PSFA was found to contain C_3S (whereas STT PSFA did not). C_3S was also detected in dSTT WBFA-1. Both WBFA-1 and WBFA-2 could be autogenously doped. In the case of adSTT WBFA-1 there was no C_2S formed (as was the case for STT and dSTT) however small quantities of C_3S were still achieved.

1 INTRODUCTION

Variations in the chemical composition of cement clinker kiln feed can have drastic effects on the resulting product. Not only is the presence of particular elements essential, but their mineralogical form and concentration are also critical. Furthermore, the ratios between the individual components are decisive for the clinker quality. Historically, cement was manufactured on the basis of practical experience derived from the production process. However, analysis of the chemical composition of the raw feed, clinker, and cement showed that specific relations exist between composition of the raw feed and the functional performance of the resulting product [1].

Previous chapters have focused on the ash compositions based on calculated oxide components (as listed for the individual ashes in Table 12). This is a typical approach to express the chemical composition of cements, clinkers, and individual phases. Values derived from these analyses characterize to a certain extent the quality of the product in terms of potential hydraulic performance. Such values include the lime saturation factor (LSF), the silica ratio (SR), and the alumina ratio (AR). In terms of cement raw feed, it is crucial to examine the ratio of the required elements in addition to the composition to get an indication of the quality of the resulting product.

The lime saturation factor (LSF) is used in practice as an indicative parameter for the quality of the bulk chemical composition and the resulting reactivity (after thermal treatment). By governing the ratio of calcium and silicium, both present albeit in different ratios in C_2S and C_3S after thermal treatment, this value denotes whether the clinker will or will not contain an excessive amount of free lime. Excess free lime should be avoided. Not only does it correlate to a limitation in the total amount of calcium silicates formed, but its presence can also negatively affect the resulting cement performance in terms of strength reduction, volume instability, and cracking of the derived concrete [2]. The LSF determines the maximum acceptable content of calculated CaO in raw feed so as not to exceed the maximum free lime tolerated in Portland cement clinker [3]. The lime saturation factor in the resulting cement is the ratio $(CaO)/(2.8\ SiO_2+1.18\ Al_2O_3+0.65\ Fe_2O_3)$. If the LSF is too large, an excess of calcium oxide will be present in the resulting clinker; regardless of the extent of mixing or the duration of the exposure to clinkering temperatures, this CaO will not be incorporated into the clinker minerals and will remain unincorporated as part of the final product. Typical values for Portland cement are in the range 0.92-0.98; however, values up to 1.02 are acceptable. Ideally, a clinker will approach a LSF of one but not exceed it. A lower LSF will result in an increased belite content at the expense of the alite. With a LSF of 0.75 a virtually alite-free clinker is formed and $C_{12}A_7$ replaces C_3A resulting in a 'slow' cement [2]. Other researchers have suggested another formula allowing for a small amount of MgO, which can be incorporated into C_3S. The formula, $(CaO + 0.75\ MgO) / (2.80\ SiO_2 + 1.18\ Al_2O_3 + 0.65\ Fe_2O_3)$, should only consider MgO to a maximum value of 2% since any value greater results in the presence of free MgO (generally in the form of periclase) which results in degradation of the hydrated product due to delayed expansion [2]. This ratio is indicated by L(Mg)SF in this work.

The silica ratio (SR) determines the proportion of silicate phases in the clinker based on the raw feed's composition. The ratio is given as $SiO_2/(Al_2O_3+Fe_2O_3)$. A higher silica ratio reduces the liquefaction of the raw materials in the kiln at any given temperature and makes the clinker formation more difficult to achieve. As such, the SR should lay in the range of 2-3 to ensure sufficient burning [4]. Similarly, the alumina ratio ($AR = (Al_2O_3/Fe_2O_3)$) determines the quantity of liquid formed at relatively low temperatures. The quantity of liquid theoretically passes through a maximum at an AR of 1.38 at 1338°C [4]. Ideally the AR will fall between 1.0 and 4.0 [4].

The particular chemical composition impacts the thermal properties of the ash through alterations to the sintering temperature. This is illustrated by the burnability, a measure for the amount of mass transfer from the raw materials to the clinker phases. The burnability indicates the ease with which free lime can be reduced in the kiln (i.e. incorporated into other minerals) and can be defined by the

quantity of free lime present after heat treatment [4]. The burnability of a mix increases with decreasing LSF or increasing SR. An increase in the LSF corresponds to an increase in the CaO content, designating a larger CaO content which must react. Increasing SR implies less liquid at a given temperature.

The mineral form and microstructure in which elements are present can also impact the burnability of the mix. Calcium oxide has a melting point of 2613°C, however calcium can also be present in other minerals like gehlenite and C_2S which have melting points of 1584 and 1540°C respectively. To further complicate the thermal properties, calcium carbonate in the form of calcite has a melting point of 1339°C, while calcium carbonate in the form of aragonite has a melting point of 825°C. CaO is thermally more stable than SiO_2. The silica present in this ash has a melting point between 1670 and 1713°C. It is hypothesized that an overabundance of CaO (particularly in relation to the SiO_2 present) in the raw feed will reduce the burnability and increase the necessary sintering temperature above what was explored in the previous chapter.

While the LSF value is a helpful indicator for the required calcium content in traditional inorganic raw feeds, in the case of alternative raw feeds (as is the circumstances with biomass derived ash), it should be more of a guidance than a rule; the contents of SiO_2, Fe_2O_3 and Al_2O_3, as well as minor oxides, are not identical to that of typical raw feed. The SR and AR give valuable information regarding the burnability of the composition but are not the most pivotal parameter since the elements are not necessarily present in just the oxide form. The available elements in the original biomass or biomass derived ash may be present in different compounds or minerals and thus have different melting points and reactivities. In addition to these ratios, most essentially, the ash composition should have a Ca to Si ratio that allows for the formation of C_2S and C_3S. Thus the C:S ratio should fall between 2 and 3. In a typical OPC raw feed, the C:S ratio falls closer to 3 [1]. In order to achieve a better quality clinker than was obtained in chapter 6, the biomass derived ashes in this study were doped with either CaO or SiO_2 to achieve more ideal LSF, AR, SR and C:S ratio before secondary thermal treatment.

2 Materials and Methods

2.1 Doping of Raw Ashes

The investigations focus on three raw woody biomass-derived ashes provided by the Energy Research Center of The Netherlands (ECN), referred to as PSFA (paper sludge fly ash), WBFA-1 (woody biomass fly ash 1) and WBFA-2 (woody biomass fly ash 2). The calculated oxide composition according to the cement oxide method of these ashes can be found in Table 12. For a full description of the biomass source, conversion technology, ash type, elemental composition, and mineralogical composition, refer to chapters three and four.

Table 17: Calculated oxide composition of raw biomass derived ash (obtained from primary thermally treated biomass) as determined using the cement oxide method [M.-%] PSFA: paper sludge fly ash; WBFA-1 and 2: woody biomass fly ashes.

Compound	CaO	SiO_2	Al_2O_3	Fe_2O_3	SO_3	TiO_2	MgO	K2O	ZnO	LOI 950 °C
PSFA	74.00	10.46	4.20	1.84	1.19	1.04	0.99	0.56	0.49	3.99
WBFA-1	44.63	8.15	1.15	3.92	4.63	0.36	1.79	14.03	0.23	15.29
WBFA-2	40.71	17.94	2.24	2.75	7.47	0.27	3.29	8.23	0.42	10.26

This investigation seeks to improve upon the functional cementitious binder performance of these ashes relative to the non-doped ashes (STT ashes) which have undergone a secondary thermally treatment (as described in chapter 6) by altering the chemical composition of the ashes prior to said secondary thermal treatment. First, the composition will be altered through doping from an external source i.e. pure chemicals/oxides (dSTT) and when possible, the chemical composition will subsequently be altered through autogenous doping i.e. doping from sievings of the same ash. The doping diagnosis for the individual biomass derived ashes was developed using the LSF, SR and AR (Table 18).

Table 18: LSF, L(Mg)SF, SR and AR for the original biomass derived ashes PSFA, WBFA-1 and WBFA-2.

	LSF	L(Mg)SF	SR	AR
PSFA	2.1	2.2	1.7	2.3
WBFA-1	1.7	1.9	1.6	0.3
WBFA-2	0.7	0.7	3.6	0.8
OPC raw materials	0.92-0.98	0.92-0.98	2-3	1-4

2.1.1 PSFA Doping Diagnosis

Raw PSFA consisted of lime, quartz, belite, gehlenite and portlandite prior to secondary thermal treatment and the composition was heavily dominated by lime (see chapter 4). Following secondary thermal treatment, the ash contained α'_H-C_2S, β-C_2S and gehlenite (see chapter 6). Despite the 74,0 M-% of CaO (Table 12) in the raw ash, only a high temperature polymorph of C_2S was produced from PSFA after secondary thermal treatment and no C_3S. The ash was fired at various temperatures between 1100°C and 1600°C. Above 1238°C no more changes in mineral formation were observed (see chapter 6). In typical OPC production, after the formation of belite, the material is exposed to higher temperatures inciting the partial melting of C_2S which allows CaO to combine and form C_3S. No free lime was found in the secondary heat-treated ash, despite the excessive amounts of calcium in the raw feed and the lack of C_3S in the secondary thermally treated ash.

To exclude the possibility that alite did not form due to a lack of CaO, the fly ash was subjected in this study to CaO doping prior to the secondary thermal treatment (at replacement rates of 1, 5, 10, 15, 20, 25, 30 and 35%). Results of this study show that despite the excessive amounts of CaO, no C_3S was formed and free lime did not appear until a doping rate of 20 M.-% and beyond (i.e. ≥ 78.3 M.-% CaO). As such a lack of CaO was excluded as the cause of no C_3S formation and an elemental imbalance is hypothesized as a possible cause and was therefore also investigated in this study.

Table 19: Characteristic composition ratios for PSFA before and after doping.

	C:S	LSF	SR	AR
Raw PSFA	7.6	2.1	1.7	2.3
Doped PSFA	3	0.9	4.4	2.3

A preferable composition for the raw feed is 43.2 M.-% CaO and 14.0 M.-% SiO_2 [2]. In PSFA, the content of CaO falls well over that which is used in practice and the SiO_2 slightly below (74.00 and 10.46 M.-% respectively). These two factors influence the characteristic ratios. The C:S ratio is significantly higher than a desirable ratio (7.6 vs 3.1). PSFA has a LSF of 2.1 which is significantly higher than 1 used for OPC. The SR of PSFA is 1.7 which is relatively low since it lies slightly below the target range of 2-3. This is indicative of a low SiO_2 content rather than too high quantities of Al_2O_3 and Fe_2O_3 (more Al_2O_3 and Fe_2O_3 will create a melt at lower temperatures). Therefore, as a correction to the chemical composition, the C:S ratio should be reduced to 3 through the addition of powder amorphous SiO_2 purified, washed and ignited. By doping the fly ash with silica to achieve a C:S ratio of 3, the LSF concomitantly dropped to 0.9 and the SR increased to 4.4 while the AR stayed constant (see Table 19).

Since alterations to the ash chemical composition result in variations to the thermal behaviour, the doped PSFA was subjected to DSC to ensure an appropriate firing temperature was implemented. Using the information gained in chapter 6 and subsequently from the DSC results obtained in this study a firing temperature of 1305°C was selected to fire the doped PSFA sample for the ash to reach a sintering point without achieving a full melt. It is hypothesized that lowering the C:S ratio will besides correcting the chemical composition also positively affect the thermal behaviour of the ash allowing for the formation of clinker minerals.

2.1.2 WBFA-1 Doping Diagnosis

Raw WBFA-1 was composed of quartz, calcite, and arcanite and heavily dominated by quartz. The STT ash was composed of merwinite, akermanite and C_2S (see chapter 6). While thermal treatments did produce a STT ash containing belite, it was never the most prominent phase. Furthermore, alite was not produced from the ash. Changes to the firing temperatures and treatments shifted the concentrations of merwinite and akermanite, but had no major impact on the minerals present. Both akermanite and merwinite are calcium-rich minerals with the chemical formulas $Ca_2MgSi_2O_7$ and $Ca_3MgSi_2O_8$ respectively. Their presence along with the knowledge that 44.6 M.-% CaO was present in the raw ash indicates that there is plenty of calcium available to form larger quantities of C_2S and potentially also C_3S, whereas the presence of magnesium disrupts the clinker mineral formation.

As can be seen from Table 20, the C:S ratio of the raw fly ash is 5.9. This is significantly higher than the requirement for C_2S and C_3S formation. The LSF also lies above what is desired. In the case of WBFA-1 the LSF accounting for the inclusion of up to 2 M.-% MgO is also important to consider since MgO is present in the minerals of the STT. The MgO concentration of WBFA-1 is 1.79 M.-%. When this is accounted for in the LSF, the number shifts from 1.7 to 1.9. This is moving even farther away from the desired LSF of 1.

Table 20: Characteristic ratios for WBFA-1.Top line being the fly ash in the state received and the lower rows being the ratios after doping with SiO_2.

	C:S	LSF	L(Mg)SF	SR	AR
WBFA-1	5.9	1.7	1.9	1.6	0.3
WBFA-1 (doped 4)	4	1.2	1.3	2.4	0.3
WBFA-1 (doped 3.5)	3.5	1.1	1.2	2.7	0.3
WBFA-1 (doped 3)	3	0.9	1.0	3.1	0.3

It is hypothesized that a reduction in the C:S ratio will produce more desirable clinker minerals. The fly ash was therefore doped in this study with amorphous SiO_2 with a purity of 99.5% powder SiO_2 purified, washed and ignited (J.T. Baker Inc.) to reduce the C:S ratio to 4, 3.5 and 3. The L(Mg)SF reached a desirable value when the C:S ratio was dropped to 3 and the LSF reached a desirable value when the C:S ratio was dropped to 3.5. The addition of SiO_2 to the ash resulted in an increase in the SR. The SR is within the desired range when the C:S is at 3.5 or 4. The AR does not change with doping and it remains below the lower limit of 1.0 for all samples. This will most likely result in less liquid being formed at lower temperatures and therefore require higher firing temperatures. However relative to the initial composition there is no change and as such the temperature should not be higher as a result of the low AR.

A DSC was performed on the mixture to determine the ideal firing temperature and based on these results it was decided that the firing temperature should be increased from 1214 to 1220°C to accommodate the added SiO_2. With the new firing temperature, the SiO_2 doped sample was fired according to the apparently most appropriate method determined for this ash.

2.1.3 WBFA-2 Doping Diagnosis

Raw WBFA-2 was composed of quartz, calcite, arcanite, portlandite and lime and heavily dominated by quartz. The STT ash was composed of wollastonite and pseudowollastonite (see chapter 6). It can be postulated that the chemical makeup is hindering the production of clinker minerals since both wollastonite and pseudowollastonite have the chemical formula $CaSiO_3$. In order to achieve alite or belite more calcium must be incorporated into these minerals.

Table 21: Characteristic ratios for WBFA-2.Top line being the fly ash in the state received and the lower rows being the ratios after doping with Ca).

	C:S	LSF	SR	AR
Raw WBFA-2	2.3	0.7	3.6	0.8
WBFA-2	3	0.9	3.6	0.8
WBFA-2	3.5	1.1	3.6	0.8
WBFA-2	4	1.2	3.6	0.8

The undoped ash had a CaO to SiO_2 ratio of 2.3. While this ratio is potentially sufficient to produce belite, it falls below the ratio necessary for alite (or a combination of alite and belite). To rectify the imbalance in C:S, the ash was doped with pure calcium oxide powder (J.T. Baker Inc.) to reach ratios of 3, 3.5 and 4. Doping the ash to achieve a CaO to SiO_2 ratio of 3.5 produced an ash with a LSF which falls within the desired range. Since in the case of WBFA-2 the chemical composition was altered with the addition of CaO, there were no changes to either the SR or the AR. The AR remains fairly close to the lower limit of 1.0 and should not impact the temperature significantly. The SR continues to be in excess of what is desirable. This will most likely result in a reduction of the liquid content making the clinker formation more difficult. However, the alterations to the Al_2O_3 and Fe_2O_3 content will change the properties of the ash and make it difficult to ascertain the impact of the CaO doping. To avoid complications and confusion, problems associated with AR and SR out of the target range will be addressed through alterations to the firing temperature.

The CaO content can greatly affect the burnability making higher firing temperature necessary to achieve sintering. The doped samples were therefore subjected to an additional DSC in this study to

ascertain new firing temperatures. The optimum firing temperatures for C:S ratios of 3, 3.5 and 4 were 1220, 1250 and 1275 °C respectively.

2.2 Characterization of Doped Ashes After Secondary Thermal Treatment

The individual biomass derived ashes from the previous chapter were investigated to determine potential routes to enhance the clinker mineral content by adapting the chemical composition prior to a secondary thermal treatment.

Samples were doped and then subjected to a secondary thermally treatment (dSTT). Mineralogical analysis was performed with XRD to determine the minerals present and the relative quantities. The mineral composition of the dSTT ash was then compared to STT ash and raw ash to see if the types and quantities of functional hydraulic cementitious minerals were increased, and ideally more similar to that of OPC.

In an additional trial with the objective of avoiding the use of pure chemicals as an attempt to keep all raw materials biologically based and with a limited CO_2 footprint, attempts were made to dope the individual ashes based on mixing different size fractions. Therefore, each of the three biomass derived ashes were sieved into the fraction sizes 0-45, 45-63, 63-90, 90-125 and 125+ μm. The individual sieving fractions were then examined using XRF and XRD to identify potential chemical differences that could be used to alter the composition. When autogenous doping was possible (which was the case for WBFA-1 and WBFA-2) the autogenously doped ashes were subjected to a secondary thermal treatment (adSTT) under the same firing regime as the chemically doped ashes. The mineralogical composition was subsequently determined with XRD and then compared to STT and dSTT to evaluate its effectivity.

3 Results

3.1 Doped Secondary Thermally Treated Ashes (dSTT)

3.1.1 PSFA dSTT

Doping PSFA with SiO_2 in order to reach a CaO to SiO_2 molar ratio of 3 prior to secondary thermal treatment resulted in changes to the mineral composition. After doping, the most intense peak obtained corresponds to gehlenite. While β-C_2S was still identified in the dSTT, α-C_2S was no longer present. In addition to these two phases alite was also present. These three phases accounted for the entirety of the crystalline fraction (Figure 57). Alite is however difficult to detect and differentiate from belite and gehlenite since the most prominent alite peaks are overlapped by these other two phases. The two strongest alite peaks are located at 32.1 2θ and 32.5 2θ however these are completely masked by C_2S. The third strongest peak is located at 29.3 2θ and this is masked by a gehlenite peak at 29.1 2θ, however a slight shift towards the left can be observed as well as a hump exactly in line with the alite reflection. Additionally, the range between 51 and 52 2θ distinguishes the presence of alite. While these reflections are not as intense they are still present.

Since gehlenite is not appreciably reactive, altering the chemical composition of PSFA alone appears insufficient to produce the best dSTT. The doped ash was also subjected to a 24 hour heat treatment, in an attempt to compensate for the lack of mixing in the laboratory oven since a longer firing time could potentially allow for interactions that would otherwise be achieved with mixing. Increasing the firing time again produced an ash composed of gehlenite, belite and alite (see Figure 58). This sample, however, contained α_H'-C_2S instead of the lesser reactive β-C_2S. Furthermore, this sample was superior to that of the undoped sample and the doped sample with a short firing time since the two most present minerals obtained are alite and belite.

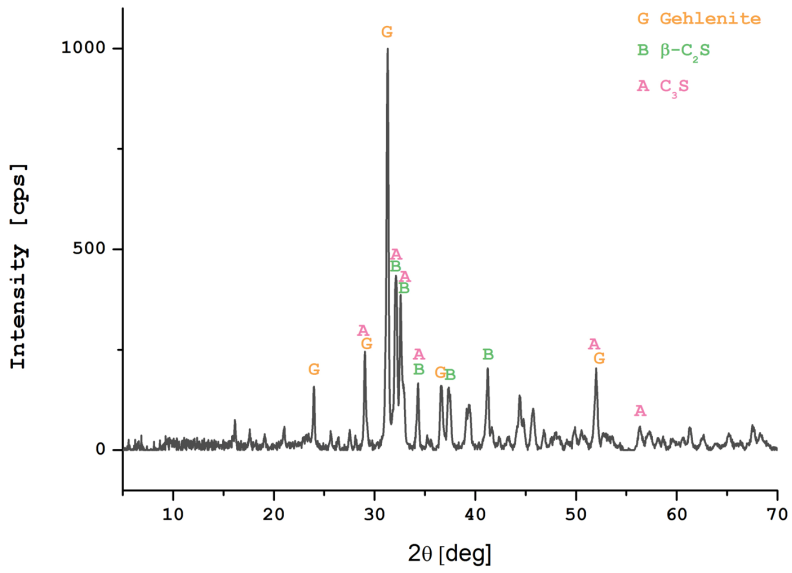

Figure 57: XRD of dSTT PSFA (C:S=3) showing the presence of gehlenite, β-C_2S and C_3S. The composition is dominated by gehlenite

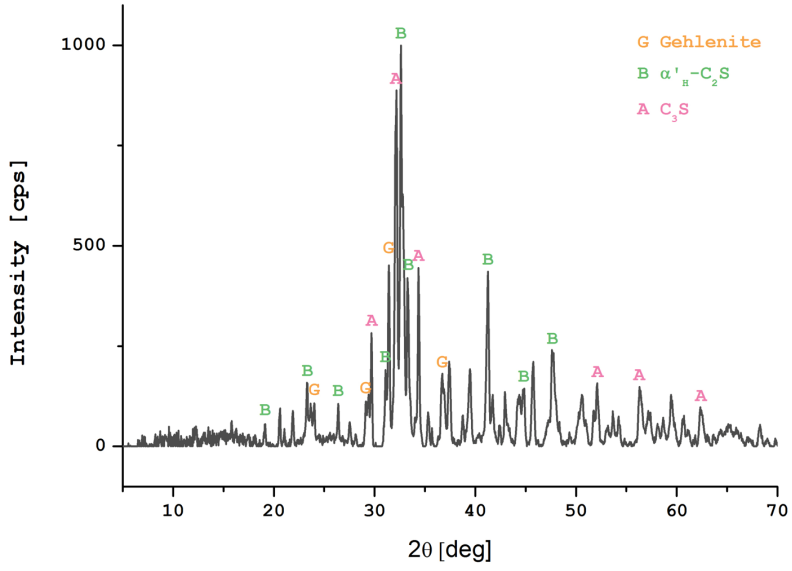

Figure 58: XRD of dSTT PSFA (C:S=3) fired for 24 hours. α'$_H$-C_2S, C_3S and gehlenite are present but the longer firing time has shifted the quantities and gehlenite is no longer the most prominent mineral.

3.1.2 WBFA-1 dSST

In the case of WBFA-1, all doping quantities produced remarkably similar reflection patterns. This appears due to akermanite heavily dominating the composition, supressing the intensity of other phases. The doped samples no longer contained any merwinite and the doped sample with C:S = 3 apparently contained only akermanite. A closer examination of the minor phases present shows that when the ash was doped to a C:S ratio of 3.5 and 4 both α-C_2S and C_3S were detected. Minor differences in the reflection patterns despite the same mineralogical composition are due to different C_3S polymorphs. Both of these minor phases were present in significantly lower quantities than akermanite. It was decided that C:S=4 (Figure 59) was the best ratio for the production of dSTT ash due to the (minor) incorporation of C_3S and the lack of merwinite.

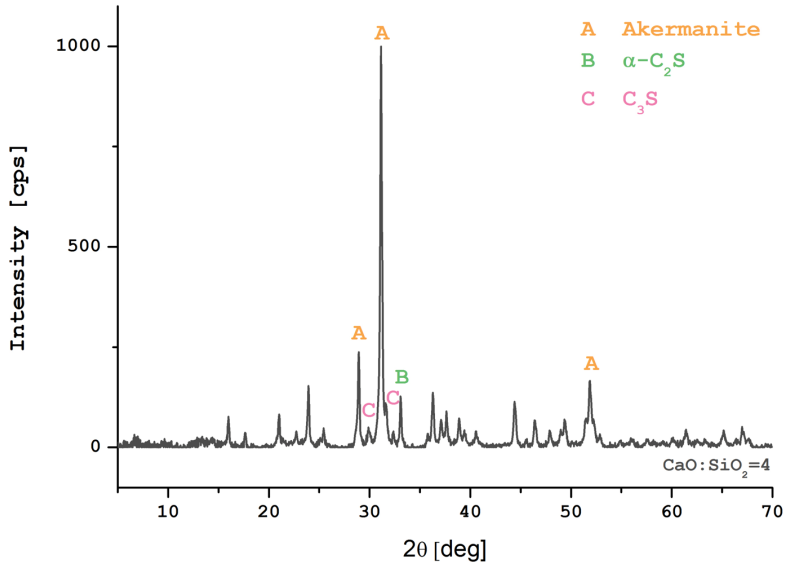

Figure 59: XRD pattern for dSTT WBFA-1 doped to a C:S=4. Akermanite is the most abundant mineral but α-C_2S and C_3S are also present.

3.1.3 WBFA-2 dSST

As was the case with the other two ashes, doping altered the mineralogical composition of the dSTT ash produced from WBFA-2. When doped prior to firing, wollastonite was no longer formed in any of the samples. Pseudowollastonite and α-C_2S were still present; additionally, the mineral akermanite was also detected.

In the case of doping to C:S = 3 akermanite was the most prevalent mineral, as can be seen by the most intense peak at 31.18 2θ (Figure 60). Pseudowollastonite was demoted to the second most abundant phase as evident by the peak at 27.55 2θ. α-C_2S remained the third most abundant phase with a peak at 33.03 2θ. When the sample was doped to a C:S ratio of 3.5, the mineral composition remained the same but the quantities of pseudowollastonite and α-C_2S increased drastically. Akermanite remained the most prominent mineral but pseudowollastonite and α-C_2S are almost as plentiful. The C:S =4 sample was composed primarily of α-C_2S although some peak shifting was detected primarily for the second most intense peak. In addition to α-C_2S minor amounts of akermanite were also detected (Figure 61).

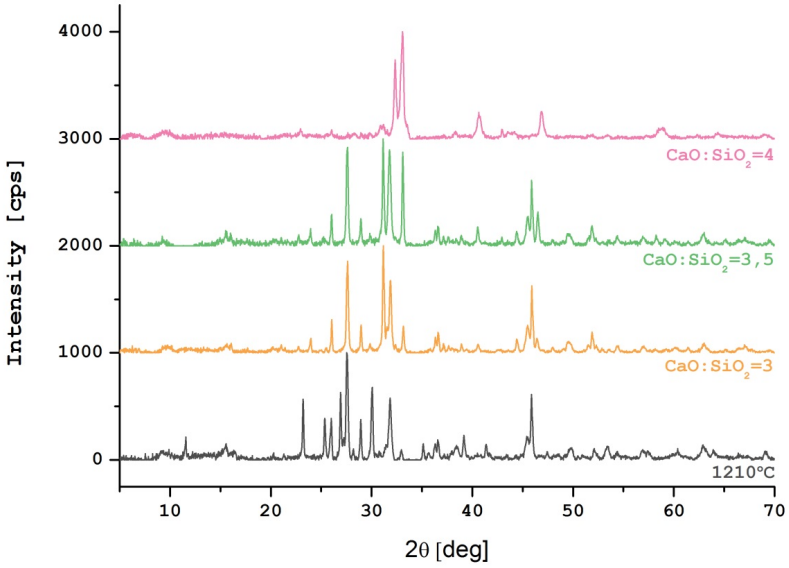

Figure 60: XRD of dSTT WBFA-2 doped to achieve a C:S of 3 (orange) 3,5 (green) and 4 (pink) showing that the same peaks are present however in different quantities.

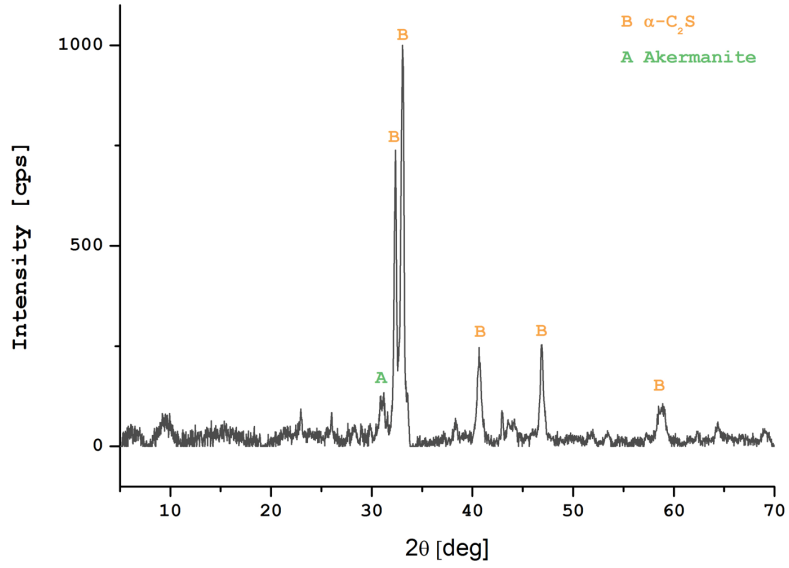

Figure 61: XRD pattern for dSTT WBFA-2 doped to C:S=4. α-C_2S is the most prevalent phase.

3.2 Autogenous Doping

3.2.1 PSFA Autogenous Doping

In the case of PSFA it was found that there were no changes in composition for the different sieving fractions. As a result, autogenous doping is not a possibility with PSFA and the chemical composition could only be altered with external chemical sources.

3.2.2 WBFA-1 Autogenous Doping

Investigations into the sieved fractions of raw WBFA-1 showed extreme differences in composition as can be seen in Figure 62. The smaller fraction sizes were composed mostly of calcite. The larger particles where lower in calcite and richer in quartz. For the 125+ µm sievings, quartz was the most prominent mineral. Arcanite was present in small quantities in all fraction sizes but for 125+ µm it was barely detectable. Since WBFA-1 required more SiO_2 to bring the C:S ratio down to 4, the 125+ µm sieving fractions were selected to be blended with the complete ash to achieve this ratio.

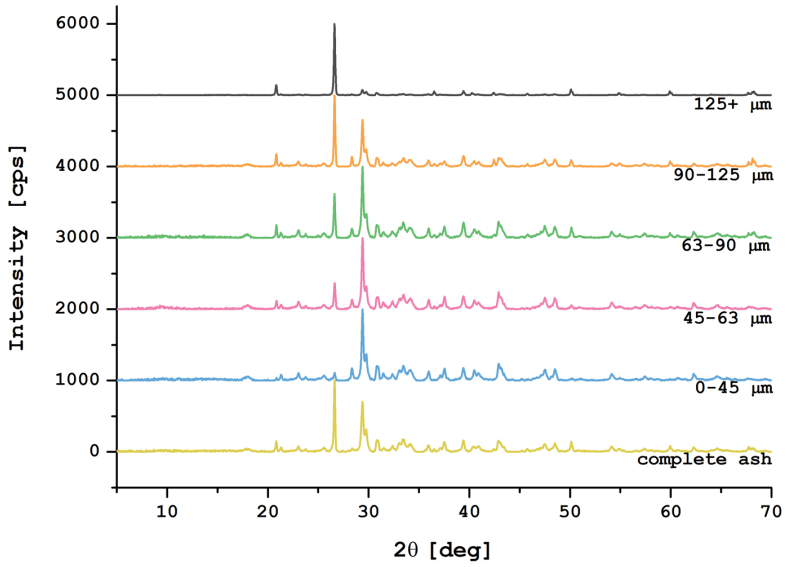

Figure 62: XRD patterns for raw but complete WBFA-1 (yellow) and it's sieved fractions 0-45 µm (blue) 45-63 µm (pink) 63-90 µm (green) 90-125 µm (orange) and 125+ µm (black). The smaller size fractions are largely dominated by calcite (29.4 2θ) while in the larger fractions, quartz (26.6 2θ) is more abundant.

Table 22: SiO2 and CaO concentrations for WBFA-1 and WBFA-1 ≥125 µm as determined by XRF.

	CaO	SiO_2
WBFA-1	42.2	11.8
WBFA-1 ≥125 µm	8.1	26.1

Based on the XRF data on the composition of the 125+ µm sievings and the completed ash, the new (autogenous doped) blend was composed of 39.3% WBFA-1 ≥ 125 µm and 60.7% complete WBFA-1 (Table 22). After blending the sample was fired at 1220°C for 24 hours. XRD analysis of the resulting adSTT WBFA-1 showed minor alterations to the mineralogical composition. Akermanite remains the

most prevalent phase and C_3S remains present. All traces of α-C_2S have vanished while minor traces of wollastonite were detected.

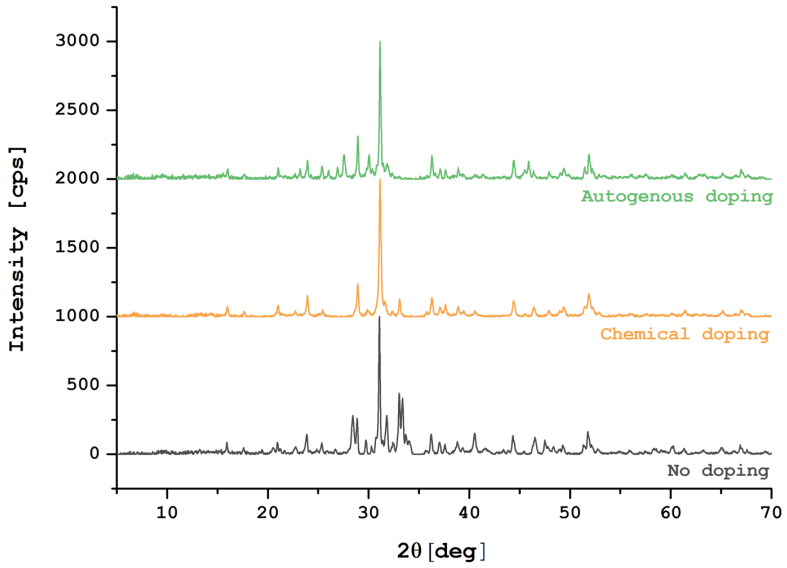

Figure 9: XRD patterns for STT WBFA-1 (black) dSTT WBFA-1 (orange) and adSTT WBFA-1 (green) showing similar reflection patterns for dSTT and adSTT with slightly more noise from the autogenously doped sample. Both Akermanite (31.1 2θ) and C_3S (32.1 2θ) are present in dSTT and adSTT, however α-C_2S (33.0 2θ) is not detected in adSTT.

3.2.3 WBFA-2 Autogenous Doping

Investigations into the sieved fractions of WBFA-2 also exhibited variance in the mineralogical composition as can be seen in Figure 63 and followed the same trend as WBFA-1. Again, the smaller fraction sizes were composed mostly of calcite. As the particle size increased the calcite content decreased and quartz became more abundant. For the 0-45μm sievings the quartz content was the smallest and the calcite was the largest. This sieving fraction also contains calcium in the form of lime and portlandite. Since WBFA-2 required more CaO to bring the C:S ratio up to 4, the 0-45μm sieving fractions were selected to be blended with the complete ash to achieve this ratio.

Based on the XRF data on the composition of the 0-45 μm sievings and the completed ash, the new (autogenous) blend was composed of 42.6% 0-45 μm WBFA-2 and 57.4% complete WBFA-2 (Table 23). After blending the sample was fired at 1220°C for 24 hours. XRD analysis of the resulting adSTT WBFA-2 showed minor alterations to the mineralogical composition.

Table 23: SiO2 and CaO concentrations for WBFA-2 and WBFA-2 0-45 μm as determined by XRF.

	CaO	SiO_2
WBFA-2	40.7	17.9
WBFA-2 0-45 μm	51.3	8.3

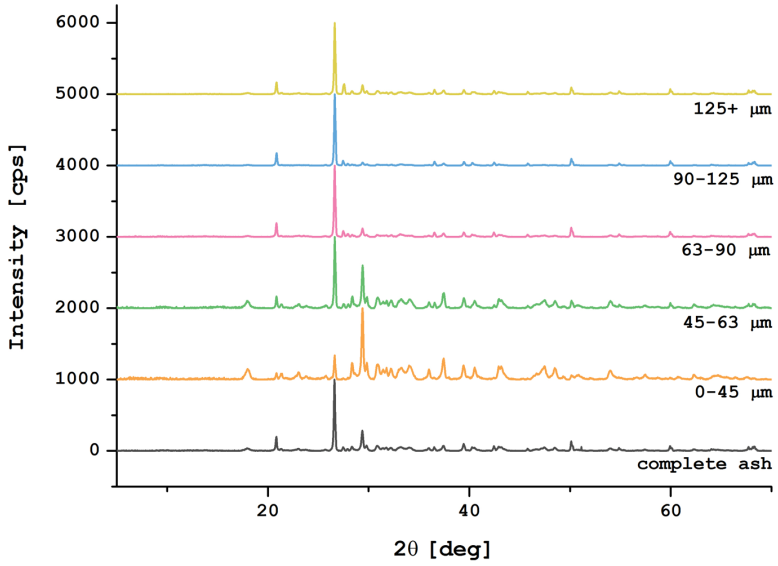

Figure 63: WBFA-2 XRD of sieved fractions XRD patterns for raw complete WBFA-2 (black) and it's sieved fractions 0-45 µm (orange) 45-63 µm (green) 63-90 µm (pink) 90-125 µm (blue) and 125+ µm (yellow). The smaller size fractions are largely dominated by calcite (29.4 2θ) while in the larger fractions, quartz (26.6 2θ) is more abundant.

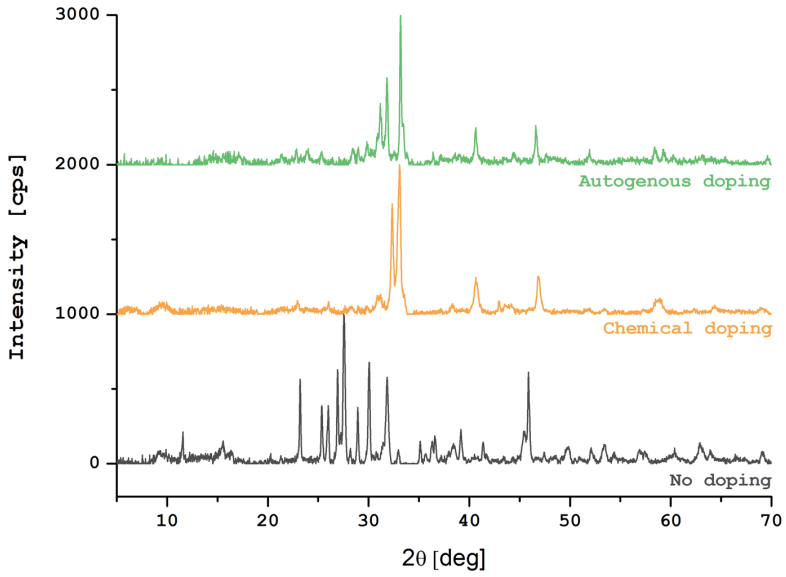

Figure 64: XRD pattern of STT WBFA-2 (black) dSTT WBFA-2 (orange) and adSTT WBFA-2 (green). Both the dSTT and adSTT samples are composed primarily of α-C_2S (33.0 2θ) but adSTT showed more akermanite (31.1 2θ).

The autogenous doping and extended firing time had no effect on the mineral composition but notable effects on the peak position and mineral quantities. This sample was also composed of α-C_2S and akermanite. While the short firing time showed shifting in the α-C_2S peaks, the longer firing time allowed sufficient time for the elements to shift into the proper place and consequently the peaks aligned better. Additionally, the content of akermanite grew somewhat however the content of α-C_2S did not decrease. With increasing firing time peaks became sharper, indicating advantages to a longer exposure to the maximum temperature. Again, the amorphous hump between 22 and 36 2θ was present and showed the highest intensity of all samples.

4 DISCUSSION

Given the extra measures taken to alter the chemical composition of the ashes and consequently the mineralogical composition of the derived dSTT, a better binder in comparison to the raw ashes and STT ashes can be created (Table 24). In the case of PSFA the best practice was doping the ash with SiO_2 to achieve a C:S ratio of 3 and then fire the blend at 1305°C for 24 hours. This resulted in an ash composed of α'_H-C_2S, C_3S and gehlenite. Autogenous doping was not an applicable upgrading method for this particular ash due to the similar element composition of the different size fractions. These experiments show that alterations to the chemical composition prior to a secondary thermal treatment are advantageous with respect to the objective to obtain OPC like mineral composition. This indicates that a longer firing time is effective when the chemical composition is corrected and effectually compensates for the lack of mixing. Thus, for this raw ash the best method to produce OPC like minerals is to dope the ash with SiO_2 in order to reduce the C:S ratio to 3 and then fire for 24 hours at 1305°C.

Table 24: Minerals present in the raw ash (PSFA, WBFA-1 and WBFA-2) and the minerals detected after secondary thermal treatment (STT), doped secondary thermal treatment (dSTT) and autogenously doped secondary thermal treatment (adSTT).

	PSFA	WBFA-1	WBFA-2
Raw ash	lime	quartz	quartz
&	quartz	calcite	calcit
BioSCM	belite	arcanite	arcanite
	gehlenite		portlandite
	portlandite		lime
STT	α'H-C_2S	merwinite	wollastonite
	β-C_2S	akermanite	pseduowollasonite
	gehlenite	C_2S	
dSTT	α'H-C_2S	akermanite	α'H-C_2S
	C_3S	α'H-C_2S	akermanite
	gehlenite	C_3S	
adSTT		akermanite	akermanite
		α'H-C_2S	α'H-C_2S
		C_3S	

Doping was proven to be advantageous for WBFA-1 as well. Secondary thermal treatment of the WBFA-1 without doping produced an ash composed of merwinite akermanite and α-C_2S. When the ash was doped to a C:S ratio of 4 all traces of merwinite vanished. The dSTT WBFA-1 was composed primarily of akermanite, which is not ideal however both α-C_2S and C_3S were also present. Further chemical alterations to the raw WBFA-1 could result in an ash that has more C_2S and C_3S and less akermanite. For WBFA-1 autogenous doping was a possibility and it was found that the best practice was doping the ash with the sieving fraction 125+ μm to alter the C:S ratio to 4 and then fire at 1220°C for 24 hours. This resulted in an ash composed of akermanite, C_3S and wollastonite. This practice shows that autogenous doping is capable of correcting the chemical composition, but further fine-tuning of the chemical composition and firing parameters could result in more OPC minerals and less akermanite and wollastonite.

In both dSTT and adSTT WBFA-1, the most prominent mineral was akermanite which in itself is not hydraulic. However, this material still has the potential to act as a binder particular with alkali activation. For example, blast furnace slag is commonly used as a cementing component in alkali activated cements [9]. Slow cooling of slag produces a stable solid that is composed of melilite, a solid solution of gehlenite and akermanite. Slag composition is fairly similar to that of akermanite [10]. So, while not directly applicable as an OPC replacement the dSTT WBFA-1 still has potential to act as binder in cementitious materials.

Alterations to the chemical composition of WBFA-2 also proved beneficial. Secondary thermal treatment of the WBFA-2 without doping produced an ash composed of wollastonite and pseudowollastonite. Doping WBFA-2 to a C:S of 4 produced and ash that was composed almost entirely of α-C_2S and minor amounts of akermanite. For WBFA-2 autogenous doping was also a possibility and the best practice was to dope the ash with the sieving fraction 0-45 μm to achieve a C:S ratio of 4. After altering the chemical composition, the blended ash should be fired at 1275°C for 24 hours. This resulted in an ash composed of akermanite and α-C_2S.

It is an interesting occurrence that for dSTT WBFA-2, when the C:S ratio was increased to 3 and 3.5, akermanite was the most abundant mineral since there was previously no akermanite present nor was there any magnesium containing phase detected. A possible explanation is that the XRF indicates the presence of magnesium in the raw ash and it was most likely contained in an amorphous phase prior to doping and thermal treatments. Furthermore, the raw data for all the doped samples showed a hump in the range between 22 and 36 2θ which is indicative of the incorporation of amorphous compounds. The intensity of the hump was higher for lower C:S ratios where the magnesium was not present in the identified crystals.

For all ashes the best dSTT ash produced was the result of extended firing times. The extended firing length is intended to provide sufficient time for particle interaction and mineral formation in compensation for the lack of mixing. As such, it is presumed that the elevated firing time will not be necessary given the intimate mixing provided in a rotary kiln. Furthermore, the reactivity, strength development and hydration products for the dSTT ashes produced in these experiments needs to be verified.

In conclusion: based on the best dSTT formed for each ash, PSFA most resembles OPC in that it contains both alite and belite. There are some differences namely the belite is the most prominent phase instead of alite. However, the belite obtained in the ash is of a higher reactivity than the β-C_2S typically found in OPC. As such this blend could potentially show an acceptable reactivity. The second best dSTT was produced from WBFA-2. While this blend did not contain any alite, it was mostly composed of belite. Again, it was a belite polymorph of a higher reactivity. Doping of raw WBFA-1 ash, either chemically or autogenously, did produce an ash containting alite, however the most abundant mineral (akermanite), while functional, is not an OPC mineral.

5 CONCLUSION

In this chapter modifying the chemical composition of biomass ash in order to upgrade its ability to act as a hydraulic binder is studied. For this purpose, doping with pure chemicals and ash sievings (autogenous doping) was used. Based on the presented results and discussion the following conclusions can be drawn:

- Based on the qualification of the minerals present in dSTT PSFA a crystalline fraction with hydraulic minerals can be produced from the biomass derived ash PSFA. The performance still needs to be validated to determine hydraulic properties.
- The best method to produce dSTT ash from PSFA is to dope the ash with SiO_2 in order to reduce the C:S ratio to 3 and then fire for 24 hours at 1305°C to achieve a mineralogical composition most similar to OPC.
- A hydraulic binder can also be produced from the biomass derived ash WBFA-1. This dSTT contained C_2S and C_3S but was composed mostly of akermanite. While this dSTT ash is less similar to OPC in terms of mineralogy, it can be created autogenously and still has functional properties. Due to the origin of the doping material being biomass, further alterations to the secondary thermal treatment have potential to produce a BioCement.
- Doping WBFA-2 to achieve a more desirable composition (i.e. more similar to OPC) did not form any C_3S, however both doping and autogenous doping produce an ash mostly composed of α-C_2S. In the case of adSTT WBFA-2, there is potential to produce a BioCement since the origin of the doping material is biomass, however further alterations to the secondary thermal treatment are necessary to reduce the amount of akermanite and increase the amount of α'H-C_2S.

6 REFERENCES

1. Aldieb, M.A. and H.G. Ibrahim. *Variation of feed chemical composition and its effect on clinker formation—simulation process*. in *Proceedings of the World Congress on Engineering and Computer Science (WCECS)*. 2010.
2. Hewlett, P.C., *Lea's chemistry of cement and concrete*. 2004: A Butterworth-Heinemann Title.
3. Lea, F.M. and T.W. Parker, *The Quaternary System CaO-A1203-Si02-Fe203 in Relation to Cement Technology*. 1935.
4. Taylor, H.F.W., *Cement chemistry*. 1997: Thomas Telford Services Ltd.
5. Lindberg, D., et al., *Towards a comprehensive thermodynamic database for ash-forming elements in biomass and waste combustion — Current situation and future developments.* Fuel Processing Technology, 2013. **105**: p. 129-141.
6. Lau, K., et al., *Studies of the vaporization/decomposition of alkali sulfates.* Journal of The Electrochemical Society, 1985. **132**(12): p. 3041-3048.
7. Armatys, K., M. Miller, and A. Wolter, *Thermochemical characterization of the gas circulation in the relevant cement industry processes.* ECS Transactions, 2013. **46**(1): p. 259-269.
8. Phemister, J., R. Nurse, and F. Bannister, *Merwinite as an Artificial Mineral.* Mineralogical Magazine, 1942. **26**(177): p. 225-230.
9. Shi, C., D. Roy, and P. Krivenko, *Alkali-activated cements and concretes*. 2006: CRC press.
10. Kirkpatrick, R., *MAS NMR-spectroscopy of minerals and glasses.* Reviews in Mineralogy, 1988. **18**: p. 341-403.
11. Puertas, F., et al., *Alkali-activated fly ash/slag cements: strength behaviour and hydration products.* Cement and Concrete Research, 2000. **30**(10): p. 1625-1632.
12. Wang, S.-D. and K.L. Scrivener, *Hydration products of alkali activated slag cement.* Cement and Concrete Research, 1995. **25**(3): p. 561-571.

CHAPTER 8

QUANTIFICATION OF THE REDUCTION IN CO_2 EMISSIONS ASSOCIATED WITH THE PRODUCTION OF BIOCEMENT RELATIVE TO PORTLAND CEMENT

ABSTRACT

The intent of this research is to explore bio-based alternatives to the production of cement and concrete with the objective of reducing the overall CO_2-emission associated with the production. The proceeding chapters outlined methods to produce binders from biomass derived ashes as alternatives to Portland cement. If, after secondary thermal treatments (STT), the ash is composed of at least 50 M.-% reactive calcium silicates (alite and belite) and it originates from biomass, it is considered a BioCement. Biomass derived ashes (which have not undergone a secondary thermal treatment) used to partially replace OPC are termed BioSCMs.

Based on these outlined methods, the reduction in CO_2 emissions will be calculated in this chapter using a basic life cycle analysis. This chapter will focus on quantifying the reduction in CO_2 emissions when BioCement (as well as OPC with BioSCM replacement and BioCement with BioSCM replacement) is produced relative to clinker. Emissions associated with the production of Biocement and BioSCMs will be based on the production methods determined in Chapters 6 and 7 for BioCement and Chapter 4 and 5 for BioSCMs and extrapolated for the larger scale installation necessary for industrial application. From this work, it was determined that partial replacement of OPC with BioSCM has the potential to reduce the CO_2eq emission while providing sufficient performance parameters. Replacement of OPC with BioCement has the potential to reduce CO_2 emissions by at least 70% and even by 80% when replaced by a BioSCM, under the assumption of equal performance.

1 INTRODUCTION

Production of construction materials is often cited as one of the most promising technologies to make an impact on reducing CO_2 emissions [1]. Of all construction materials concrete is the largest contributor to CO_2 emissions, based on a high Portland cement content. Portland cement production is characterized by high emission rates stemming from the production process and from the fact that it is being consumed in large quantities. It has been estimated that if 50% of Portland cement were replaced by a low-carbon alternative, then an annual saving of up to 1 billion tonnes of CO_2 could be reached [2]. In 2014, the global average gross CO_2 emission per ton of clinker was 842 kg [3]. Cement production is held accountable for roughly 8% of anthropogenic global CO_2 emissions [4]. Due to this, the carbon dioxide emission stemming directly from Portland cement manufacturing is the most acute sustainability issue confronting the construction industry.

In the production of Portland cement, CO_2 emissions stem from two discrete sources, namely, the thermal decomposition of calcium carbonate (calcination) and the combustion of fossil fuel. These two categories can be divided into process emissions and production emissions respectively. The calcination process is responsible for 62% of the CO_2 emissions while the remaining 38% stems from the fossil fuels which are combusted to drive the calcination process [5]. The process emissions, or the CO_2 emissions resulting from conversion of limestone into calcium oxide, are fairly constant. Since multiple factors are involved, such as the thermal efficiency of the kilns, the CO_2 emissions resulting from the combustion of fossil fuels required for the production of a ton cement fluctuate. A breakdown of the CO_2 sources and the factors influencing their quantities can be seen in Figure 65.

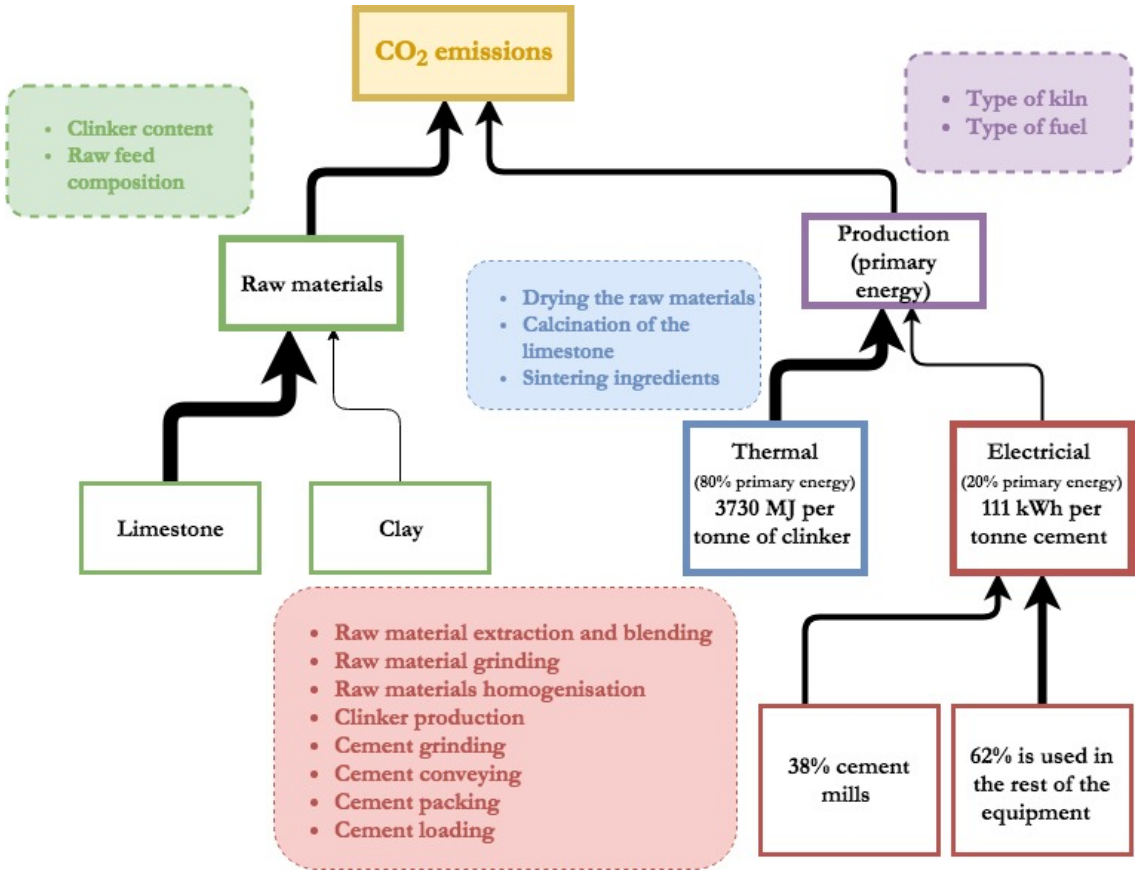

Figure 65: Breakdown of the CO_2 sources and the factors influencing their quantities in the production of Portland cement.

Clinker is made from 64-67% CaO which traditionally comes from limestone ($CaCO_3$). As one of the initial chemical reactions in OPC production, limestone is calcined to produce CaO and in this process, CO_2 is released into the atmosphere. Process CO_2 can be expressed and quantified by the following equation:

$$CaCO_3 \rightarrow CaO + CO_2 \quad (1)$$

$$1\,kg \rightarrow 0.56\,kg + 0.44\,kg \quad (2)$$

For every tonne of calcium carbonate calcined, 440 kg of CO_2 are released into the atmosphere [6]. The specific process CO_2 emission for cement production depends on the exact clinker recipe as well as the amount of clinker in the cement. This can vary between 30 and 95% [6]. For the most commonly used form of cement, Portland cement (OPC), clinker comprises typically around 95%. Therefore for every tonne of OPC, approximately 530 kg of calcium carbonate-derived CO_2 is released [7].

As previously mentioned in addition to process emissions, 38% of CO_2 stems from production. Cement production is extremely energy-intensive and the industry accounts for about 2% of the global primary energy consumption, or up to 5% of the total global industrial energy consumption [8]. Thermal energy accounts for around 80% of the primary energy consumed and the remaining 20% is consumed in the form of electrical energy [9]. Predominantly, carbon intensive fuels like coal are used to provide the thermal energy [6]. Practically all fuel is used for pyro-processing where water is removed from the raw meal and the limestone subsequently calcined at temperatures between 900 and 1000°C, and the resulting products sintered at about 1500°C. The theoretical energy consumption is based on the heat requirement to produce clinker minerals which is theoretically calculated to be 1750 MJ per tonne of clinker [10]. However, in 2008 the European weighted-average for thermal energy consumption in the production of clinker was 3730 MJ per tonne of clinker [9].

The discrepancy between the theoretical and weighted-average values lies in the specific process applied. The type of kiln technology, the number of cyclone stages in the pre-heater and type of cooling system are all influential on the thermal energy consumption [5]. This is illustrated in

Table 25, which shows the brake down of the thermal energy consumption (in MJ/tonne clinker) dependent on the type of kiln technology averaged out for the EU 28 as well as the world for the years 1990, 2000, 2010 and 2014. It is advantageous to examine the consumption rates for both Europe and the world at distinct time periods because they have experienced technological advancements at different times. Historical variances in energy prices have been critical in the development of different processes. When spikes in energy costs occurred, pressure was applied to the industry. If the climate was right for domestic infrastructure development this pressure helped to drive installation upgrades for lower energy processes [11].

Table 25: Thermal energy consumption per tonne of clinker per type of kiln technology (MJ/tonne clinker) for the EU 28 and world between 1990 and 2014.

Kiln technology	EU 28				World			
	1990	2000	2010	2014	1990	2000	2010	2014
Dry rotary kiln with preheater & precalciner	3711	3517	3581	3570	3620	3403	3391	3376
Dry rotary kiln with preheater	3836	3591	3704	3692	3853	3676	3692	3670
Dry long rotary kiln without preheater	3871	3936	3641	3751	4584	4336	4016	3794
Semi-wet & semi dry rotary kiln	3999	3745	3829	4035	4006	3776	3824	3989
Wet rotary kiln & shaft kiln	5821	5330	5044	5184	6315	6031	5982	5711

Table 26 Energy saving measures in clinker production and potential emissions reduction according to [12].

Energy saving measures	Emission reduction (kg CO_2/ton)
Conversion of long dry kilns to pre-heater/pre-calciner Kiln for clinker making in rotary kilns	169.07
Dry process upgrade to multi stage pre-heater kiln for clinker making in rotary kilns	141.44
Replacing vertical shaft kilns with new suspension pre-heater/pre-calciner kilns for clinker making in vertical shaft kilns	62
Installation or upgrade of a pre-heater to a pre-heater/pre-calciner kiln for clinker making in rotary kilns.	45.69
Conversion to reciprocating grate cooler for clinker making in rotary kilns	43.13
Kiln combustion system improvements for clinker making in rotary kilns.	40.68
Energy management and process control systems for clinker making in all kilns	21
Low temperature heat recovery for power generation for clinker making in rotary kilns	19.18
High temperature heat recovery for power generation for clinker making in rotary kilns	18.03
Optimize heat recovery/upgrade clinker cooler for clinker making in rotary kilns	15.38
High pressure (hydraulic) roller press for finish grinding	13.63

The different kiln technologies are typically broken down into seven distinct categories, however in

Table 25 the semi-wet and semi-dry rotary kiln consumptions were grouped together as well as the wet rotary kiln and shaft kiln due to the similarity in rates. The different processes involve varying quantities of water, and the necessary energy demand to evaporate that water correlates to varying quantities of fuels. Consequently different volumes of CO2 are emitted [11]. Furthermore, lower thermal energy consumption corresponds to more advanced kiln technology with clinker-coolers, preheaters with more cyclone stages and higher efficiencies in general. Higher thermal energy consumption corresponds to production processes that are less efficient in the reuse of waste and latent heat, and these technologies are forced to remove more moisture during the processing with primary thermal energy. Converting long dry kilns to kilns with a pre-heater and a pre-calciner has the potential to save 169 kg of CO_2 for every ton of clinker produced [12].

Ali et al. investigated potential measures to save energy in clinker production and reduce emissions [12] based on the works of [13-15]. Table 26 shows a summary of the measures with the highest impact. Techniques which reduced energy consumption center around additional recovery, production of electricity from exhaust gases, increased recovery of the heat of the exhaust gases to dry and preheat the raw materials.

Most attempts to lower the CO_2 footprint of cement (like the ones listed above) are focused on reducing the production-CO_2. Attempts to reduce the process-CO_2 also exist but are typically limited to reducing the clinker fraction in the cement or reducing cement content in concrete through the introduction of secondary cementitious materials (SCM). Since the process-CO_2 stems from the decarbonation of limestone, alternative sources of CaO need to be identified and explored to truly make an impact on the process-CO_2 emissions. The concept behind the present work is to explore biobased materials which can be used to replace limestone. The biobased materials are then processed in a way that mitigates production CO_2 as well (schematically depicted in Figure 66).

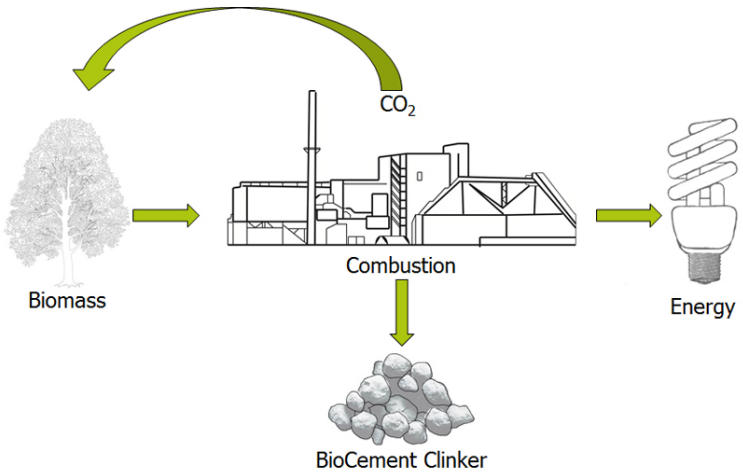

Figure 66: Concept: Biomass is thermally treated to produce energy (in the form of heat and/or electricity) and in the process hydraulic minerals are produced as a byproduct. Emitted CO_2 is part of the short-term CO_2 cycle resulting in no net emission.

In this work, to be classified as a BioCement, the binder must have a mineralogical composition that satisfies the European Standard ENV 197-1 [16]. The described binder must be comprised of at least 50 M.-% reactive dicalcium silicate (C_2S) and tricalcium silicate (C_3S or alite) and originate from recent biomass. This can be directly produced in the production of energy or after secondary thermal treatment (STT ash) or doping and secondary thermal treatment (dSTT ash). Ashes directly stemming from the combustion of recent agricultural biomass which are used to partially replace OPC are referred to as BioSCM. However, the functional performance is a critical factor when designing a sustainable material and must be qualified and quantified. If the environmental impact decreases but at the cost of performance or service life, then the overall sustainability does not increase. A sustainable building material can be thought of as: (functional performance x service life) / environmental impact.

BioCement theoretically has the distinct advantage of significantly reducing both the process and the production CO_2 emissions. The burning of biomass and the resulting decomposition of $CaCO_3$ into CaO does not contribute new CO_2 into the atmosphere, unlike the combustion of fossil fuels or the decomposition of limestone which release carbon that has been stored for millions of years. By replanting harvested biomass, the emitted CO_2 will be absorbed and returned for a new growth cycle. This cyclical process ensures that no "new" CO_2 will be released into the atmosphere [17]. So, in line with the IPCC GWP100 model [18], this work assumes that biogenic CO_2 does not contribute to global warming. Since firing of the biomass will be done in conjunction with energy production, the biomass derived ashes and ultimately BioCement can be viewed as a by-product. In this regard, a fraction of the energy invested in harvesting, processing and preparing the biomass will be allocated with energy production and not with BioCement production.

Based on the current standard of CO_2 emissions for OPC and the proposed changes for the production of BioCement a 62% reduction in CO_2 emissions can initially be estimated due to the replacement of limestone with biomass derived ashes. However other emissions which stem from the necessary additional steps to process the biomass are introduced while other emissions become obsolete. The 38% of emissions that are associated with the production of OPC would also be reduced through the implementation of BioCement since the thermo-processing during the energy production already removes all moisture and CO_2. Some energy is still needed for the higher temperature phase changes and material preparation (i.e. grinding and milling) however this energy would be required in the traditional approach anyway and it is significantly less.

The complexity is further compounded by logistics, such as the locations of the biomass reactors, the cement plants, the biomass waste streams and the distances between. In a hypothetical situation, they would all be located in the same area and produce locally the building materials, energy and agriculture (and thereby biomass waste) to service the community. Furthermore, such installations could exist at various scales depending on the demands and resources of the community. However, this is not the current state of things and to obtain an accurate estimation of the current potential for CO_2 reduction we must model these factors in. One advantage to this is that in the future, smart planning and future construction can allow for a further reduction in the CO_2 emissions associated with the production of BioCement.

Quantification of both input flows (such as energy, water, materials), and output flows (such as CO_2 emission) creates a foundation to estimate the potential impact on humans and nature [1]. It is important to analyze and compare the potential environmental impacts related to the production of concrete made from both OPC and alternative binders, like those proposed in this work. Comparison allows for claims to be made regarding the environmental advantages but also gives insight into where those reductions stem from [19]. Furthermore, an LCA offers further optimization and reduction of the impacts through the identification of areas with improvement potential [20]. In order to derive a realistic estimation of the potential reduction of CO_2 emissions obtained through the production of BioCement a simplified LCA was conducted.

The consensual framework, terminology and methodological phases for an LCA are outlined in the ISO 14040 standard. The implementation of an LCA is based chronologically on the following four phases:

1. goal and scope definition
2. inventory analysis
3. impact assessment
4. interpretation

First the goal and scope are defined, or more specifically, the purpose, objectives, product system, boundaries and functional unit are made explicit. Then, the data necessary to analyse the life cycle of the product is collected for the inventory analysis. Subsequently the life cycle inventory (LCI) flows are classified, characterized and normalized. This is performed using one of many possible Life Cycle Impact Assessment (LCIA) methodologies and serves to estimate the potential environmental impacts. Lastly, the interpretation phase is performed to identify, quantify and evaluate the information that results from the last two phases. Additionally, the phase includes communicating the information in a correct way, as well as recommending improvements within the analyzed system.

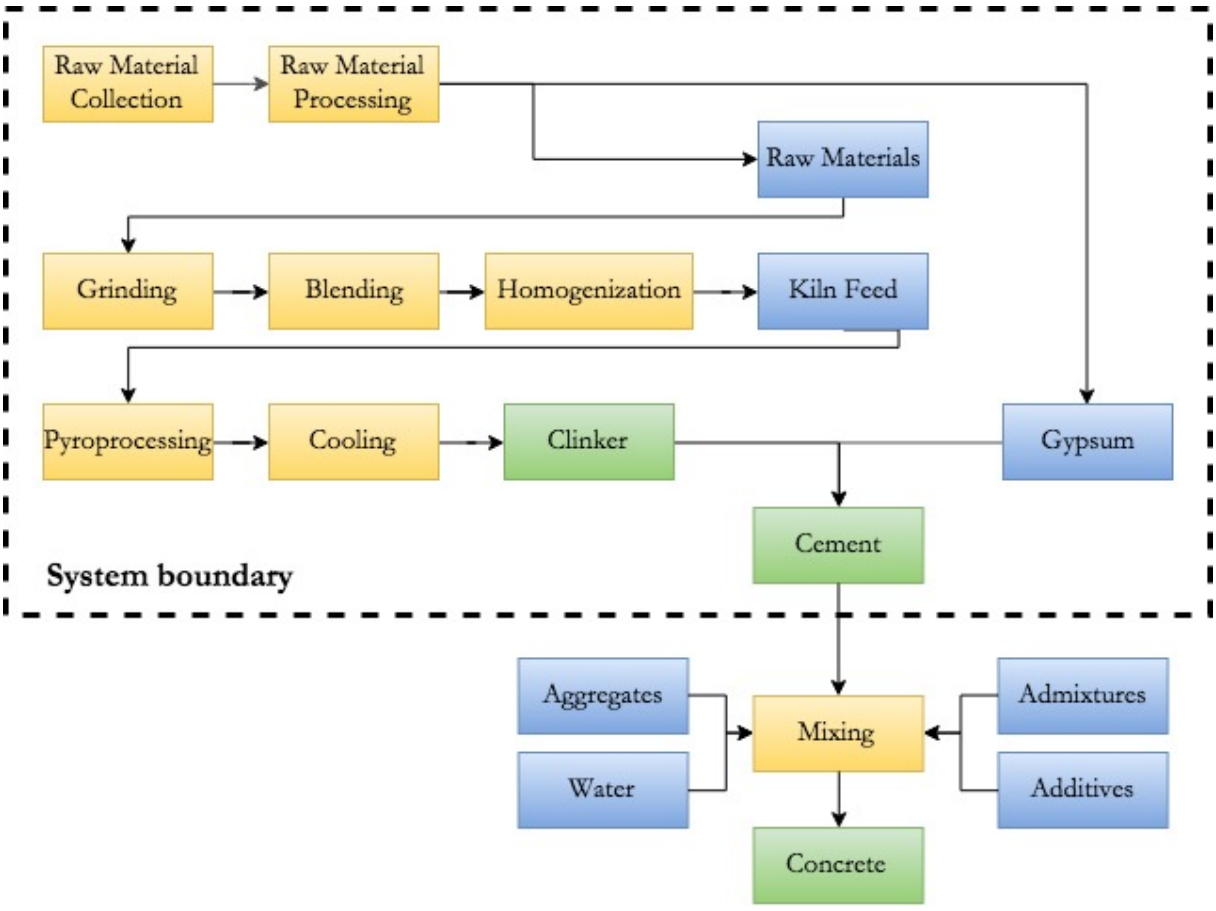

Figure 67: Simplification of the processes included in the LCA analysis and the boundaries of the study. The system presented was adapted according to the mixture in question.

This paper aims to access the greenhouse gas emission potential for alternative biomass derived binders, relative to standard cement. Greenhouse gas emission was expressed as CO_2-eq. The following binding systems were evaluated: (1) OPC (2) OPC + BioSCM (3) BioCement and (4) BioCement + BioSCM

The scope of the study includes the extraction of raw materials, production and upgrading of materials, the manufacturing of the binder and transportation (see Figure 67). The use and disposal phases are the same for the proposed binders, so the scope was limited to cradle-to-gate. Since the scope excludes the use phase, the functional unit was defined as 1 ton of binder with the assumption that the performance characteristics are equal to that of CEM I 42.5. Setting the functional unit as a binder and not concrete allows for the assessment of several different products with divergent qualities and applications. Expanding the scope to concrete would have unnecessarily expanded the complexity; as such a common approach to LCA studies of cement is to limit the perspective to cradle-to-gate [19, 21-24] It is important to note that the different binders have different chemical and mineralogical compositions which influence their performance. In the discussion, the CO_2 saving abilities of the different binders will be evaluated in the context of their relative performance.

2 Materials and Methods

2.1 Materials

This investigation evaluates emissions associated with the production of alternative binders, relative to OPC. The alternative binders are composed of various quantities of OPC, BioSCM and BioCement blended together; a table stipulating the various quantities of the different components can be found below (Table 27).

Table 27: composition of the different binders being explored in the investigation [M.-%].

	OPC	BioSCM	BioCement
Control	100		
20 %	80	20	
40 %	60	40	
BioCement			100
20 %		20	80
40 %		40	60

As elaborated in previous chapters, both BioSCM and BioCement are produced from biomass derived fly ash. Specific details on the formation of BioSCM and BioCement can be found in chapters 4-7. The ash could be directly applied as a BioSCM or after processing could be transformed into BioCement. For this investigation, three types of biomass derived fly ash were considered in the calculations since previous chapters explored the binding potential for three different ashes. All ashes considered were derived from woody biomass since they showed the most potential as a cement

replacement. The differentiating factor between these ashes is the primary product in the biomass combustion. The raw material input for the production of the theoretical BioSCM and BioCements emission calculations were derived from the following three scenarios:

- Heat production, hardwood chips from forest, at furnace 5000kW, state-of-the-art 2014 - CH
- Heat and power co-generation, wood chips, 6667 kW, state-of-the-art 2014 - BE
- Heat and power co-generation, wood chips, 6667 kW, state-of-the-art 2014 - NL

The CO_2eq value was selected as the key indicator to evaluate the different products since the objective of this work is to achieve a CO_2 neutral binder. The CO_2eq value for each of the fly ashes was calculated based on the data obtained from the Ecoinvent database. The Ecoinvent database is one of the most internationally accredited generic environmental databases which covers the average inventory data of different building materials and processes in regional contexts [20]. A CO_2eq value for OPC was obtained from [19]. This value originates from an LCA study conducted by the authors as a typical attributional and comparative LCA in line with the ISO 14040 and 14044 standards.

2.2 Methods

The products described in this work are entirely theoretical and as a result no site-specific data exists. This necessitates an LCA constructed of hypotheticals and assumptions. The simplified model used here is derived from generic LCA data obtained from literature and the Ecoinvent database. Typically in an initial LCA study where the main goal is to compare different design scenarios, generic data is used [20]. This helps to reduce the complexity and the complications associated with assumptions without sacrificing too much accuracy.

For OPC, BioSCM and BioCement a process flow was established. Identification of differences in input flows and output flows for the three different processes showed where the calculations of the CO_2eq was different. At these stages, instead of using the CO_2eq for the OPC relevant values for BioCement and BioSCM were applied. The framework and input values used for this LCA were obtained from the same extensive LCA study which provided the CO_2eq value for OPC [19]. That particular study provided the process emissions associated with cement production which were then altered to fit cement production from biomass (based on the results of chapters 6 and 7). Alterations were made to the flow to account for the different processes involved in BioCement production versus OPC production. This ultimately resulted in a CO_2eq value for each of the binders investigated.

3 Results

3.1 Modelling the Production Process

A simplified overview of OPC production is outlined in Figure 68. Prior to obtaining OPC the intermediate product, clinker, is produced. OPC consists typically of 93-97% clinker. The clinker is ground to a fine powder and blended with gypsum to create OPC. Additionally, other types of hydraulic cements can be made from clinker and these are defined by the European cement standard EN 197-1 (2011). Five main cement types are outlined (CEM I to V) and each main type has a few sub-types. In total, there are 27 different cement varieties which are differentiated by their material content. CEM I has the highest clinker content and corresponds to OPC.

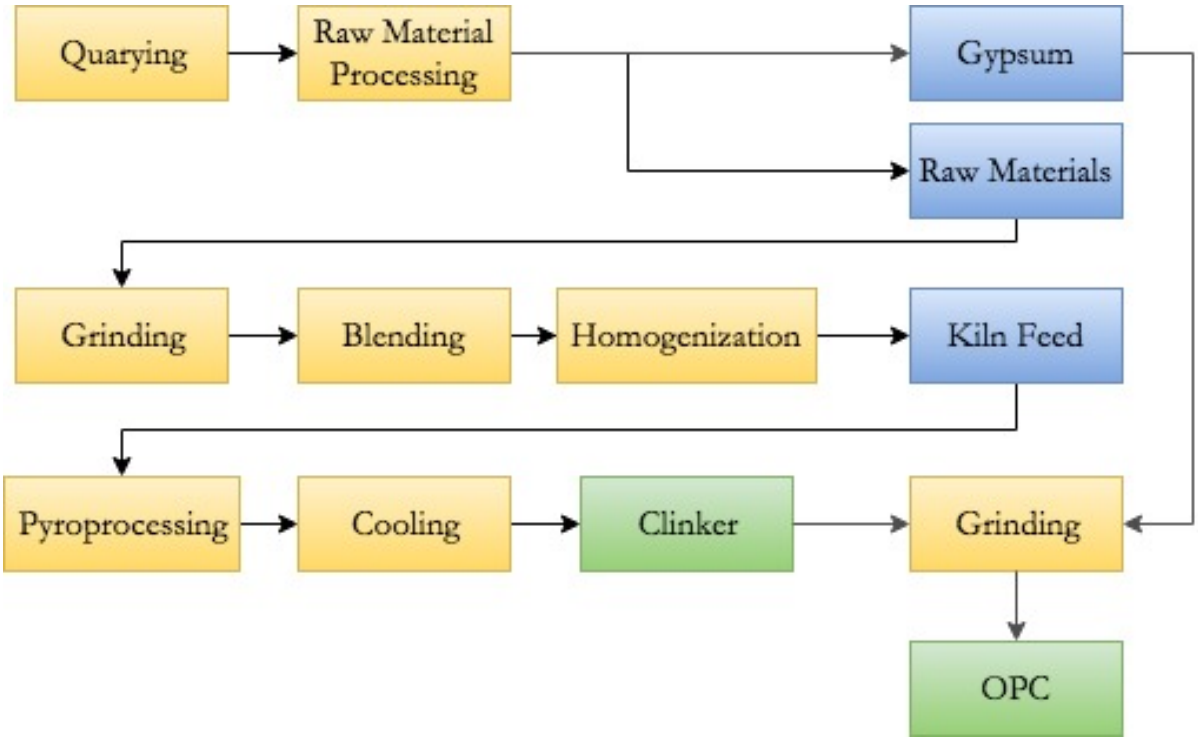

Figure 68: Flow chart identifying the processes involved in cement production.

Biomass combustion to produce heat and electricity follows the path depicted in Figure 69. In addition to the primary energy products fly ash is also produced. Depending on the exact biomass used and the conversion process these ashes have the potential to act as either pozzolans (non-cementitious siliceous materials that become hydraulically cementitious when reacted with free lime) or latent cements (weakly hydraulically cementitious materials that become strongly cementitious when reacted). Due to these reactive properties, the fly ash can be used to partially replace clinker as a supplementary cementitious material (BioSCM).

Alternatively, these ashes can be subjected to further thermal treatment to enhance the hydraulic activity. When the biomass derived fly ash is used as a raw material in the production of OPC-like cement a product called BioCement is produced. As shown in Figure 70, the BioCement can also be partially replaced by BioSCMs to achieve the highest reductions in CO_2 emissions.

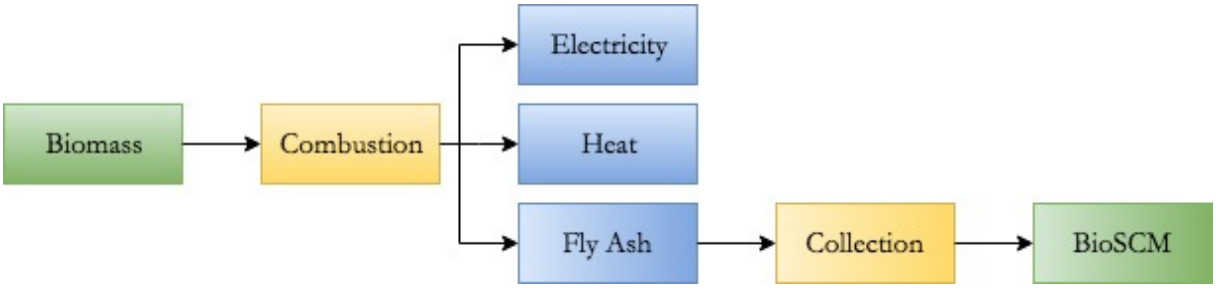

Figure 69: Flow chart identifying the processes involved in biomass fly ash production.

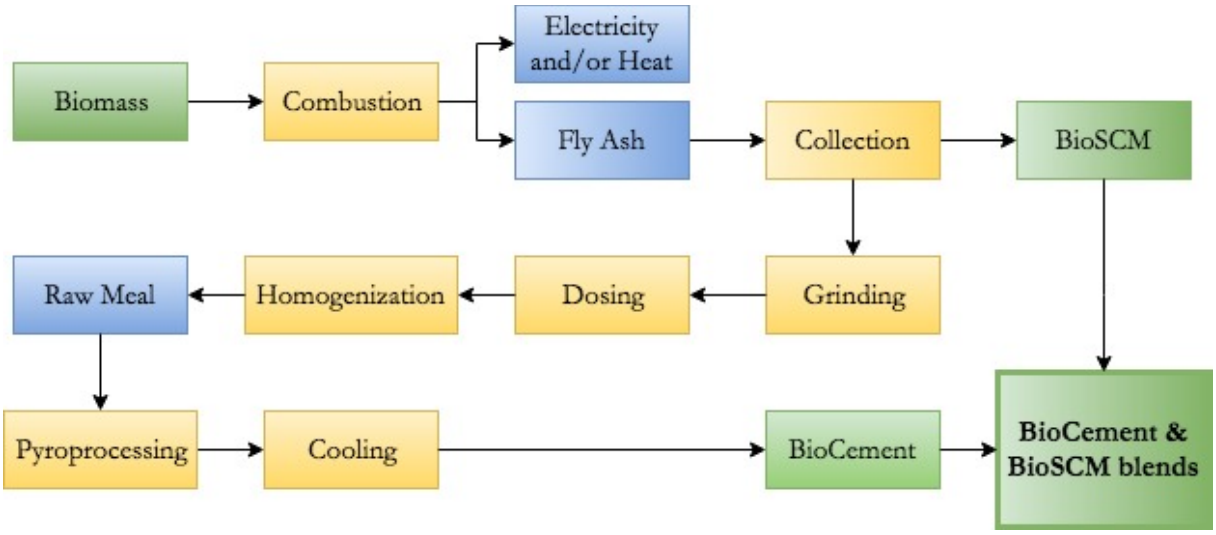

Figure 70: BioCement and BioSCM flowchart.

3.2 Calculating the CO_2eq for Fly Ash

For the three-selected biomass types, the amount of ash and the CO_2eq produced per 1 MJ of energy yield can be obtained from the Ecoinvent database. Based on these values the quantity of CO_2 for every tonne of ash produced can be calculated (see Table 28)

Table 28: Calculation of kg CO2/tonne ash based of the MJ energy yield per biomass type.

	PSFA	WBFA1	WBFA2
Reference product	1 MJ	1 MJ	1 MJ
Ash produced [kg]	6.250E-04	3.970E-04	3.970E-04
CO_2 eq [kg]	4.126E-03	2.639E-03	2.639E-03
kg CO_2/kg ash	6.60	6.65	6.65
kg CO_2/tonne ash	6602	6647	6647

However not all of these emissions can be attributed to the fly ash since this is not the primary product. The primary product is energy (in the form of heat). In order to determine the share of emissions attributed to the fly ash an economic allocation was implemented. Economic allocation shares the impacts according to a coefficient (*Ce*) calculated from the ratio between the market prices (€) and the quantity of products (m). The following equation can be used:

$$Ce = \frac{(€ \cdot m)Fly\ ash}{(€ \cdot m)Energy + (€ \cdot m)Fly\ ash} \quad (3)$$

In Europe, biomass derived fly ash is typically considered a waste product and consequently should afforded no economic value. The European standard EN 450-1 (CEN TC 104) regulates the use of fly ash as a mineral admixture and only allows as cement replacement fly ash derived primarily from

coal combustion (with tolerance for a 20% replacement of coal with biomass), as such there is no real market price for biomass derived fly ash. However, this work operates under the assumption that in the future biomass derived fly ash will be tolerated and regulated similar to that of coal fly ash. Therefore, the economic allocation was employed with the monetary value of coal derived fly ash. In a sensitivity analysis where biomass cost was equal to that of coal, [20] found that the results will remain similar since the energy production still has a significantly higher economical revenue. The individual coefficient for each type of ash can be seen in Table 29

Table 29: Calculation of economic allocation based on the market prices (€) and the quantity of products (m) for energy and ash.

	Products	Market price (€)		quantity (m)		Ce
PSFA	Wood ash	40	€/ton	6.25E-07	ton	0.0024
	Heat	0.0106	€/MJ	1	MJ	
WBFA1	Wood ash	40	€/ton	3.97E-07	ton	0.0010
	Electricity	0.0977	€/kWh	0.0472	kWh	
	Heat	0.0106	€/MJ	1	MJ	
WBFA2	Wood ash	40	€/ton	3.97E-07	ton	0.0011
	Electricity	0.084	€/kWh	0.0472	kWh	
	Heat	0.0106	€/MJ	1	MJ	

Implementation of these coefficient results in the following CO_2eq for the production of the three different ashes after economic allocation:

Table 30: kg CO_2/tonne ash after economic allocation.

	kg CO2eq/ton ash
PSFA	15.8
WBFA 1	6.7
WBFA 2	7.3

3.3 Calculating the CO_2eq for BioSCM

To calculate the CO_2 saving potential of using BioSCM in conjuncture with OPC, the CO_2eq values for both the fly ash and the OPC are used. Since the replacement rate indicates the mass fraction of both components and the CO_2eq is based on mass the total CO_2eq of the binding system can be calculated. Based on the stipulated replacement rate (r), the following formula can be used:

$$r(FA\ CO_2e) + (1 - r)(OPC\ CO_2e) = \ Binder's\ total\ CO_2e \quad (4)$$

Based on the above-mentioned equation the following values were derived for the kg of CO_2eq emissions associated with the replacement of OPC by the two variants of FA at rates between 0 and 100 by increments of ten (see Table 31)

Table 31: CO_2eq for 1 ton binder composed of % OPC and % BioSCM for three different biomass derived fly ashes [kg CO_2eq/ton binder].

	OPC percentage										
	0%	10%	20%	30%	40%	50%	60%	70%	80%	90%	100%
PSFA	850.0	766.6	683.2	599.7	516.3	432.9	349.5	266.1	182.6	99.2	15.8
WBFA 1	850.0	765.7	681.3	597.0	512.7	428.4	344.0	259.7	175.4	91.0	6.7
WBFA 2	850.0	765.7	681.5	597.2	512.9	428.7	344.4	260.1	175.8	91.6	7.3

While great CO_2 saving can be achieved with the implementation of BioSCMs, performance still needs to be considered because SCMs are notably less reactive than OPC. Figure 71 shows the CO_2eq emissions relative to the achieved 28 day strength for three different ashes used to replace one tonne of OPC at 0, 20 and 40% (see chapter 4 for strength results).

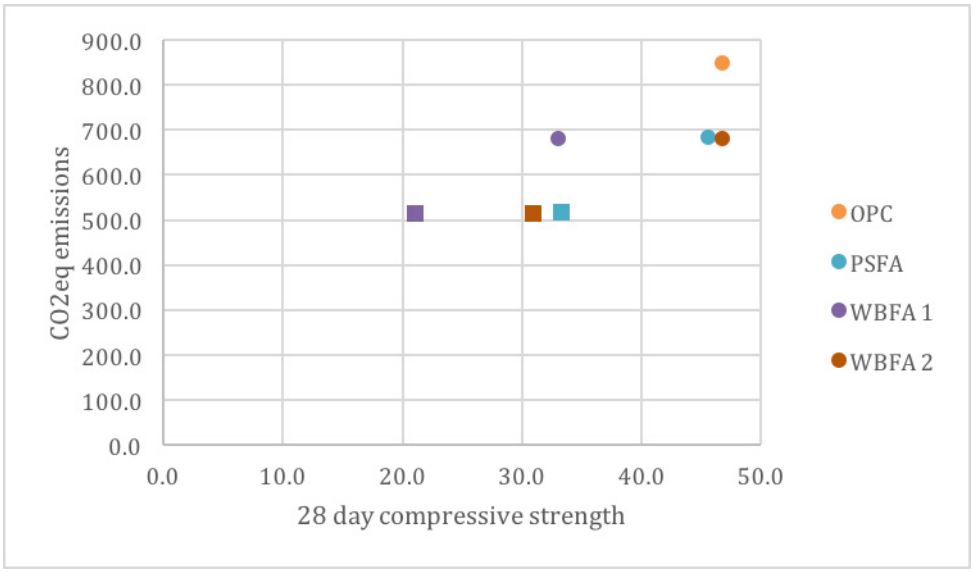

Figure 71: CO_2eq emissions related to strength for replacement rates of 0, 20 (square) and 40% (circle) for three different ashes.

A critical point is the 28 day strength of 42.5 MPa which is the target strength. Three binders were able to reach that target, one of which was the OPC control. In the case of PSFA 20% and WBFA2 20% we observe sufficient strength development at CO_2eq emission reductions (around 25% reduction). Another group of samples fell short of the 28 day strength requirement however they displayed even more significant decreases in emissions. Specifically, PSFA 40% and WBFA2 40%. While WBFA1 20% also performed in the same strength range, its emission reduction was on par with PSFA 20% and WBFA2 20%, thus it is not the best option. WBFA1 40% as well was not a good option despite the low emission rate since its strength was far too low.

3.4 Calculating the CO_2eq for BioCement

Calculation of the CO_2eq for BioCement is slightly more complicated that BioSCM since additional processing is required. To avoid the complexity and uncertainty of a full attributional LCA study, a simplified model was implemented based on a detailed quantitative attributional LCA of cement by [25]. Table 32 lists all the processes associated with the production of clinker and their associated emissions.

Based on the simplified model where biomass derived fly ash is used as an input for the production of BioCement (as seen in Figure 70) alterations were made to the processes included in the calculation. According to the authors, raw material extraction, upgrading and transport to the plant contribute emissions for clinker which can be separated from the production emissions and those stemming from the calcination of the raw materials. The raw material extraction and the raw material calcination are not included in the BioCement emission calculations, however these values were replaced with the extraction and combustion of the biomass. The values for the “combustion of biomass” were taken from Table 30, and represent the CO_2eq after economic allocation.

Table 32: The processes associated with the production of clinker and BioCements and their associated emissions in kg CO_2eq / tonne binder based on a detailed quantitative attributional LCA of cement by [25] and adapted for economic allocation of the Biomass derived ashes (Table 30).

	Process	Clinker	PSFA	WBFA-1	WBFA-2
Raw material extraction	Electricity	46	0	0	0
	Upgrading of animal meal	39	0	0	0
	Kiln coal	12	0	0	0
	Transport (road)	3	0	0	0
	Transport (rail)	1	0	0	0
	Calcareous marl	2	0	0	0
	Upgrading of RDF-fluff (silo)	1.2	0	0	0
	Limestone	0.9	0	0	0
	Refractory waste	0.6	0	0	0
	Light fuel oil	0.3	0	0	0
	Lignite	0.2	0	0	0
	Upgrading of RDF fluff (kiln)	0.1	0	0	0
	Upgrading of tires	0.1	0	0	0
	Combustion of RDF fluff (agglomerate)	0.0	0	0	0
	Calcination of raw materials	541	0	0	0
Production	Combustion of kiln coal	89	89	89	89
	Combustion of RDF fluff (silo)	71	71	71	71
	Combustion of lignite	31	31	31	31
	Combustion of tires	4.7	4.7	4.7	4.7
	Combustion of RDF fluff (agglomerate)	3.2	3.2	3.2	3.2
	Combustion of RDF fluff (kiln)	2.0	2.0	2.0	2.0
	Combustion of light fuel oil	1.3	1.3	1.3	1.3
	Combustion of biomass	0	15.8	6.7	7.3
	SUM	**849.6**	**218.0**	**208.9**	**209.5**

The values for the BioCements are believed to be conservative estimations. As seen in chapters 6 and 7 the biomass derived fly ashes (BioSCMs) need less grinding, lower temperatures and lower firing times for conversion into BioCement in comparison to conversion of cement raw feed into clinker. Furthermore, since the ashes have already undergone declination the energy investment for BioCement is lower.

3.5 BioCement with BioSCM Replacement

Similar to the replacement of OPC with a biomass derived fly ash, the BioCement can also be partially replaced with BioSCMs to obtain an even larger reduction in CO_2eq emissions. In Table 33, the CO_2eq emissions associated with the BioCement being partially replaced with BioSCM at rates between 10 and 90% can be seen. As expected the emissions approach zero as the replacement rates rises, however this does not correlate to a functioning binder. Based on the hydraulic minerals detected in the BioCement and the observations of the BioSCM replacing OPC at 20% it is suggested that 20% replacement of BioCement with BioSCM will provide sufficient strength, however this needs to be corroborated with strength tests.

Table 33: CO_2eq emissions associated with the BioCement with BioSCM replacement at rates between 10 and 90% under the assumption of similar performance characteristics.

	OPC percentage								
	10%	20%	30%	40%	50%	60%	70%	80%	90%
PSFA	197.8	177.6	157.3	137.1	116.9	96.7	76.5	56.2	36.0
WBFA1	188.7	168.5	148.2	128.0	107.8	87.6	67.4	47.1	26.9
WBFA2	189.3	169.1	148.8	128.6	108.4	88.2	68.0	47.7	27.5

4 Discussion

In open loop recycling, products or wastes from one product system are used as raw materials in the other product system. This concept has proven to significantly reduce the environmental impact of concrete [26-30]. Not only does the use of byproducts, such as fly ash, promote CO_2 emission reduction, it also avoids the need for disposal of those materials and can increase the lifetime of concrete structures. [31, 32]. While wastes and by-products can be incorporated into concrete to improve product performance and its environmental impact this is not as yet the case for those of biological origin.

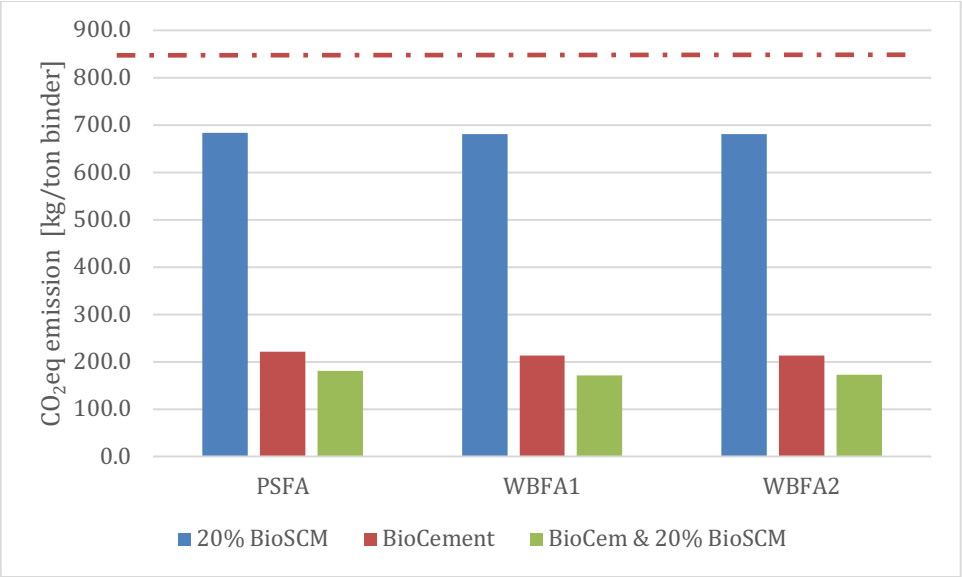

Figure 72: CO_2eq emission for the three different ash types when used as a BioSCM to replace 20% OPC, after secondary thermal treatment as 100% BioCement and as 80% BioCement and 20% BioSCM. The red dotted line represents the CO_2eq emission for traditional OPC.

From the results obtained in this study, we can see that a reduction can be made simply with cement replacement with SCM derived from biomass. However, besides functional performance, there is a limit as to how much replacement material can be used, as stipulated by standards. We have seen in chapters 4 and 5 that strength reduction can be even more profound and the results less predictable when organic material is used. This was illustrated by the two different woody biomasses having drastically different strength performances when used as a 40% replacement of OPC.

It is clear that the largest reduction in emissions comes into play when the biomass derived ash is used as the raw material replacement in the production of cement. Based on the research conducted in chapters 6 and 7 we can also say that these emission calculations are overestimates since energy and time input is necessary to thermally treat the ashes in order to get a functionally more reactive material. For all ashes explored here, PSFA showed a reduction potential in CO_2 emissions on the order of 74% whereas both WBFA1 and WBFA2 show reductions of 75%.

However, these emissions can be further reduced through the introduction of BioSCMs to BioCement. The same untreated ash can be used as partial replacement for BioCement just as it was for OPC. When 20% of the PSFA ash is used to directly replace BioCement produced out of PSFA a CO_2eq emission reduction of 79% can be achieved. When 20% of the WBFA 1 or WBFA 2 is used to partially replace the corresponding BioCement then a total CO_2 reduction of 80% can be realized.

5 CONCLUSION

Based on the presented results and discussion the following conclusions can be drawn:

- The replacement of OPC with biomass derived ash (BioSCM or BioCement) has the potential to reduce the CO_2eq emission.
- The production of BioCement has the potential to reduce OPC production related CO_2eq emissions on the order of 70-75%.
- The replacement of BioCement with 20% BioSCM has the potential to even further reduce CO_2eq emissions in the order of 75-80%.
- The functional performances of BioCement and BioCement replaced with BioSCM are worthy of being qualified and optimized due to the large potential reductions in CO_2 emissions.

6 REFERENCES

1. Celik, K., et al., *Mechanical properties, durability, and life-cycle assessment of self-consolidating concrete mixtures made with blended portland cements containing fly ash and limestone powder.* Cement and Concrete Composites, 2015. **56**: p. 59-72.
2. Tomkins, C., *Redefining what's possible for clean energy by 2020.* San Francisco: Gigaton Throwdown, 2009.
3. Initiative, C.S., *Cement Industry Energy and CO2 Performance,"Getting the Numbers Right"*, in *World Business Council for Sustainable Development*. 2016.
4. Olivier, J., et al., *Trends in Global CO2 Emissions: 2014 Report*. 2015, PBL Netherlands Environmental Assessment Agency.
5. Schorcht, F., et al., *Best Available Techniques (BAT), Reference Document for the Production of Cement, Lime and Magnesium Oxide: Industrial Emissions Directive 2010/75/EU:(Integrated Pollution Prevention and Control).* JRC Reference Reports; Publications Office of the European Union, 2013.
6. Hendriks, C.A., et al. *Emission reduction of greenhouse gases from the cement industry.* in *Proceedings of the Fourth International Conference on Greenhouse Gas Control Technologies*. 1998.
7. Damtoft, J.S., et al., *Sustainable development and climate change initiatives.* Cement and concrete research, 2008. **38**(2): p. 115-127.
8. Worrell, E., et al., *Carbon dioxide emissions from the global cement industry.* Annual Review of Energy and the Environment, 2001. **26**: p. 303-329.
9. Pardo, N., J.A. Moya, and A. Mercier, *Prospective on the energy efficiency and CO2 emissions in the EU cement industry.* Energy, 2011. **36**(5): p. 3244-3254.
10. Taylor, H.F.W., *Cement chemistry*. 1997: Thomas Telford Services Ltd.
11. Chateau, B. and B. Lapillonne, *Energy demand: facts and trends: a comparative analysis of industrialized countries*. 2012: Springer Science & Business Media.
12. Ali, M.B., R. Saidur, and M.S. Hossain, *A review on emission analysis in cement industries.* Renewable and Sustainable Energy Reviews, 2011. **15**(5): p. 2252-2261.
13. Worrell, E. and C. Galitsky, *Energy efficiency improvement opportunities for cement making.* Ernest Orlando Lawrence Berkeley National Laboratory, 2004.
14. Hasanbeigi, A., C. Menke, and A. Therdyothin, *The use of conservation supply curves in energy policy and economic analysis: the case study of Thai cement industry.* Energy Policy, 2010. **38**(1): p. 392-405.
15. Worrell, E., N. Martin, and L. Price, *Potentials for energy efficiency improvement in the US cement industry.* Energy, 2000. **25**(12): p. 1189-1214.
16. Hewlett, P.C., *Lea's chemistry of cement and concrete*. 2004: A Butterworth-Heinemann Title.
17. McKendry, P., *Energy production from biomass (part 1): overview of biomass.* Bioresource Technology, 2002. **83**(1): p. 37-46.
18. Change, I.C., *The Fourth Assessment Report of the Intergovernmental Panel on Climate Change.* Geneva, Switzerland, 2007.
19. Feiz, R., et al., *Improving the CO 2 performance of cement, part I: utilizing life-cycle assessment and key performance indicators to assess development within the cement industry.* Journal of Cleaner Production, 2015. **98**: p. 272-281.
20. Teixeira, E.R., et al., *Comparative environmental life-cycle analysis of concretes using biomass and coal fly ashes as partial cement replacement material.* Journal of Cleaner Production, 2016. **112**: p. 2221-2230.

21. Chen, C., et al., *LCA allocation procedure used as an incitative method for waste recycling: An application to mineral additions in concrete.* Resources, Conservation and Recycling, 2010. **54**(12): p. 1231-1240.

22. Boesch, M.E. and S. Hellweg, *Identifying improvement potentials in cement production with life cycle assessment.* Environmental science & technology, 2010. **44**(23): p. 9143-9149.

23. Josa, A., et al., *Comparative analysis of available life cycle inventories of cement in the EU.* Cement and Concrete Research, 2004. **34**(8): p. 1313-1320.

24. Huntzinger, D.N. and T.D. Eatmon, *A life-cycle assessment of Portland cement manufacturing: comparing the traditional process with alternative technologies.* Journal of Cleaner Production, 2009. **17**(7): p. 668-675.

25. Ammenberg, J., et al., *Industrial symbiosis for improving the CO2-performance of cement production.* Final report of the CEMEX-Linköping University industrial ecology project, 2011.

26. Ahlman, A.P., et al. *System Wide Life Cycle Benefits of Fly Ash*. in *2015 World of Coal Ash (WOCA) Conference*. 2015.

27. De Schepper, M., et al., *Life cycle assessment of completely recyclable concrete.* Materials, 2014. **7**(8): p. 6010-6027.

28. Dosho, Y., *Development of a sustainable concrete waste recycling system.* Journal of Advanced Concrete Technology, 2007. **5**(1): p. 27-42.

29. Ondova, M. and A. Estokova, *LCA and multi-criteria analysis of fly ash concrete pavements.* International Journal of Environmental, Ecological, Geological and Mining Engineering, 2014. **8**(5): p. 308-13.

30. Schuurmans, A., et al., *LCA of Finer Sand in Concrete (5 pp).* The International Journal of Life Cycle Assessment, 2005. **10**(2): p. 131-135.

31. Flower, D.J. and J.G. Sanjayan, *Green house gas emissions due to concrete manufacture.* The international Journal of life cycle assessment, 2007. **12**(5): p. 282.

32. Turk, J., et al., *Environmental evaluation of green concretes versus conventional concrete by means of LCA.* Waste Management, 2015. **45**: p. 194-205.

CHAPTER 9

RETROSPECTION, CONCLUSIONS AND RECOMMENDATIONS

ABSTRACT

This Chapter presents a brief summary of the objective of this dissertation. The current and future outlook of the biomass streams discussed in this work are explored in terms of quantity. General conclusions drawn from this work are presented and as recommendations for future research in this field are proposed.

1. RETROSPECTION

The aim of this project was the development of the scientific basis for methodologies that enable the production of renewable sustainable cement (i.e. BioCement) based on ashes derived from the conversion of biomass residues. Within this project, biomass ash and derived products were developed at the laboratory scale, and their functionality was tested with respect to sustainability and composition (relative to OPC). The ultimate goal was to prove the possibility of replacing traditional Portland cement with a renewable BioCement in typical cement-based products such as concrete. The environmental superiority of theoretical BioCement is based on assumed negligible CO_2 emissions during production. Through a Life Cycle Analyses on the developed biomass ashes (and preferably fully functional BioCement), the environmental impact and the potential to replace Portland cement with theoretical BioCement was quantified. The investigations included three types of biomass (ash) utilization:

1. Partial cement replacement with biomass derived ash as a secondary cementitious material (BioSCM)
2. Thermally treated biomass derived ash to serve a full cement replacement (STT ash)
3. Chemically and thermally altered biomass derived ash to serve a full cement replacement (dSTT ash)

Currently the application of biomass derived ash as a SCM is not tolerated under EN-450. However, there is a need to explore the potential of biomass derived ashes as supplementary cementing materials due to the impending reduction in availability of coal-based fly ashes and the impact that will have on the cement production industry. Furthermore, the utilization of the ashes provides a solution to waste disposal which would otherwise be landfilling since this is the most economical solution [1]. The utilization of biomass, particularly those stemming from landscaping and agricultural residues, provides a solution for their disposal as well. Integrating biomass ash into concrete as a SCM offers solutions to many problems, however the research is limited and focused on silica rich ashes which rely on the pozzolanic reaction. This work seeks to expand that knowledge to included ashes with full hydraulic potential.

Examination of the chemical and mineralogical composition of biomass-derived ash has shown that in addition to CaO and SiO_2, clinker minerals can be found. The investigation into STT ash serves as a foundation for the use of Biomass ashes as a complete cement replacement directly after combustion. Changes to the thermal treatment parameters have the potential to produce larger quantities of more valuable clinker minerals. Alterations to the thermal treatment would potentially reduce the efficiency and quantity of the primary product (energy in the form of heat or electricity) produced, however this would create a value-added product from the waste.

Alterations to the chemical composition prior to thermal treatment (dSTT) demonstrate that the biomass derived ash has the potential to act as a replacement for the raw materials in clinker production. Biomass ashes with sufficient quantities and ratio of CaO and SiO_2 can either be blended together to obtain the desired chemical composition of the raw material required for clinker production and yield typical clinker minerals after further heat treatment.

These approaches to replacing or producing cement from Biomass all have the potential to reduce the CO_2 emissions associated with cement to varying degrees. Most importantly they all reduce the amount of limestone consumed to obtain a final concrete product. Since the decomposition of limestone produces more than half of the CO_2 emissions, avoiding this step alone can yield drastic reductions. This work proves that the utilization of biomass ash in cement and concrete products is possible and with further research and control over the process a significant reduction of CO_2 emissions can be achieved.

2. Current Potential and Future Outlook

Investigation of land use and industry in The Netherlands showed different biomass wastes streams and residues with energetic potential. As shown in this work, the combustion of these resources can produce ashes with binding potential. To understand how much cement could be replaced with BioCement the current amount of biomass available for combustion and the amount of thereby derived ash must be quantified.

Most supplementary biomass is produced in agricultural and forestry practices as well as in the maintenance of nature areas and public parks [2]. Additionally, in The Netherlands industrial practices produce relevant amounts of biomass waste. To simplify the calculation of available biomass, sources have been broken down into three different categories; maintenance, agriculture and industry.

Maintenance biomass is the waste produced in the maintenance of different types of land areas and is typically verge grass or woody biomass. Table 34 gives a breakdown on the different land uses in The Netherlands, their area and the amount of biomass they produce annually [3, 4].

Table 34: Maintenance biomass produced in The Netherlands based on surface area and dry matter yield.

	Surface Area [10^3 ha]	Biomass dry matter yield [tonnes DM/ha/year]	Available biomass dry matter ktonnes/year
Transportation	116	3	348
Built up area	356	1	356
Semi built area	51	2	102
Recreation	103	3	309
Forest and nature	490	3.5	1715
Inland waterway	368	1	368
Total	1484		3198

Assuming that verge grass has an average ash content of 13.9% and woody biomass has an average ash content of 5.2% [5] the derived ash can be calculated (see Table 35). The total amount of maintenance biomass derived ash which could theoretically replace cement is over 295 ktonnes.

The amount of biomass waste stemming from agricultural practices can be similarly calculated (Table 36). In 2012 there was 2251000 ha of farm land from which about 12 tonnes of dry matter can be extracted per ha per year. This results in 27012 ktonnes of biomass. However not all of this biomass is waste; using an average harvest index for the main crops cultivated in The Netherlands (0.45) the amount of biomass waste can be calculated to be 14857 ktonnes. Based on an average ash fraction of 9.35 this results in 1389 ktonnes of ash after combustion (see Table 37) [5].

Table 35: Calculation of maintenance biomass ash quantity.

	Available biomass dry matter [ktonnes/year]	Ash fraction [%]	Available ash [ktonnes]
Transportation	348	13.9	48.4
Built up area	356	13.9	49.5
Semi built area	102	13.9	14.2
Recreation	309	13.9	43.0
Forest and nature	1715	5.2	89.2
Inland waterway	368	13.9	51.2
Total	3198		295.3

Table 36: Calculation of biomass waste based off of agricultural land surface area, dry matter (DM) yield and harvest index.

Surface Area [10 ^ 3 ha]	Biomass DM yield [tonnes DM/ha/year]	Available biomass DM [ktonnes/year]	Harvest index	available waste [ktonnes]
2251	12	27012	0.45	14857

Table 37: Calculation of agricultural waste biomass derived ash.

Available biomass waste [ktonnes]	Ash fraction	Available biomass ash [ktonnes]
14856.6	9.35	1389

Industrial wastes can also provide streams of biomass waste and this work has particularly identified paper waste as a functional cement raw material replacement. Paper waste is typically recycled and reused in the production of new paper. This process can only be repeated so many times before the fibres degrade too much and the quality of the paper is too low. At this point the paper is still suitable for combustion and since the original material was biomass, yet it is still considered biomass combustion. It was reported that in 2012 of the total recyclable waste produced in The Netherlands 24.3% was paper waste which is about 4.0 Mtonnes (see Chapter 2 [4]). Assuming an average ash content of 8.6% roughly 344 ktonnes of ash result [5].

Table 38: Total amount of biomass derived ash from the three identified categories which is available for cement replacement based on the 2012 estimates [tonnes].

	Biomass derived ash
Maintenance	295 000
Agricultural	1 389 000
Industrial	344 000
Total	2 028 000

From the three identified biomass categories, combustion of the ash would result in more than 2.0 Mtonnes of biomass ash for cement application. In 2013, no clinker was produced in The Netherlands per Eurostat, however, ENCI Maastricht has reported the production of less than 600 tonnes of clinker [6, 7]. Since The Netherlands has a limited supply of raw materials for clinker production, namely limestone consequently all cement manufactured in the country is produced by blending imported clinker with domestically produced waste streams such as slag. Per the United Nations Department of Economic and Social Affairs Statistics Division, The Netherlands imported a net 0.63 Mtonnes of cement clinker in 2013 (0.63 Mtonne imported and 0.002 Mtonnes exported) [8]. All the imported cement clinker could potentially be replaced by domesticly produced biomass derived ash. Additionally, The Netherlands imported a net 2.7 Mtonnes of Portland cement and hydraulic binders, for a total of 3.3 Mtonnes Portland cement, hydraulic binders and cement clinker. This statistic fits with the reported usage of 4.2 Mtonnes of hydraulic binders consumed in The Netherlands in 2013 [9] given that the imported clinker was blended with industrial wastes to produce cements like CEM II-S and CEM III. If 100% of these biomass waste streams were combusted and applied as a cement replacement (and negating the difference in chemical composition), theoretically 100% of clinker imports could be avoided. The amount of hydraulic binder imports could also be reduced by 52% (or more given the potential to blend with industrial wastes). This oversimplification serves as an indication of potential impact, however more investigations into the functional properties of BioCements is necessary for specific values to be calculated.

While these estimates do make many assumptions, they also negate the growing stake of biomass in energy production and the vested interest in a circular economy. Given the current potential and the environmentally minded changes being made in society [10] the use of biomass derived ash as a cement replacement holds definite potential and deserves further research.

3. CONCLUSIONS

It is well established that further actions need to be taken by the cement industry to reduce the overall CO_2 production associated with clinker production [11-13]. This directive coincides with a renaissance in the development and utilization of biomass as an energy source. Numerous biomass waste streams are available in The Netherlands, which have the potential to act as a source of energy and thereby produce a valuable ash which can function as a binder in construction applications thereby helping to alleviate a portion of the CO_2 emissions associated with cement production.

A potentially ideal ash for clinker replacement or clinker production can be achieved based on the ashes of particular biomass streams. SiO_2 can be obtained from OR-CB (organic residues and contaminated biomass) or possibly HBA (herbaceous and agricultural biomass) but then from the sub categories husk shell pits or organic residues. CaO can be obtained from WWB (wood and woody biomass) bark and hardwood specifically. Ashes derived from the OR-CB category paper sludge showed the potential to provide both CaO and SiO_2 however the extent of their reactivity remains to be investigated.

In general, OR-CB provided the highest average ash content. Circulating fluidized beds (CFB) and bubbling fluidized beds (BFB) produce ashes that on average have higher contents of the desired oxides CaO and SiO_2 with a smaller deviation range and are also more desirable concerning minor elemental oxides since they had more Al_2O_3 and less K_2O.

Three ashes were chosen as the most suitable for further investigations:

- WBFA-1 (wood pellets, pulverized fuel combustion, 180 MW, fly ash) should be used for further investigations due to the highest amount of Ca present for all WWB ashes.
- WBFA-2 (mixed clean biomass, bubbling fluidized bed combustor, 80 MW, fly ash) should also be further investigated due to the higher Si content with coexistent significant Ca content.
- PSFA (de-inking sludge + demolition wood, bubbling fluidized bed combustor, 75 MW, fly ash) should also be subjected to further investigation due to the presence of calcium silicate in the derived ash.

To achieve the best suited ash for clinker replacement, pelletized wood should be combusted in a fluidized bed with quartz sand as bed material. The derived fly ash should have the potential to act as clinker due to the enhance calcium content introduced in the pelletization process and the enhanced silica content introduced from the bed material. Furthermore, a clearly defined biomass stream in terms of element composition is necessary for the production of ashes that can function directly as either clinker replacement or indirectly as a raw feed for clinker production.

When used as a cement replacement in mortar production, all biomass derived ashes showed a reduction in strength development. Replacement of 20% OPC with the woody biomass and paper sludge-derived ashes WBFA-2 and PSFA respectively provided sufficient strength to satisfy the 42.5 MPa standard. The strength with 20% replacement using WBFA-1 however fell short of this goal. At 40% replacement, the PSFA mixture still achieved a relatively high strength (40.1 MPa) by 90 days. PSFA performed presumably better than both the WBFA ashes due to the presence of reactive calcium silicates. Both WBFA-1 and WBFA-2 contributed more to early strength development whereas the positive effect of PSFA increased with time. At 3 and 7 days WBFA-2 even provided strengths higher than pure OPC when used to replace 20%.

Methods of upgrading the biomass derived ash (i.e. alterations to the particle size and distribution) to improve their performance as a BioSCM and increase the possible replacement rate were also explored. It was found that when strength development is an important parameter in the concrete, the content of biomass derived ash as a direct replacement should not reach 40%. If the ash is used

in higher replacements, then it is best to use the ash directly as-is and not make any modifications to the particle size or composition.

In this work, it was concluded that hydraulic minerals can be formed from biomass derived ashes when these are subjected to a secondary thermal treatment (see Table 39). The specific minerals formed, as well as their quantity and quality, can be manipulated by specific pre-treatments (feed, form and firing regimes) and post-treatment firing regimes. PSFA could be converted from an ash composed of lime, quartz, β-C_2S, gehlenite and portlandite to a SST ash composed of α'H-C_2S β-C_2S and gehlenite when treated at 1238°C. WBFA-1 could be converted form an ash composed of quartz, calcite and arcanite into a SST ash composed of merwinite, akermanite and α-C_2S when treated at 1214°C. WBFA-2 could be converted form an ash composed of quartz, calcite, arcanite, portlandite and lime into a SST ash composed of wollastonite and pseudowollastonite when treated at 1210°C. High concentrations of potassium in the raw ash correlated with lower sintering temperature, however they may also have inhibited the production of alite. A reduction in particle size and compaction of the powder proved beneficial to clinker mineral formation. Ideally, samples should be fired in tablet or compacted nodule form and the D(90) should be less than 45 μm. All of the ashes benefited from a longer dwelling time. There was no new mineral formation with a longer exposure time, however the quantity and the crystallinity of the desired minerals appeared to improve with firing time. Staged heating appeared beneficial when the raw ashes contain significant contents of volatile compounds (i.e. hydroxides and carbonates) indicated by a higher loss on ignition. Rapidly cooling (particularly by submerging the crucible in a water bath) helped to expedite the removal of embodied heat and minimize the reversal of the metastable minerals back to less reactive low temperature polymorphs.

Modifying the chemical composition of biomass ash with pure chemicals or ash sievings helped to upgrade the quantity and quality of the clinker minerals formed. Chemical alterations to PSFA prior to secondary thermal treatment made the mineralogical composition of the dSTT PSFA more like that of OPC. It was determined that the best method to produce dSTT PSFA is to dope the ash with SiO_2 to reduce the C:S ratio to 3 and then fire for 24 hours at 1305°C. A hydraulic binder can also be produced from the biomass derived ash WBFA-1. This dSTT contained C_2S and C_3S but was composed mostly of akermanite. While this dSTT ash is less like OPC in terms of mineralogy, it can be created autogenously and still has functional properties. Doping WBFA-2 to achieve a more desirable composition did not form any C_3S, however both doping and autogenous doping produce an ash mostly composed of α-C_2S.

Under the assumption that the BioCement or BioCement BioSCM blend has the ability to perform as well as OPC a drastic reduction in CO_2eq emission can be achieved. With assumed (but not quantified in this work) equivalent functional performance the production of BioCement has the potential to reduce cement production related CO_2eq emissions on the order of 70-75% when used as an alternative to OPC. The replacement of BioCement with 20% BioSCM has the potential to even further reduce CO_2eq emissions in the order of 75-80%.

Table 39: Composition of the Raw ashes (BioSCM), the secondary thermally treated ashes (STT), the doped secondary thermally treated ashes (dSTT), and the autogenously doped secondary thermally treated ashes (adSTT) for the paper sludge fly ash (PSFA) the woody biomass fly ash (WBFA-1) and the second woody biomass fly ash (WBFA-2).

	PSFA	WBFA-1	WBFA-2
Raw ash & BioSCM	lime	quartz	quartz
	quartz	calcite	calcit
	belite	arcanite	arcanite
	gehlenite		portlandite
	portlandite		lime
STT	α'H-C_2S	merwinite	wollastonite
	β-C_2S	akermanite	pseduowollastonite
	gehlenite	C_2S	
dSTT	α'H-C2S	akermanite	α'H-C_2S
	C_3S	α'H-C_2S	akermanite
	gehlenite	C_3S	
adSTT		akermanite	akermanite
		α'H-C_2S	α'H-C_2S
		C_3S	

4. RECOMMENDATIONS

The use of biomass derived ash to replace cement, either as a secondary cementitious material in concrete or as the raw materials in clinker production has the potential to lower anthropogenic CO_2 emissions but to what extend is still not entirely clear. The LCA values derived in this work are based on the assumption that the BioCements produced will have similar performance and durability characteristics to OPC. Similarly, the quantity estimations on the potential supply of biomass waste streams as raw materials for clinker production assume that these streams are equally suitable and available for this application. These topic need to be further explored.

To meet the 2030 climate and energy targets more biomass combustion is foreseeable. However, the selection/use of biomass must be done in a sustainable manner. Thus, it is important to note that the biomass should not be grown at the expense of land devoted to food production (i.e. no biofuels or energy crops). Biomass for energy should not displace other existing uses of the biomass and should be in line with the principles of cascading use and the waste hierarchy (contribute to a circular economy). High risk biomass sources, like those from protected areas, should not be used. The extraction of agricultural and forest residues should be done at safe levels.

There is still a lot of work to be done; the ideas contained within this body of work are just the first step in producing a binder based on biomass and in terms of reducing the overall global CO_2 emissions they are only one piece of the puzzle. This work seeks to prove the possibility of making a cement replacement with negligible CO_2 emissions. However, making that theory a reality will still take a lot of research but also support of government and various industries.

It is recommended that the research conducted in this work be scaled up. Paper sludge fly ash should be blended together with verge grass ash to produce BioCement in a rotary kiln. Lager scale production should be performed not only to test the concept in a real-world application but also to provide sufficient quantities of BioCement to test strength and durability characteristics.

5. REFERENCES

1. Pels, J.R., D.S. de Nie, and J.H. Kiel. *Utilization of ashes from biomass combustion and gasification*. in *14th European Biomass Conference & Exhibition*. 2005.
2. Faaij, A., et al., *Exploration of the land potential for the production of biomass for energy in The Netherlands.* Biomass and Bioenergy, 1998. **14**(5–6): p. 439-456.
3. Rabou, L., et al., *Biomass in the Dutch energy infrastructure in 2030*. 2006, Wageningen UR.
4. Netherlands, S., *CBS statline*. 2013.
5. Phyllis, E., *Database for biomass and waste.* Energy Research Centre of The Netherlands, 2012.
6. ENCI, *Milieu- en veiligheidsverslag Maastricht 2013-2014.* 2014.
7. Eurostat. *Total production by PRODCOM list (NACE Rev. 2) - annual data*. 2013; Available from: https://ec.europa.eu/eurostat/data/database.
8. Division, U.N.S. *Commodity Trade Statistics Database*. 2018; Available from: http://data.un.org/
9. CEMBUREAU, *World Statistical Review 2004-20014*. 2017.
10. Commission, E., *A Roadmap for moving to a competitive low carbon economy in 2050* 2011.
11. Kajaste, R. and M. Hurme, *Cement industry greenhouse gas emissions–management options and abatement cost.* Journal of cleaner production, 2016. **112**: p. 4041-4052.
12. Shen, W., et al., *Quantifying CO2 emissions from China's cement industry.* Renewable and Sustainable Energy Reviews, 2015. **50**: p. 1004-1012.
13. Supino, S., et al., *Sustainability in the EU cement industry: the Italian and German experiences.* Journal of cleaner production, 2016. **112**: p. 430-442.

SUMMARY

The aim of this project was the development of the scientific basis for methodologies that enable the production of renewable sustainable cement (i.e. BioCement) based on ashes derived from the conversion of biomass residues. Within this project, biomass ash and derived products were developed at the laboratory scale, and their functionality was tested with respect to sustainability and composition (relative to OPC). The ultimate goal was to prove the possibility of replacing traditional Portland cement with a renewable BioCement in typical cement-based products such as concrete. The environmental superiority of theoretical BioCement is based on assumed negligible CO_2 emissions during production. Through a Life Cycle Analyses on the developed biomass ashes (and preferably fully functional BioCement), the environmental impact and the potential to replace Portland cement with theoretical BioCement was quantified. The investigations included three types of biomass (ash) utilization:

4. Partial cement replacement with biomass derived ash as a secondary cementitious material (BioSCM)
5. Thermally treated biomass derived ash to serve a full cement replacement (STT ash)
6. Chemically and thermally altered biomass derived ash to serve a full cement replacement (dSTT ash)

These approaches to replacing or producing cement from Biomass all have the potential to reduce the CO_2 emissions associated with cement to varying degrees. Most importantly they all reduce the amount of limestone consumed to obtain a final concrete product. Since the decomposition of limestone produces more than half of the CO_2 emissions, avoiding this step alone can yield drastic reductions.

Examination of the chemical and mineralogical composition of biomass-derived ash has shown that in addition to CaO and SiO_2, clinker minerals can be found. The investigation into STT ash serves as a foundation for the use of Biomass ashes as a complete cement replacement directly after combustion. Alterations to the thermal treatment would potentially reduce the efficiency and quantity of the primary product (energy in the form of heat or electricity) produced, however this would create a value-added product from the waste. Alterations to the chemical composition prior to thermal treatment (dSTT) demonstrate that the biomass derived ash has the potential to act as a replacement for the raw materials in clinker production. Biomass ashes with sufficient quantities and ratio of CaO and SiO_2 can either be blended together to obtain the desired chemical composition of the raw material required for clinker production and yield typical clinker minerals after further heat treatment. SiO_2 can be obtained from OR-CB (organic residues and contaminated biomass) or possibly HBA (herbaceous and agricultural biomass). CaO can be obtained from WWB (wood and woody biomass) bark and hardwood specifically. Ashes derived from the OR-CB category paper sludge showed the potential to provide both CaO and SiO_2.In this work, it was concluded that hydraulic minerals can be formed from biomass derived ashes when these are subjected to a secondary thermal treatment. The specific minerals formed, as well as their quantity and quality, can be manipulated by specific pre-treatments (feed, form and firing regimes) and post-treatment firing regimes.

Under the assumption that the BioCement or BioCement BioSCM blend has the ability to perform as well as OPC a drastic reduction in CO_2eq emission can be achieved. Given equivalent functional performance the production of BioCement has the potential to reduce cement production related CO_2eq emissions on the order of 70-75% when used as an alternative to OPC. The replacement of BioCement with 20% BioSCM has the potential to even further reduce CO_2eq emissions in the order of 75-80%.

CURRICULUM VITAE

EMPLOYMENT HISTORY

3/2018 – Present	SGS Intron, Project Engineer
4/2016 – 4/2017	MgAubel R&D, Chief Technology Officer
1/2012 – 4/2016	Delft University of Technology Faculty of Civil Engineering and Geosciences, Department of Materials and Environment, PhD Candidate
2/2009 – 12/2011	Ingenieurbüro Schießl Gehlen Sodeikat GmbH, Munich, Scientific Assistant
11/2010 – 12/2011	Centre for Building Materials and Testing at the TU München, Scientific Assistant
1/2009 – 10/2010	Centre for Building Materials and Testing at the TU München, Tutor
1/2009 – 4/2009	Department of Building Physics at the TU München, Scientific Assistant for the Plus Energy House

EDUCATIONAL HISTORY

10/2008 – 12/2011	Technische Universität München, Building Materials, Building Chemistry and Maintenance, Masters of Science
9/2002 – 5/2006	University of California, Berkeley, California, Architecture, Bachelor of Arts
9/1998 – 6/2002	Livermore High School, Livermore, California, High School Diploma

PUBLICATIONS

Carr, N. Jonkers, H. (2013) Towards the Development of CO2 Neutral Cement, Proceedings of the 2013 International Concrete Sustainability Conference, San Francisco, May 6-8th 2013.

Carr, N. Jonkers, H. (2014) Towards the Development of BioCement, Proceedings of the 34th Conference on Cement and Concrete Science Conference, Sheffield, September 14-16th 2014.

Tosti, L. Carr, N. (2015) Life cycle assessment (LCA) of cement containing biomass fly ash as secondary cementitious material (SCM), STW BioGeoCivil Summit, Delft, November 18-19th 2015.

Tosti, L. van Zomeren, A. Pels, J. Carr, N. Comans, R. (2015) Development of new cement formulations containing paper sludge fly ash as secondary cementitious material. Proceedings of the 9th International Conference on the Environmental and Technical Implications of Construction with Alternative Materials - Resource Efficiency in Construction Santander, SPAIN, June 10-12th 2015.

Tosti, L. van Zomeren, A. Pels, J. Carr, N. Comans, R. (2016). Life Cycle assessment of the reuse of fly ash from paper sludge combustion in cement formulations. Proceedings of the 5th International Conference on Industrial and Hazardous Waste Management, Chania, September 27-30th 2016.